

---

Theses and Dissertations

---

Spring 2010

# Modulatory activities of glycosaminoglycans and other polyanionic polysaccharides on cationic antimicrobial peptides

Beth Ellen Miskimins Mills  
*University of Iowa*

Copyright 2010 Beth Ellen Miskimins Mills

This dissertation is available at Iowa Research Online: <http://ir.uiowa.edu/etd/557>

---

## Recommended Citation

Miskimins Mills, Beth Ellen. "Modulatory activities of glycosaminoglycans and other polyanionic polysaccharides on cationic antimicrobial peptides." PhD (Doctor of Philosophy) thesis, University of Iowa, 2010.  
<http://ir.uiowa.edu/etd/557>.

---

Follow this and additional works at: <http://ir.uiowa.edu/etd>

 Part of the [Pharmacy and Pharmaceutical Sciences Commons](#)

MODULATORY ACTIVITIES OF GLYCOSAMINOGLYCANS AND OTHER  
POLYANIONIC POLYSACCHARIDES ON CATIONIC ANTIMICROBIAL  
PEPTIDES

by

Beth Ellen Miskimins Mills

An Abstract

Of a thesis submitted in partial fulfillment  
of the requirements for the Doctor of  
Philosophy degree in Pharmacy  
in the Graduate College of  
The University of Iowa

May 2010

Thesis Supervisor: Associate Professor Robert J. Kerns

## ABSTRACT

Cationic antimicrobial peptides (CAPs) are an important component of the innate immune system and are instrumental in the elimination of bacteria, viruses, protozoa, yeast, fungi and cancerous cells from the body. CAPs have a net positive charge due to a multitude of basic residues in their primary sequences. CAPs exert their antimicrobial activity primarily through the formation of pores in microbial membranes, but also play important immunostimulatory roles in the body. Glycosaminoglycans (GAGs) are negatively charged, polydisperse linear polysaccharides found at cellular surfaces. Although many protein-binding interactions of the GAG family, including heparin and heparan sulfate, have been well-characterized, it is not known to what extent endogenous GAGs affect the innate immune system.

In this work the modulatory activities of GAGs and other polyanionic polysaccharides (PPSs) on CAPs were probed. Initial studies focused on interactions between a short peptide derived from bovine lactoferricin and GAGs. GAGs and other PPSs were then tested for their ability to modulate the antimicrobial activities of a number of CAPs against Gram-positive and –negative organisms. GAGs were also tested for the ability to modulate CAPs binding to bacterial lipopolysaccharide. CAP affinities for the GAGs were determined from lipopolysaccharide competition binding assays. Finally GAGs were evaluated for the ability to protect CAPs from proteolytic degradation. The modulatory activities of GAGs and other PPSs are largely dependent upon all components of the test system and, to a lesser extent, the charge of the molecule.

Abstract Approved: \_\_\_\_\_  
Thesis Supervisor  
\_\_\_\_\_  
Title and Department  
\_\_\_\_\_  
Date

MODULATORY ACTIVITIES OF GLYCOSAMINOGLYCANS AND OTHER  
POLYANIONIC POLYSACCHARIDES ON CATIONIC ANTIMICROBIAL  
PEPTIDES

by

Beth Ellen Miskimins Mills

A thesis submitted in partial fulfillment  
of the requirements for the Doctor of  
Philosophy degree in Pharmacy  
in the Graduate College of  
The University of Iowa

May 2010

Thesis Supervisor: Associate Professor Robert J. Kerns



Graduate College  
The University of Iowa  
Iowa City, Iowa

CERTIFICATE OF APPROVAL

---

PH.D. THESIS

---

This is to certify that the Ph.D. thesis of

Beth Ellen Miskimins Mills

has been approved by the Examining Committee  
for the thesis requirement for the Doctor of Philosophy  
degree in Pharmacy at the May 2010 graduation.

Thesis Committee: \_\_\_\_\_  
Robert J. Kerns, Thesis Supervisor

\_\_\_\_\_  
Michael Duffel

\_\_\_\_\_  
Kevin Rice

\_\_\_\_\_  
Jonathan Doorn

\_\_\_\_\_  
Daniel Quinn

Thank you to my family for all of your love and support! Love, Dr. Mills

## ABSTRACT

Cationic antimicrobial peptides (CAPs) are an important component of the innate immune system and are instrumental in the elimination of bacteria, viruses, protozoa, yeast, fungi and cancerous cells from the body. CAPs have a net positive charge due to a multitude of basic residues in their primary sequences. CAPs exert their antimicrobial activity primarily through the formation of pores in microbial membranes, but also play important immunostimulatory roles in the body. Glycosaminoglycans (GAGs) are negatively charged, polydisperse linear polysaccharides found at cellular surfaces. Although many protein-binding interactions of the GAG family, including heparin and heparan sulfate, have been well-characterized, it is not known to what extent endogenous GAGs affect the innate immune system.

In this work the modulatory activities of GAGs and other polyanionic polysaccharides (PPSs) on CAPs were probed. Initial studies focused on interactions between a short peptide derived from bovine lactoferricin and GAGs. GAGs and other PPSs were then tested for their ability to modulate the antimicrobial activities of a number of CAPs against Gram-positive and –negative organisms. GAGs were also tested for the ability to modulate CAPs binding to bacterial lipopolysaccharide. CAP affinities for the GAGs were determined from lipopolysaccharide competition binding assays. Finally GAGs were evaluated for the ability to protect CAPs from proteolytic degradation. The modulatory activities of GAGs and other PPSs are largely dependent upon all components of the test system and, to a lesser extent, the charge of the molecule.

## TABLE OF CONTENTS

LIST OF TABLES .....	vii
LIST OF FIGURES .....	ix
CHAPTER I BACKGROUND .....	1
1.1 Antimicrobial Peptides .....	1
1.1.1 Modes of Actions of AMPs .....	2
1.1.2 Degradation of AMPs by proteases .....	3
1.2 Lactoferricin Peptide .....	4
1.3 Magainin II .....	5
1.4 Cecropins .....	7
1.5 LL-37 .....	9
1.6 Glycosaminoglycans .....	11
1.6.1 Heparan sulfate and heparin .....	13
1.6.2 Low molecular weight heparins .....	15
1.6.3 Other GAGs .....	17
1.6.4 Preparation of GAGs .....	19
1.6.5 Other Polyanionic Polysaccharides .....	20
1.6.6 Heparin binding sequences .....	22
1.6.7 GAGs and proteases .....	22
1.7 Cationic antimicrobial peptide interactions with glycosaminoglycans .....	23
1.7.1 Early efforts .....	23
1.7.2 GAGs and lactoferrin-derived peptides .....	24
1.7.3 GAGs and cathelicidin CAPs .....	26
1.7.4 GAG-binding peptides and antimicrobial activity .....	30
1.7.5 Virulence traits that exploit interactions between GAGs and AMPs .....	31
1.8 Bacterial Cell Wall Components .....	33
1.8.1 Lipopolysaccharide .....	33
1.8.2 LPS of <i>E. coli</i> .....	34
1.8.3 LPS of <i>P. aeruginosa</i> .....	36
1.8.4 Lipoteichoic acid .....	37
1.8.5 Modification of cell wall components in response to CAPs .....	38
CHAPTER 2 STATEMENT OF THE PROBLEM .....	40
CHAPTER 3 INTERACTION BETWEEN LACTOFERRICIN PEPTIDE AND GLYCOSAMINOGLYCANS .....	42
3.1 Antimicrobial activity of GAGs – Experimental techniques and results .....	42
3.2 Modulation of LP antimicrobial activity by GAGs .....	44
3.2.1 Minimum inhibitory concentrations for LP – experimental techniques and results .....	44
3.2.2 Single point screen accessing the ability of GAGs to modulate the antimicrobial activity of LP – experimental technique and results .....	45

3.2.3 Concentration dependent ability of GAGs to modulate the antimicrobial activity of LP – experimental technique and results .....	47
3.3 LP binding to GAGs .....	48
3.3.1 LP-GAG binding studies - Experimental technique.....	48
3.3.2 Results of LP-GAG binding studies .....	49
3.3.2 Sulfate determination of heparin and LMWHs – Experimental technique and results.....	52
3.3 Conclusions.....	55
CHAPTER 4 MODULATION OF ANTIMICROBIAL ACTIVITY OF MAGAININ II, CECROPIN A, CECROPIN B AND LL-37 .....	57
4.1 Antimicrobial activity of GAGs and other polyanionic polysaccharides – experimental technique and results .....	57
4.2 Modulation of antimicrobial activity of magainin II, cecropin A, cecropin B and LL-37 .....	62
4.2.1 Minimum inhibitory concentrations – Experimental technique and results .....	62
4.2.2 Single point screens for reversal of antimicrobial activity – Experimental technique and results.....	66
4.2.3 Concentration dependent reversal of antimicrobial activity by GAGs, charge-reduced heparin analogs and LMWHs – experimental techniques .....	74
4.2.4 Modulation of magainin II antimicrobial activity by GAGs, charge-reduced heparin analogs and LMWHs .....	75
4.2.5 Modulation of cecropin A antimicrobial activity by GAGs, charge-reduced heparin analogs and LMWHs .....	79
4.2.6 Modulation of cecropin B antimicrobial activity by GAGs, charge-reduced heparin analogs and LMWHs .....	83
4.2.7 Modulation of LL-37 antimicrobial activity by GAGs, charge-reduced heparin analogs and LMWHs .....	88
4.3 Conclusions.....	99
CHAPTER 5 MODULATION OF CATIONIC ANTIMICROBIAL PEPTIDE BINDING BACTERIAL MEMBRANE COMPONENTS BY GLYCOSAMINOGLYCANS.....	101
5.1 CAPs binding to lipopolysaccharides and lipoteichoic acid.....	101
5.1.1 Experimental techniques .....	101
5.1.2 Cecropin A binding to <i>P. aeruginosa</i> and <i>E. coli</i> LPS.....	103
5.1.3 Cecropin B binding to <i>P. aeruginosa</i> and <i>E. coli</i> LPS .....	104
5.1.4 LL-37 binding to <i>P. aeruginosa</i> and <i>E. coli</i> LPS .....	106
5.2 Evaluation of CAP affinity for LPS or LTA by competition binding assays.....	107
5.2.1 Experimental technique .....	107
5.2.2 Measure of affinity of cecropin A for LPS and LTA by competition binding assay .....	109
5.2.3 Affinity of cecropin B for LPS and LTA measured by competition binding assay .....	113
5.2.4 Competition binding assays showing LL-37 affinity for LPS and LTA.....	117
5.3 Competition binding assays measuring the affinity of CAPs for GAGs .....	121

5.3.1 Experimental techniques .....	121
5.3.2 Competition binding studies for cecropin A and GAGs .....	122
5.3.3 Competition binding studies on cecropin B binding to GAGs.....	126
5.3.4 Competition binding studies for LL-37 and GAGs.....	131
5.4 Correlation between LL-37 affinity for glycosaminoglycans and the ability of glycosaminoglycans to reversal of antimicrobial activity of LL-37 .....	152
5.5 Conclusions.....	154
 CHAPTER 6 PROTECTION OF CATIONIC ANTIMICROBIAL PEPTIDES FROM PROTEOLYTIC DEGRADATION BY GLYCOSAMINOGLYCANS.....	156
6.1 Inhibition of trypsin and <i>Pseudomonas aeruginosa</i> elastase by glycosaminoglycans.....	156
6.1.1 Experimental techniques .....	156
6.1.2 Results .....	159
6.2 Protection of CAPs from trypsin degradation by GAGs .....	160
6.2.1 Experimental technique.....	160
6.2.2 Protection of LL-37 from trypsin degradation by GAGs .....	161
6.2.3 Protection of cecropin A from trypsin degradation by GAGs.....	166
6.2.4 Protection of cecropin B from trypsin degradation by GAGs.....	169
6.3 Protection of LL-37 from <i>Pseudomonas aeruginosa</i> elastase degradation by glycosaminoglycans.....	171
6.4 Conclusions.....	176
 CHAPTER 7 CONCLUSIONS AND FUTURE DIRECTIONS .....	178
REFERENCES .....	180

## LIST OF TABLES

Table 1	The most common repeating disaccharides of endogenous mammalian GAGs.....	12
Table 2	Molecular weights and preparation methods for LMWHs. ....	16
Table 3	Calculated binding constants for GAGs binding LP.....	52
Table 4	MIC values for magainin II, cecropin A, cecropin B and LL-37 against <i>P. aeruginosa</i> , <i>E. coli</i> and <i>S. aureus</i> . ....	65
Table 5	Binding constants calculated from cecropin A saturation of immobilized <i>P. aeruginosa</i> LPS. ....	134
Table 6	Binding constants calculated from cecropin A saturation of <i>E. coli</i> LPS.....	135
Table 7	Binding constants calculated from cecropin B saturation of <i>P. aeruginosa</i> LPS.....	136
Table 8	Calculated binding constants for cecropin B binding to immobilized <i>E. coli</i> LPS.....	137
Table 9	Binding constants calculated for LL-37 binding to <i>P. aeruginosa</i> LPS.....	138
Table 10	Calculated binding constants for LL-37 binding to <i>E. coli</i> LPS.....	139
Table 11	Binding constants calculated from LPS and LTA competition binding studies on cecropin A binding to immobilized <i>P. aeruginosa</i> LPS. ....	140
Table 12	Calculated binding values from LPS and LTA competition binding studies on cecropin A binding to immobilized <i>E. coli</i> LPS. ....	141
Table 13	Calculated binding values from LPS and LTA competition binding studies on cecropin B binding to immobilized <i>P. aeruginosa</i> LPS. ....	142
Table 14	Binding constants calculated from LPS and LTA competition binding assays on cecropin B binding to immobilized <i>E. coli</i> LPS. ....	143
Table 15	Calculated binding constants for LL-37 binding to <i>P. aeruginosa</i> LPS.....	144
Table 16	Calculated binding constants for LL-37 binding to <i>E. coli</i> LPS.....	145
Table 17	Binding constants calculated for GAG competition binding assays on cecropin A binding to immobilized <i>P. aeruginosa</i> LPS. ....	146
Table 18	Binding constants calculated for GAG competition binding assays on cecropin A binding to immobilized <i>E.coli</i> LPS. ....	147
Table 19	Calculated binding constants for GAG competition binding studies for cecropin B binding to <i>P. aeruginosa</i> LPS.....	148

Table 20	Binding constants calculated from GAG competition binding curves on cecropin B binding to immobilized <i>E. coli</i> LPS.....	149
Table 21	Binding constants for GAG competition binding assays for LL-37 binding immobilized <i>P. aeruginosa</i> LPS.....	150
Table 22	Binding constants calculated from GAG competition binding curves on LL-37 binding to immobilized <i>E. coli</i> LPS.....	151
Table 23	Calculated inhibition constants for GAGs inhibiting trypsin.....	159
Table 24	Calculated inhibition constants for GAGs inhibiting <i>P. aeruginosa</i> elastase. ....	160



## LIST OF FIGURES

Figure 1	CAP modes of actions: Barrel-stave model (left), carpet model (middle) and toroidal pore model (right). Figures are modified from Brogden, 2005. <sup>39</sup> .....	3
Figure 2	Sequence (A) and secondary structure of magainin II. Magainin II forms an $\alpha$ -helix (B) that contains cationic (red) and hydrophobic (green) domains (C). <sup>9</sup> .....	6
Figure 3	Sequences of cecropin A (A) and cecropin B (B) and the secondary structure of cecropin A (C). <sup>116</sup> Predicted trypsin cleavage sites are on the C-terminal sides of basic residues. ....	9
Figure 4	Primary sequence of LL-37 (A) and 3-dimensional models of LL-37 showing hydrophilic (blue/dark gray) and hydrophobic (white/light gray) residues (B and C). <sup>126</sup> Degradation pattern for LL-37 by trypsin (C-terminal side of basic residues) and <i>P. aeruginosa</i> elastase (denoted by arrows) (D). <sup>42</sup> .....	10
Figure 5	Representation of the domains found in HS where uronic acids are represented by diamonds, glucosamine is represented by squares and sulfate groups are indicated above or below the residue symbols. <sup>150</sup> .....	14
Figure 6	3-dimensional model of the solution conformation of a heparin dodecasaccharide (PDB entry 1HPN). ....	15
Figure 7	Structure of lipid A with inner core Kdo residues.....	35
Figure 8	Antimicrobial activity of GAGs and other PPSs against <i>E. coli</i> . PPSs were tested at two concentrations and growth of the bacteria was evaluated at three different time points. Data is presented as the means of triplicate data points $\pm$ standard error. A positive growth control, in the form of bacteria incubated with sterile water is shown. ....	43
Figure 9	Antimicrobial activity of PPSs against <i>E. coli</i> after 53 hours. Data points represent the mean of triplicate determinations $\pm$ standard error. ....	44
Figure 10	Single point screen accessing the modulatory activities of PPSs on the antimicrobial activity of LP. LP was tested at the MIC for <i>E. coli</i> (16.0 $\mu\text{g}/\text{mL}$ , red) and two-fold the MIC (32.0 $\mu\text{g}/\text{mL}$ , blue). ....	46
Figure 11	Negative modulatory activity of the GAGs on the antimicrobial activity of LP against <i>E. coli</i> . LP was used at two-fold the MIC for <i>E. coli</i> . Data points represent the mean of duplicate measurements.....	48
Figure 12	Saturation binding curves for heparin (black), enoxaparin (dotted line) and DS (red) binding LP generated from tryptophan fluorescence data. Data points represent the means of 12 determinations (heparin) or 6 determinations (enoxaparin and DS) $\pm$ standard error.....	50
Figure 13	Comparision of the concentration of GAG at which 50% of maximal fluorescence is achieved calculated from tryptophan fluorescence data. C4S did not achieve maximal binding in the range of 0-3330 $\mu\text{g}/\text{mL}$ . ....	50

Figure 14	Saturation binding curves for GAGs binding to LP. The fits of the one-site binding model are shown for heparin (A), HS (B), enoxaparin (C), ardeparin (D) and DS (E). The means of 12 determinations (A), 9 determinations (B), or 6 determinations (C-E) $\pm$ standard error are shown.....	51
Figure 15	Potassium sulfate standard curve generated for GAG total sulfate determination.....	53
Figure 16	Total sulfate levels of heparin, centaxarin and enoxparin samples calculated using the standard curve in Figure 15. ....	54
Figure 17	Antimicrobial activity of GAGs, charge-reduced heparin analogs and LMWHs versus <i>P. aeruginosa</i> . Data points represent the mean of triplicate determinations $\pm$ standard error.....	58
Figure 18	Antimicrobial activity of GAGs, charge-reduced heparin analogs and LMWHs versus <i>E. coli</i> (A) and <i>S. aureus</i> (B). Measurements were done in triplicate and data points are shown as the mean $\pm$ standard error. ....	59
Figure 19	Antimicrobial activity of 6- <i>O</i> -desulfated heparin and other PPSs versus <i>P. aeruginosa</i> (A) and <i>E. coli</i> (B). Mean of six data points $\pm$ standard error shown.....	60
Figure 20	Antimicrobial activity of 6- <i>O</i> -desulfated heparin and other polyanionic polysaccharides versus <i>S. aureus</i> . Mean of six data points $\pm$ standard error shown.....	61
Figure 21	Magainin II MIC determination against <i>P. aeruginosa</i> and <i>E. coli</i> . Data points represent the mean of duplicate data points.....	63
Figure 22	Cecropin A MICs (A) and cecropin B MICs (B) against <i>P. aeruginosa</i> and <i>E. coli</i> . Data points represent the mean of duplicate determinations.....	64
Figure 23	LL-37 MICs against <i>P. aeruginosa</i> , <i>E. coli</i> and <i>S. aureus</i> . Data points represent the mean of duplicate measurements.....	65
Figure 24	Effect of GAGs, charge-reduced heparin analogs and LMWHs on the antimicrobial activity of magainin II at 4.0, 16.0 and 32.0 mg/mL versus <i>P. aeruginosa</i> (A) and <i>E. coli</i> (B). Single data points shown.....	68
Figure 25	Effect of GAGs, charge-reduced heparin analogs and LMWHs on the antimicrobial activity of cecropin A four-fold below MIC, at MIC and 2-fold above MIC versus <i>P. aeruginosa</i> . Single data points shown.....	69
Figure 26	Effect of GAGs, charge-reduced heparin analogs, LMWHs and other PPSs on the antimicrobial activity of cecropin A versus <i>P. aeruginosa</i> at 0.325, 1.25 and 2.5 $\mu$ g/mL. Single data points shown.....	70
Figure 27	Effect of GAGs, charge-reduced heparin analogs and LMWHs on the antimicrobial activity of cecropin B 4-fold below MIC, at MIC and 2-fold above MIC versus <i>P. aeruginosa</i> (A) and <i>E. coli</i> (B). Single data points shown.....	71

Figure 28	Effect of GAGs, charge-reduced heparin analogs, LMWHs and other PPSs on the antimicrobial activity of LL-37 versus <i>P. aeruginosa</i> (A) and <i>E. coli</i> (B). Single data points shown.....	72
Figure 29	Single point screen showing the effect of GAGs, charge-reduced heparin analogs, LMWHs and other PPSs on the antimicrobial activity of LL-37 against <i>S. aureus</i> . .....	73
Figure 30	Reversal of magainin II antimicrobial activity versus <i>P. aeruginosa</i> by GAGs, charge-reduced heparin analogs and LMWHs. Average of duplicate data points shown.....	76
Figure 31	Reversal of antimicrobial activity of magainin II versus <i>P. aeruginosa</i> by GAGs. Average of duplicate data points shown.....	76
Figure 32	Reversal of antimicrobial activity of magainin II versus <i>P. aeruginosa</i> by heparin and charge-reduced heparin analogs. Average of duplicate data points shown. ....	77
Figure 33	Reversal of antimicrobial activity of magainin II versus <i>P. aeruginosa</i> by heparin and LMWHs. Average of duplicate data points shown.....	77
Figure 34	Reversal of antimicrobial activity of magainin II versus <i>E. coli</i> by GAGs, charge-reduced heparin analogs and LMWHs. Average of duplicate data points shown.....	78
Figure 35	Reversal of antimicrobial activity of cecropin A versus <i>P. aeruginosa</i> by GAGs, charge-reduced heparin analogs and LMWHs. Average of triplicate data points shown with error bars omitted for ease of viewing.....	80
Figure 36	Reversal of antimicrobial activity of cecropin A versus <i>P. aeruginosa</i> by GAGs. Data points represent the mean $\pm$ standard error of triplicate determinations. ....	80
Figure 37	Reversal of antimicrobial activity of cecropin A versus <i>P. aeruginosa</i> by heparin and charge-reduced heparin analogs. Data points represent the mean $\pm$ standard error of triplicate measurements.....	81
Figure 38	Reversal of antimicrobial activity of cecropin A versus <i>P. aeruginosa</i> by heparin and LMWHs. Data points represent the mean $\pm$ standard error of triplicate measurements. ....	82
Figure 39	Reversal of antimicrobial activity of cecropin A versus <i>E. coli</i> by GAGs, charge-reduced heparin analogs and LMWHs. Means of triplicate data points are plotted.....	83
Figure 40	Reversal of antimicrobial activity of cecropin B versus <i>P. aeruginosa</i> by GAGs, charge-reduced heparin analogs and LMWHs. Means of duplicate data points are shown.....	84
Figure 41	Reversal of antimicrobial activity of cecropin B versus <i>P. aeruginosa</i> by GAGs. Data points represent the mean of duplicate measurements.....	85

Figure 42	Reversal of antimicrobial activity of cecropin B versus <i>P. aeruginosa</i> by heparin and charge-reduced heparin analogs. Mean of duplicate data points shown.....	86
Figure 43	Reversal of antimicrobial activity of cecropin B versus <i>P. aeruginosa</i> by heparin and LMWHs. Data points represent the mean of duplicate measurements. ....	87
Figure 44	Reversal of antimicrobial activity of cecropin B versus <i>E. coli</i> by GAGs, charge-reduced heparin analogs and LMWHs. Data points represent the mean of duplicate determinations. ....	88
Figure 45	Reversal of antimicrobial activity of LL-37 versus <i>P. aeruginosa</i> by GAGs. Average of duplicate data points shown.....	89
Figure 46	Reversal of antimicrobial activity of LL-37 versus <i>P. aeruginosa</i> by GAGs. Average of duplicate data points shown.....	90
Figure 47	Reversal of antimicrobial activity of LL-37 versus <i>P. aeruginosa</i> by heparin and charge-reduced heparin analogs. Average of duplicate data points shown.....	91
Figure 48	Reversal of antimicrobial activity of LL-37 versus <i>P. aeruginosa</i> by heparin and LMWHs. Average of duplicate data points shown.....	92
Figure 49	Reversal of antimicrobial activity of LL-37 versus <i>E. coli</i> by GAGs, chemically-modified heparins and LMWHs. Average of duplicate data points shown.....	93
Figure 50	Reversal of antimicrobial activity of LL-37 versus <i>E. coli</i> by GAGs. Average of duplicate data points shown.....	94
Figure 51	Reversal of antimicrobial activity of LL-37 versus <i>E. coli</i> by heparin, chemically-modified heparin analogs. Average of duplicate data points shown.....	95
Figure 52	Reversal of antimicrobial activity of LL-37 versus <i>E. coli</i> by heparin and LMWHs. Average of duplicate data points shown.....	95
Figure 53	Reversal of antimicrobial activity of LL-37 against <i>S. aureus</i> by GAGs, LMWHs and chemically-modified heparin analogs. Single data points shown.....	96
Figure 54	Reversal of antimicrobial activity of LL-37 versus <i>S. aureus</i> by GAGs (A) and heparin and charge-reduced heparin analogs (B). Single data points shown.....	97
Figure 55	Reversal of antimicrobial activity of LL-37 versus <i>S. aureus</i> by heparin and LMWHs. Single data points shown.....	98
Figure 56	Cecropin A binding to <i>P. aeruginosa</i> LPS. Mean of triplicate data points $\pm$ standard error shown. Line shows the fit of Equation 2.....	103

Figure 57	Cecropin A binding to <i>E. coli</i> LPS. Data points represent the mean of triplicate measurements $\pm$ standard error. Line shows the fit of Equation 2.....	104
Figure 58	Cecropin B binding to immobilized <i>P. aeruginosa</i> LPS (A) and <i>E. coli</i> LPS (B). Means of triplicate data points $\pm$ standard error shown. Data in A and B is fit to Equation 1.....	105
Figure 59	LL-37 binding to immobilized <i>P. aeruginosa</i> LPS. Data points represent the mean of triplicate measurements $\pm$ standard error. The fit of Equation 1 is shown. ....	106
Figure 60	LL-37 binding to immobilized <i>E. coli</i> LPS. The mean of triplicate data points $\pm$ standard error is shown. Data are fit to Equation 1. ....	107
Figure 61	Competition binding curve for free <i>P. aeruginosa</i> LPS binding cecropin A off <i>P. aeruginosa</i> LPS. Means of triplicate measurements $\pm$ standard error. The fit of Equation 5 is shown.....	109
Figure 62	Competition binding curve for <i>E. coli</i> LPS binding cecropin A on immobilized <i>P. aeruginosa</i> LPS. Data points represent the mean of triplicate determinations $\pm$ standard error. The fit of Equation 5 is shown.....	110
Figure 63	Competition binding curve for <i>S. aureus</i> LTA binding cecropin A on <i>P. aeruginosa</i> LPS plates. Mean of triplicate data points $\pm$ standard error shown. The fit of Equation 5 is shown.....	110
Figure 64	Competition binding curve for free <i>E. coli</i> LPS binding cecropin A off <i>E. coli</i> LPS plates. Means of triplicate data points $\pm$ standard error shown. The fit of Equation 5 is shown.....	111
Figure 65	Competition binding curves for <i>P. aeruginosa</i> LPS (A) and <i>S. aureus</i> LTA (B) competition binding cecropin A on <i>E. coli</i> LPS plates. Data points represent the mean of triplicate measurements $\pm$ standard error. The fit of Equation 5 is shown in A and B.....	112
Figure 66	<i>P. aeruginosa</i> LPS competition binding cecropin B on <i>P. aeruginosa</i> LPS. Data points represent the mean of triplicate determinations $\pm$ standard error. The fit of Equation 5 is shown.....	113
Figure 67	Competition binding curve for <i>E. coli</i> LPS binding cecropin B on <i>P. aeruginosa</i> LPS. The means of triplicate data points $\pm$ standard error are shown. Data are fit to Equation 5. ....	114
Figure 68	Competition binding curves for <i>S. aureus</i> LTA binding cecropin B on immobilized <i>P. aeruginosa</i> LPS. The means of triplicate data points $\pm$ standard error are shown. The fits of Equation 5 (left) and Equation 6 (right) are shown.....	114
Figure 69	<i>E. coli</i> LPS competition binding cecropin B on immobilized <i>E. coli</i> LPS. Means of triplicate data points $\pm$ standard error shown. The line is fit to Equation 5. ....	115

Figure 70	Competition binding curve for <i>P. aeruginosa</i> LPS binding to cecropin B on <i>E. coli</i> LPS. Means of triplicate measurements are shown $\pm$ standard error. The fit of Equation 5 is shown.....	116
Figure 71	Competition binding curves <i>S. aureus</i> LTA binding to cecropin B on immobilized <i>E. coli</i> LPS. Data points represent the mean of triplicate determinations $\pm$ standard error. The fits of Equation 5 (left) and Equation 6 (right) are shown.....	117
Figure 72	Competition binding curves for free <i>P. aeruginosa</i> LPS binding to LL-37 on immobilized <i>P. aeruginosa</i> LPS. Data points represent the mean of triplicate measurements $\pm$ standard error. Lines are the fit of Equation 5 (left) and Equation 6 (right). .....	117
Figure 73	Competition binding curves for <i>E. coli</i> LPS binding to cecropin B on <i>P. aeruginosa</i> LPS plates. The mean of triplicate data points $\pm$ standard error is shown. Data are fit to Equation 5.....	118
Figure 74	Competition binding curves for <i>S. aureus</i> LTA competition binding to LL-37 on <i>P. aeruginosa</i> plates. The means of triplicate measurements $\pm$ standard error are shown. Lines are fit to Equation 5 (left) and Equation 6 (right).....	118
Figure 75	Competition binding curve for free <i>E. coli</i> LPS binding to LL-37 on immobilized <i>E. coli</i> LPS. Data points represent the mean of triplicate measurements $\pm$ standard error. Fit of Equation 5 is shown. ....	119
Figure 76	Competition binding curve of <i>P. aeruginosa</i> LPS binding to LL-37 on immobilized <i>E. coli</i> LPS. Mean of triplicate data points $\pm$ standard error shown. The line is fit to Equation 5.....	120
Figure 77	Competition binding curves showing <i>S. aureus</i> LTA binding to LL-37 on <i>E. coli</i> LPS plates. The mean of triplicate measurements $\pm$ standard error is shown. The fits of Equation 5 (left) and Equation 6 (right) are shown.....	120
Figure 78	Competition binding curves showing heparin (A), HS (B), DS (C) and HA (D) binding cecropin A on immobilized <i>P. aeruginosa</i> LPS. The fits of Equation 5 are shown.....	122
Figure 79	Competition binding curves for enoxaparin binding cecropin A on <i>P. aeruginosa</i> LPS. The fits of Equation 5 (left) and Equation 6 (right) are shown.....	123
Figure 80	Competition binding curves for C4S binding cecropin A on immobilized <i>P. aeruginosa</i> LPS. The fits of Equation 5 (left) and Equation 6 (right) are shown.....	123
Figure 81	Competition binding curves showing heparin (A), enoxaparin (B), HS (C), DS (D) and HA (E) binding cecropin A on immobilized <i>E. coli</i> LPS. The fit of Equation 5 is shown in A-E.....	124

Figure 82	Competition binding curves showing C4S binding cecropin A on immobilized <i>E. coli</i> LPS. The fits of Equation 5 (left) and Equation 6 (right) are shown.....	125
Figure 83	Competition binding curves showing heparin (A), enoxaparin (B) and DS (C) binding to cecropin B on immobilized <i>P. aeruginosa</i> LPS. The fits of Equation 5 are shown.....	126
Figure 84	Competition curves for HS binding cecropin B on immobilized <i>P. aeruginosa</i> LPS. Means of triplicate data points $\pm$ standard error are shown. The fits of Equation 5 (A) and Equation 6 (B) are shown. ....	127
Figure 85	Competition binding curves for HA binding to cecropin B on immobilized <i>P. aeruginosa</i> LPS. Data points represent the mean of triplicate measurements $\pm$ standard error. The fits of Equation 5 (left) and Equation 6 (right) are shown. ....	127
Figure 86	Competition binding curves for C4S binding cecropin B on immobilized <i>P. aeruginosa</i> LPS. Means of triplicate determinations $\pm$ standard error shown. The fits of Equation 5 (left) and Equation 6 (right) are shown.....	128
Figure 87	Competition binding curves for DS (A), C4S (B), HA (C) and enoxaparin (D) binding to cecropin B on immobilized <i>E. coli</i> LPS. Means of triplicate data points $\pm$ standard error shown. The fits of Equation 5 are shown. ....	129
Figure 88	Competition binding curves for heparin binding cecropin B on immobilized <i>E.coli</i> LPS. Data points represent the means of triplicate determinations $\pm$ standard error. The fits of Equation 5 (left) and Equation 6 (right) are shown. ....	130
Figure 89	Competition binding curves for HS binding to cecropin B on immobilized <i>E. coli</i> LPS. Data points represent the mean of triplicate measurements $\pm$ standard error. Lines are fit to Equation 5 (left) and Equation 6 (right).....	130
Figure 90	Competition binding curves for heparin (A), enoxaparin (B), HS (C), DS (D), HA (E) and C4S (F) binding to LL-37 on immobilized <i>P. aeruginosa</i> LPS. The means of triplicate data points $\pm$ standard error are shown. The fits of Equation 5 are shown. ....	132
Figure 91	Competition binding curves for heparin (A), enoxaparin (B), HS (C), DS (D), HA (E) and C4S (F) binding to LL-37 on immobilized <i>E. coli</i> LPS. Means of triplicate data points $\pm$ standard error shown. The fits of Equation 5 are shown. ....	133
Figure 92	Correlation plot comparing the concentration of GAG required to reverse the antimicrobial activity of LL-37 against <i>P. aeruginosa</i> vs. the $K_i$ value for each GAG binding LL-37 on <i>P. aeruginosa</i> LPS. A linear fit is shown for the data. ....	152

Figure 93	Correlation plot comparing the concentration of GAG required to reverse the antimicrobial activity of LL-37 against <i>E. coli</i> vs. the $K_i$ value for each GAG binding LL-37 on <i>E. coli</i> LPS. A linear fit is shown for the data.....	153
Figure 94	Example of a Dixon plot and determination of the inhibition constant.....	158
Figure 95	Concentration-dependent trypsin digestion of LL-37. 15 minute (A) and 30 minute (B) digestions shown. Lanes 1-2: MWMs, Lane 3: LL-37, Lanes 4-10: LL-37 + trypsin. Lane 4 contains 1000 U. 1:10 trypsin dilutions were used in subsequent lanes, giving 1 mU trypsin in lane 10.....	162
Figure 96	Tris-tricine PAGE showing concentration-dependent protection of LL-37 from trypsin degradation by heparin (A) and HS (B). Lanes 1-2: MWMs, Lane 3: LL-37, Lane 4: LL-37 + 1 U trypsin, Lanes 5-14: LL-37, 1 U trypsin + GAGs.....	163
Figure 97	Tris-tricine PAGE showing concentration-dependent protection of LL-37 from trypsin degradation by DS (A), C4S (B), C6S (C), HA (D), enoxaparin (E), and ardeparin (F). Lanes 1-2: MWMs, Lane 3: LL-37, Lane 4: LL-37 + 1 U trypsin, Lanes 5-15: LL-37, 1 U trypsin + GAGs.....	164
Figure 98	Concentration-dependent protection of LL-37 from trypsin degradation by GAGs (A) and heparin and LMWHs (B). .....	165
Figure 99	Concentration-dependent digestion of cecropin A by trypsin. Lanes 1-2: MWMs, Lanes 3-4: cecropin A, Lanes 5-13: cecropin A + trypsin. Lane 5 contains 5,500 U of trypsin. 1:10 dilutions of trypsin were used in subsequent lanes, where lane 13 has 55 nU of trypsin.....	166
Figure 100	Tris-tricine PAGE showing concentration-dependent protection of cecropin A from trypsin degradation by heparin (A), enoxaparin (B), ardeparin (C), dermatan sulfate (D) and hyaluronic acid (E). Lanes 1-2: MWMs, Lane 3: cecropin A, Lane 4: cecropin A + 5.5 U trypsin, Lanes 5-13: cecropin A, 5.5 U trypsin and GAGs.....	167
Figure 101	Concentration-dependent protection of cecropin A by heparin, dermatan sulfate and hyaluronic acid (A) and heparin and LMWHs (B).....	168
Figure 102	Concentration-dependent digestion of cecropin B by trypsin. Lanes 1-2: MWMs, Lane 3: cecropin B, Lanes 4-13: cecropin B + trypsin. Lane 4 contains 55,000 U of trypsin. 1:10 dilutions of trypsin were used in subsequent lanes, where lane 13 has 55 nU of trypsin.....	169
Figure 103	Tris-tricine PAGE showing concentration-dependent protection of cecropin B by heparin (A), ardeparin (B), dermatan sulfate (C) and hyaluronic acid (D). Lanes 1-2: MWMs, Lane 3: cecropin B, Lane 4: cecropin B + 550 mU trypsin, Lanes 5-13: cecropin B, 550 U trypsin + GAGs.....	170
Figure 104	Concentration-dependent protection of cecropin B from trypsin degradation by GAGs. ....	171



Figure 105	Concentration-dependent PAELA digestion of LL-37. Lanes 1-2: MWMs, Lane 3: LL-37, Lanes 4-14: LL-37 + PAELA. Lane 4 contains 10.0 U of PAELA. 1:10 dilutions of PAELA were used in subsequent lanes, where lane 14 contains 1.0 nU PAELA.....	172
Figure 106	Tris-tricine PAGE showing concentration-dependent protection of LL-37 from PAELA degradation by heparin (A), HS (B), DS (C), C4S (D) and C6S (E). Lanes 1-2: MWMs, Lane 3: LL-37, Lane 4: LL-37 + 10 mU PAELA, Lanes 5-15: LL-37, 10 mU PAELA + GAGs.....	173
Figure 107	Tris-tricine PAGE showing concentration-dependent protection of LL-37 from PAELA degradation by HA (A), enoxaparin (B) and ardeparin (C).....	174
Figure 108	Concentration-dependent protection of LL-37 from PAELA degradation by GAGs (A) and heparin and LMWHs (B). .....	175

## CHAPTER I BACKGROUND

### 1.1 Antimicrobial Peptides

Antimicrobial peptides (AMPs) are a component of the innate immune system, a basic line of defense.<sup>1,2</sup> Peptides with antimicrobial activity were first described by Zeya and Spitznagel in 1966 and named defensins because of their function in host defense.<sup>3,4</sup> AMPs act as endogenous antibiotics by direct destruction of microorganisms. AMPs are polypeptides containing fewer than 100 amino acid residues and have broad antimicrobial activity spectra that are unique for each peptide.<sup>5</sup> The antibiotic spectra of AMPs are determined by their amino acid sequence and structural conformation.<sup>6</sup> Organisms producing AMP include virtually all higher eukaryotes—including plants and invertebrates, and also eubacteria and archaea.<sup>7-9</sup> In humans, several cell types synthesize and secrete AMPs - epithelial and professional host-defense cells such as neutrophils, macrophages, and natural killer cells.<sup>10</sup>

On the basis of structural homology motifs, two main families of eukaryotic AMPs can be described: cationic antimicrobial peptides (CAPs) and noncationic antimicrobial peptides.<sup>11</sup> CAPs, the largest group of AMPs, include defensins and cathelicidins. The other classes of cationic peptides are the amino acid enriched class (including histatins), cecropins/magainins, and peptides related to histones or lactoferrin.<sup>10</sup> CAPs are multifaceted molecules that possess antimicrobial, chemoattractant and wound healing properties. CAPs consist of basic and hydrophobic residues that allow them to interact with the membranes bacteria and fungi.<sup>12</sup> Additionally they can serve as chemoattractants for neutrophils, monocytes and lymphocytes.<sup>13-15</sup> Antimicrobial peptides have also been implicated as positive effectors of wound repair.<sup>12,16-18</sup>

### 1.1.1 Modes of Actions of AMPs

In general, antimicrobial peptides have evolved to target bacterial rather than mammalian cells due to a fundamental difference in the composition of the cell membrane. The outer surface of Gram-negative bacteria is covered in lipopolysaccharides and Gram-positive bacteria present a surface of teichoic acids, resulting in both classes of bacteria having negatively charged cell surfaces. In contrast, most mammalian cell membranes have an outer leaflet comprised of zwitterionic phosphatidylcholine and sphingomyelin phospholipids, while the inner leaflet is composed of phosphatidylserine leading to an essentially neutral surface. The negative charge associated with bacterial cells means that CAPs are primarily attracted to the pathogenic membrane rather than that of mammalian cells.<sup>19</sup> Similar to bacteria, many cancer cells carry a net negative charge due to their elevated expression, relative to non-transformed cells, of anionic molecules such as phosphatidylserine and *O*-glycosylated mucins on the outer membrane leaflet.<sup>20-23</sup> This net negative charge allows electrostatic interactions to occur between CAPs and the surface of many cancer cells.

Amphipathic  $\alpha$ -helical peptides act via a non-receptor-mediated pathway and elicit the release of contents from lipid vesicles and cells (**Figure 1**). Originally, they were thought to form pores in membranes. According to the barrel-stave model<sup>24</sup>,  $\alpha$ -helical bundles of six or more peptides would insert into the membrane and form a water-filled pore, exposing the hydrophilic face of the helices to water and the hydrophobic face to the lipid bilayer interior. The model was believed to apply to alamethicin, melittin, and  $\delta$ -lysin. However, it was subsequently shown that it is unlikely for melittin<sup>25</sup> and incorrect for  $\delta$ -lysin.<sup>26,27</sup> It now appears that most peptides follow other mechanisms<sup>28,29</sup>, including the toroidal hole model<sup>30-32</sup>, the carpet model<sup>29,33,34</sup>, the sinking raft model<sup>26,27</sup> and other less structured types of pores<sup>35</sup>. The question of whether membrane disruption is the function of these peptides is also still under debate.<sup>36,37</sup> It is possible that the real targets are intracellular components and that membrane perturbation might be only a side

effect. Nevertheless, interaction with the bilayer is essential for the function of these peptides<sup>38</sup>.

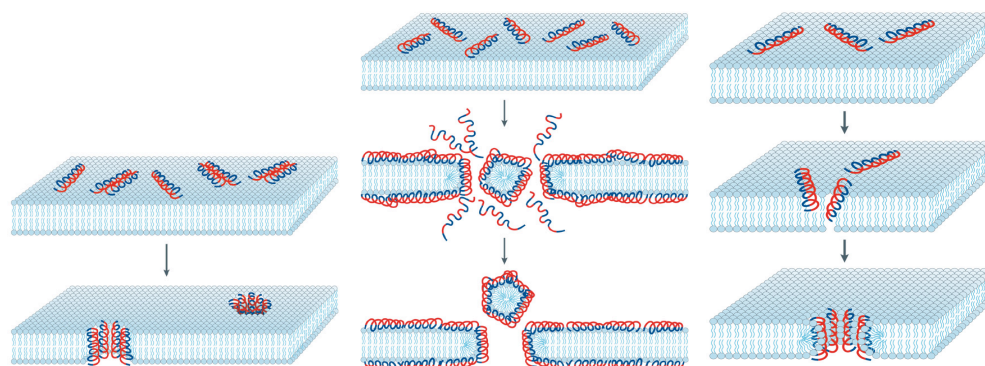


**Figure 1** CAP modes of actions: Barrel-stave model (left), carpet model (middle) and toroidal pore model (right). Figures are modified from Brogden, 2005.<sup>39</sup>

### 1.1.2 Degradation of AMPs by proteases

CAPs are degraded and inactivated by a number of both host and pathogen proteases. Cathepsins B, L and S inactivate  $\beta$ -defensins 2 and 3 by proteolytic degradation.<sup>40</sup> Proteinases of significant pathogens including aureolysin of *Staphylococcus aureus*<sup>41</sup> and elastase of *Pseudomonas aeruginosa* have been shown to degrade LL-37.<sup>42</sup> Bergsson *et al.* recently demonstrated that physiological concentrations of LL-37 are not active against *P. aeruginosa* in cystic fibrosis bronchoalveolar lavage fluid due to proteolytic degradation of LL-37 by neutrophil elastase and cathepsin D.<sup>43</sup> They also demonstrated that a mixture of heparan sulfate, chondroitin sulfate and hyaluronic acid inhibited the proteolytic degradation of LL-37 by cathepsin D.<sup>43</sup> These interactions also inhibited the antimicrobial activity of LL-37.<sup>43</sup> Interestingly, cathepsin D is induced by *P. aeruginosa* in cystic fibrosis individuals, thus this may be described as another virulence factor of *P. aeruginosa* along with the production of elastase.<sup>44,45</sup> Trypsin, a serine protease found in the digestive system of many vertebrates and a

common biotechnology tool, is commonly used to evaluate the proteolytic stability of CAPs.<sup>46-48</sup>

LL-37 induces degranulation in purified human lung mast cells at physiological concentrations and as a result induces its own degradation. As a result of mast cell degranulation,  $\beta$ -trypstase is released, degrading LL-37 into peptides 8-18 residues in length. These LL-37 fragments lost the capacity to activate mast cells, to neutralize LPS-induced dendritic cell activation and to kill Gram-positive and –negative bacteria.<sup>49</sup>

## 1.2 Lactoferricin Peptide

Lactoferricin is an amphipathic CAP produced by acid-pepsin hydrolysis of lactoferrin, a member of the transferrin family of iron-binding glycoproteins.<sup>50</sup> It is widely distributed in the physiological fluids of mammals and is a major component of polymorphonuclear leukocytes.<sup>51-53</sup> It has multiple functions, including antimicrobial and anti-tumor activities and a role in immune regulation.<sup>54,55</sup> Lactoferrin has several regions with high concentration of positive charge, resulting in a high isoelectric point (pI~9).<sup>56</sup> The most notable region of positive charges is found in the N-terminus of the polypeptide chain and this gives the protein some unique properties. For example, this region provides a binding site for heparin and other GAGs, making it an important region for binding to many different cell types.<sup>57,58</sup>

Bovine lactoferricin has attracted considerable interest because lactoferricin of bovine origin exhibits greater antimicrobial activity than lactoferricins of human, murine or caprine origin.<sup>59</sup> Bovine lactoferricin (lactoferricin B) consists of 25 amino acids consisting of residues 17-41 in bovine lactoferrin. In lactoferrin, this region forms an amphipathic helix with an overall positive charge. As a peptide lactoferricin B forms a distorted  $\beta$ -sheet with a disulfide bridge.<sup>60</sup> Lactoferricin B is active against a wide range of bacteria, fungi, protozoa and cancers.<sup>54,61</sup> Many smaller fragments of bovine lactoferricin have been investigated for their antimicrobial activities. The antimicrobial

center of lactoferricin B consists of six residues (RRWQWR-NH<sub>2</sub>) and possesses similar bactericidal activity to lactoferricin B.<sup>62</sup> In our experiments we worked with a shorter peptide derived from bovine lactoferricin that we termed lactoferricin peptide (LP). LP has a primary sequence of RRWQWRMKKLG and has similar antimicrobial activity to lactoferricin B.<sup>63</sup>

### 1.3 Magainin II

Magainin II was first isolated, along with magainin I, from the skin of the African clawed frog *Xenopus laevis*.<sup>64</sup> Magainin II, along with other amphibian antimicrobial peptides, is stored within the neuroendocrine granular glands in the skin, and is released in response to stress, injury or challenge by foreign organisms.<sup>65</sup> Accordingly, magainin II exhibits a wide range of potent anti-bacterial activity against a variety of Gram-negative and Gram-positive bacteria. Magainin II can also inhibit the growth of fungi and viruses and induce osmotic lysis in protozoa.<sup>64,66</sup> Although many AMPs are nonspecific in their activity, magainin 2 is non-hemolytic towards human erythrocytes.<sup>64</sup> More recently, magainins were shown to selectively lyse tumor cells without killing healthy vertebrate cells.<sup>67-69</sup>

Magainin II has a primary sequence of 23 residues and a net charge of +4.<sup>64</sup> All-D-magainins cause channel formation and cell lysis of the same organisms sensitive to the L-isomer.<sup>70,71</sup> These results, the lack of primary sequence homology within the magainin family as well as a strong correlation between antibiotic activity and peptide amphiphilicity indicate that the structural and physico-chemical properties of magainins, rather than specific receptor-ligand interactions are responsible for their biological activity.<sup>72</sup> The secondary structure of magainin II is not well-defined in a neutral aqueous environment.<sup>73</sup> Magainin II forms a right-handed  $\alpha$ -helix in the presence of organic solvents or after binding to negatively charged lipid membranes via electrostatic interactions.<sup>64,73-78</sup> Helical wheel projections show that such a helix is amphipathic with

the polar and hydrophobic amino acid side chains neatly separated on opposite faces of the helix.<sup>79</sup>

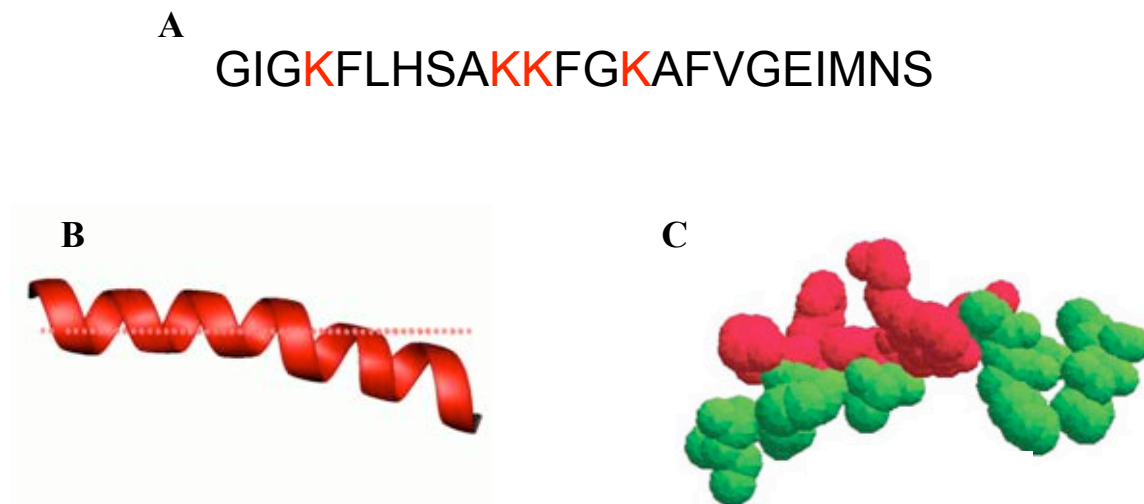


**Figure 2** Sequence (A) and secondary structure of magainin II. Magainin II forms an  $\alpha$ -helix (B) that contains cationic (red) and hydrophobic (green) domains (C).<sup>9</sup>

Magainin II has been widely studied and reported to form pores at cell membranes.<sup>74,80,81</sup> The peptide interacts and kills the cells by penetrating the membrane structure by arranging perpendicular to the lipid interface and adopting a helical conformation.<sup>31,80,81</sup> Research has shown that the interaction is stronger if the lipid layer is anionic and that a critical concentration of peptide in the surface region appears to be required before pore formation and cell death occur.<sup>31,80,82,83</sup> Magainin II can then self-assemble into transmembrane pores that make the cell membrane leaky and can also lead to cell lysis, preferentially in bacterial cells. The size of pores formed by magainins in lipid bilayers is estimated to be approximately 1 nm diameter.<sup>84,85</sup> It has also been suggested that magainin II forms a toroidal pore with a diameter of 1-2 nm, inducing lipid flip-flop and the translocation of peptides into the inner leaflet of the bilayer coupled to membrane permeabilization.<sup>85,86</sup> Magainin II at sub-MIC levels crosses the *E. coli*

cytoplasmic membrane and can be found in the cytoplasm.<sup>87</sup> Additionally, it has been reported that glycosaminoglycans are not involved in the permeabilization of mammalian cells by magainin II.<sup>88</sup>

#### 1.4 Cecropins

Cecropin was one of the first inducible insect antibacterial proteins identified in the study of immunity in the moth *Hyalophora cecropia* and proteins from this family have since been found to be widely distributed.<sup>89-95</sup> The cecropin family consists of small, strongly basic peptides of approximately 4 kD. Sequencing has shown that typically each insect has several related cecropins.<sup>96</sup> Cecropins A, B and D are close homologues which consist of 35-39 residues and have been found in the pupae of the cecropia moth.<sup>89,97,98</sup> Cecropin B differs from cecropin A in 5 of 39 residues.<sup>93</sup> Porcine cecropin homolog is found in pig intestine and shows 64-75% homology with the two insect cecropins.<sup>99</sup>

Cecropin A and B exert strong antibiotic activity against both Gram-positive and -negative bacteria in micromolar concentrations.<sup>100,101</sup> Cecropins have the ability to form specific amphipathic  $\alpha$ -helices, which allow them to target nonpolar lipid cell membranes. Upon membrane targeting, they form ion-permeable channels subsequently causing cell depolarization, irreversible cytolysis and cell death.<sup>79,102</sup> Spectrofluometric studies show that fluorophore-labeled cecropin B binds to lipid membranes in a noncooperative manner, suggesting that they associate with membranes in a monomeric form. The same studies indicate a localization of the N-terminus along the bilayer surface.<sup>103</sup> At lethal dose concentrations the amount of radioactively-labeled cecropins bound to cells has been estimated to be sufficient to cover the bacterial membrane surface with a polypeptide monolayer.<sup>104,105</sup> Interestingly, bacteria resistant to the antibiotic activity of cecropins are loaded with cecropins to a similar extent whereas nonpermissive



erythrocytes are not. Therefore, factors other than binding affinity must also play an important role in determining the susceptibility to these peptides.<sup>105,106</sup>

Natural cecropins show strong antibiotic activity against a variety of Gram-negative and Gram-positive bacteria without lysing mammalian cell lines or yeast.<sup>89,107,108</sup> The cell killing activity of cecropins is not mediated through specific, chiral receptor interactions, but rather their ability to form  $\alpha$ -helical secondary structures in membrane environments as well as with their binding affinity to liposomes.<sup>109</sup> Additionally, cecropins and other related peptides have been shown to release respiratory control, to inhibit protein import, and at higher concentrations also to inhibit respiration. When comparing the concentration-dependent effects of cecropins and its biosynthetic precursors, however, no simple correlation can be established between antibacterial activity and the uncoupling of the respiratory phosphorylation in mitochondria.<sup>110</sup> This mechanism explains the specificity of this peptide for Gram-negative bacteria.<sup>104</sup> Both cecropin A and cecropin B show cytolytic activity against several different human cancer cell lines, including leukaemia and lymphoma cells, but do not lyse normal fibroblasts, lymphocytes or mammalian erythrocytes at peptide concentrations that are lethal to transformed cells.<sup>111-113</sup>

Cecropin A assumes a predominantly random coil conformation in water and adopts a highly ordered structure in 15% (v/v) hexafluoroisopropanol.<sup>101,114</sup> The conformation of cecropin A is characterized by two amphipathic helical regions extending from residues 5 to 21 and 24 to 37 that are connected by a flexible hinge region. The length and continuous disruption of basic residues along one face of the amphipathic N-terminal helix closely resembles the amino acid distribution of magainins. In contrast, the central part of the C-terminal helix (25-33) is much more hydrophobic. The first eleven N-terminal residues have been shown to be particularly important for the high antibiotic activity of cecropins, although the short peptide consisting of just these residues is inactive.<sup>101,105,115</sup>

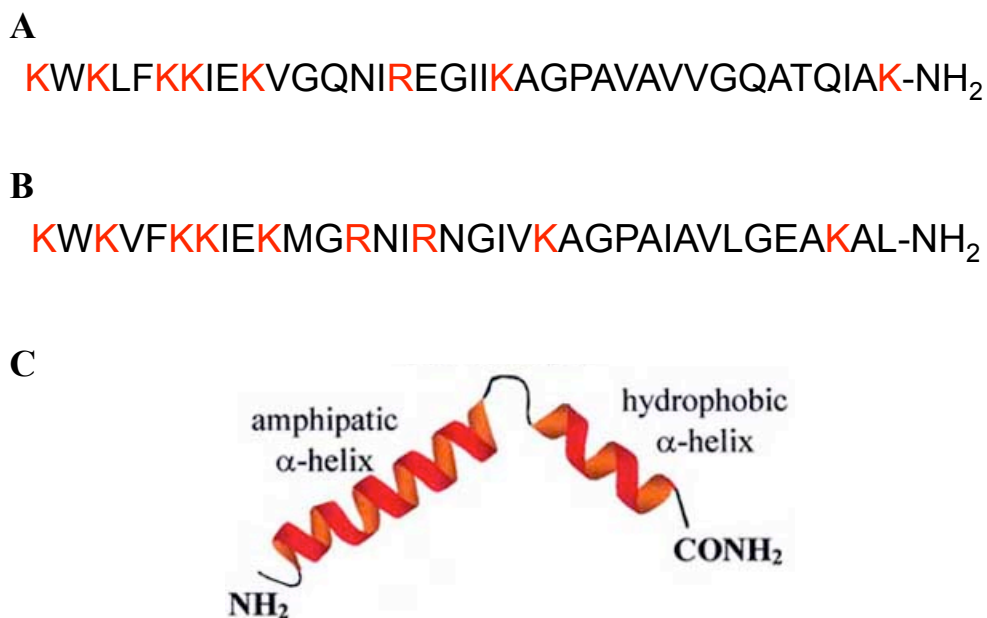


**Figure 3** Sequences of cecropin A (A) and cecropin B (B) and the secondary structure of cecropin A (C).<sup>116</sup> Predicted trypsin cleavage sites are on the C-terminal sides of basic residues.

### 1.5 LL-37

The human cathelicidin propeptide, designated 10-kDa cationic antimicrobial protein (hCAP18), has been identified in peripheral blood neutrophils, lung epithelium and alveolar macrophages.<sup>117-119</sup> hCAP18 is composed of a conserved N-terminal prodomain (cathelin domain) and a C-terminal antimicrobial peptide domain. The C-terminal domain is released from the propeptide by proteolytic processing by proteinase 3 to give the cationic α-helical peptide LL-37 in neutrophils and ALL-38 by prostate-derived protease gastricin in the vagina.<sup>119-121</sup> LL-37 has been isolated from neutrophils and sub-populations of lymphocytes and monocytes.<sup>117,122</sup> LL-37 is also found in seminal plasma, in the lung and in keratinocytes during inflammation.<sup>118,123,124</sup> The actual release of LL-37 is proposed to occur at the cell surface as, on stimulation of the

neutrophil, hCAP-18 locates to the plasma membrane, potentially through an interaction with an hCAP-18 specific receptor.<sup>125</sup>

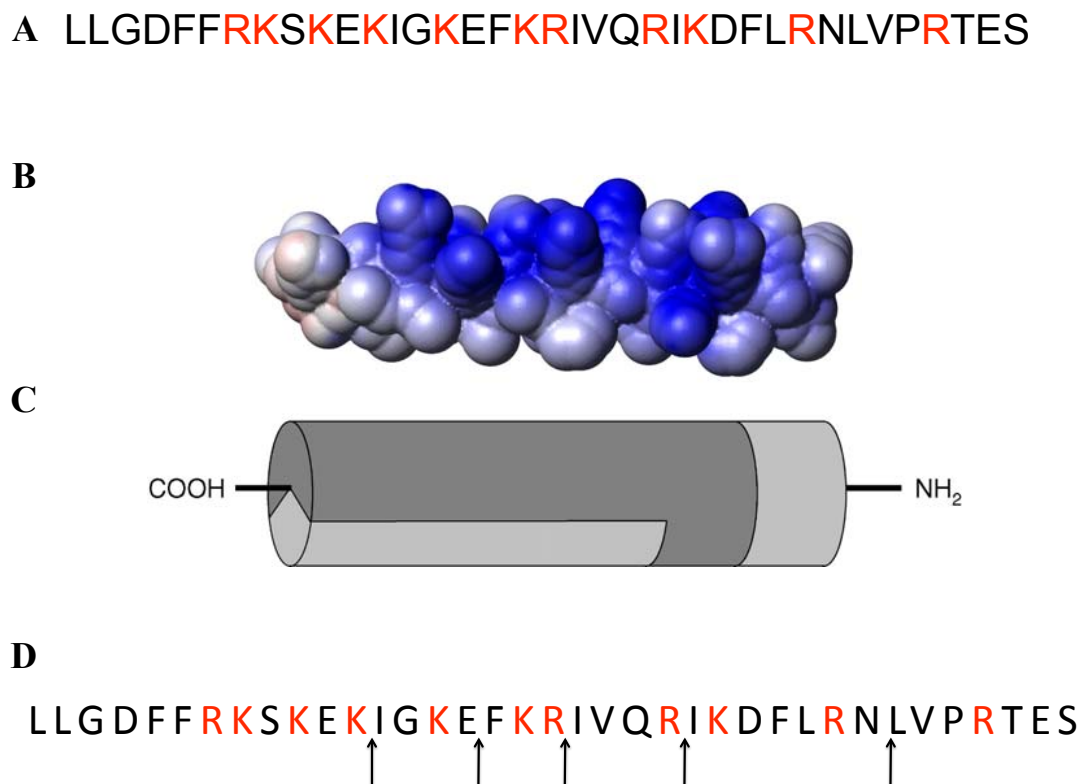


**Figure 4** Primary sequence of LL-37 (A) and 3-dimensional models of LL-37 showing hydrophilic (blue/dark gray) and hydrophobic (white/light gray) residues (B and C).<sup>126</sup> Degradation pattern for LL-37 by trypsin (C-terminal side of basic residues) and *P. aeruginosa* elastase (denoted by arrows) (D).<sup>42</sup>

As suggested by the name, LL-37 is a 37 residue peptide that adopts an  $\alpha$ -helical structure in lipid membranes, micelles, and ions such as hydrocarbonate and sulfate, but is a random coil in pure water.<sup>127</sup> LL-37 exhibits antimicrobial activity against a wide range of microbes including viruses, fungus, and both Gram-positive and Gram-negative bacteria, such as *S. aureus* and *P. aeruginosa*.<sup>128-130</sup> LL-37 binds electrostatically to bacterial membranes, followed by insertion into and disruption of the membrane.<sup>131</sup>

Furthermore, LL-37 acts as a multifunctional immunomodulator, and has been shown to be chemotactic to human neutrophils, monocytes, T cells and mast cells and stimulate phagocytosis, reactive oxygen species production, and the synthesis of leucotriene B4 by neutrophils, degranulation of mast cells and induce chemokine response in monocytes, airway epithelia and keratinocytes.<sup>15,132-139</sup> The mature LL-37 has been shown to be further degraded to shorter peptide fragments, including KR-20, KS-30 and RK-31, by kallikrein proteases in human sweat. Studies suggest that proteolytically cleaved LL-37 fragments have altered antimicrobial activity and reduced immunomodulatory host response compared with LL-37.<sup>140</sup> LL-37 also binds and neutralizes lipopolysaccharide (LPS), thus protecting against endotoxic shock.<sup>131,141</sup>

### 1.6 Glycosaminoglycans

Glycosaminoglycans (GAGs) are linear, sulfated, negatively charged polysaccharides composed of disaccharide repeating units made up of an amino sugar (N-acetylglucosamine or N-acetylgalactosamine) and an uronic acid (glucuronic acid or iduronic acid). As a consequence GAGs differ according to the type of hexosamine, hexose or hexuronic acid unit that they contain, as well as the geometry of the glycosidic linkage between these units. GAGs also differ in their sulfation pattern, as can be seen in **Table 1**. At physiological pH, all carboxylic acid and sulphate groups are deprotonated, giving GAGs very high negative charge densities.<sup>142</sup> In fact, heparin has the highest negative charge density of any known biomolecule.<sup>143</sup>

GAGs are the major component of proteoglycans, which consist of a core protein with one or more GAGs attached. Proteoglycans are found in the extracellular matrix, inserted in the plasma membrane or stored in secretory granules. Matrix proteoglycans include small interstitial proteoglycans, such as decorin and biglycan, and members of the aggrecan family of proteoglycans (aggrecan and versican). Some proteoglycans contain

GAG	Major Repeating Disaccharide Unit	Average MW (Da)	Average Sulfate Groups per Disaccharide
Heparin		14,000 – 15,000 <sup>144</sup>	2.7
Dermatan Sulfate		25,000 <sup>145</sup>	2
Chondroitin 4-Sulfate		20,000 <sup>146</sup>	1
Chondroitin 6-Sulfate		65,000 <sup>146</sup>	1
Heparan Sulfate		10,000 <sup>147</sup>	1
Keratan Sulfate		20,000 <sup>148</sup>	1
Hyaluronic Acid		1,000,000 <sup>149</sup>	0

**Table 1** The most common repeating disaccharides of endogenous mammalian GAGs.

only one GAG chain (e.g., decorin), while others, such as aggrecan, contain more than 100 chains.<sup>150</sup>

All endogenous GAGs, with the exception of hyaluronic acid, are found as components of proteoglycans. GAGs are covalently linked to core proteins via a specific trisaccharide composed of two galactose and one xylose residues. The linker connects GAGs via an *O*-glycosidic bond to a serine residue on the core protein. Matrix proteoglycans typically contain dermatan sulfate and chondroitins 4- and 6-sulfate. Heparan sulfate and chondroitin sulfate are found in membrane proteoglycans such as glypicans and syndecans.<sup>150</sup> A major component of mast cell granules is the proteoglycan serglycan which contains heparin and chondroitin sulfate E.<sup>151-153</sup> Hyaluronic acid is a major component of the extracellular matrix and can serve as a scaffold for proteoglycan aggregation, such as seen with aggrecan.<sup>154</sup>

#### 1.6.1 Heparan sulfate and heparin

Heparan sulfate (HS) and heparin are linear polysaccharides consisting of uronic acid-(1→4)-D-glucosamine repeating disaccharide subunits. Variable patterns of substitution of the disaccharide subunits with N-sulfate, O-sulfate and N-acetyl groups give rise to a large number of complex sequences. Heparin and HS are structurally the most complex members of the GAG family of polysaccharides.<sup>155</sup> Heparin is sometimes considered to be synonymous with HS, and, while they are similar, this is an oversimplification.<sup>156</sup>

Heparin consists of repeating units of 1→4-linked uronic acid and glucosamine residues. The uronic acid residues typically consist of 90% L-iduronic acid and 10% D-glucuronic acid, both of which may contain a 2-*O*-sulfate group. The amino group of the glucosamine residue may be substituted with an acetyl or sulfate group, or remain unsubstituted.<sup>142</sup> The most common disaccharide in heparin is 2-*O*-sulfated iduronic acid 1→4 linked to N-sulfated, 6-*O*-sulfated galactosamine. This disaccharide accounts for up

to 90% of heparins from bovine lung and up to 70% of those from porcine intestinal mucosa.<sup>155</sup>

HS contains predominantly D-glucuronic acid, but can also contain substantial amounts of L-iduronic acid. HS contains a higher level of N-acetylated glucosamine and has a lower degree of sulfation as compared to heparin. Heparin has 2.7 sulfate groups average per disaccharide, in stark contrast to HS which possesses on average 1 sulfate group per disaccharide.<sup>156</sup> The structure of HS is incredibly polydisperse due to variable modifications along the polysaccharide. Sulfation and epimerization tend to occur in clusters along the chain, with regions devoid of sulfate separating the modified tracts. In general, these modifications fail to go to completion, resulting in tremendous chemical heterogeneity within the modified regions.<sup>150</sup> HS has a domain structure consisting of segregated blocks of repeating glucuronic acid 1→4 N-acetylglucosamine disaccharides (NA domains) and blocks of highly sulfated, heparin-like iduronic acid 1→4 N-sulfated galactosamine disaccharides (NS domains). The NA and NS domains are separated by NA/NS transition segments that consist of both N-acetylglucosamine and N-sulfated glucosamine-containing disaccharides.<sup>157</sup> The diversity of HS structures gives rise to a wide range of biological functions and specific binding sequences for ligands.<sup>150</sup>

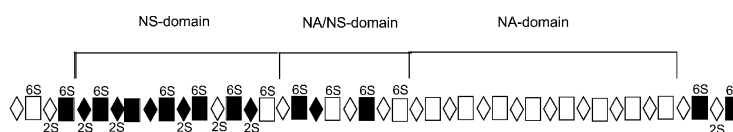


**Figure 5** Representation of the domains found in HS where uronic acids are represented by diamonds, glucosamine is represented by squares and sulfate groups are indicated above or below the residue symbols.<sup>150</sup>

In solution heparin exists primarily as an extended helical structure.<sup>158</sup> Heparin maintains a degree of conformational flexibility due to multiple conformations of

iduronic acid.<sup>143,158,159</sup> This conformational flexibility allows for diverse spatial displays of negative charge thought to facilitate specific interactions with proteins through induced fit binding mechanisms.<sup>160</sup> A significant driving force behind heparin-protein interactions is the entropically favorable displacement of the counter-ion shell during the binding interaction with basic residues on the binding partner.<sup>161</sup>

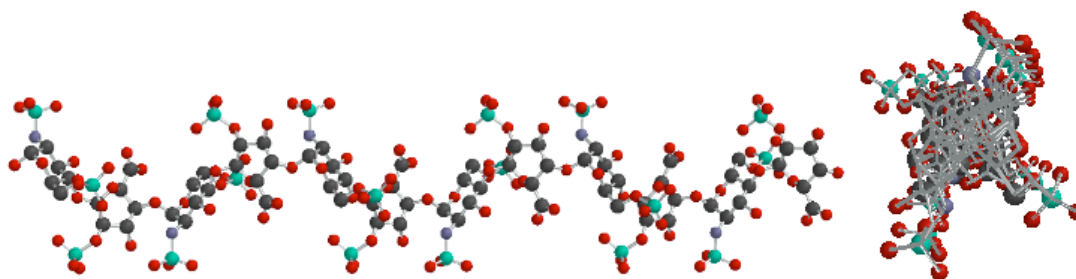


**Figure 6** 3-dimensional model of the solution conformation of a heparin dodecasaccharide (PDB entry 1HPN).

The anticoagulant and antithrombotic properties of heparin involve binding to antithrombin, heparin cofactor II, and tissue factor pathway inhibitor. The “minimal” binding sequence is a specific pentasaccharide binding site, distributed randomly in the unfractionated heparin, which is prevalently responsible for heparin antithrombotic activity.<sup>162</sup> Heparin inhibits thrombogenesis through the inactivation of factors IIa and Xa. The use of unfractionated heparin presents limitations mostly related to its nonspecific binding to proteins and cells. Such binding activity results in low availability and variable anticoagulant effectiveness.<sup>163</sup>

### 1.6.2 Low molecular weight heparins

Low-molecular weight heparins (LMWHs), as compared with unfractionated heparin, present superior bioavailability, much longer plasma half-life, and lower



incidence of side effects. For these reasons, LMWHs have become the drugs of choice for the treatment of deep venous thrombosis, pulmonary embolism, arterial thrombosis, and unstable angina over the past two decades.<sup>164</sup>

The internal structure of LMWHs should ideally match that of the parent heparin in terms of monosaccharide composition, substitution pattern, and oligosaccharide sequence. However, the depolymerization processes involved in the manufacturing of LMWHs usually involves some structural modification. Such differences are due mostly to modifications of the monosaccharide units at the site of cleavage and are characteristic for each depolymerization procedure. The monosaccharidic sequence of LMWHs can also be different, according to the cleavage point along the heparin polysaccharide chain. For example, the cleavage of heparin chains at the more heavily sulfated sites, rather than undersulfated sites, influences preservation and position of the specific pentasaccharide motif of the active site for antithrombin III along the oligosaccharidic chains.<sup>164</sup>

<b>LMWH Supplier</b>	<b>Average MW (Da)</b>	<b>Method of depolymerization</b>
Ardeparin (Centaxarin) Celsus	5500	Oxidative depolymerization of heparin using peroxide
Enoxaparin Sequoia Research	3200	Cleavage by $\beta$ -elimination of benzyl ester by alkaline treatment
3 kD heparin (Dalteparin) Celsus	3000	Nitrous acid deamination of heparin
Ultra LMWH Sigma	3000	Free-radical induced cleavage of heparin

**Table 2** Molecular weights and preparation methods for LMWHs.

LMWHs can be prepared by a variety of techniques. Enoxaparin is prepared by  $\beta$ -cleavage of the benzyl ester by alkaline treatment and has an average molecular weight of 3200 Da. This preparation results in a complex structure with eight possible reducing residues and two possible non-reducing residues.<sup>164</sup> Centaxarin, also called ardeparin, is prepared by periodate-oxidation of heparin and has an average MW of 5500. Two different 3000 Da heparin preparations were used in our experiments. The first preparation, termed 3 kD heparin in our experiments, is prepared by the nitrous acid deamination of heparin and is available from Celsus. Ultra LMWH, the second 3 kD LMWH, is available from Sigma-Aldrich and is prepared by free-radical induced cleavage of heparin. Interestingly, this type of reaction is also likely to occur *in vivo*. Mast cells store heparin in their granules and release it upon phagocytosis. Simultaneously, free radicals produced by the phagocytic cell could attack and depolymerize heparin.<sup>163</sup> Distinct pharmacological and biochemical profiles of LMWHs are claimed and can be associated with structural modifications resulting from differences in preparative techniques.<sup>162</sup> Despite these differences in molecular weight and structures, LMWHs are considered interchangeable by many health care practitioners.

### 1.6.3 Other GAGs

Chondroitin sulfate is made up of major disaccharide units of glucuronic acid and N-acetylgalactosamine connected by  $\beta$ -1,3 linkages. Sulfate groups can be found at the C4 or C6 position of N-acetylgalactosamine residues, thus giving populations of chondroitin 4-sulfate (C4S) and chondroitin-6 sulfate (C6S). Dermatan sulfate (DS), also called chondroitin sulfate B, has a major disaccharide repeating unit in which iduronic acid and N-acetylgalactosamine are linked together by  $\alpha$ -1,3 linkages. In DS sulfate groups are found at the C4 and C6 position of N-acetylgalactosamine. DS is less sulfated on average than heparin since its N-acetylgalactosamine is exclusively N-acetylated and its iduronic acids are primarily nonsulfated.<sup>165</sup> C4S, C6S and DS have the potential to

display an enormous structural diversity, comparable to that of HS, by embedding multiple overlapping sequences constructed with distinct disaccharide units modified by different patterns of sulfation.<sup>166</sup> Chondroitin sulfate and DS are often found as copolymeric structures.

The large structural diversity of chondroitin sulfate and DS is the basis for their wide variety of functions. Growing evidence suggests that CS and DS chains play roles in the development of the central nervous system, wound repair, infection, growth factor signaling, morphogenesis and cell division, in addition to their conventional structural roles.<sup>166</sup> DS is found in skin, blood vessels and heart valves of humans while chondroitin sulfate is found primarily in cartilage, tendons and ligaments, as well as in the aorta.<sup>142</sup>

Hyaluronic acid (HA) is an extremely simple polysaccharide composed of repeating disaccharide units in which N-acetylglucosamine and glucuronic acid are linked together by alternating  $\beta$ -1,3 and  $\beta$ -1,4 linkages.<sup>167</sup> HA is unique among the GAGs because it is not sulfated or modified in any other way throughout its length.<sup>154</sup> HA is distributed widely in nature, from the capsules of *Streptococcus* to tissues of invertebrate and vertebrate organisms. In mammals, HA is abundant in skin, skeletal tissues, the vitreous of the eye, umbilical cord, and synovial fluid. HA functions as an extracellular molecule transmitting signals and regulates a variety of cell behaviors, such as cell adhesion, motility, growth and differentiation.<sup>168</sup> HA has also recently been shown to play a role in wound healing.<sup>169</sup> Excess HA accumulation has been implicated in the promotion of cardiovascular diseases and malignant cancers produce excessive amounts of HA, leading to increased serum levels.<sup>170-174</sup> HA also acts as a lubricant of synovial joints and joint movement, and its function has been described as space filler, wetting agent, flow barrier within the synovium and protector of cartilage surfaces.<sup>175</sup> In solution, HA has an extended structure. Because of its length, it tends to entangle into a mesh-like structure. At a concentration of 10 mg/ml, its viscosity is about 5000 times that of water, which confers rigidity to tissues when HA is present at high concentrations.<sup>150</sup>

Keratan sulfate is a sulfated polyglucosamine chain identical to the type found on conventional glycoproteins and mucins and found primarily in the cornea of mammals.<sup>150</sup> Keratan sulfate and chondroitin sulfate are components of the proteoglycan aggrecan found in cartilage.<sup>142</sup> The level of keratan sulfate found in the cornea is 10 fold higher than it is in cartilage.<sup>176</sup> As keratan sulfate is found primarily in the eye and cartilage, we chose to omit it from our studies.

#### 1.6.4 Preparation of GAGs

Heparin and HS are prepared from either beef lung or porcine intestinal mucosa.<sup>177</sup> DS is most commonly prepared from porcine mucosa and skin.<sup>165</sup> C4S is isolated from bovine trachea and C6S is isolated from shark cartilage.<sup>178</sup> HA has been traditionally extracted from rooster combs and bovine vitreous humor, but is now commonly prepared by bacterial fermentation.<sup>179</sup>

Carboxyl-reduced heparin is prepared by the reaction of heparin with a water soluble carbodiimide (EDC), which yields a polymer in which all the uronic acid carboxyl groups are activated so that they can be reduced to hydroxyl groups with sodium borohydride.<sup>180</sup> This results in a heparin molecule where a portion of the carboxyl groups of uronic acid are reduced to alcohols and where the most common disaccharide units are either glucose→glucosamine or idose→glucosamine.<sup>181</sup> Methods for the selective removal of sulfate groups from heparin have been developed to systematically reduce anionic charge along the polysaccharide chain and to identify sequences that bind proteins. Methods for the selective 2-*O* and 6-*O*-desulfations of heparin have been reported.<sup>182-184</sup> In 1997, Jaseja *et al.* reported the selective 2-*O*-desulfonation of heparin following lyophilization of an alkaline solution of heparin. A selective 6-*O*-desulfonation procedure for sulfated polysaccharides was reported in 1993 by Matsuo *et al.* The method exposes the pyridinium salt of heparin suspended in pyridine to *N,O*-bis(trimethylsilyl)trifluoroacetamide (BTSA).<sup>185</sup> This reagent selectively removes

primary sulfoxyl groups to yield a silyloxyl group, which is easily desilylated by addition of water to obtain the hydroxyl group. The procedure was later optimized for selective 6-*O*-desulfation of heparin by Takano *et al.*<sup>186</sup> In these methods the *O*-sulfate groups on C2 of uronic acid or C6 of glucosamine residues are removed. Phenoxyaniline was coupled to heparin using a modification of the method reported by Danishefsky *et al.*<sup>187</sup> Carboxyl-reduced heparin, 6-*O*-desulfated heparin, 2-*O*-desulfated heparin and phenoxyaniline heparin were prepared by other members of the Kerns lab.

#### 1.6.5 Other Polyanionic Polysaccharides

Cyclodextrins are a family of cyclic oligosaccharides, and several members of this family are used industrially in pharmaceutical and allied applications. Cyclodextrins are manufactured from starch, which consists of D-glucopyranoside building blocks that have both  $\alpha$ -1,4- and  $\alpha$ -1,6-glycosidic linkages. The degradation of starch by glucosyltransferase generates, by chain splitting and intramolecular rearrangement, primary products that are cyclic oligomers of  $\alpha$ -1,4-D -glucopyranoside, or cyclodextrins. Cyclodextrins are named based on the number of glucose residues in their structure, such that the glucose hexamer is referred to as  $\alpha$ -cyclodextrin and the heptamer as  $\beta$ -cyclodextrin. The three-dimensional structure of cyclodextrins endows them with properties that are useful for pharmaceutical applications. Because of the large number of hydroxyl groups on cyclodextrins, they are water-soluble. Cyclodextrins form a cup-like structure that has a hydrophilic cavity exterior and a hydrophobic cavity interior. These properties are responsible for their aqueous solubility and ability to encapsulate hydrophobic moieties within their cavities.<sup>188</sup> The incorporation of 'guest' molecules in cyclodextrin inclusion complexes in aqueous media has been the basis for most pharmaceutical applications.<sup>189</sup> Cyclodextrins are used in the pharmaceutical industry for a variety of reasons, including enhanced solubility, bioavailability and stability.<sup>190,191</sup>

The hydroxyl groups on cyclodextrins can be modified with a variety of substitutions, including sulfate groups.

Dextrin sulfate is a sulfonated polysaccharide of  $\alpha$ -1,4-linked glucose residues with  $\alpha$ -1,6 branch points. Dextrin 2-sulfate, marketed as Emmelle™ by M-L Laboratories PLC, inhibits the growth HIV-1 strains in a variety of human cell lines, lymphocytes and macrophages.<sup>192,193</sup> Dextrin 2-sulfate interacts with target cells to inhibit viral entry, but does not neutralize virions directly.<sup>194</sup> Dextrin 2-sulfate has been the subject of multiple clinical trials testing its efficacy as a topical anti-HIV microbicide, but its potential is limited due to a variable toxicity profile.<sup>195,196</sup>

Sulodexide is a GAG obtained by a patent process from porcine mucosa.<sup>197</sup> Sulodexide is comprised of four naturally occurring GAG polysaccharides:  $\approx$ 80% electrophoretically “fast-moving” heparin,  $\approx$ 20% dermatan sulfate, and lesser populations of “slow-moving” heparin and chondroitin sulfate. Sulodexide has been marketed by Alfa Wassermann S.p.A. since 1982 for the indication of “vascular pathologies with thrombotic risk” in Italy and many other countries in Eastern Europe, Asia, and Central and South America.<sup>198</sup> The simultaneous presence of a heparin fraction and dermatan sulfate provides the product with particular synergistic characteristics which increase the antithrombotic potential in comparison to heparin with less bleeding.<sup>199</sup>

Dextran is high molecular weight polysaccharide produced from sucrose by bacteria. Its backbone consists primarily of  $\alpha$ -(1 $\rightarrow$ 6) linked D-glucose units. Dextran can differ in chain length and degree of branching and branching occurs via  $\alpha$ -(1 $\rightarrow$ 3) and  $\alpha$ -(1 $\rightarrow$ 4) branch points. Dextran fractions of varying molecular weights can be prepared by partial hydrolysis.<sup>200</sup> Dextran sulfate is a polyanionic derivative of dextran and is prepared by sulfating a selected fraction of dextran. Dextran sulfate was developed as an anticoagulant to delay clotting of blood in people who had heart disease or strokes.<sup>201</sup> More recently dextran sulfate has shown anti-HIV activity, and now plays an important role in low-density lipoprotein-apheresis.<sup>202,203</sup>

### 1.6.6 Heparin binding sequences

The structural requirements of heparin binding and the presence of heparin-binding motifs in various proteins are well documented. After examining a series of heparin-binding sequences Cardin and Weintraub proposed that those were arranged in pattern XBBBXXBX or XBBXBX (where X represents hydrophobic or uncharged residues and B represents a basic residue). Molecular modeling of these sequences predicts the arrangement of amino acids in  $\alpha$ -helices or  $\beta$ -strands.<sup>204</sup> Additional analyses of heparin-binding peptide sites have revealed that these consensus sequences may not constitute absolute requirement. Sobel *et al.* proposed a third consensus sequence, XBBBXXBBBXXBBX<sup>205</sup> and Lindhardt's group found an additional heparin-binding sequence, TXXBXXTBXXXTBB (where T defines a turn), in heparin-binding sites of growth factors.<sup>143,206</sup> Based on studies of heparin-binding sites, Margalit *et al.* reported that a distance of approximately 20 Å between basic residues constituted a prerequisite for heparin binding irrespective of peptide conformation.<sup>207</sup> Thus, spacing of basic amino acids in heparin-binding peptides facilitates formation of ion pairs with spatially defined sulpho- or carboxyl-groups in heparin and heparan sulfate. Furthermore, *N*-acetyl and hydroxyl groups in heparin and, to a greater extent, in heparan sulfate, require matching residues, such as alanine, leucine or tyrosine, and glutamine or asparagine, enabling hydrophobic interactions and hydrogen bonding, respectively.<sup>143</sup>

### 1.6.7 GAGs and proteases

Approximately 50% of the weight of a mature mast cell consists of various neutral proteases stored in the cell's secretory granules electrostatically bound to serglycin proteoglycans that contain heparin and/or chondroitin sulfate chains.<sup>208</sup> Cells with storage granules concentrate proteoglycans along with other secretory products. These proteoglycans typically contain highly sulfated forms of CS, although the secretory granules of connective tissue mast cells contain mostly heparin. Secretory granule

proteoglycans are thought to help sequester and regulate the availability of positively charged components, such as proteases and bioactive amines.<sup>150</sup>

Heparin is known to inhibit proteinase activity of leukocyte elastase, cathepsin G and trypsin.<sup>209-211</sup> However, this inhibitory activity is not linearly dependent on dose and at high concentrations reversal of the inhibitory effects has been observed.<sup>212,213</sup>

Additionally, inhibition of trypsin by heparin was dependent upon the molecular weight of the GAG where LMWHs are inhibitors.<sup>211</sup> Heparin showed differential inhibitory activity towards *P. aeruginosa* elastase as well. When a model peptide substrate was used no inhibition of *P. aeruginosa* elastase was seen. However, inhibition of *P. aeruginosa* elastase was observed when elastin was used as the substrate.<sup>210</sup>

## 1.7 Cationic antimicrobial peptide interactions with glycosaminoglycans

### 1.7.1 Early efforts

The earliest interaction between heparin and a CAP was reported by Thorne *et al.* where they found that the anti-herpes simplex virus activity of a lysosomal cationic protein isolated from ruminant neutrophils was inhibited by heparin.<sup>214</sup> This cationic protein content was later identified as bactenin-5 and -7 purified from the large granules of bovine neutrophils.<sup>215</sup> Interactions between bactenecin-7 and glycosaminoglycans were later investigated by Park *et al.* They found that the *P. aeruginosa*-induced shedding of HS syndecan domains and heparin negatively modulated the antimicrobial activity of bactenecin-7, PR-38 and cecropin B.<sup>216</sup>

Little *et al.* investigated the heparin-binding properties of a recombinant 23-kDa amino-terminal fragment of BPI, a Gram-negative active protein found in the azurophilic granules of neutrophils.<sup>217</sup> They found that the recombinant BPI peptide has three separate domains. All three domains bound heparin and LPS, but only one domain was responsible for the antimicrobial activity of the peptide. The authors made note of the



correlation between heparin-binding and neutralization of LPS, but did not speculate the effect of this on the antimicrobial activity of the peptide.<sup>218</sup>

While investigating the ability of short cecropin-melittin hybrid peptides to permeabilize the inner mitochondrial membrane Díaz-Achirica *et al.* found the heparin had potentiating effects at low concentrations and inhibitory effects at higher concentrations. The authors postulate that heparin interactions with the peptides lead to further structural changes, thus altering the peptide interaction with the mitochondrial membrane.<sup>103</sup> The binding of melittin to heparan sulfate induces a conformational change from unstructured to a predominantly  $\alpha$ -helical structure. Circular dichroism spectra for melittin binding to heparin and DS were qualitatively and quantitatively very similar to those obtained for melittin binding to HS.<sup>219</sup>

James *et al.* found that antimicrobial peptides could be purified by exploiting their affinity for heparin. Antimicrobial peptides from the skin of *Xenopus laevis*, such as magainin 1 and magainin 2, were purified using heparin-affinity HPLC.<sup>220</sup> This technique has been utilized to purify antimicrobial peptides from hydra<sup>221</sup>, worms<sup>222,223</sup>, plants<sup>224,225</sup>, fish<sup>226</sup>, frogs<sup>227</sup>, rabbit<sup>228,229</sup>, lactoferrin from cattle<sup>230</sup> and humans.<sup>231-235</sup>

### 1.7.2 GAGs and lactoferrin-derived peptides

Biotin-labeled heparin was examined for binding to immobilized lactoferrin. Binding was found to be dependant upon pH and ionic conditions and concentrations of sodium, calcium, copper, zinc and iron affected heparin binding to lactoferrin. Zou *et al.* also investigated the binding of other GAGs to lactoferrin. The relative degree of heparin-binding inhibition by GAGs for both lactoferrin and lactoferricin was heparin > HS > C6S > HS. This binding pattern corresponds to their degree of sulfation, suggesting that the polyanionic nature of GAGs is more important than the saccharide sequence.<sup>236</sup>

The *in vitro* uptake of lactoferrin by cultured cells including hepatocytes and macrophages, and its clearance *in vivo*, is inhibited by sulfated polysaccharides such as

fucoidin and dextran sulfate.<sup>237-239</sup> Mann *et al.* established that human lactoferrin binds to GAGs through a region of the protein localized to the first 33 residues of the mature protein. This region contains two clusters of basic residues that resemble the putative heparin-binding sites (BBXB) and these two regions act synergistically to facilitate binding between lactoferrin and GAGs. The authors termed this GAG-binding structure a cationic cradle. Lactoferrin and lactoferricin B interfere with the cellular entry of herpes simplex virus-1 and -2 via this binding structure. Lactoferrin binds to heparan sulfate and thereby blocks the initial binding of the virus. The antiviral activity of lactoferricin B is dependant on heparan sulfate, but has an additional antiviral activity after the initial binding of the virus to the host cell.<sup>240</sup>

Fadnes *et al.* explored the effect of glycosaminoglycans on the anticancer activity of lactoferricin B and an idealized  $\alpha$ -helical amphipathic peptide, KW5. Using cell lines that express different amounts of GAGs at the cell surface, the colon carcinoma cell line HT-29 and FEMX cells, which express a larger amount of GAGs compared to HT-29 cells. Both peptides displayed higher cytotoxic activity against the FEMX cells. This agrees with previous studies showing that an increased negative charge on the cell surface of target cells enhances the cytotoxic activity of lytic peptides.<sup>241,242</sup> In addition, the sulfation of the GAGs was reduced by adding sodium chlorate to the culture medium prior to exposure to the peptides. Chlorate reduces the overall sulfation of GAGs by competing with sulfate ions for binding to ATP-sulphyrolase.<sup>243</sup> Fadnes *et al.* found that the peptides displayed a significantly greater cytotoxic activity against chlorate-treated cells, indicating that the negatively charged GAGs at the cell surface reduced the cytotoxic activity of the peptides. The peptides also exhibited significantly higher cytotoxic activity against GAG-deficient pgsA-745 cells compared to wild type CHO cells expressing normal levels of GAGs, clearly showing that GAGs have an inhibitory effect of the cytotoxic activity of these peptides. This is in contrast to reports showing that the anionic cell surface molecules, sialic acid and phosphatidylserine, have been

shown to enhance the anticancer activity of CAPs.<sup>241,242</sup> FEMX cells express cell surface proteoglycans mostly substituted with chondroitin sulfate, whereas the proteoglycans at the surface of the HT-29 cells were mostly substituted with HS.<sup>244</sup> Thus, the lower cytotoxic activity of the peptides against the HT-29 cells compared to the FEMX cells suggests that the inhibitory effect of GAGs is attributable to HS, not chondroitin sulfate. The addition of soluble heparin and chondroitin sulfate to cell cultures is widely used to study the interaction between various molecules and cell surface heparan sulfate and chondroitin sulfate.<sup>245,246</sup> Exogenously added heparin had a stronger inhibitory effect on the cytotoxic activity of the peptides, compared to chondroitin sulfate. These results indicate that HS can sequester the CAPs away from the phospholipid bilayer and thereby hinder their ability to induce cytolysis.<sup>244</sup>

### 1.7.3 GAGs and cathelicidin CAPs

The antimicrobial activity of LL-37 is inhibited by apolipoprotein A-1, other factors in human plasma and serum and is influenced by pH and ion composition.<sup>127,247</sup> The Schmidtchen group previously demonstrated that LL-37 binds to DS and heparin, and that these interactions block the bacteriocidal effect of the peptide.<sup>42,248</sup> It is also important to note that GAGs occur in wound fluid in significant concentrations.<sup>249</sup> Barańska-Rybak *et al.* found that plasma fractions and wound fluids affect the antibacterial action of LL-37 to differing degrees, where inhibition was most pronounced in GAG-rich wound fluids and heparin-treated plasma.<sup>250</sup> The authors postulate that high GAG levels in wound fluids may affect the antimicrobial effects of LL-37 during wound healing *in vivo* and may predispose to bacterial colonization and infection.

Endocan-1, an endothelial proteoglycan, has been shown to possess properties as a marker for sepsis.<sup>251</sup> In addition, urine levels of GAGs in patients with meningococcal sepsis have been related to the severity of the disease.<sup>252</sup> Nelson *et al.* reported that circulating levels of GAGs and syndecan-1 are increased in septic shock patients,

indicating a deranged GAG turnover. The increased GAG levels also correlated to increased mortality. Nelson *et al.* found that select GAGs, at concentrations present in the sepsis patients with a poor prognosis, inhibit the antibacterial activity of plasma, as well as LL-37 and BPI *in vitro*. This suggests that an increased plasma GAG level per se could impair the innate immune system by binding locally released AMPs as well as activated complement fragments as previously demonstrated by Nordahl *et al.*<sup>253</sup> The authors suggest that the inhibitory effects exerted by the negatively charged GAGs, at least partly, are caused by electrostatic interactions with the positively charged endogenous AMPs such as LL-37 and BPI.<sup>254</sup>

Bergsson *et al.* demonstrated the high degree of electrostatic binding between LL-37 and GAGs by showing that hypertonic saline can release LL-37 from glycosaminoglycans.<sup>43</sup> Increased NaCl concentration is known to enhance the antimicrobial activity of LL-37<sup>127,129</sup> but reduce the effect of defensins.<sup>255</sup> Indeed, Bergsson *et al.* showed that there are synergistic effects between NaCl concentration and LL-37 antimicrobial activity against *P. aeruginosa*.<sup>43</sup>

Recent studies have shown that small fragment HA is generated by inflammation or injury, inducing cytokine release from macrophages.<sup>169,256</sup> These findings have led to the hypothesis that the release of HA fragments after physical or chemical trauma serves as an endogenous signal of inflammation in both the lung and the skin.<sup>257,258</sup> Morioka *et al.* demonstrated that cathelicidins inhibit HA function and produce anti-inflammatory activity *in vitro* and *in vivo*. The cathelicidins mCRAMP, LL-37 or two alternatively processed hCAP-18 peptides inhibited HA-induced cytokine release in macrophages and HA-mediated cell binding, and cathelicidin deficiency exacerbated the development of chronic allergic dermatitis.<sup>259</sup> Preincubation of LL-37 with excess HA did not affect LL-37-induced IL-8 release in keratinocytes, thus suggesting that the inhibitory activity of cathelicidins is not due to direct binding of HA. The authors suggest that the cathelicidin

peptides may block the formation of the TLR4-CD44 complex needed for HA-induced cytokine release.<sup>258,259</sup>

PR-39, the cathelicidin found in porcine leukocytes, is chemoattractive for neutrophils in a calcium-dependent and pertussis toxin-inhibitable reaction and contributes to wound healing by stimulating the expression of syndecans, cell-surface HS proteoglycans.<sup>13</sup> Removal of HS proteoglycans from the surface of neutrophils eliminates their migratory response to PR-39.<sup>260</sup> The lack of surface HS does not eliminate neutrophil migratory response to N-formyl-methionyl-leucyl-phenylalanine (fMLP), suggesting that cell surface receptors are involved in PR-39 functions.<sup>260</sup> PR-39 has been identified in human-skin wound fluid and has been shown to increase levels of cell surface HS proteoglycans syndecan-1 and -4 in NIH 3T3 fibroblasts.<sup>16</sup> Interestingly, the human wound fluid was passed through a heparin-sepharose column prior to these experiments, thus PR-39 was not bound by heparin in these experiments.<sup>16</sup> PR-39 was also found to increase the expression of syndecan-1 in hepatocellular carcinoma cells, resulting in a suppression of motile activity, altered actin structure and a suppression of the carcinoma cells' invasive activity.<sup>261</sup> The modification of HS proteoglycans with sodium chlorate or removal of HS or chondroitin sulfates from cellular surfaces using heparinase or chondroitinase inhibited PR-39 induced migration of neutrophils.<sup>260</sup> This indicates HS proteoglycans, likely syndecans, in cathelicidin peptide-mediated regulation of the antimicrobial host defense and these observations tightly link HS proteoglycans and PR-39 in cathelicidin-induced immunomodulatory functions.<sup>262</sup>

Leukocyte and vascular HS proteoglycans may change the chemical structure of the HS chains they express in response to cathelicidins and thereby alter the inflammatory response with changes in chemokine and growth factor binding known to be important for leukocyte function, angiogenesis and tissue remodeling, but little is known about this possibility. LL-37 induces keratinocyte migration via metalloproteinase-induced release of heparin-binding EGF from the cell surface that

mediates transactivation of EGFR, which stimulates this migration.<sup>263</sup> Purified syndecan-1 ectodomains, through their HS chains, bind tightly to peptides of the cathelicidin family, such as PR-39, and inhibit their antibacterial activities.<sup>248</sup> Similar observations have been reported on where shed DS-domains inactivate defensins.<sup>264</sup> Soluble heparin can inhibit the activity of several cytokines involved in phagocyte recruitment, suggesting that HS chains of shed ectodomains may act similarly.<sup>265</sup>

LL-37 is present in large quantities, but essentially inactive against microbes in the cystic fibrosis lung.<sup>266</sup> It has been demonstrated that the antimicrobial activity of LL-37 is inhibited *in vitro* by lipopolysaccharide<sup>267,268</sup> and mucins<sup>269</sup> and in cystic fibrosis sputum by F-actin bundles and DNA.<sup>268</sup> Bergsson *et al.* recently demonstrated that LL-37 in cystic fibrosis bronchoalveolar lavage fluid is protected from proteolytic degradation by GAGs.<sup>43</sup> However, interactions between LL-37 and a mixture of HS, chondroitin sulfate and HA in a 1:10 (w/w) ratio inhibited activity against *P. aeruginosa*.<sup>43</sup> The importance of this interaction was further demonstrated when the antimicrobial activity of cystic fibrosis sputum was activated following the use of GAG lyases, disrupting the LL-37 complexation with GAGs.<sup>43</sup> When LL-37 is free in the lung it is quickly degraded and inactivated by proteinase 3 and cathepsin D.<sup>43</sup>

There is now ample evidence that HS proteoglycans participate in many aspects of inflammation. Following an infectious stimulus, leukocytes and other tissue cells produce and release heparin-binding molecules, such as chemokines, growth factors, heparin-binding proteins and antimicrobial peptides, including cathelicidins that bind with high affinity to host or bacterial binding sites and associate with diverse HS-binding domains of proteoglycans.<sup>262</sup> Ligand affinity and concentration determine competitive displacement of HS-bound mediators. Activation or inhibition of proteases and heparanases alter constitutive shedding of HS proteoglycans. Binding of cathelicidins to HS proteoglycans may alter directly focal adhesion kinase signaling of syndecan-4; affect coreceptor function of syndecans and glypicans, e.g., by activation of metalloproteinase

and shedding of syndecan extodomains or by modification of enzymatic degradation of heparan sulfates by heparanase; and transactivation of surface receptors of inflammatory cells, including formyl peptide receptor, FPRL1, purinergic receptor, EGFR, and chemokine receptors. At the same time, binding of cathelicidins to HS and shedding of HS proteoglycans from cell surfaces affects microbial virulence and the antimicrobial potential of the peptides.

#### 1.7.4 GAG-binding peptides and antimicrobial activity

Zaleski *et al.* investigated the ability of HA binding peptides to protect from Staphylococcal infection. HA binding peptides have previously been shown to modulate cellular trafficking during host responses by blocking skin-directed trafficking of inflammatory leukocytes.<sup>270-272</sup> The authors found that treatment with HA binding peptides significantly reduced bacterial burden in staphylococcal wound infections. The HA binding peptides did not possess antimicrobial activity against *S. aureus*. Accordingly, the reduction in bacterial burden was attributed to the ability of the peptides to modulate the development of host inflammatory responses and a decrease in inflammation was seen at the site of infection.<sup>273</sup>

The requirements for interactions between heparin and peptides, such as amphipathicity, cationicity, and select secondary structures, are remarkably similar to the structural features of many known AMPs. Andersson *et al.* demonstrated that amphipathic motifs, such as heparin-binding consensus sequences exhibit potent antibacterial effects, exerting similar effects on bacterial membranes as endogenous AMPs.<sup>248</sup> Indeed, well known AMPs contain heparin-binding motifs, evidenced by the heparin-binding sequence XBBXB found in LL-37. Heparin-binding peptides derived from laminin, fibronectin, histidine-rich glycoprotein, domain 5 of high molecular weight kininogen, von Willebrand factor, vitronectin, protein C inhibitor, complement factor C3, proline arginine-rich end leucine-rich repeat protein (PRELP) and thrombospondin

exerted antimicrobial activities against Gram-positive and Gram-negative bacteria.<sup>248,264,274,275</sup> In addition, model peptides of consensus heparin-binding sequences exert direct antimicrobial effects against Gram-positive and Gram-negative bacteria, suggesting that these sequences may serve as templates for *de novo* synthesis of novel antimicrobial molecules.<sup>248,276</sup> Heparin-binding peptides are multifunctional and are active growth stimulus and angiogenesis, protease inhibition, anti-angiogenesis and chemotaxis.<sup>143</sup>

The antiangiogenesis activity of lactoferricin B has been attributed to the binding of lactoferricin B to heparan sulfate proteoglycans on the cell surface, thus blocking the binding of bFGF and VEGF<sub>165</sub> to their respective receptors and thereby preventing receptor-stimulated angiogenesis.<sup>277</sup> The proteoglycan involved is most likely glypican-1. A comparison of binding capacities to cell surfaces between native lactoferricin B and a scrambled lactoferricin B peptide with the same net charge showed that the structure of lactoferricin B rather than its charge is a major factor in its binding to cell surface proteoglycans.<sup>277</sup>

#### 1.7.5 Virulence traits that exploit interactions between GAGs and AMPs

Bacteria utilize a variety of virulence traits during infections. Release of various proteinases, such as the cysteine proteinase by *Streptococcus pyogenes*<sup>278</sup> modulates host responses involving kallikreins, coagulation factors, complement, cytokines and antiproteinases.<sup>279-283</sup> Other common pathogenic bacteria, such as *Pseudomonas aeruginosa* and *Enterococcus faecalis*, produce the proteinases elastase, alkaline proteinase and gelatinase.<sup>284-288</sup> Degradation of complement, antiproteinases and matrix components *in vitro* closely resembles the degradation pattern of these molecules in wound fluid *in vivo*.<sup>289,290</sup>



Park *et al.* showed that the *P. aeruginosa* virulence factor LasA enhances the *in vitro* shedding of syndecan-1, the predominant cell-surface HS proteoglycan.<sup>291</sup> They later showed that the shedding of syndecan-1 is also activated by *P. aeruginosa in vivo*, and that HS chains released from syndecan-1 are the effectors of bacterial virulence. Park *et al.* found that purified syndecan-1 ectodomains, through their HS chains, bind tightly to CAPs of the (proline/arginine)-rich cathelicidin family, including bactenecins 5 and 7 and PR-39. They also showed that syndecan-1 ectodomains inhibit the antibacterial activity of bactenecin 7 and that heparin inhibits the antibacterial activity of bactenecin 7, PR-39 and cecropin B.<sup>216</sup> Thus, inhibition of soluble, innate host defense factors, such as CAPs, may be one of the underlying mechanisms used by bacteria to shift host defense in their favor.

Schmidtchen *et al.* found that growth media from *P. aeruginosa* or *E. faecalis*, as well as purified enzymes from *P. aeruginosa*, *E. faecalis* or *S. pyogenes*, release dermatan sulfate from the proteoglycan decorin. DS was shown to bind  $\alpha$ -defensin-1 (HNP-1). C4S and C6S were not able to displace DS from binding  $\alpha$ -defensin-1. Only HS fractions with higher sulphation and iduronic acid contents and heparin could displace DS, suggesting that iduronic acid residues are needed to bind  $\alpha$ -defensin-1. In addition, Schmidtchen *et al.* found that DS could completely reverse the antimicrobial activity of  $\alpha$ -defensin-1 using *S. pyogenes* as the test organism, while HS, C4S and C6S each yielded less than 20% inhibition of  $\alpha$ -defensin-1 activity. DS also reversed the antimicrobial activity of  $\alpha$ -defensin-1 against *E. faecalis* and *P. aeruginosa*. The authors conclude that pathogenic bacteria use host-derived proteoglycans to release soluble DS, which subsequently binds to and inactivates neutrophil-derived defensins.<sup>264</sup>

## 1.8 Bacterial Cell Wall Components

### 1.8.1 Lipopolysaccharide

The cell wall of Gram-negative bacteria contains two distinct membranes, an inner and an outer membrane separated by periplasm, a hydrophilic compartment that includes a layer of peptidoglycan.<sup>292</sup> The inner membrane, also known as the cytoplasmic or cell membrane, is a symmetrical phospholipid bilayer in which proteins are embedded.<sup>293,294</sup> The outer membrane is an asymmetric lipid bilayer with phospholipids forming the inner leaflet and lipopolysaccharides (LPS) forming the outer leaflet. Proteins and lipoproteins are also inserted in the outer membrane lipid bilayer.<sup>292,295</sup>

LPS is a complex glycolipid that can be structurally divided in three parts: Lipid A, the oligosaccharide core region and the O-antigen polysaccharide chain. Lipid A is the hydrophobic moiety that anchors LPS to the outer membrane. The core oligosaccharide of LPS can be further divided into inner core, composed of Kdo (3-deoxy-D-manno-oct-2-ulosonic acid) and heptose (L-glycero-D-manno-heptopyranose), and outer core, which exhibits a greater structural diversity and provides the attachment site for the O-polysaccharide chain.<sup>296</sup> The O-polysaccharide chains, or O-antigens, are responsible for conferring serogroup specificity, defined by antibodies specific to the different variants of this antigen. The core and O-antigen domains are required for virulence and consequently are present in most clinical and environmental isolates.<sup>295</sup> LPS is essential for the viability of most Gram-negative bacteria and the Kdo<sub>2</sub>-lipid A moiety represents the minimal structure required for growth.<sup>296</sup>

Lipid A, also called endotoxin, has powerful biological effects in mammals, causing fever, septic shock, and other deleterious physiological effects. When released into the circulation, LPS binds to CD14 and Toll-like receptor 4 on monocytes and macrophages, which triggers secretion of proinflammatory mediators. At low levels,

lipid A serves as an adjuvant causing polyclonal expansion of B cells, but at high levels, it causes morbidity and mortality.<sup>297</sup>

### 1.8.2 LPS of *E. coli*

Lipid A, the hydrophobic anchor of LPS, is a glucosamine-based phospholipid that makes up the outer monolayer of the outer membranes of most Gram-negative bacteria.<sup>298,299</sup> Lipid A contains an *N*- and *O*-acylated diglucosamine bisphosphate backbone with chemical variation in the number of primary acyl groups and the types of fatty acid substituting the primary and secondary acyl groups. There are  $\sim 10^6$  lipid A residues per *E. coli* cell and these constitute 75% of outer membrane surface area.<sup>300</sup>

Much of the knowledge on the structure and biosynthesis of the core oligosaccharide is founded on work in *E. coli* and *Salmonella*.<sup>296</sup> The core oligosaccharides are conceptually divided into two regions: inner core (lipid A proximal) and outer core. The outer core region provides an attachment site for O antigen. Mucosal pathogens often lack O polysaccharides, instead producing lipooligosaccharides that contain a recognizable inner core from which extend one or more mono- or oligosaccharide branches which are equivalent to the outer core.<sup>296</sup> The inner core of *E. coli* contains Kdo and heptose and is further substituted with non-stoichiometric substitutions, including rhamnose, galactose, glucosamine, *N*-acetylglucosamine, Kdo, phosphate and phosphorylethanolamine residues.<sup>301-303</sup> Negative charges provided by the phosphate residues on heptose in the inner core play an important role in maintaining the barrier function of the outer membrane by providing sites for cross-linking of adjacent LPS molecules with divalent cations or polyamines.<sup>292,298,304</sup> In addition, the negative charges are important in mediating interactions between LPS and the positively-charged outer membrane proteins.<sup>305,306</sup>

The outer core of *E. coli* shows more structural diversity as might be expected for a region with more exposure to the selective pressures of host responses, bacteriophages,

and environmental stresses.<sup>298</sup> The outer core consists of glucose residues, differing in the specific sugar residues and the linkages between them. It is primarily differences in the outer core that define the five core types in *E. coli* (K12, R1-R4).<sup>307</sup> The R1 core predominates among strains that cause extraintestinal infections<sup>308,309</sup> and the R3 core is found in most verotoxigenic isolates such as O157:H7.<sup>310,311</sup>

The O-polysaccharide repeat unit structures can differ in the monomer glycoses, the position and stereochemistry of the O-glycosidic linkages, and the presence or absence of noncarbohydrate substituents. O-repeat units from different structures may comprise varying numbers of monosaccharides, they may be linear or branched, and they can form homopolymers (i.e. a single monosaccharide component) or, more frequently, heteropolymers. In some cases, nonstoichiometric modifications (e.g. O-acetylation or glycosylation) complicate the identification of a precise O-repeat unit. When the LPS molecules extracted from any smooth LPS-containing strain are separated by SDS-PAGE, it is apparent that there is extensive heterogeneity in the sizes of the molecules due to variations in the chain length of the O polysaccharides.<sup>298</sup>

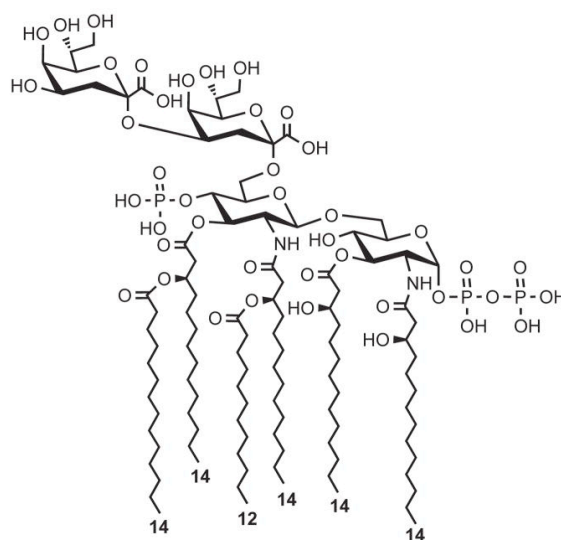


**Figure 7** Structure of lipid A with inner core Kdo residues.

The structure of the O polysaccharide defines the O-antigen serological specificity in an organism. *E. coli* produces approximately 176 O-serotypes. Common monosaccharides found in the O antigens of *E. coli* include glucose, rhamnose, galactose and fucose. A number of unusual sugars are found in the O antigens of *E. coli*, including pentoses, deoxyhexoses, lactyl substituted hexoses, heptoses and nonuloses. The number of sugar residues in the O-antigen repeating unit ranges from two to seven and the topology of the repeats may be described as linear, branched or double branched. The most common topology contains four sugars in the backbone being linear or containing a single terminal residue in the side-chain. The 3- and 5-residue backbones are also common, whereas the 2- and 6-residue backbones are only present in a few cases.<sup>312</sup>

### 1.8.3 LPS of *P. aeruginosa*

The LPS of *P. aeruginosa* contains lipid A and an inner core region that are relatively conserved among other Gram-negative bacteria.<sup>313</sup> The inner core structure contains two Kdo residues and two heptose residues with a 7-O-carbamyl group bound to the second heptose residue.<sup>314-316</sup> Both lipid A and the inner core region are usually highly phosphorylated and may also contain substituents with free amino acids. *P. aeruginosa* LPS has a higher phosphorus content at 4-5% compared to other Gram-negative LPSs. While enterobacterial LPS contains approximately 4 phosphate residues in the inner core region and an additional two to three in lipid A, LPS from *P. aeruginosa* can contain 10 or more residues per LPS molecule.<sup>317</sup> The two heptose residues in the inner core are often phosphorylated at positions 2 and 4 of Hep<sup>I</sup> and position 6 of Hep<sup>II</sup>.<sup>318-320</sup> Phosphate substituents can be mono-, di- or tri-phosphates and most *P. aeruginosa* LPS contain some triphosphate.<sup>313</sup>

The outer core of *P. aeruginosa* LPS is usually synthesized as two different isoforms or glycoforms by an individual strain.<sup>315,318,320</sup> Both outer core glycoforms contain an *N*-acetylated galactosamine residue, three D-glucose residues and one L-

rhamnose residue the position of which differs in the two glycoforms. There is extensive *O*-acetylation of the hydroxyl groups in the outer core carbohydrates, but the acetates are not present in high amounts at any one position. The *O*-antigen is attached to glycoform 2.<sup>318</sup>

The *O*-antigens of *P. aeruginosa* LPS diverge into at least eleven structural variants.<sup>315</sup> Eleven groups of *O*-antigen biosynthetic gene clusters have been found among the 20 IATS-prototype strains analyzed, corresponding precisely with the chemical structures reported for the eleven serogroups.<sup>321</sup> Typical sugars within the *O*-antigen for *P. aeruginosa* include *N*-acyl derivatives of different amino sugars along with rhamnose.<sup>315</sup> The monosaccharides are arranged in repeat units containing three to four individual monosaccharides. The linkage of the monosaccharide in the first repeat unit to the rhamnose residue in glycoform 2 of the outer core is usually a 2-*N*-acetyl derivative of a 6-deoxy-D-hexosamine.

#### 1.8.4 Lipoteichoic acid

Gram-positive bacteria lack an outer membrane and have a thicker peptidoglycan layer than Gram-negative bacteria. In Gram-positive organisms, the polysaccharide backbone of peptidoglycan typically contains 100 disaccharides and the peptide/peptide cross-bridge between strands varies. On average, every tenth unit contains a teichoic acid. The teichoic acids impart a high negative charge to the cell wall, which may have a role in selective uptake of charged molecules or as a barrier to uptake of antibiotics. Not all Gram-positive organisms contain teichoic acids, but those that lack them contain other types of polyanionic cell wall constituents, such as succinylated lipomannan. Under conditions of phosphate limitation, some bacteria produce teichuronic acids containing glucuronic acid–glucose or galacturonic acid–glucose copolymers instead of polyribitolphosphate and polyglycerophosphate polymers, demonstrating the necessity of

charged constituents in the cell wall. Although the precise function of teichoic acids is unknown, mutant cells that do not synthesize these compounds are unable to grow.<sup>150</sup>

LTA is the major amphiphilic molecule of gram-positive bacteria. The physiochemical properties of LTA are similar to those of LPS in gram-negative bacteria. Lipoteichoic acid is commonly composed of a hydrophilic backbone with repetitive glycerophosphate units and D-alanine or hexose substituents as well as a lipophilic glycolipid.<sup>322</sup> Staphylococcal LTA consists of about 25 poly(1-3)-glycerol phosphate linked to a diacylglycerolipid anchor. The hydrophilic polyglycerol phosphate chain is long enough to penetrate the peptidoglycan, and the lipid moiety attaches the polymer to the surface of the cytoplasmic membrane.<sup>323</sup> LTA from *S. aureus* has been shown to provoke secretion of cytokines and chemoattractants (TNF- $\alpha$ , IL-1 $\beta$ , IL-10, IL-12, IL-8, leukotriene B4, complement factor 5a, MCP-1, MIP-1 $\alpha$  and granulocyte colony-stimulating factor) from monocytes or macrophages.<sup>324-329</sup> Comparison of the activity of LPS versus LTA showed that staphylococcal LTA is able to promote the same strong induction of chemoattractants (IL-8, MIP-1 $\alpha$ , MCP-1, complement factor 5a, and leukotriene B4), granulocyte colony-stimulating factor, and anti-inflammatory cytokines (IL-10) as LPS, whereas it is a weaker inducer of TNF- $\alpha$ , IL-1 $\beta$ , and IL-6.<sup>329,330</sup> Thus, staphylococcal LTA is a strong inducer of chemoattractant and granulocyte colony-stimulating factor release, suggesting that it is not just a weak LPS-like molecule but indeed displays activities distinct from LPS.<sup>323</sup>

#### 1.8.5 Modification of cell wall components in response to

##### CAPs

Bacteria can reduce the net anionic charge of their cell wall in order to develop resistance to CAPs. This decrease in negative charge reduces the affinity of CAPs for the bacterial membrane and conveys protection for the bacteria.<sup>331</sup> As described above, the teichoic acid polymers found in Gram-positive bacteria have strong anionic properties

due to alternating glycerophosphate and ribitolphosphate units.<sup>332</sup> *S. aureus*, *S. pyogenes*, *Streptococcus agalactiae*, *Listeria monocytogenes* and many other bacteria can partially neutralize the anionic content of their cell walls by modifying their teichoic acid chains with D-alanine residues that bear positively charged amino groups.<sup>333-336</sup> This modification limits the interaction of CAPs with the cell wall and decreases susceptibility to cationic host factors, such as defensins.<sup>335</sup> *S. aureus* can also partially neutralize its cell wall by modifying membrane phosphatidylglycerol with L-lysine.<sup>337</sup> This neutralization of cell surface net charge reduces binding of CAPs and other cationic host defense molecules.<sup>338,339</sup>

Gram-negative bacteria neutralize their outer membranes through modifications to lipid A, which contains anionic phosphate groups. *S. enterica*, *P. aeruginosa* and several other bacteria can incorporate positively charged aminoarabinose into lipid A, thereby reducing the affinity of CAPs for the molecule and rendering the bacteria resistant to CAPs.<sup>340,341</sup> Bacteria also induce changes in the hydrophobicity of LPS<sup>342</sup>, alter the permeability of their outer membrane<sup>343</sup> and form biofilms in order to increase their resistance to CAPs.<sup>344,345</sup>



## CHAPTER 2 STATEMENT OF THE PROBLEM

CAPs are an important component of the innate immune system for their direct antimicrobial activity as well as their many immunomodulatory activities. These peptides depend upon electrostatic binding, rather than receptor-mediated targeting, for their antimicrobial activity. Additionally, there has been a great deal of interest in the commercial development of CAP-based antibiotics since bacteria develop resistance to CAPs at a much lower rate than to traditional antibiotics. Thus, it is important to understand any endogenous or exogenous factors that may decrease the activities of CAPs.

GAGs are endogenous and exogenously used polyanionic polysaccharides (PPSs). Although many protein-binding interactions of the GAG family, including heparin and HS, have been well-characterized, it is not known to what extent these PPSs affect the innate immune system. The use of polyanion-based therapeutics is increasing as additional applications for these agents are discovered. Traditionally polyanions, such as heparin and chemically and structurally-modified heparinoids, are used therapeutically as anticoagulants.<sup>346</sup> In addition, polyanions are currently the basis for therapeutics in pre-clinical and clinical development as anticancer, anti-inflammatory, anti-HIV, anti-STD and microbicidal agents.<sup>347,348</sup> The increasing prevalence of polyanion-based therapeutics necessitates a thorough investigation for possible adverse interactions within the human body.

It has recently been shown that a number of polyanions have the ability to inhibit the antimicrobial activity of certain CAPs. Bacteria utilize a multitude of virulence traits to evade the host immune system, including the inactivation of CAPs. A number of bacterial human pathogens secrete extracellular proteases that degrade cellular proteoglycans, resulting in the release of the highly anionic GAGs. Dermatan sulfate and syndecan-1, a cell-surface heparan sulfate, are two sulfated GAGs that demonstrate this

type of interactions with CAPs. Heparin has also demonstrated inhibitory interactions with a limited number of CAPs. A limited number of GAGs have also been shown to protect a small number of CAPs from proteolytic degradation.

The goal of this work was to work towards understand the complex and often overlooked relationship between innate host defenses and polyanionic therapies or endogenous GAGs. While a number of interactions have been documented between GAGs and CAPs, this field has not been studied from a chemical and structural perspective. Thus, the hypothesis of this work is that **specific endogenous GAGs and exogenous PPSs are direct and indirect modulators of specific CAP activities.**

Given the lack of knowledge in this field when this work was initiated, the first goal was to analyze the ability of GAGs and other PPSs to modulate the antimicrobial activity of 5 CAPs – lactoferricin peptide, magainin II, cecropin A, cecropin B and LL-37. The second goal was to measure the affinity of the CAPs for the specific GAGs and PPSs to facilitate correlations of the antimicrobial activity modulatory activity. To do this the affinity of cecropin A, cecropin B and LL-37 was measured for LPS for *P. aeruginosa* and *E. coli* and competition binding experiments were performed to measure the affinity of the CAPs for select GAGs. Finally, the third goal of this work was to explore the ability of GAGs to protect cecropin A, cecropin B and LL-37 from proteolytic degradation. Trypsin and *P. aeruginosa* LPS were used to test the ability of GAGs to modulate the proteolytic degradation of cecropin A, cecropin B and LL-37.

Going into this work we postulated that the unique properties of specific GAGs and PPSs would provide optimal binding sites for individual CAPs, leading to the modulation of their antimicrobial activity, bacterial-membrane binding and proteolytic degradation. Indeed we found that some modulatory activities of the GAGs were dependent upon specific structural and chemical features. Additionally, we found that the modulatory activities of the GAGs were dependent upon all components of the system, as opposed to depending solely on the CAP interacting with the GAG.

## CHAPTER 3 INTERACTION BETWEEN LACTOFERRICIN PEPTIDE AND GLYCOSAMINOGLYCANS

### 3.1 Antimicrobial activity of GAGs – Experimental techniques and results

Because we are interested in studying the ability of GAGs to modulate the antimicrobial activity of bovine lactoferricin peptide (LP), it was important to first establish that GAGs have no innate antimicrobial activity. PPSs were obtained from the following sources: Unfractionated heparin (Sigma H4784), heparan sulfate (Celsus HO-03102), dermatan sulfate (Celsus DS-03123), chondroitin 4-sulfate (Sigma C9819), chondroitin 6-sulfate (Sigma C4384), hyaluronic acid (Fluka 53747), enoxaparin (Sequoia Research SRP0108755e), ardeparin (Celsus FH-03093), 3 kD heparin (deaminated heparin, Celsus DH-03253), dextran sulfate (MP Biomedicals 101518) and sulodexide (Celsus DX-03633). Carboxyl-reduced heparin, 2-*O*-desulfated heparin and phenoxyaniline heparin amide were prepared in the Kerns laboratory as discussed in the background. Overnight cultures of *E. coli* ATCC 33876 and *S. epidermidis* ATCC 14990 were grown in Mueller-Hinton broth (Difco # 275710). The cultures were diluted with 1% (w/v) Peptone water minimal media (Difco 218071) pH 6.8, to an Optical Density at 600 nm of 0.1, corresponding to a bacterial suspension of approximately  $10^8$  colony forming units (CFU)/mL. These suspensions were further diluted using 1% (w/v) Peptone Water Minimal Media pH 6.8 to obtain a bacterial suspension of  $2-7 \times 10^5$  CFU/mL. Aliquots of 0.1 mL of the *E. coli* or *S. epidermidis* bacterial suspensions were incubated with 10 and 20  $\mu$ g of the GAGs in triplicate. Sterile water was used in the place of GAG solution as a negative control and is shown as the “+ Growth” category in **Figure 8**. Ciprofloxacin (Sigma Aldrich 17850) at its appropriate minimum inhibitory concentration was used as a positive control. Following incubation at 37°C, growth was

evaluated by measuring the optical density (OD) at 600nm. Peptone minimal media was used in these experiments in order to limit the interaction between the GAGs or PPSs and the contents of the growth medium.

None of the GAGs tested showed antimicrobial activity against *E. coli* (**Figure 8**) or *S. epidermidis*. Looking at the trends as the incubation time increased the GAGs showed positive support of bacterial growth rather than inhibition. This is especially seen in the 53 hour time points (**Figure 9**). Since 20  $\mu\text{g}/\text{well}$  of each GAG did not inhibit the growth of *E. coli* we felt confident using this amount in assays looking at the ability of GAGs to modulate the antimicrobial activity of LP.

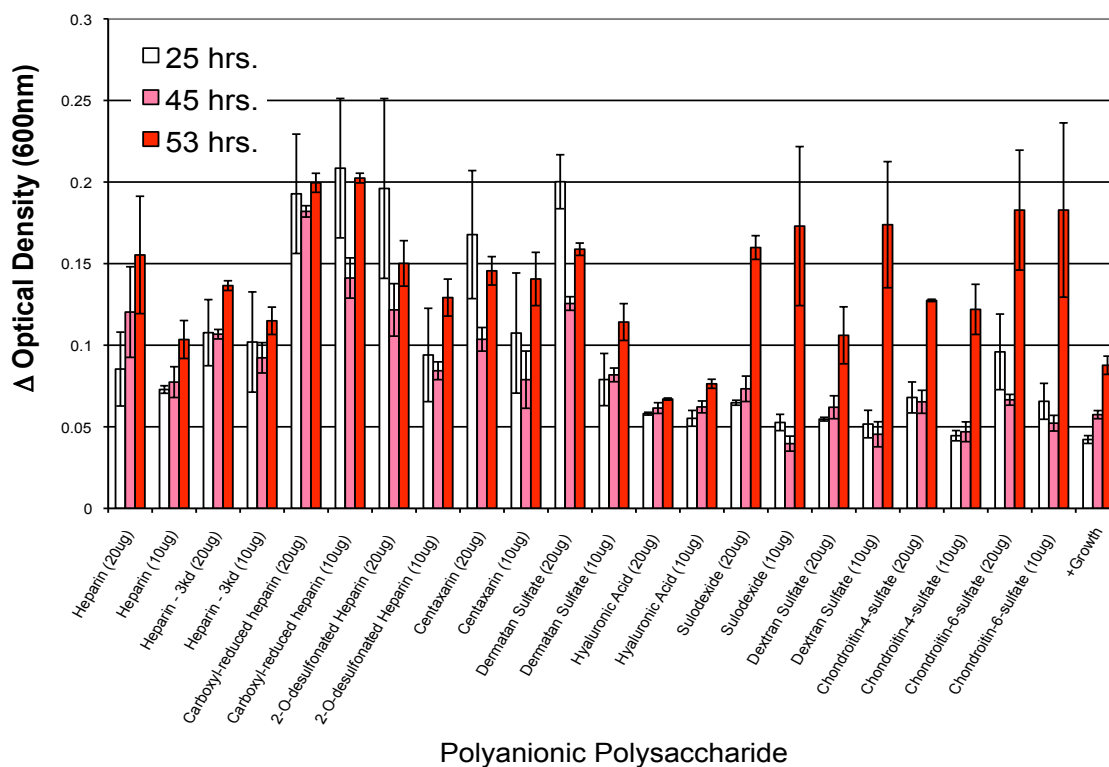


**Figure 8** Antimicrobial activity of GAGs and other PPSs against *E. coli*. PPSs were tested at two concentrations and growth of the bacteria was evaluated at three different time points. Data is presented as the means of triplicate data points  $\pm$  standard error. A positive growth control, in the form of bacteria incubated with sterile water is shown.

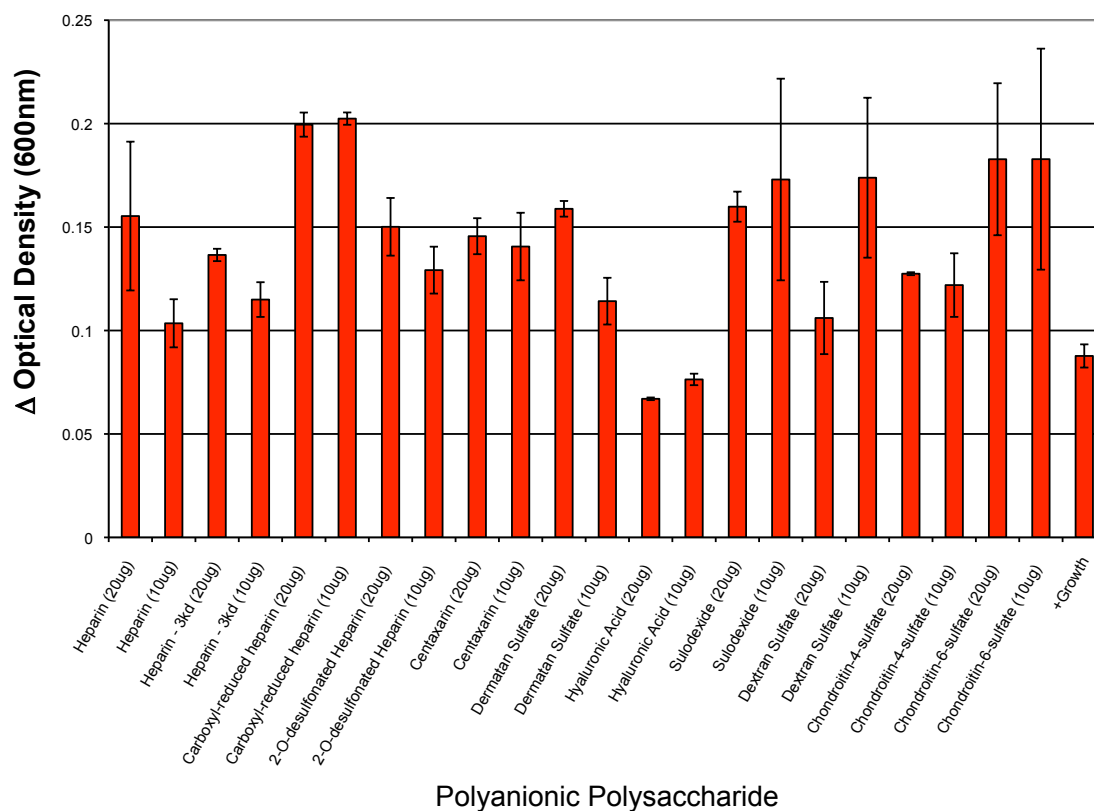


**Figure 9** Antimicrobial activity of PPSs against *E. coli* after 53 hours. Data points represent the mean of triplicate determinations  $\pm$  standard error.

### 3.2 Modulation of LP antimicrobial activity by GAGs

#### 3.2.1 Minimum inhibitory concentrations for LP – experimental techniques and results

The bacterial strains *Escherichia coli* ATCC 33876 and *Staphylococcus epidermidis* ATCC 14990 were used to investigate the antimicrobial activity of LP. *E. coli* was chosen as a model of Gram-negative bacteria and *S. epidermidis* was used as a Gram-negative model. Overnight cultures of each organism were first grown in Mueller-Hinton Broth at 37°C. The cultures were diluted with 1% (w/v) Peptone water minimal media, pH 6.8, to an OD<sub>600</sub> of 0.1. These suspensions were further diluted using 1%

(w/v) Peptone Water Minimal Media, pH 6.8, to obtain a bacterial suspension of approximately  $2-7 \times 10^5$  CFU/mL. A polypropylene 96-well plate, pre-sterilized with 80% ethanol and overnight UV exposure, was used for this assay. LP (American Peptide 72-1-31) was dissolved in 0.01% Acetic Acid, 0.2% BSA to a final concentration of 1 mg/mL. Using the modified microdilution technique, a series of concentrations of LP was added to wells of a 96-well plate. 0.1 mL of the *E. coli* or *S. epidermidis* bacterial suspensions was added to the wells containing LP and the plate was sealed and incubated overnight at 37°C. Again, sterile water was used as a negative control and ciprofloxacin at the appropriate MIC was used as a positive control. The MIC was defined as the lowest concentration of the peptide at which there was no growth after 24 hours, as evaluated by measuring the absorbance at 600nm.

The MIC of LP for *E. coli* was identified as 16.0 µg/mL (10.4 µM) and 8.0 µg/mL (5.17 µM) for *S. epidermidis*.

### 3.2.2 Single point screen accessing the ability of GAGs to modulate the antimicrobial activity of LP – experimental technique and results

*E. coli* ATCC 33876 was used to investigate the modulation of LP antimicrobial activity by GAGs. Overnight cultures were diluted as previously described using 1% Peptone Water Minimal Media, pH 6.8. Using a single point screen, three concentrations of LP, corresponding to one-fourth the MIC, at the MIC and 2-fold the MIC (4.0, 16.0 or 32.0 µg/mL), were evaluated for antimicrobial activity in the presence of 20 µg of 11 GAGs. Sterile water was used to give a positive growth control.

In this single point screen 0.1 mL of the  $2-7 \times 10^5$  CFU/mL *E. coli* solution was incubated with 20 µg of each GAG and 0.5, 2 or 4 µg LP in 1% Peptone Water Minimal Media, pH 6.8. Following incubation at 37°C for 24 hours, bacterial growth was evaluated by measuring OD at 600nm. The percent recovery of growth was calculated by

dividing the OD<sub>600</sub> value for each well by the OD<sub>600</sub> value for the positive growth controls and multiplying by 100. We decided to focus on the ability of GAGs to modulate the antimicrobial activity of LP because they are found endogenously and also, in the case of heparin, used therapeutically.

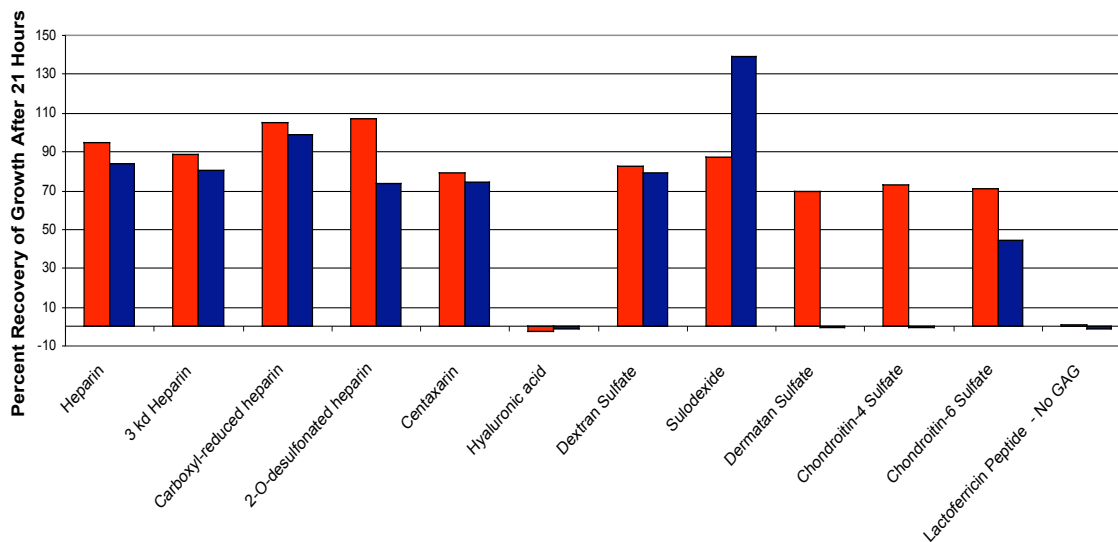


**Figure 10** Single point screen accessing the modulatory activities of PPSs on the antimicrobial activity of LP. LP was tested at the MIC for *E. coli* (16.0 µg/mL, red) and two-fold the MIC (32.0 µg/mL, blue).

All of the GAGs, with the exception of HA, were able to modulate the antimicrobial activity of LP against *E. coli* (**Figure 10**). At the concentrations tested, DS and C4S were only able to reverse the antimicrobial activity of LP at the MIC while the other GAGs reversed the antimicrobial activity of LP at the MIC and 2-fold the MIC. Since this was a single point screen few other conclusions can be drawn from these results. Having determined that specific GAGs modulate LP differently, we performed concentration-dependent studies analyzing the ability of GAGs to modulate the anti-*Escherichia* activity of LP.

### 3.2.3 Concentration dependent ability of GAGs to modulate the antimicrobial activity of LP – experimental technique and results

Heparin, carboxyl-reduced heparin, a heparin amide previously prepared in our laboratory, Enoxaparin, Centaxarin, HS, DS, C4S and C6S were further investigated for their ability to inhibit the antimicrobial activity of LP. For these experiments 4 µg of LP was added to a  $2-7 \times 10^5$  CFU/mL *E. coli* suspension in 1% Peptone Water Minimal Media pH 6.8. Each GAG was added to the lactoferricin-*E. coli* suspension in the following amounts: 40, 20, 10, 5, 1.0, 0.5, 0.1 and 0 µg. Assay volumes were kept equal by the addition of sterile water. After 24 hours of incubation at 37°C growth was assayed by measuring the absorbance at 600nm.

These experiments revealed three classes of LP antimicrobial activity modulators (**Figure 11**). Heparin and the phenoxyaniline heparin amide were the best negative modulators of LP antimicrobial activity. Carboxyl-reduced heparin, ardeparin (centaxarin) and enoxaparin were in the second class of LP anti-*Escherichia* activity modulators. The rest of the GAGs tested, HS, DS, C4S and C6S, were in the third class of modulators of LP antimicrobial activity.

These results are intriguing for a variety of reasons. First we saw that heparin was a better modulator of antimicrobial activity as compared to the LMWHs tested. Secondly, charge reduction of heparin affects its ability to modulate the antimicrobial activity of LP. When the carboxyl group is replaced with a hydroxyl group, as is the case for carboxyl-reduced heparin, the ability of the heparinoid to negatively modulate the antimicrobial activity of LP was decreased. Alternatively, when the charged group was replaced with a larger hydrophobic group (phenoxyaniline) the modulatory activity of the heparinoid was not decreased. Additionally, the lower anionic charge of the other GAGs tested may explain their lesser negative modulatory activities. Thus we can say that the molecular



weight molecular weight and charge of heparin contribute to the negative modulatory activity against the anti-*Escherichia* activity of LP.

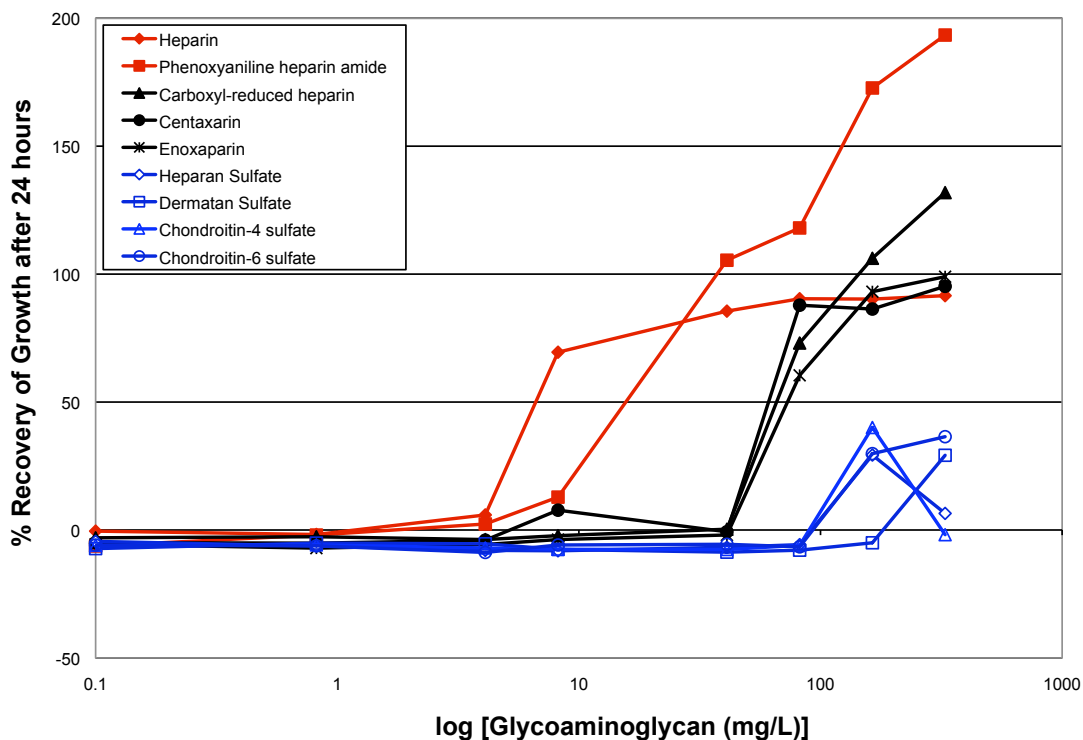


**Figure 11** Negative modulatory activity of the GAGs on the antimicrobial activity of LP against *E. coli*. LP was used at two-fold the MIC for *E. coli*. Data points represent the mean of duplicate measurements.

### 3.3 LP binding to GAGs

#### 3.3.1 LP-GAG binding studies - Experimental technique

Tryptophan fluorescence was used as an indicator of binding interactions between LP and each of the six GAGs tested. Solutions of 5.9 mM LP were incubated with each GAG at final concentrations between 0 and 1.0 mg/mL in tris buffer (50 mM Tris-HCl, 100 mM NaCl, 0.02% Tween-20, pH 7.4). 200  $\mu$ L samples of the LP-GAG solutions

were read in a microcuvette using a PerkinElmer LS55 Luminescence Spectrophotometer. Emission scans were performed using an excitation wavelength of 280nm, an emission range of 300-400nm, excitation slit width of 5 nm, emission wavelength of 6.5 nm and a scanning speed of 500 nm/min. LP emission was measured at 354nm.  $F_1-F_0$  values were calculated by subtracting the fluorescence or light scattering of the peptide alone from the fluorescence or light scattering of each sample solution. Percentage of maximal fluorescence (% Max F) was calculated using the following formula:  $(F_1-F_0/F_{Max})\times 100$ , where  $F_{Max}$  is an average of the maximum fluorescence data points and is unique for each GAG. Each experiment was done in triplicate and the data were averaged. The data were fit using a single binding site model in SigmaPlot. From the binding data we compared the concentration of each GAG at which 50% maximal lactoferricin peptide binding is observed. The tryptophan fluorescence binding data were also fit to single site saturation model using GAG molecular weights calculated based on average disaccharide molecular weight in SigmaPlot. This gave us  $K_{d_{app}}$  values to compare for the GAGs binding to LP.

Light scattering experiments were performed using the synchronous delta lambda mode with a difference between monochromators of 0 nm, scanning from 450nm to 550 nm with emission and excitation slit widths of 2.5nm and a scanning speed of 500 nm/min. Light scattering was detected at 492nm.

### 3.3.2 Results of LP-GAG binding studies

The LP-GAG binding studies revealed that the GAGs have different affinities for LP (**Figure 12**). By comparing the concentration required for 50% maximal binding we were able to compare the apparent affinities of the GAGs for LP (**Figure 13**). In this comparison heparin, enoxaparin and ardeparin (centaxarin) required equal concentrations to achieve 50% of the maximal binding to LP. HS and DS required significantly more to

achieve 50% maximal LP binding while C4S never achieved 100% binding in the tryptophan fluorescence assay.

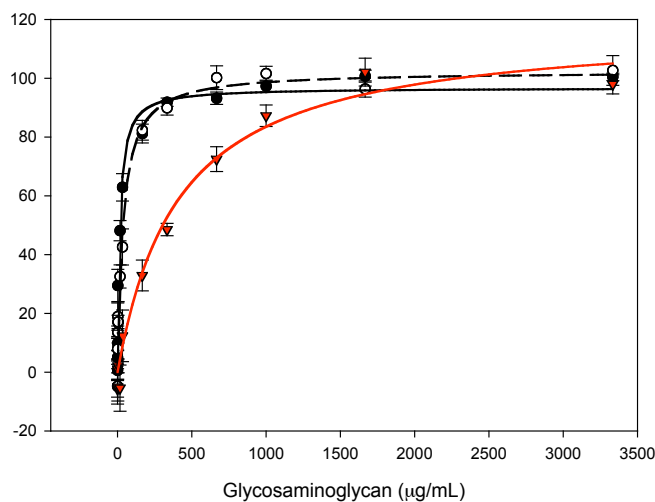


**Figure 12** Saturation binding curves for heparin (black), enoxaparin (dotted line) and DS (red) binding LP generated from tryptophan fluorescence data. Data points represent the means of 12 determinations (heparin) or 6 determinations (enoxaparin and DS)  $\pm$  standard error.

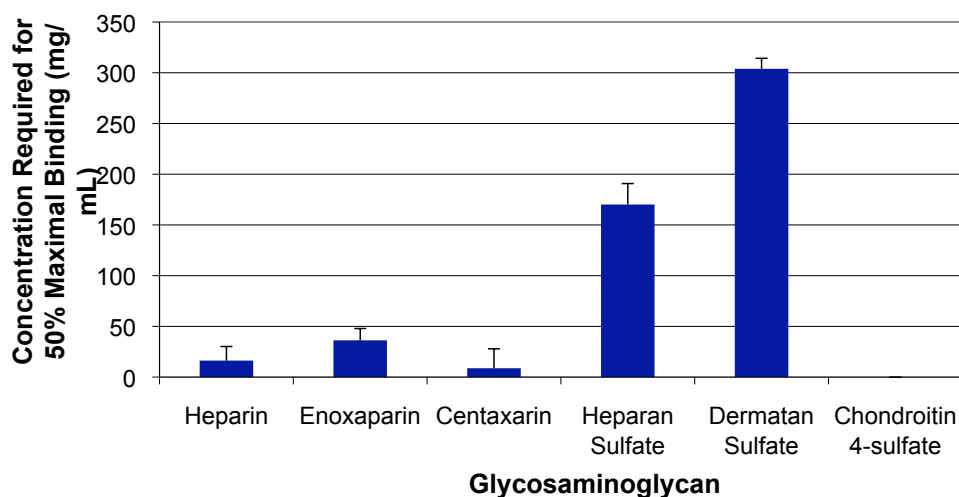


**Figure 13** Comparison of the concentration of GAG at which 50% of maximal fluorescence is achieved calculated from tryptophan fluorescence data. C4S did not achieve maximal binding in the range of 0-3330  $\mu\text{g/mL}$ .

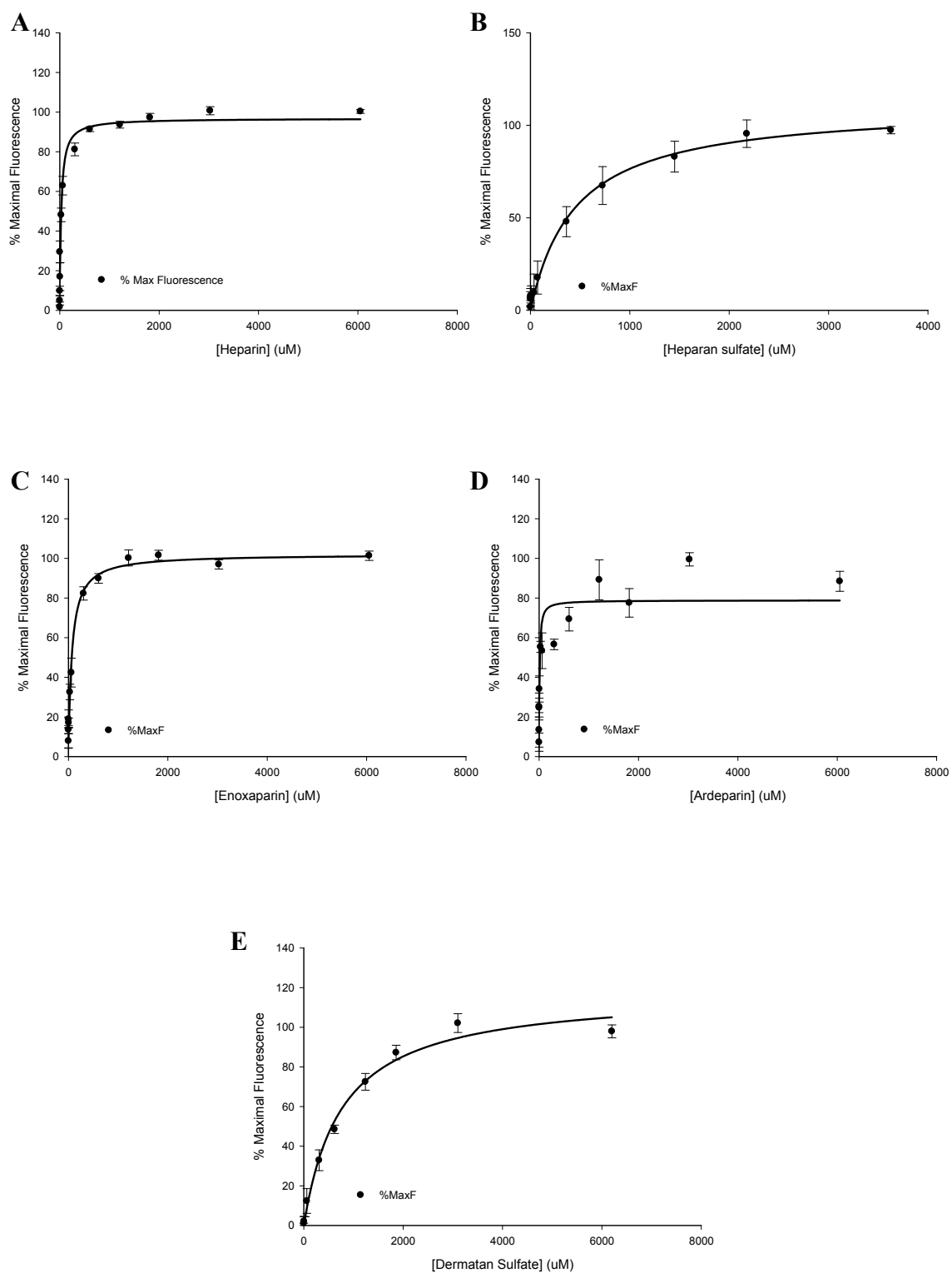


**Figure 14** Saturation binding curves for GAGs binding to LP. The fits of the one-site binding model are shown for heparin (A), HS (B), enoxaparin (C), ardeparin (D) and DS (E). The means of 12 determinations (A), 9 determinations (B), or 6 determinations (C-E)  $\pm$  standard error are shown.

GAG	K <sub>d</sub> <sub>app</sub> (μM)	B <sub>max</sub>	R <sup>2</sup>
Heparin	3.31 ± 1.74	1.74 ± 3.31	0.8890
Ardeparin	9.16 ± 2.66	78.8 ± 3.17	0.6653
Enoxaparin	67.5 ± 9.16	102 ± 2.27	0.9294
Heparan sulfate	449 ± 118	111 ± 7.96	0.7666
Dermatan sulfate	769 ± 104	118 ± 4.89	0.9445

**Table 3** Calculated binding constants for GAGs binding LP.

Calculating K<sub>d</sub><sub>app</sub> values (**Table 3**) from the single binding site saturation curves in **Figure 14** gives similar results. Heparin and ardeparin have very similar K<sub>d</sub><sub>app</sub> values while enoxaparin has a slightly lower affinity for LP. Again, HS and DS have a much lower affinity for LP as compared to heparin and the LMWHs. These results indicate that there is no difference in affinities of LP for heparin and the LMWHs.

We postulated that aggregation of LP by the GAGs would result in the reduction of effective LP concentration in solution with the bacteria, thereby decreasing the concentration of LP to below the MIC. To test this hypothesis, light scattering experiments were performed on the same solutions used to collect the tryptophan fluorescence affinity data. These experiments did not detect LP-GAG aggregates that caused measurable light scattering, indicating that aggregation is not the likely cause for the modulation of the LP antimicrobial activity by the GAGs tested.

### 3.3.2 Sulfate determination of heparin and LMWHs –

#### Experimental technique and results

Since heparin and the LMMHs showed distinct modulation of LP antimicrobial activity, but similar affinities, we postulated that heparin could have a higher degree of sulfation. Furthermore, we postulated that a higher degree of sulfation would correlate to an increased ability to negatively modulate the antimicrobial activity of LP against *E. coli*.

The sulfate content of heparin, enoxaparin and ardeparin (centaxarin) were measured using the methodology of Dodgson and Price.<sup>349,350</sup> Briefly, this method involves acid hydrolysis of sulfate followed by the turbidimetric measurement of barium sulfate. Gelatin is used as a cloud stabilizer and decreases the amount of substrate needed to perform these measurements. The use of a potassium sulfate standard curve allowed for quantitative sulfate measurements of heparin, centaxarin and enoxaparin.

One milliliter volumes of 400 $\mu$ g/mL, 200 $\mu$ g/mL and 100 $\mu$ g/mL solutions of heparin, aredeparin (centaxarin) and enoxaparin in 2N HCl were prepared from the stock solutions. One milliliter volumes of K<sub>2</sub>SO<sub>4</sub> in 2N HCl were also prepared in concentrations ranging from 25  $\mu$ g/mL to 5.0 mg/mL for the standard curve. All solutions, including 2 N HCl for use as a blank, were transferred to glass ampules and were heated to and held at 105°C for 5 hours. During this time BaCl<sub>2</sub> (SigmaAldrich

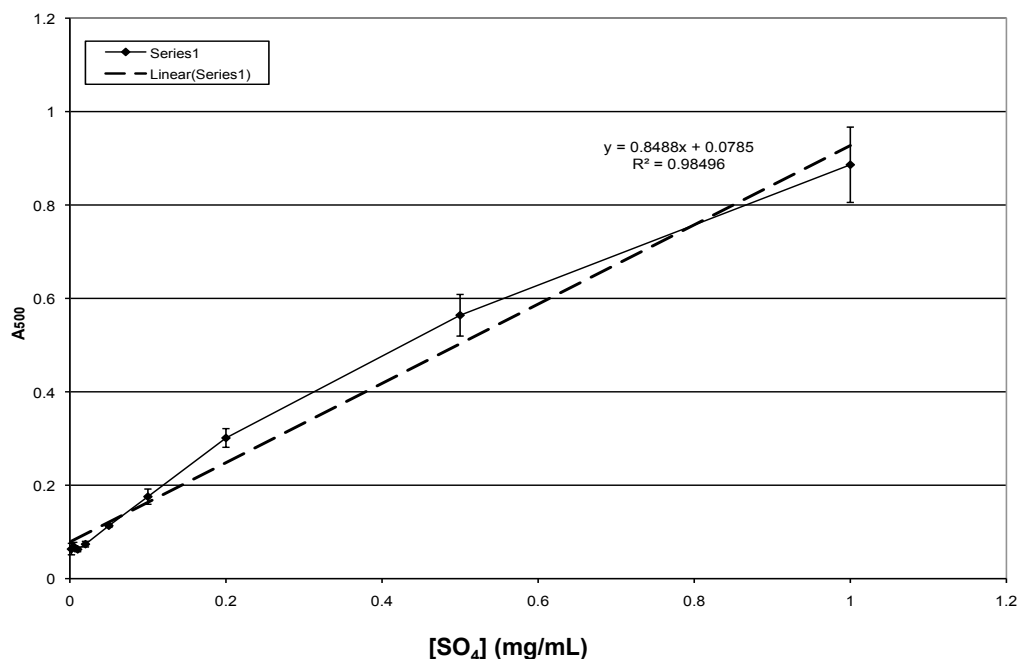


**Figure 15** Potassium sulfate standard curve generated for GAG total sulfate determination.

202738) was added to a 1% (w/v) gelatin to make a 0.24 M BaCl<sub>2</sub>-gelatin solution. In triplicate, 200 μL of each GAG or K<sub>2</sub>SO<sub>4</sub> solution was added to 3.8 mL 3.8% trichloroacetic acid, followed by the addition of 1 mL of BaCl<sub>2</sub>-gelatin solution and mixing for 20 minutes. The absorbance of each sample was read at 500nm using a Shimadzu UV-2101PC UV-VIS scanning spectrophotometer. A standard curve was generated using the absorbance values from the K<sub>2</sub>SO<sub>4</sub> solutions (**Figure 15**). Quantitative sulfate measurements for heparin, ardeparin and enoxaparin were calculated from this standard curve (**Figure 16**).

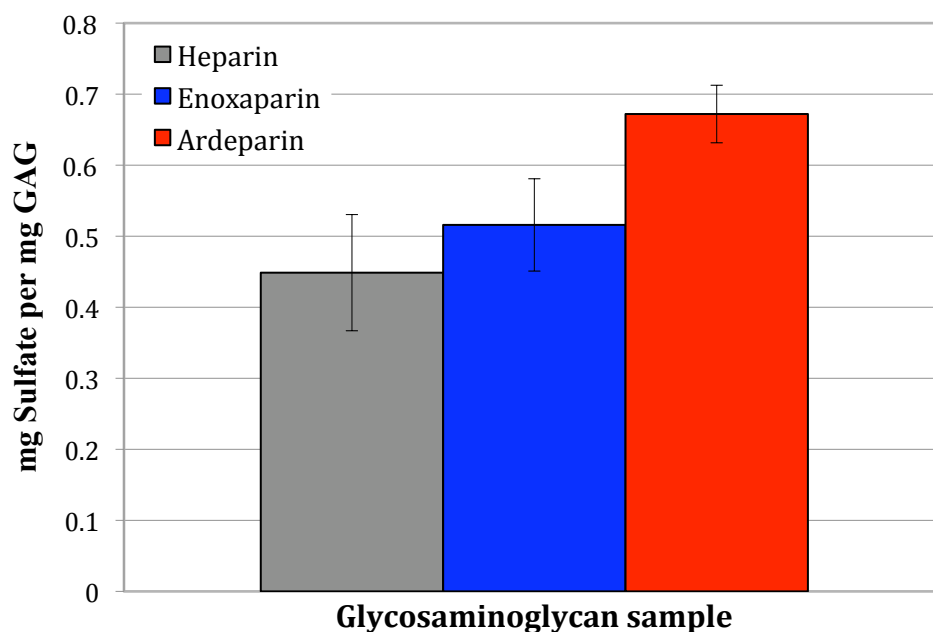


**Figure 16** Total sulfate levels of heparin, centaxarin and enoxparin samples calculated using the standard curve in **Figure 15**.

Based on these results we concluded that the sulfate levels of heparin, enoxaparin and ardeparin are not significantly different. Thus, difference in anionic charge cannot be

used to explain the difference in LP antimicrobial activity modulatory activities of heparin and LMWHs.

### 3.3 Conclusions

Most importantly, we demonstrated that GAGs can modulate the antimicrobial activity of LP, a linear CAP. We found that there were three classes of LP antimicrobial activity reversal capacities. Heparin and a phenoxyaniline heparin amide were in the first class of antimicrobial activity modulators. The LMWHs enoxaparin and ardeparin as well as carboxyl-reduced heparin made up the second, less active class of antimicrobial activity modulators. All of the other GAGs tested made up the third level of LP antimicrobial activity modulators, which were very poor at reversing the antimicrobial activity of LP. To determine if affinity for LP correlated to the ability to reverse antimicrobial activity, we then measured the affinity of LP for the GAGs using tryptophan fluorescence. From these experiments we found that heparin and the LMWHs show similar affinities for LP, despite their different abilities to modulate the antimicrobial activity of LP against *E. coli*. DS and HS showed lower affinities for LP and C4S did not fully bind LP in the concentration range tested. The binding results led us to question the reason for heparin's superior reversal activity of LP antimicrobial activity over the LMWHs. We postulated that heparin could have a higher anionic charge as compared to the LMWHs due to the depolymerization methods used to produce the LMWHs. Thus, the total sulfate levels of heparin, enoxaparin and ardeparin were determined and all three GAGs had approximately equal sulfate levels, indicating that heparin does not have a higher anionic charge than the LMWHs. Thus we conclude that the higher molecular weight of heparin confers a higher reversal activity against LP antimicrobial activity as compared to the LMWHs. We hypothesize that more LP molecules can bind to a full-length heparin molecule as compared to the LMWHs. Thus,



one molecule of heparin can bind more LP molecules and more efficiently block LP binding to the bacterial membrane.

CHAPTER 4 MODULATION OF ANTIMICROBIAL  
ACTIVITY OF MAGAININ II, CECROPIN A,  
CECROPIN B AND LL-37

4.1 Antimicrobial activity of GAGs and other polyanionic  
polysaccharides – experimental technique and results

As we were interested in the ability of GAGs and other polyanionic polysaccharides to modulate the antimicrobial activity of different CAPs, it was important to study the inherent antimicrobial activity of the GAGs, charge-reduced heparin analogs, LMWHs and other PPSs used in subsequent experiments. It was previously shown that heparin has no significant antibacterial activity at antibiotic levels<sup>351</sup>. The antimicrobial activities of the GAGs and other PPSs were measured using a microdilution MIC determination method modified from de Leeuw *et al.*<sup>352</sup> PPSs were obtained from commercial sources previously mentioned and the following commercial sources: ultra LMWH (Sigma H3400),  $\alpha$ -cyclodextrin sulfate (CarboMer, Inc. 400,195),  $\beta$ -cyclodextrin sulfate (Sigma T3821) and dextrin sulfate (CarboMer, Inc. 502,530). Carboxyl-reduced heparin and 6-*O*-desulfated heparin were prepared in the Kerns lab as discussed previously. Overnight cultures of *P. aeruginosa* ATCC 27853, *E. coli* JM101 ATCC 33876 or *S. aureus* ATCC 25923 were grown in Mueller-Hinton broth (Difco #275710) and diluted to an optical density of 0.1 with 10 mM sodium phosphate, pH 7.4. Aliquots from GAG and other PPS stock solutions were added to individual wells of pre-sterilized 96-well polypropylene plates (Corning ClearPro #3371) and 100  $\mu$ L of the diluted bacteria solutions were added, bringing the concentration of PPSs to 0.05 or 0.1 mg/mL in sodium phosphate, pH 7.4. After an initial incubation at 37°C for 2 hours, 200  $\mu$ L of Mueller-Hinton broth was added to each well and the plate was sealed and incubated at 37°C overnight. Optical density (OD) at 600 nm was used to measure the viability of the bacteria in each well. Sterile water was used in the place of a GAG or

PPS to yield a negative growth control. Ciprofloxacin at its MIC for each organism was used as a positive control. A two-way paired student's T-test was used to determine statistical significance.

In these experiments the GAG was incubated with the appropriate bacteria in sodium phosphate buffer for 2 hours at 37°C. This approach allowed for us to detect the effect of GAG binding to the bacteria in the absence of other growth medium components that could bind the GAGs with a higher affinity. After the incubation Mueller-Hinton broth, a growth medium commonly used for MIC determinations, was added to allow us to detect bacterial growth in each well. The use of the sodium phosphate buffer in these experiments has the advantage of simplifying the aqueous binding environment, however

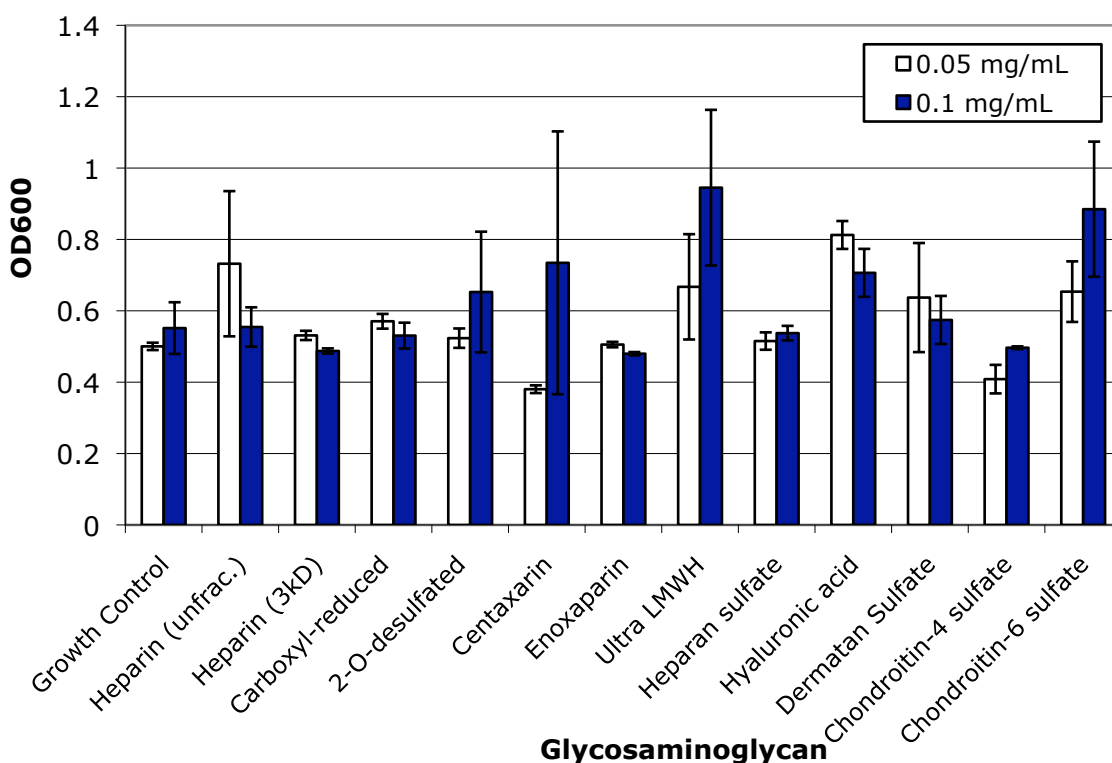


**Figure 17** Antimicrobial activity of GAGs, charge-reduced heparin analogs and LMWHs versus *P. aeruginosa*. Data points represent the mean of triplicate determinations  $\pm$  standard error.

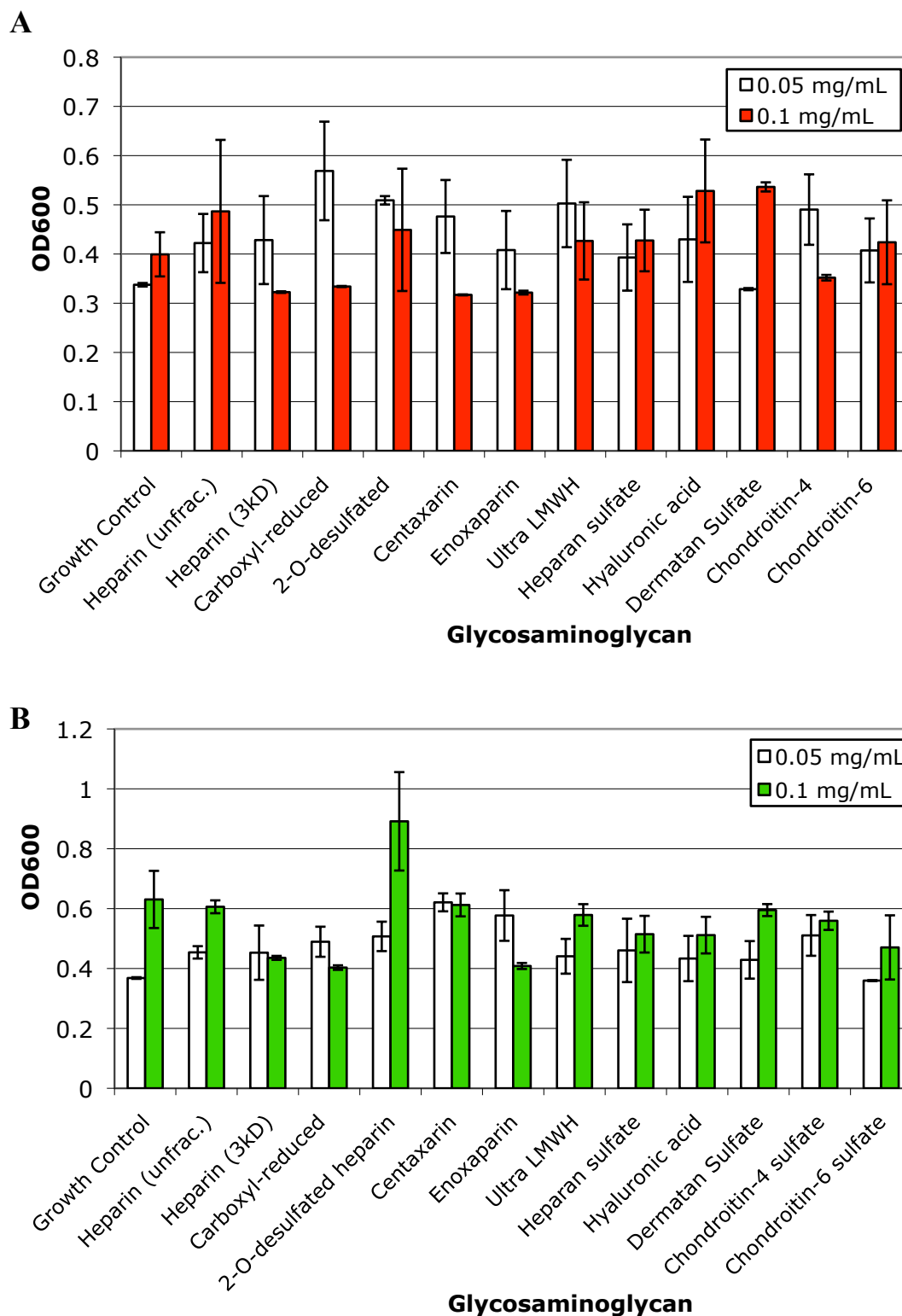


**Figure 18** Antimicrobial activity of GAGs, charge-reduced heparin analogs and LMWHs versus *E. coli* (A) and *S. aureus* (B). Measurements were done in triplicate and data points are shown as the mean  $\pm$  standard error.

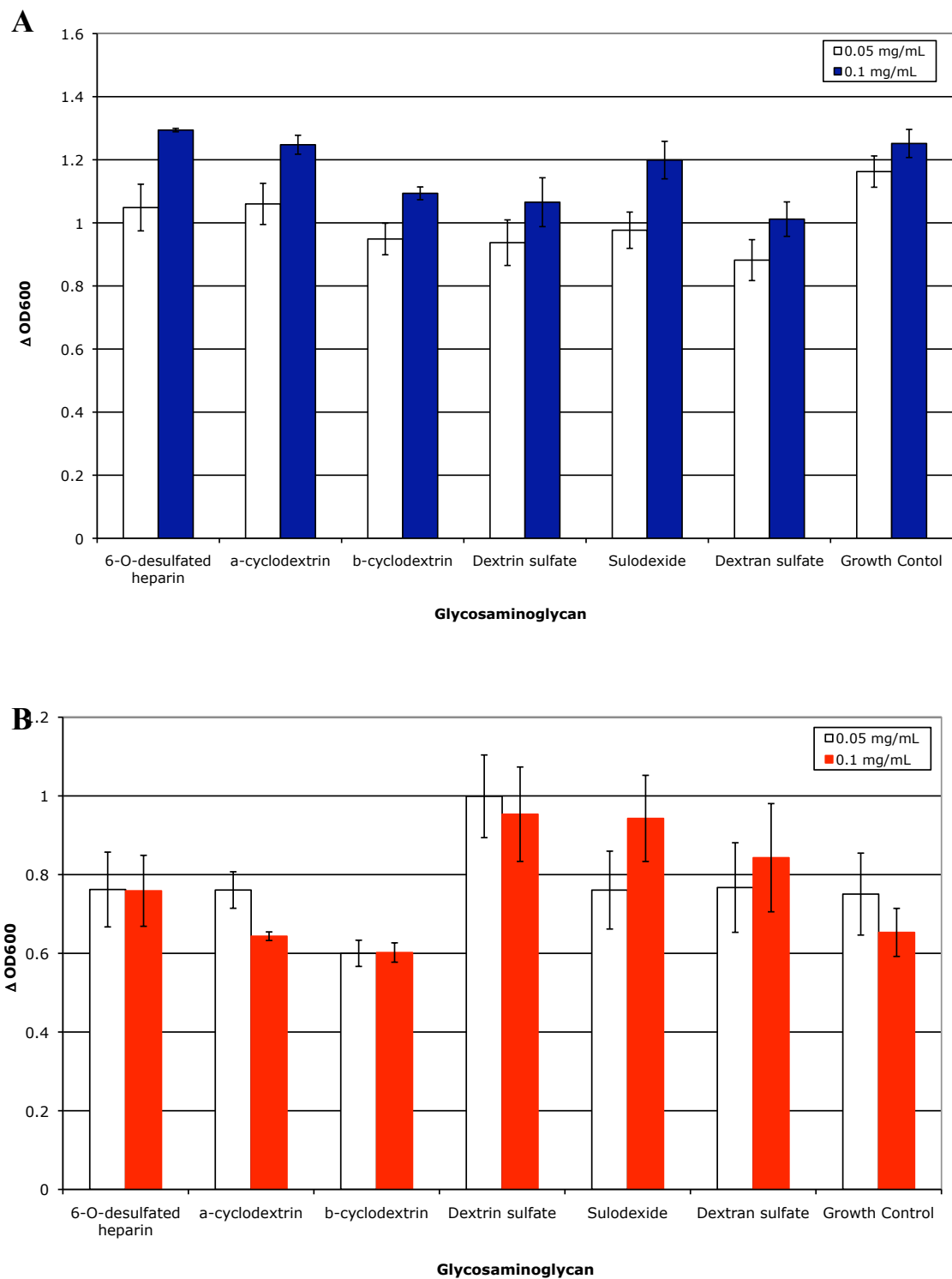


**Figure 19** Antimicrobial activity of 6-*O*-desulfated heparin and other PPSs versus *P. aeruginosa* (A) and *E. coli* (B). Mean of six data points  $\pm$  standard error shown.

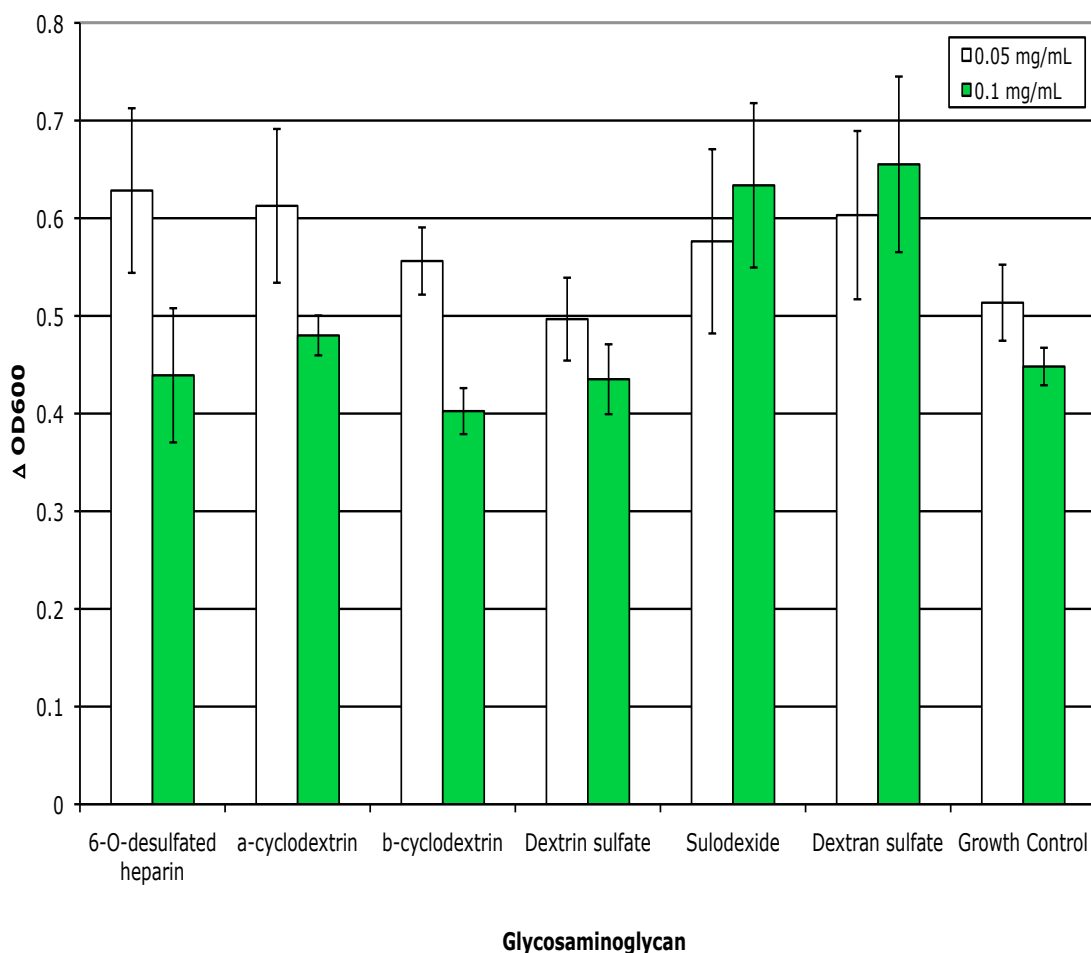


**Figure 20** Antimicrobial activity of 6-*O*-desulfated heparin and other polyanionic polysaccharides versus *S. aureus*. Mean of six data points  $\pm$  standard error shown.

it does affect the ionic strength of the aqueous binding environment. Ten mM sodium phosphate buffer, pH 7.4 has an ionic strength of 0.06. Many of the interactions between GAGs or other PPSs and their binding targets are dependent upon ionic interactions. Thus, working in buffers with low ionic strengths is best when looking for interactions with GAGs or other PPSs. In addition, solutions that have a high concentration of GAG or PPS will have a higher ionic strength due to the large amount of sulfate groups found on the GAGs and PPSs used in these studies.

None of the GAGs, charge-reduced heparin analogs, LMWHs and other PPSs displayed antimicrobial activity at both concentrations tested (**Figures 17, 18, 19 and 22**). The differences between the *P. aeruginosa* growth control and  $\beta$ -cyclodextrin at 0.05 mg/mL or dextran sulfate at 0.1 mg/mL were statistically significant at a significance level of  $P = 0.01$ . These PPSs reduced the growth of *P. aeruginosa* at these concentrations, but not at the other concentration level tested. 2-*O*-desulfated heparin at 0.05 mg/mL increased the growth of *E. coli* at a significance level of  $P = 0.01$ . Centaxarin at 0.05 mg/mL increased the growth of *S. aureus* at a significance level of  $P = 0.01$ . Many of the GAGs and other PPSs increased the growth of *P. aeruginosa*, *E. coli* and *S. aureus*. These data suggests that GAGs and other PPSs may serve as a food source for the bacteria, a subject that has been briefly addressed in the literature.<sup>353-356</sup> Since none of the PPSs showed inherent antimicrobial activity we were able to move forward with experiments studying the ability of GAGs and other PPSs to modulate the antimicrobial activity of linear CAPs.

#### 4.2 Modulation of antimicrobial activity of magainin II, cecropin A, cecropin B and LL-37

##### 4.2.1 Minimum inhibitory concentrations – Experimental technique and results

Minimum inhibitory concentrations for magainin II, cecropin A, cecropin B and LL-37 versus *P. aeruginosa* and *E. coli* were determined using the modified microdilution MIC method. Briefly, overnight cultures of *P. aeruginosa* ATCC 27853 or *E. coli* JM101 ATCC 33876 were grown in Mueller-Hinton broth (Difco) and diluted to an optical density of 0.1 with 10 mM sodium phosphate, pH 7.4. 100  $\mu$ L of the diluted bacteria solution was added to a range of concentrations of magainin II (American Peptide 72-2-26), cecropin A (Porcine, American Peptide 87-9-59), cecropin B (American Peptide 87-9-58) or LL-37 (Innovagen SP-LL37) from pre-made stock

solutions in pre-sterilized 96-well polypropylene plates. The plate was incubated at 37°C for 2 hours. Following this incubation, 200  $\mu$ L of Mueller-Hinton broth was added to each well and the plate was sealed and incubated at 37°C overnight. Optical density (OD) at 600 nm was used to measure the viability of the bacteria in each well. The MIC of LL-37 against *S. aureus* was also identified in the same manner. In these experiments the ionic strength of the sodium phosphate buffer during the binding incubation for the CAPs with the bacteria was 0.06. The MICs for magainin II, cecropin A, cecropin B and LL-37 against *P. aeruginosa*, *E. coli* and *S. aureus* are listed in **Table 4**.

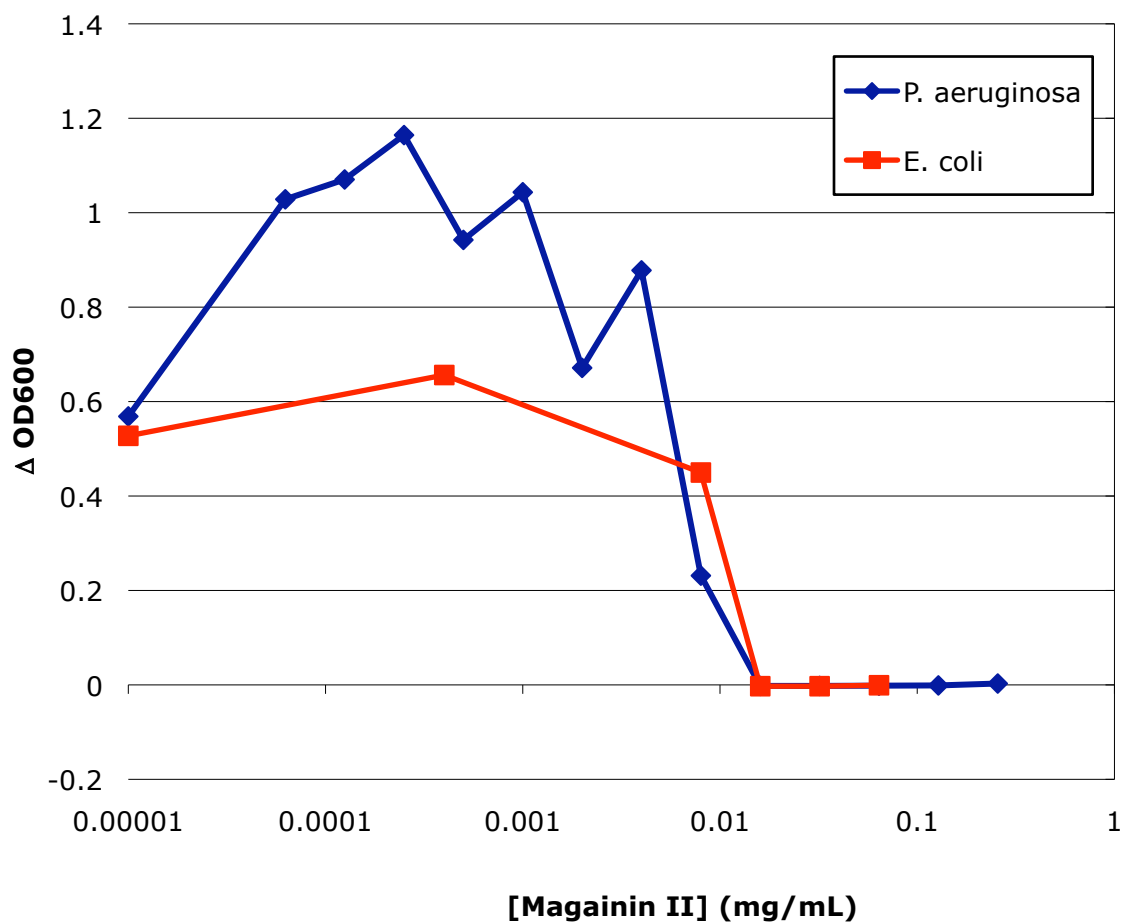


**Figure 21** Magainin II MIC determination against *P. aeruginosa* and *E. coli*. Data points represent the mean of duplicate data points.



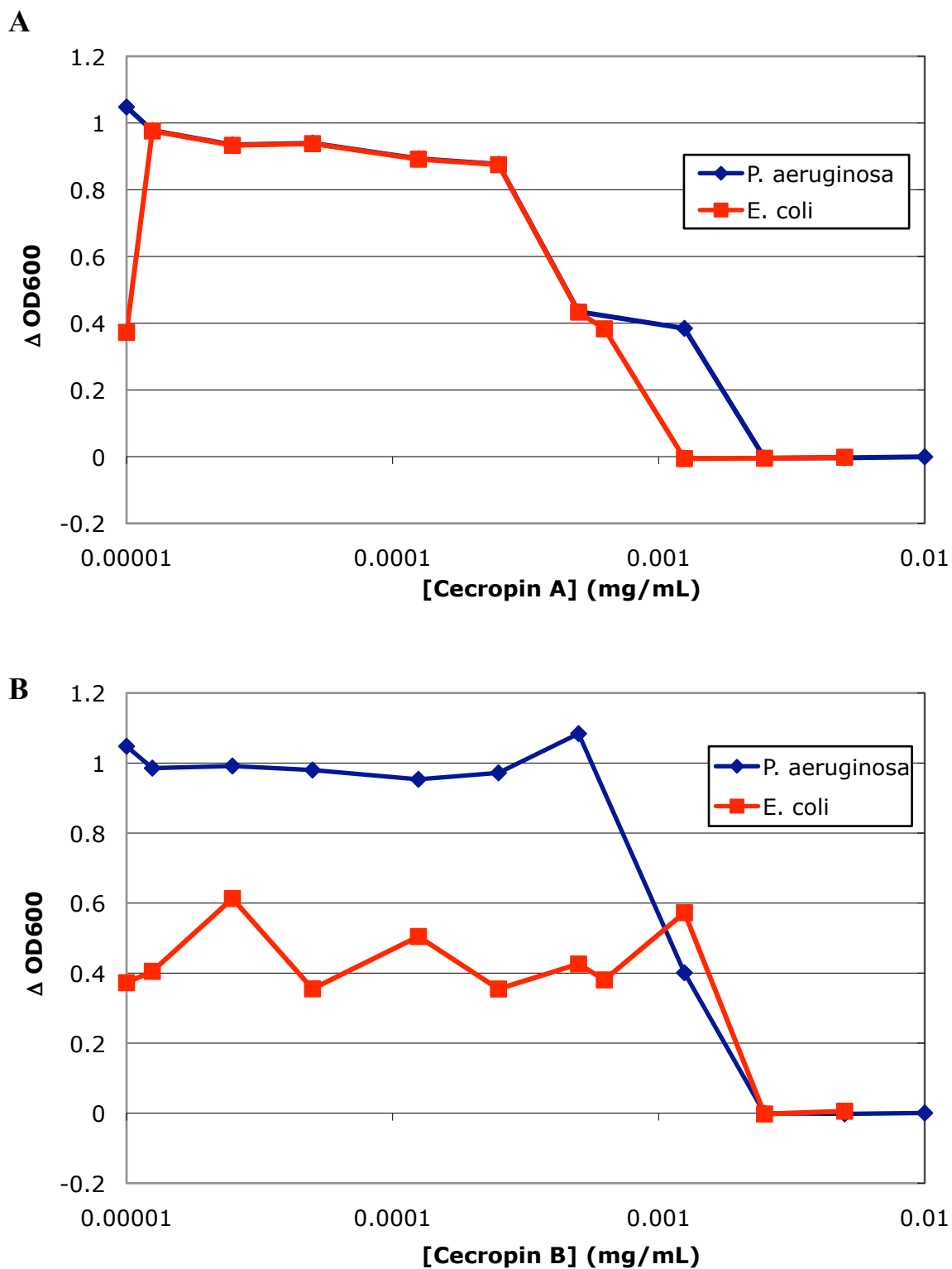


**Figure 22** Cecropin A MICs (A) and cecropin B MICs (B) against *P. aeruginosa* and *E. coli*. Data points represent the mean of duplicate determinations.

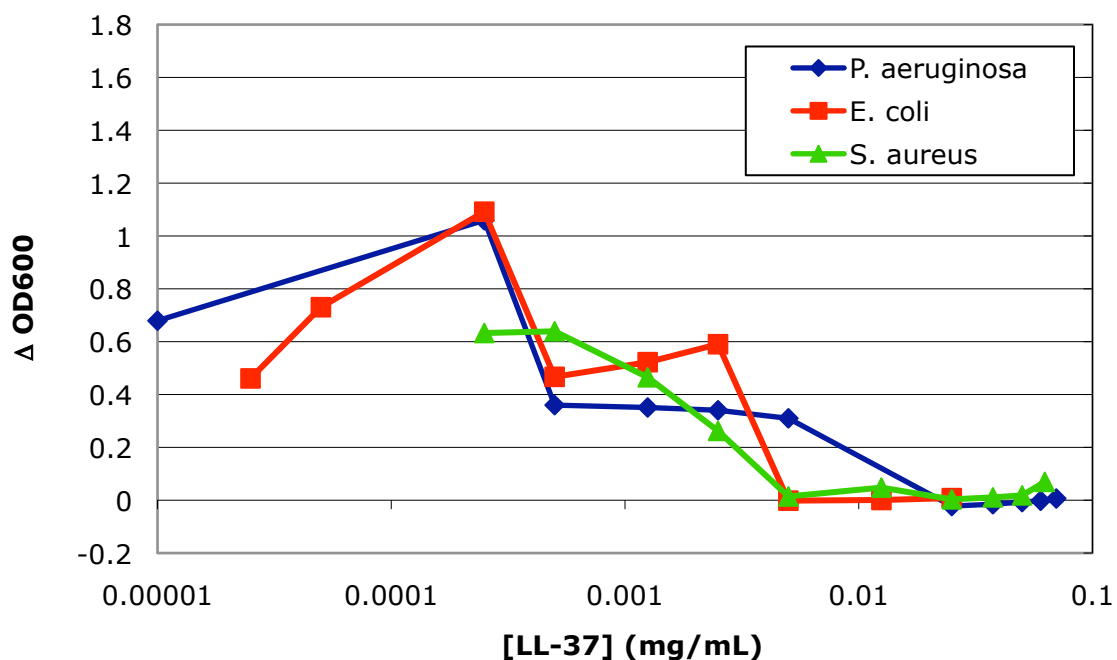


**Figure 23** LL-37 MICs against *P. aeruginosa*, *E. coli* and *S. aureus*. Data points represent the mean of duplicate measurements.

CAP	<i>P. aeruginosa</i>	<i>E. coli</i>	<i>S. aureus</i>
Magainin II	16.0 µg/mL (64.9 µM)	16.0 µg/mL (64.9µM)	NA
Cecropin A	2.5 µg/mL (6.2 µM)	2.5 µg/mL (6.2µM)	NA
Cecropin B	2.5 µg/mL (6.5 µM)	2.5 µg/mL (6.5 µM)	NA
LL-37	25.0 µg/mL (55.6 µM)	5.0 µg/mL (11.1 µM)	50.0 µg/mL (111 µM)

**Table 4** MIC values for magainin II, cecropin A, cecropin B and LL-37 against *P. aeruginosa*, *E. coli* and *S. aureus*.

Note: NA indicates that the CAP is not active against *S. aureus*.

#### 4.2.2 Single point screens for reversal of antimicrobial activity – Experimental technique and results

Once the MICs were identified against *P. aeruginosa*, *E. coli*, and *S. aureus*, single concentration screens were performed to investigate the ability of GAGs, charge-reduced heparin analogs and LMWHs to modulate the antimicrobial activity of the 4 CAPs. The reason for the single point scans was two-fold. First, we were primarily interested in the ability of PPSs to negatively modulate, or reverse, the antimicrobial activity of the 4 CAPs studied. To this end, magainin II, cecropin A, cecropin B and LL-37 were incubated at two concentrations, the MIC and 2-fold the MIC, in 0.1 mg/mL PPS solutions and either *P. aeruginosa*, *E. coli* or *S. aureus*. Secondly, we were interested in the ability of PPSs to positively modulate the antimicrobial activity of CAPs. The secondary structures of magainin II, cecropin A and LL-37 are largely undefined in aqueous environments, but form  $\alpha$ -helices when introduced to a hydrophobic environment, either in a hydrophobic solvent such as hexafluoroisopropanol or by binding to charged lipid membranes<sup>73,101,129</sup>. We hypothesized that PPSs could positively modulate, or promote, the antimicrobial activity of magainin II, cecropin A, cecropin B and LL-37 at levels below the concentration need to kill bacteria. In order to test this magainin II, cecropin A, cecropin B and LL-37 at a quarter their MIC were added to 0.1 mg/mL PPS solutions and incubated with *P. aeruginosa*, *E. coli* or *S. aureus*.

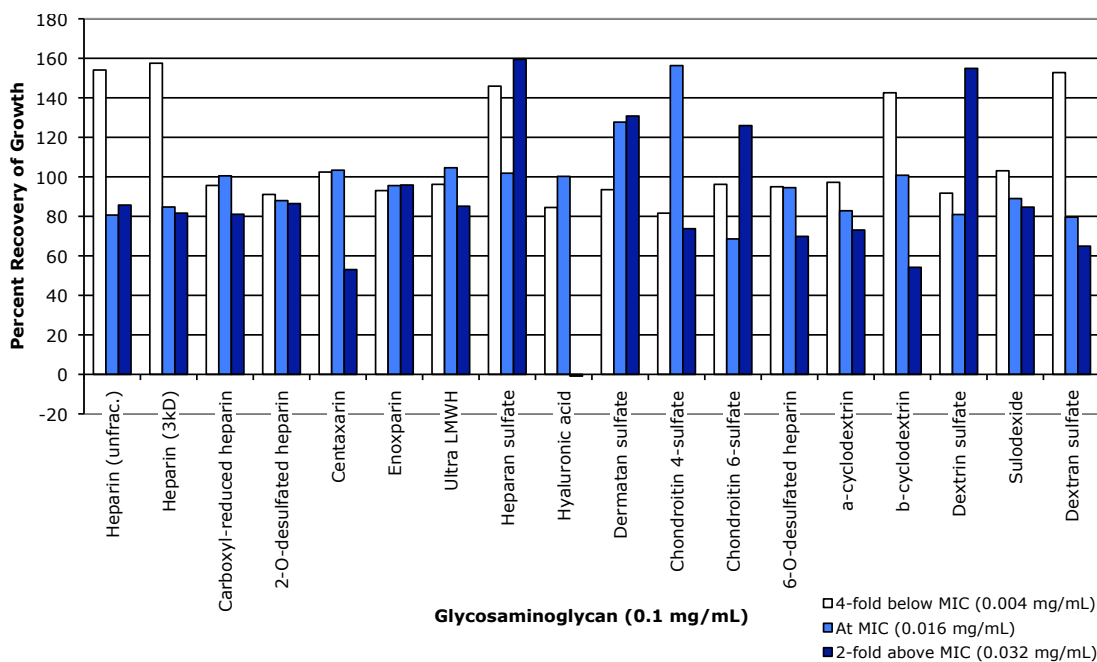
Overnight cultures of *P. aeruginosa*, *E. coli* or *S. aureus* were grown in Mueller-Hinton Broth and then diluted to an absorbance of 0.1 at 600nm using 10 mM sodium phosphate, pH 7.4. The bacteria solution was then further diluted to approximately 100 CFU/mL using 10 mM sodium phosphate, pH 7.4 (ionic strength = 0.06). Aliquots of CAP and PPS were added from stock solutions to wells in pre-sterilized polypropylene 96-well plates to achieve concentrations of magainin II, cecropin A, cecropin B or LL-37 at a quarter their MICs, at their MICs and twice their MICs in 0.1 mg/mL PPS solutions. 100  $\mu$ L of the diluted bacterial solution was then added to the appropriate wells and the

plate was incubated at 37°C for 2 hours. Following this incubation, 200 µL Mueller-Hinton broth was added to the wells and the plate was incubated at 37°C overnight. Bacterial growth was measured using optical density (OD) at 600nm to detect the turbidity in the wells. Sterile water was used in the place of a GAG or PPS to yield a negative growth control. Ciprofloxacin at its MIC for each organism was used as a positive control. These experiments were done as single point screens in order to get an initial understanding for the effect PPSs have on CAPs.

These experiments were designed to examine the ability of PPSs to modulate the antimicrobial activity of magainin II, cecropin A, cecropin B and LL-37 at concentrations below the MIC, at the MIC and above the MIC. In some earlier experiments the MIC was incorrectly identified and these concentrations were not achieved. For positive modulation of antimicrobial activity in the single point screens we expected to see killing of the bacteria at concentrations less than the MIC. In the case of negative modulation of antimicrobial activity we expected to see no killing of bacteria at concentrations at or above the MIC. In both cases this can be seen as reversal of antimicrobial activity. Magainin II showed no positive modulation of antimicrobial activity by GAGs, charge-reduced heparin-analogs, LMWHs or other PPSs (**Figure 24**). All of the PPSs tested were able to negatively modulate the antimicrobial activity of magainin II against *P. aeruginosa* and *E. coli* at 16 µg/mL, the MIC for both organisms. In addition, all PPSs, with the exception of HA, were able to reverse the activity of magainin II against *P. aeruginosa*. Only carboxyl-reduced heparin, C4S and β-cyclodextrin and, to a smaller degree dextrin sulfate and sulodexide, were able to reverse the activity of magainin II against *E. coli* at two times the MIC.

Cecropin A showed no positive modulation of antimicrobial activity by GAGs, charge-reduced heparin-analogs, LMWHs or other PPSs (**Figures 25 and 26**). In contrast to the modulation of magainin II, none of the non-heparin GAGs reversed the antimicrobial activity of cecropin A versus *P. aeruginosa* at 2.5 and 5.0 µg/mL. In

A



B

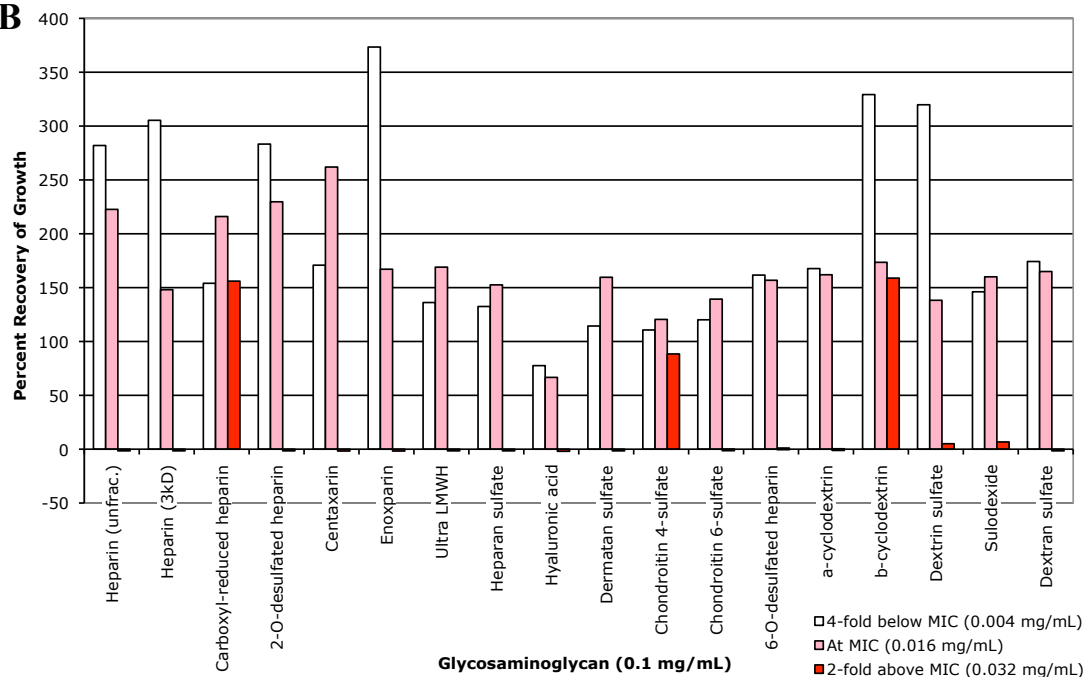


**Figure 24** Effect of GAGs, charge-reduced heparin analogs and LMWHs on the antimicrobial activity of magainin II at 4.0, 16.0 and 32.0 mg/mL versus *P. aeruginosa* (A) and *E. coli* (B). Single data points shown.

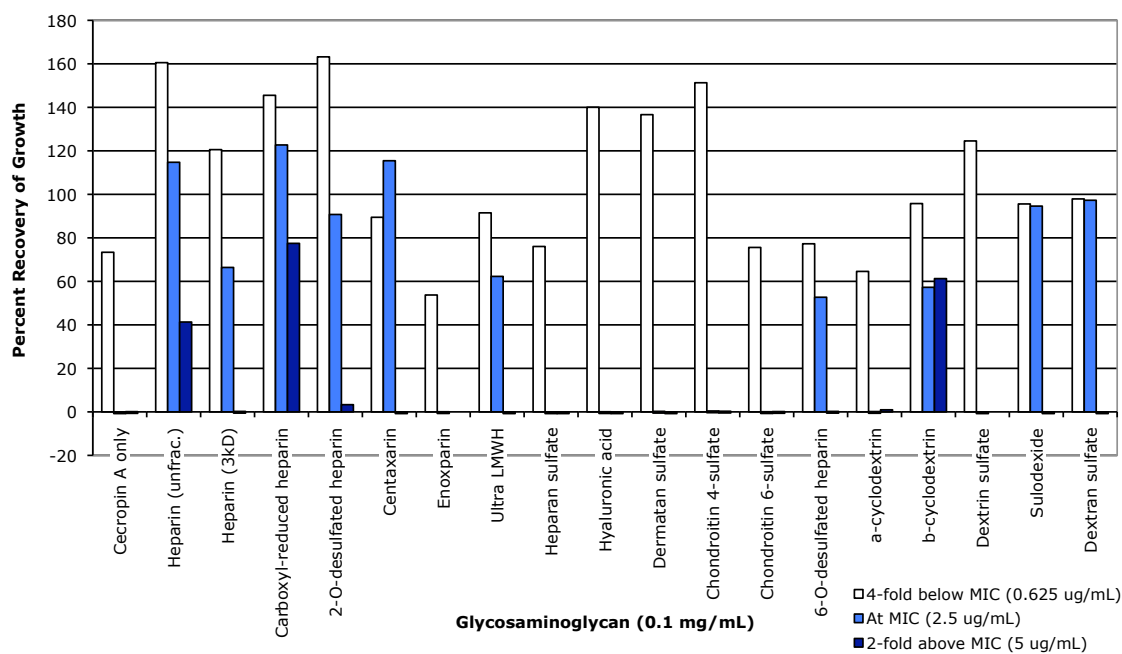


**Figure 25** Effect of GAGs, charge-reduced heparin analogs and LMWHs on the antimicrobial activity of cecropin A four-fold below MIC, at MIC and 2-fold above MIC versus *P. aeruginosa*. Single data points shown.

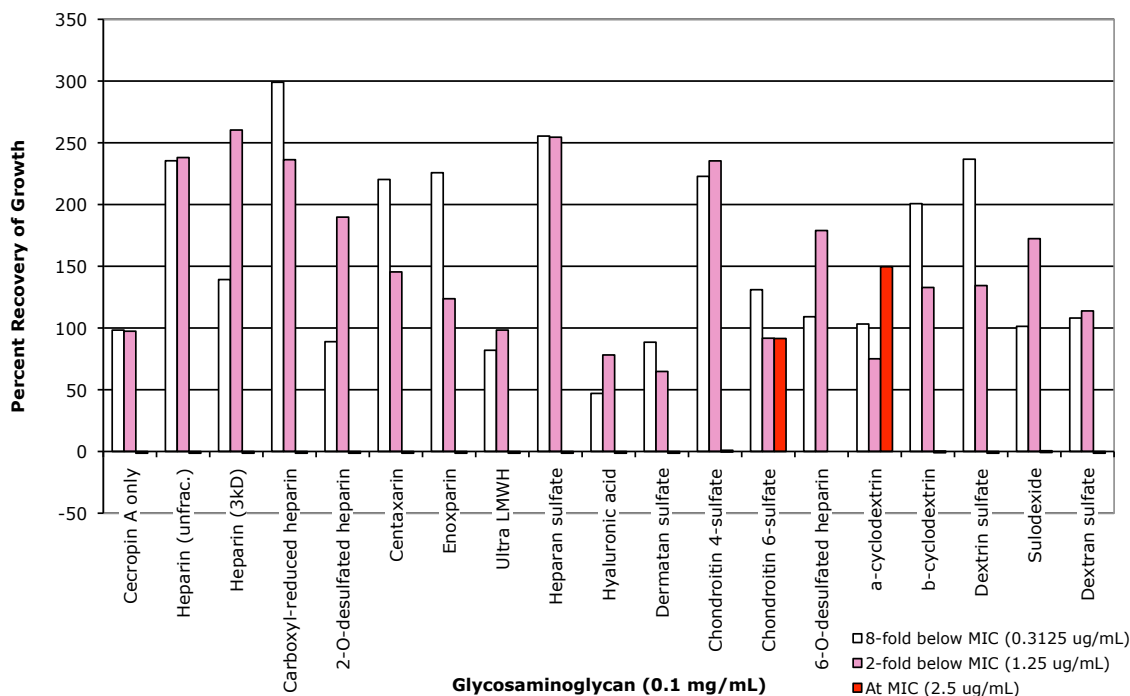
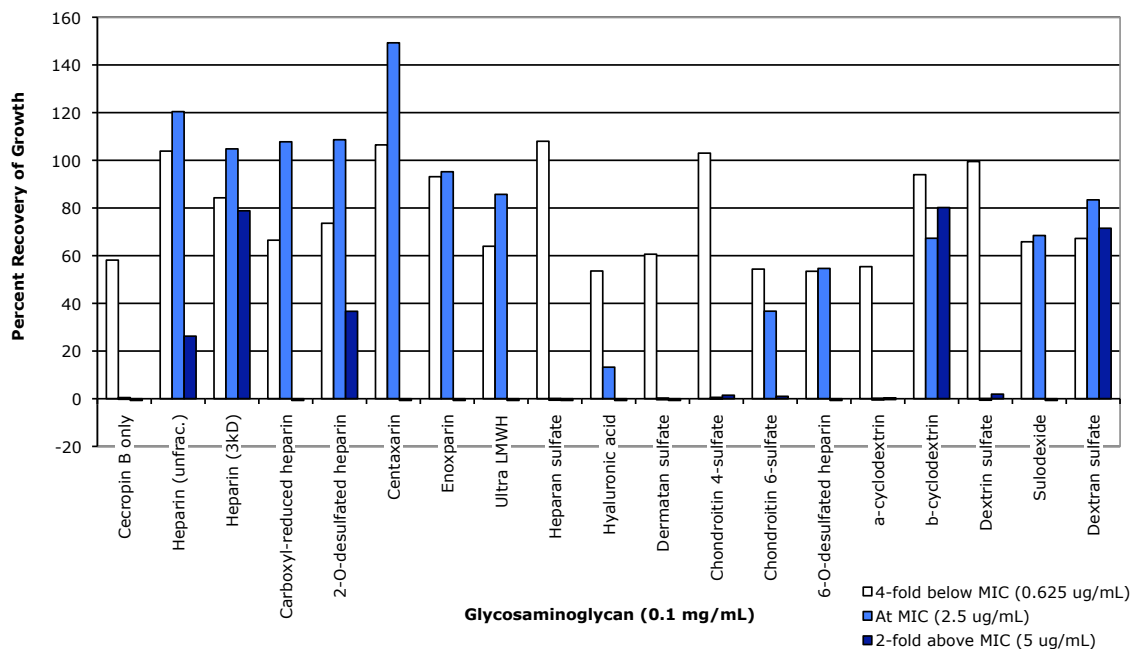


**Figure 26** Effect of GAGs, charge-reduced heparin analogs, LMWHs and other PPSs on the antimicrobial activity of cecropin A versus *P. aeruginosa* at 0.325, 1.25 and 2.5  $\mu\text{g/mL}$ . Single data points shown.

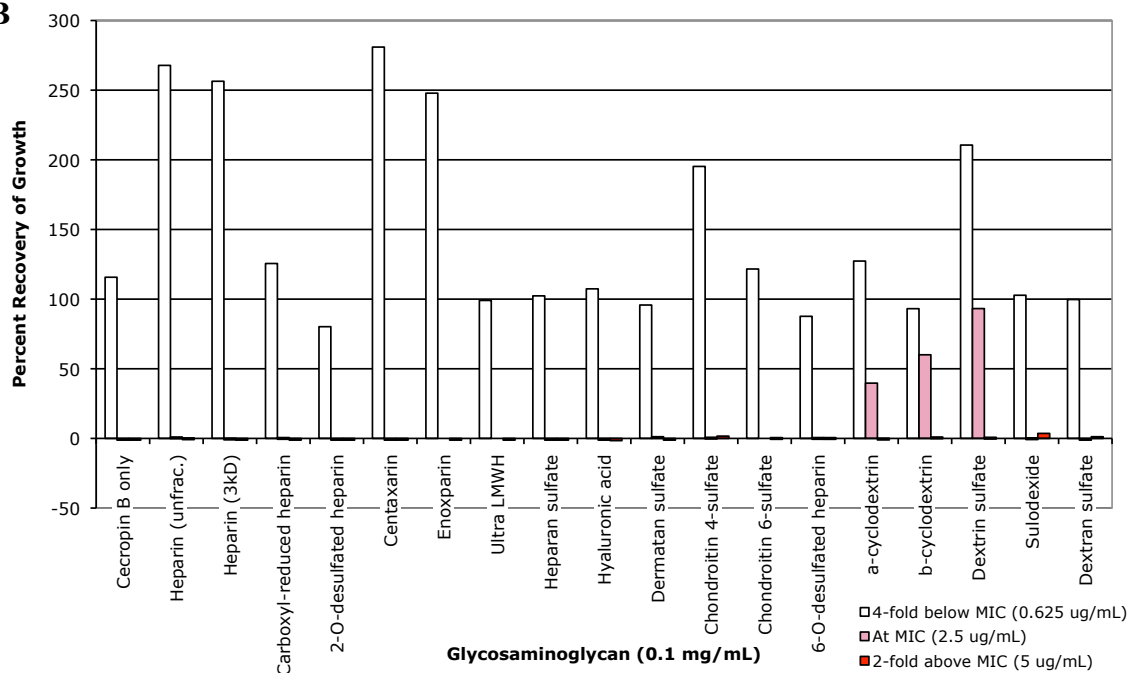
In addition, only heparin, carboxyl-reduced heparin and  $\beta$ -cyclodextrin were able to reverse the antimicrobial activity of cecropin A versus *P. aeruginosa* at 5.0  $\mu\text{g/mL}$ . Only C6S and  $\alpha$ -cyclodextrin were able to negatively modulate cecropin A versus *E. coli* at 2.5  $\mu\text{g/mL}$ . A single point screen was not performed looking at the ability of GAGs, charge-reduced heparin analogs, LMWHs and other PPSs to negatively modulate the antimicrobial activity of cecropin A at 2X the MIC versus *E. coli*. These data points were collected in later experiments.

Cecropin B showed very similar reversal patterns to cecropin A in the single point screens. None of the GAGs, charge-reduced heparin analogs, LMWHs and other PPSs were able to positively modulate the antimicrobial activity of cecropin B against *P. aeruginosa* or *E. coli* (**Figure 27**). HS, DS and C4S did not negatively modulate the antimicrobial activity of cecropin B versus *P. aeruginosa* at 2.5 or 5.0  $\mu\text{g/mL}$ . Only

A

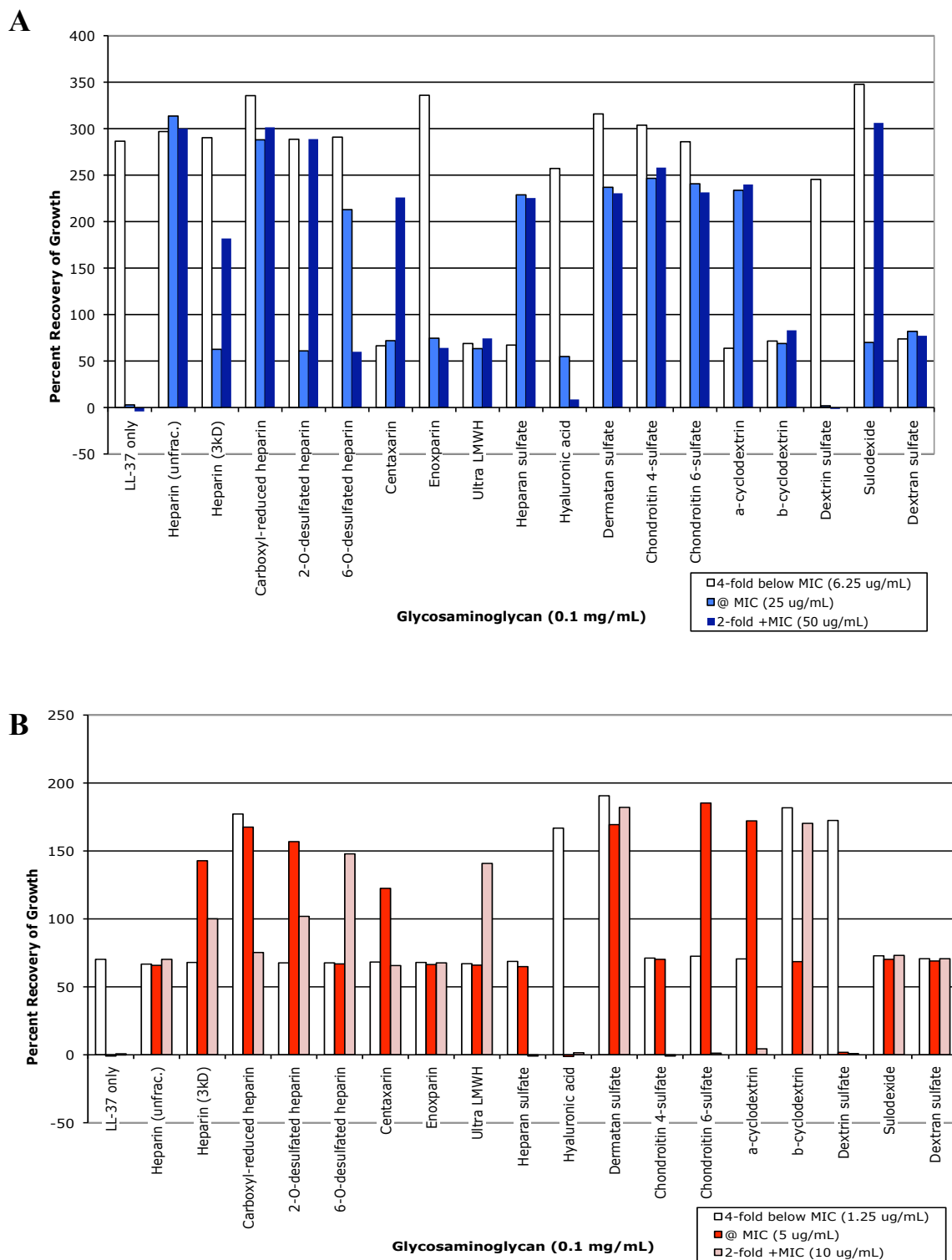


B



**Figure 27** Effect of GAGs, charge-reduced heparin analogs and LMWHs on the antimicrobial activity of cecropin B 4-fold below MIC, at MIC and 2-fold above MIC versus *P. aeruginosa* (A) and *E. coli* (B). Single data points shown.





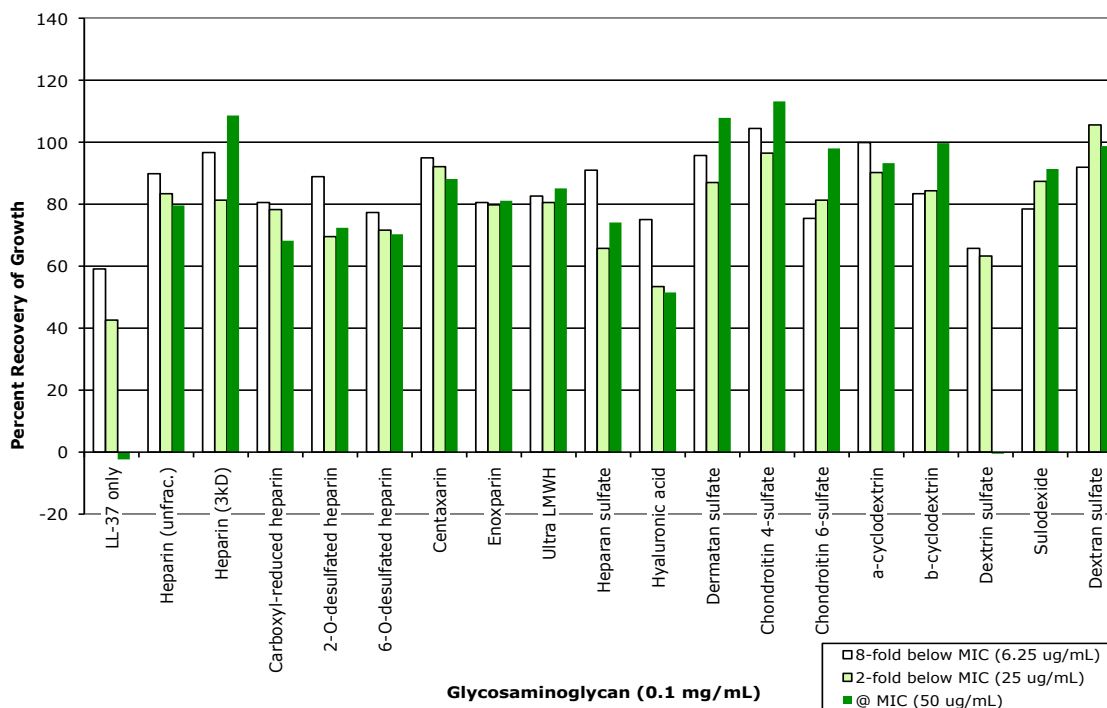


**Figure 29** Single point screen showing the effect of GAGs, charge-reduced heparin analogs, LMWHs and other PPSs on the antimicrobial activity of LL-37 against *S. aureus*.

unfractionated heparin, 3 kD heparin, 2-*O*-desulfated heparin,  $\beta$ -cyclodextrin and dextran sulfate negatively modulated cecropin B at 5.0  $\mu\text{g/mL}$  against *P. aeruginosa*.

None of the GAGs, charge-reduced heparin analogs, LMWHs or other PPSs positively modulated the antimicrobial activity of LL-37 versus *P. aeruginosa*, *E. coli* or *S. aureus* (**Figures 28** and **29**). Every PPS tested, with the exception of dextrin sulfate, reversed the antimicrobial activity of LL-37 at both 25.0 and 50.0  $\mu\text{g/mL}$  against *P. aeruginosa*. Interestingly, many of the LMWHs were not able to fully reverse the antimicrobial activity of LL-37 against *P. aeruginosa*. All of the GAGs, charge-reduced heparin analogs, LMWHs and other PPSs, with the exception of HA and dextrin sulfate, showed negative modulation of LL-37 versus *E. coli*. Of these, HS, C4S, C6S, and  $\alpha$ -cyclodextrin were not able to reverse the antimicrobial activity of LL-37 versus *E. coli* at

10.0 µg/mL. All of the PPSs tested, with the exception of dextrin sulfate, were able to negatively modulate the antimicrobial activity of LL-37 versus *S. aureus* at the MIC. A single point screen was not performed looking at the ability of GAGs, charge-reduced heparin analogs, LMWHs and other PPSs to negatively modulate the antimicrobial activity of LL-37 at 2X the MIC versus *S. aureus*. These data points were collected in later experiments.

The results of the single concentration scans were used to direct the focus of future experiments. Based on these results we decided to concentrate on the ability of GAGs, charge-reduced heparin analogs and LMWHs to modulate the antimicrobial activity of magainin II, cecropin A, cecropin B and LL-37 versus *P. aeruginosa*, *E. coli* and *S. aureus*.

#### 4.2.3 Concentration dependent reversal of antimicrobial activity by GAGs, charge-reduced heparin analogs and LMWHs – experimental techniques

Concentration dependent studies were done in the same manner as the single point screens used to study the effect of GAGs, charge-reduced heparin analogs, LMWHs and other PPSs on CAP antimicrobial activity. Briefly, cultures of *P. aeruginosa*, *E. coli* or *S. aureus* were grown overnight in Mueller-Hinton broth and diluted to an OD of 0.1 in 10 mM sodium phosphate, pH 7.4. The bacterial solution was then further diluted to approximately 100 CFU/mL using 10 mM sodium phosphate, pH 7.4 (ionic strength = 0.06). CAP, either magainin II, cecropin A, cecropin B or LL-37, was added to the wells of a pre-sterilized 96-well polypropylene plate in the appropriate volume to give a final concentration of 2X the MIC. PPSs were added to wells to give a final concentration range of 0.25 – 200 µg/mL. 100 µL of the diluted bacterial solution and 10 mM sodium phosphate, pH 7.4, were added to give a volume of 200 uL in each well. The plates were sealed and incubated at 37°C for 2 hours, followed by the addition of 200 uL Mueller-

Hinton broth and an overnight incubation at 37°C. The next day bacterial growth in each well, indicated by turbidity, was read using optical density at 600nm. Sterile water was used in the place of a GAG or PPS to yield a negative growth control. Ciprofloxacin (Sigma Aldrich 17850) at its MIC for each organism was used as a positive control. Many of the GAGs and PPSs investigated in this work are extremely heterogenous and cannot be assigned specific molecular weights. We used the average disaccharide molecular weight for each GAG or PPS to calculate the molarity of the GAG or PPS. This allowed us to compare the antimicrobial activity modulatory potentials of all the GAGs and PPSs directly. A two-way paired student's T-test was used to determine statistical significance.

#### 4.2.4 Modulation of magainin II antimicrobial activity by GAGs, charge-reduced heparin analogs and LMWHs

All but one of the GAGs, charge-reduced heparin analogs and LMWHs were negative modulators of the antimicrobial activity of magainin II against *P. aeruginosa* (**Figure 30**). Examining the reversal pattern by class of PPS (GAG, charge-reduced heparin analog or LMWH), gives some insight into the structural and chemical requirements for reversal of the antimicrobial activity. It is clear that heparin is the best GAG negative modulator of magainin II versus *P. aeruginosa* (**Figure 31**). HA is the only GAG, and only PPS tested, that does not reverse the antimicrobial activity of magainin II against *P. aeruginosa*. HS, DS, C4S and C6S reverse the antimicrobial activity of magainin II against *P. aeruginosa* with similar efficacies. It takes approximately 10X more of these GAGs to reverse the antimicrobial activity as compared to the amount of heparin needed.

Despite the reduction in negative charge, there is no significant difference between the reversal patterns of heparin and the charge-reduced heparin analogs (**Figure 3**). It takes a ratio of less than 1:1 for heparin and the charge-reduced heparin analogs to

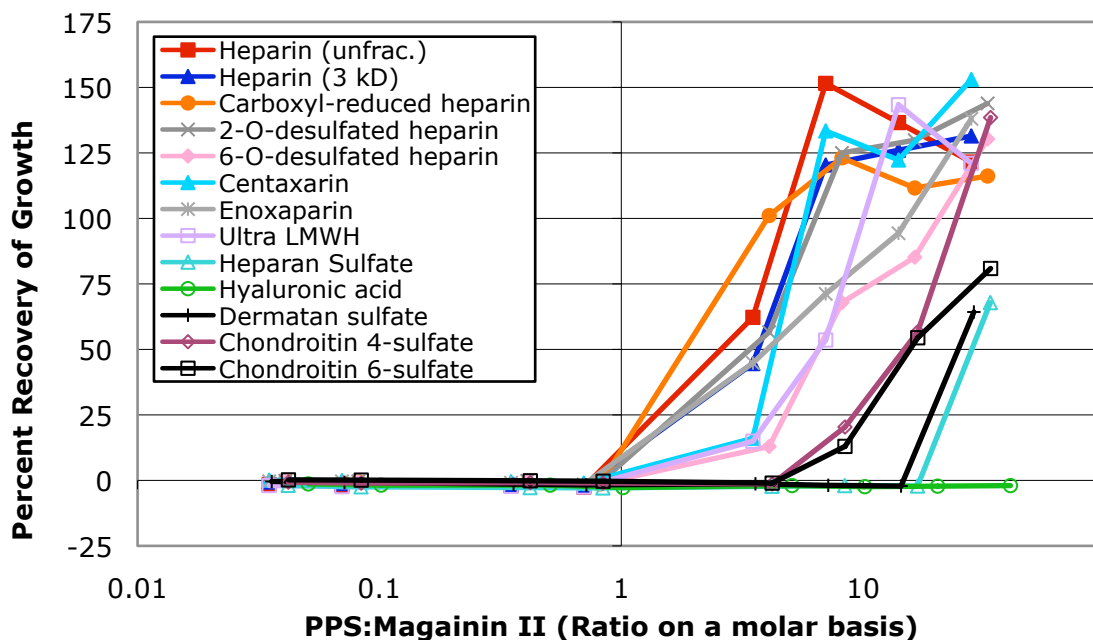


**Figure 30** Reversal of magainin II antimicrobial activity versus *P. aeruginosa* by GAGs, charge-reduced heparin analogs and LMWHs. Average of duplicate data points shown.

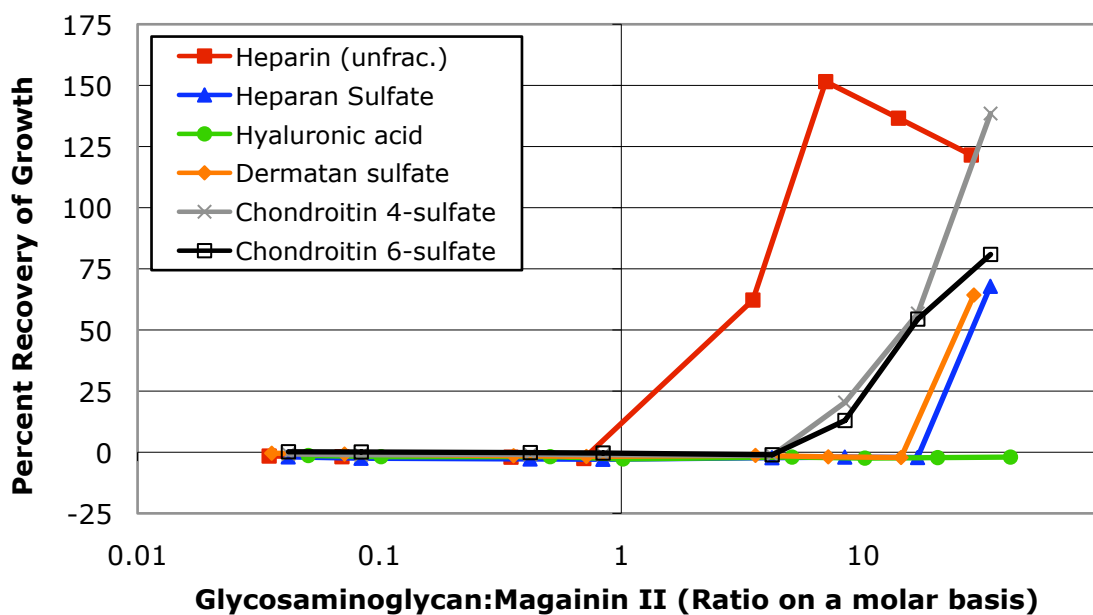


**Figure 31** Reversal of antimicrobial activity of magainin II versus *P. aeruginosa* by GAGs. Average of duplicate data points shown.

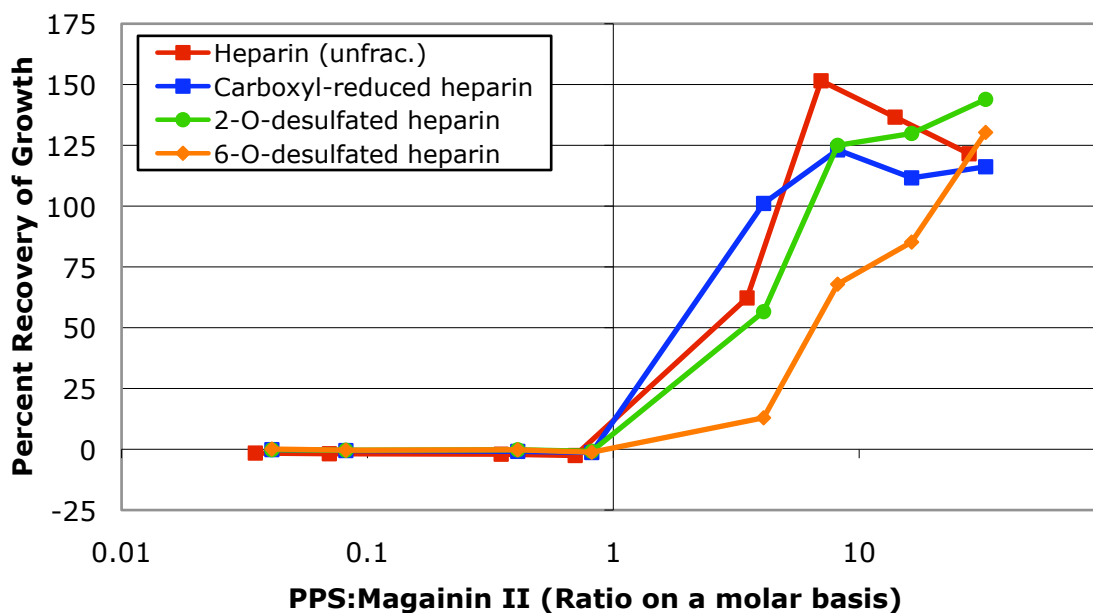


**Figure 32** Reversal of antimicrobial activity of magainin II versus *P. aeruginosa* by heparin and charge-reduced heparin analogs. Average of duplicate data points shown.

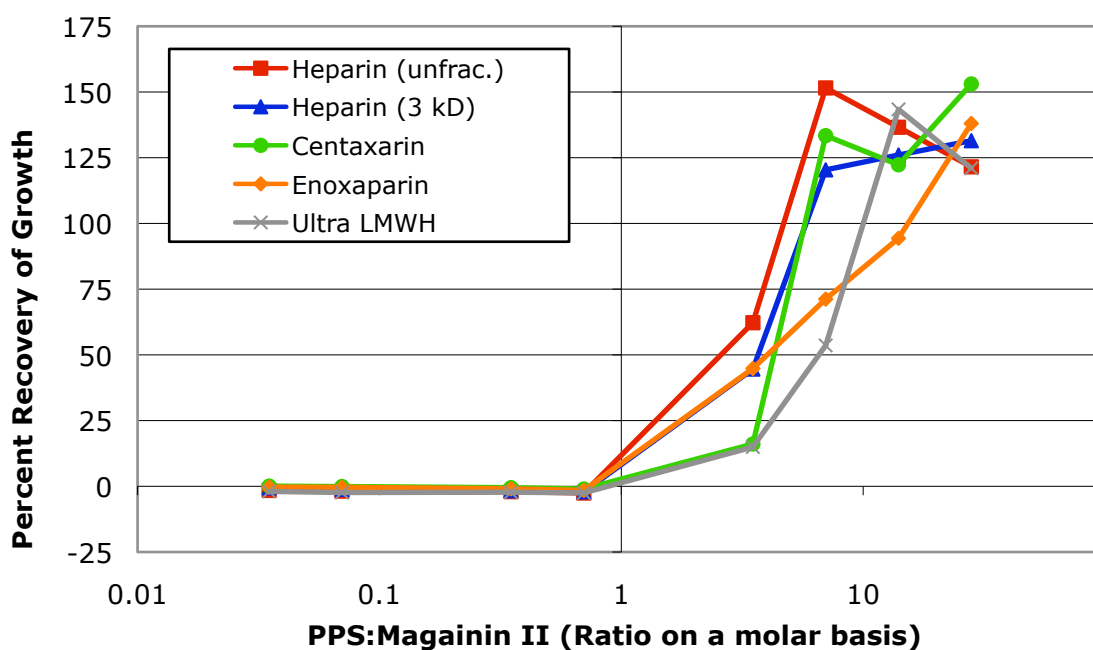


**Figure 33** Reversal of antimicrobial activity of magainin II versus *P. aeruginosa* by heparin and LMWHs. Average of duplicate data points shown.

reverse the antimicrobial activity of magainin II against *P. aeruginosa*. 6-*O*-desulfated heparin is slightly less efficient at modulating the antimicrobial activity of magainin II as compared to heparin and 2-*O*-desulfated heparin, indicating that sulfate group at the C6 position of the glucosamine residues may play a key role in the binding interaction between heparin and magainin II. Interestingly, molecular weight does not have any effect on the reversal of magainin II antimicrobial activity. There is no significant difference between the reversal patterns of heparin and the LMWHs (**Figure 33**).

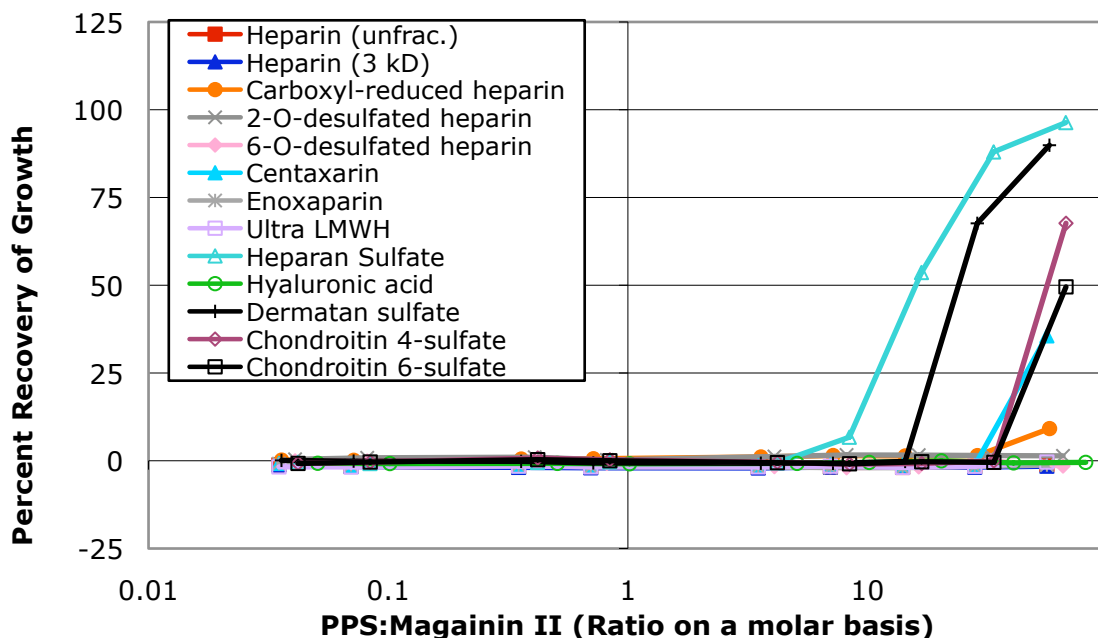


**Figure 34** Reversal of antimicrobial activity of magainin II versus *E. coli* by GAGs, charge-reduced heparin analogs and LMWHs. Average of duplicate data points shown.

Of particular interest are the differences between reversal patterns for magainin II antimicrobial activity against *P. aeruginosa* and *E. coli*. While heparin is the best negative modulator of magainin II antimicrobial activity against *P. aeruginosa*, it shows no reversal of antimicrobial activity against *E. coli*. HS and DS, two of the worst

modulators of antimicrobial activity of magainin II against *P. aeruginosa*, are the best modulators of antimicrobial activity against *E. coli* (**Figure 34**). On the whole, the PPSs are less active modulators of magainin II antimicrobial activity against *E. coli* than against *P. aeruginosa*. Reversal of antimicrobial activity against *E. coli* requires a PPS:magainin II molar ratio of greater than 10:1, while reversal against *P. aeruginosa* requires a molar ratio of 1:1 on average.

#### 4.2.5 Modulation of cecropin A antimicrobial activity by GAGs, charge-reduced heparin analogs and LMWHs

Cecropin A antimicrobial activity versus *P. aeruginosa* (**Figure 35**) is reversed by fewer PPSs as compared to the reversal pattern for magainin II activity against *P. aeruginosa*. In addition, fewer of the PPSs are able to completely reverse the antimicrobial activity versus *P. aeruginosa* as compared to the reversal pattern for magainin II. Overall more PPS is required to reverse cecropin A antimicrobial activity as compared to magainin II activity against *P. aeruginosa*. Again, heparin is one of the best negative modulators of cecropin A activity against *P. aeruginosa*.

Heparin is the only GAG capable of reversing the antimicrobial activity of cecropin A against *P. aeruginosa* (**Figure 36**). This may be due to the increased anionic charge of heparin or the unique structure of heparin. Surprisingly HS shows no reversal activity. Even though heparin and HS are commonly thought to be essentially the same by many researchers, HS is comprised of a much more diverse sequence.

The charge-reduced heparin analogs show little difference in their ability to reverse the anti-*Pseudomonas* activity of cecropin A (**Figure 37**). Heparin and carboxyl-reduced heparin show no difference in their ability to modulate cecropin A activity. 2-*O*-desulfated heparin much larger requires a larger ratio (approximately 100:1 on a molar basis) to reverse compared to heparin and carboxyl-reduced heparin, but achieves full reversal of cecropin A activity. 6-*O*-desulfated heparin, on the other hand, reverses at a



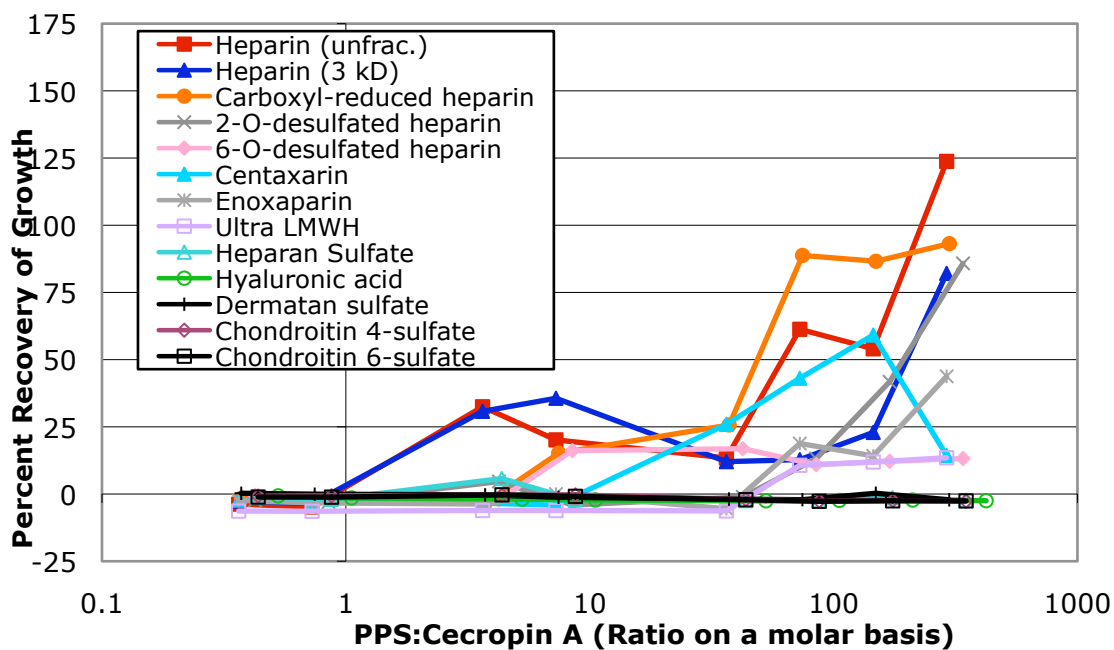


**Figure 35** Reversal of antimicrobial activity of cecropin A versus *P. aeruginosa* by GAGs, charge-reduced heparin analogs and LMWHs. Average of triplicate data points shown with error bars omitted for ease of viewing.

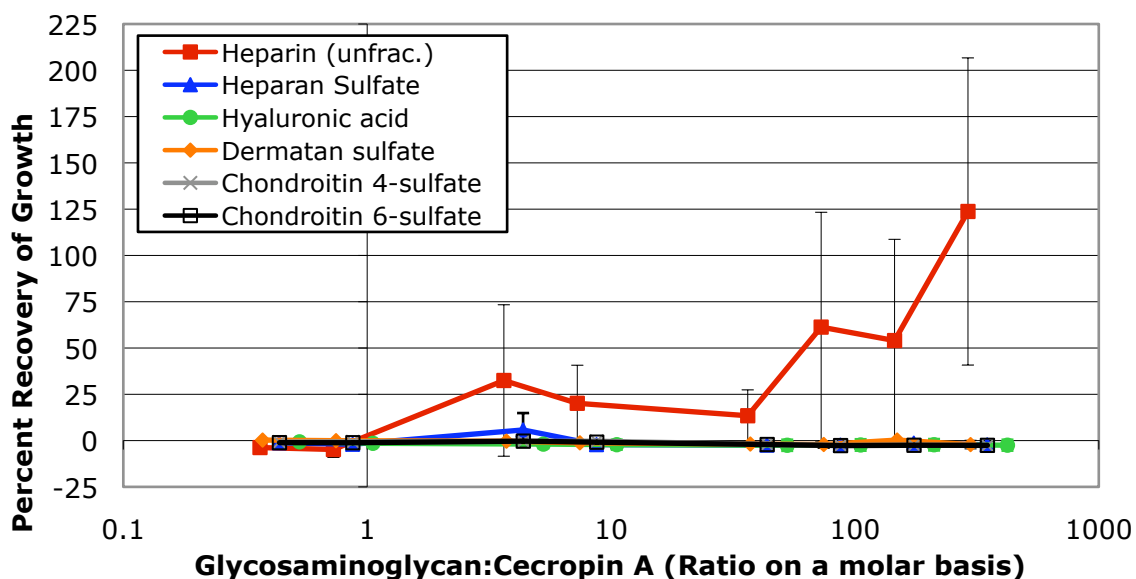


**Figure 36** Reversal of antimicrobial activity of cecropin A versus *P. aeruginosa* by GAGs. Data points represent the mean  $\pm$  standard error of triplicate determinations.

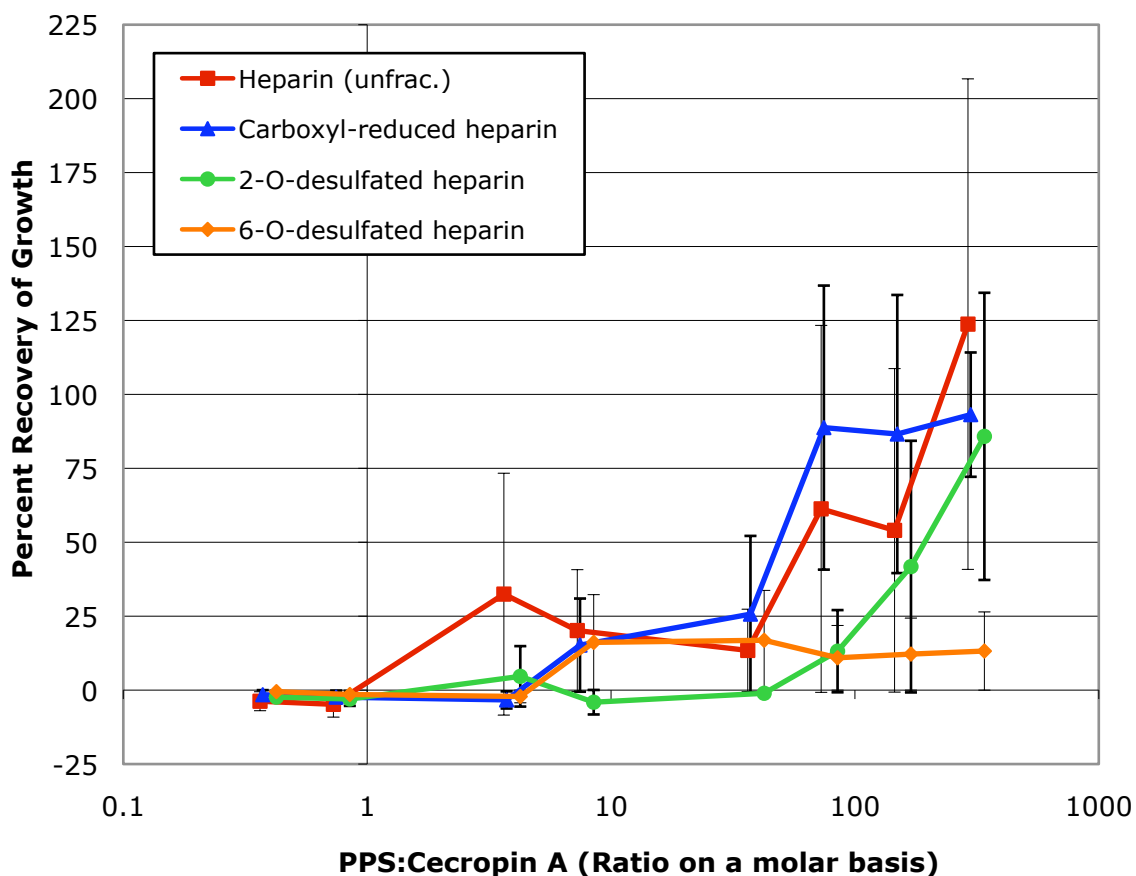


**Figure 37** Reversal of antimicrobial activity of cecropin A versus *P. aeruginosa* by heparin and charge-reduced heparin analogs. Data points represent the mean  $\pm$  standard error of triplicate measurements.

lower level (10:1), but cannot fully reverse the anti-*P. aeruginosa* activity of cecropin A. This indicates that both the 2-*O* and 6-*O* sulfate groups are fundamental for the interaction between cecropin A and heparin.

There is no significant difference between heparin and the LMWHs using a significance factor of  $P = 0.01$  (**Figure 38**). Enoxaparin and ultra LMWH are less efficient at reversing the anti-*P. aeruginosa* activity of cecropin A as compared to heparin and the other LMWHs because they can not fully reverse cecropin A activity. Both heparin and 3 kD heparin reverse cecropin A antimicrobial activity at low ratios, but they do not achieve full reversal until a PPS:cecropin A molar ratio of approximately 300:1.

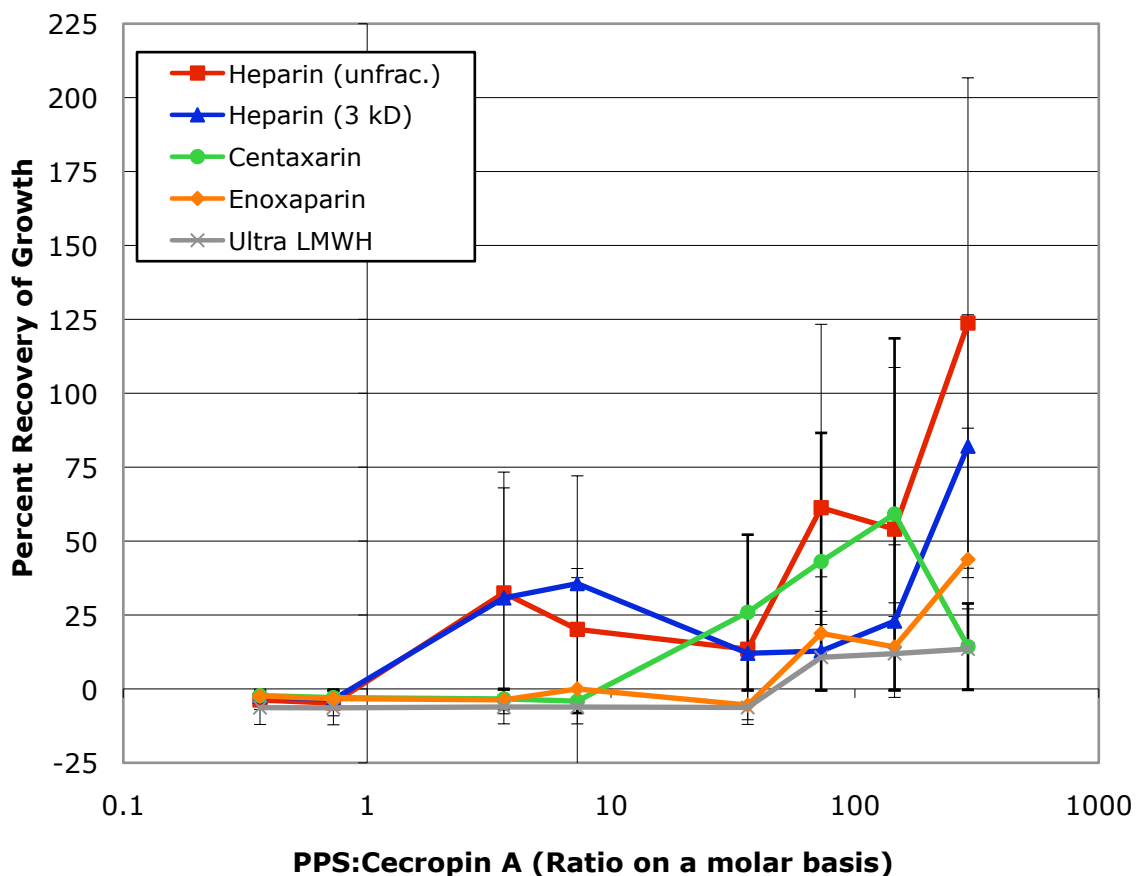


**Figure 38** Reversal of antimicrobial activity of cecropin A versus *P. aeruginosa* by heparin and LMWHs. Data points represent the mean  $\pm$  standard error of triplicate measurements.

A surprising result was the complete inability of the PPSs tested to reverse the antimicrobial activity of cecropin A against *E. coli* (**Figure 39**). This may be due to the two helices in the secondary structure of cecropin A (**Figure 3C**). Since one  $\alpha$ -helix is highly hydrophobic and the other is amphipathic it is possible that cecropin A binds too tightly to the *E. coli* outer membrane to be displaced by any of the PPSs. Another possibility is that PPSs bind to cecropin A, but cannot disrupt the CAP binding to the *E. coli* membrane and subsequent antimicrobial activity. Thus, binding of the hydrophobic tail of cecropin A to the bacterial cell can not be blocked by GAGs and other PPSs binding to the amphipathic helix.

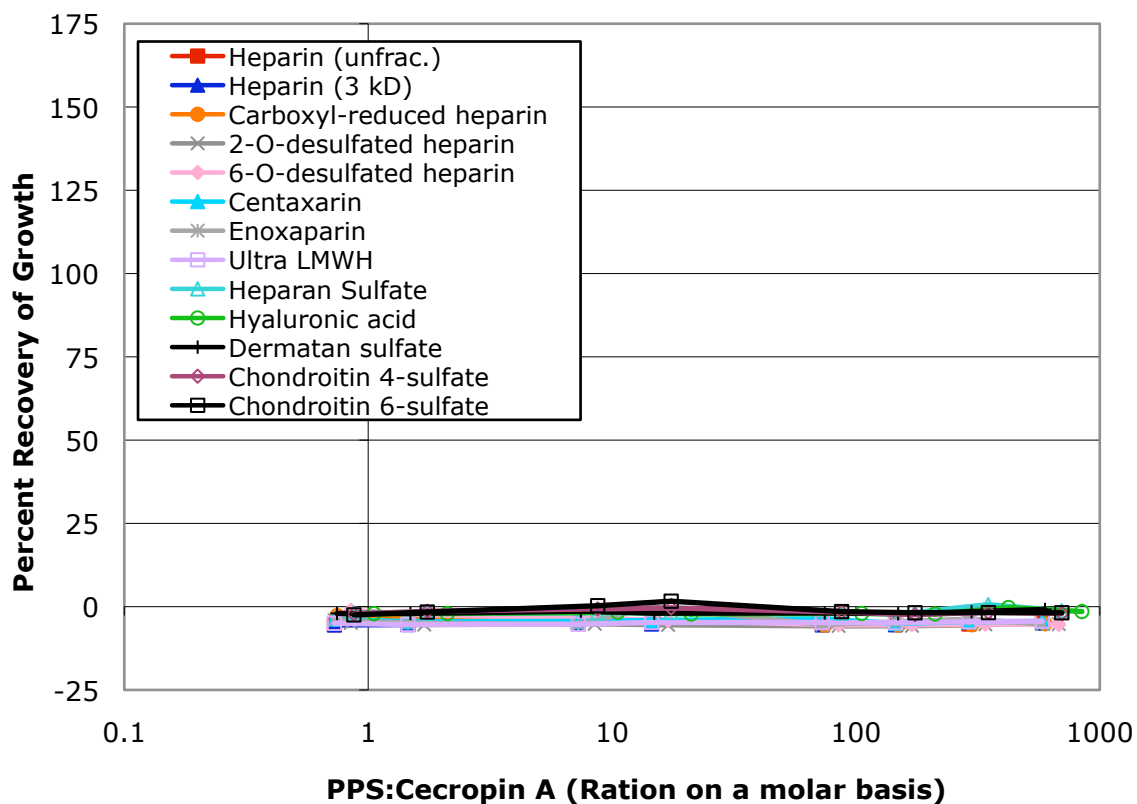


**Figure 39** Reversal of antimicrobial activity of cecropin A versus *E. coli* by GAGs, charge-reduced heparin analogs and LMWHs. Means of triplicate data points are plotted.

#### 4.2.6 Modulation of cecropin B antimicrobial activity by GAGs, charge-reduced heparin analogs and LMWHs

The reversal pattern for cecropin B antimicrobial activity versus *P. aeruginosa* (**Figure 40**) is similar to the reversal pattern for cecropin A activity against *P. aeruginosa*. As is the case for cecropin A, fewer of the PPSs are able to completely reverse the antimicrobial activity versus *P. aeruginosa* as compared to the reversal pattern for magainin II. On the whole more PPS is required to reverse cecropin B antimicrobial activity as compared to magainin II activity against *P. aeruginosa*. Yet again heparin is the best negative modulator of all the PPSs tested for their ability to reverse cecropin A activity against *P. aeruginosa*.

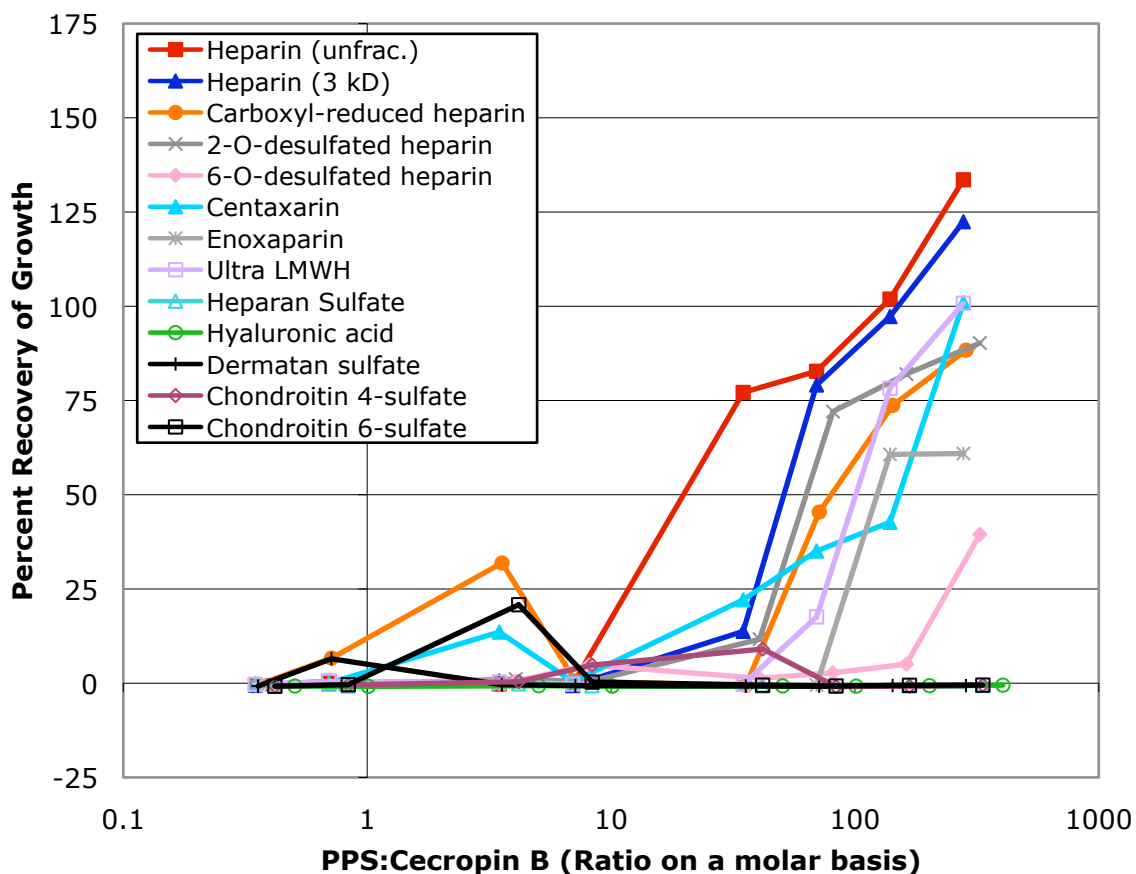


**Figure 40** Reversal of antimicrobial activity of cecropin B versus *P. aeruginosa* by GAGs, charge-reduced heparin analogs and LMWHs. Means of duplicate data points are shown.

Comparing the ability of GAGs to reverse the antimicrobial activity of cecropin B against *P. aeruginosa* (**Figure 41**) it is apparent that heparin is the only GAG able to negatively modulate cecropin B. The difference between heparin and all of the other GAGs is statistically significant at a significance level of  $P = 0.05$  between the molar ratios of approximately 300:1 to approximately 40:1. These results mirror the results of GAG reversal of cecropin A activity against *P. aeruginosa*, but in this case heparin is able to completely reverse cecropin B activity in the concentration range tested.

Heparin is the best negative modulator of cecropin B anti-*P. aeruginosa* activity when compared to the charge-reduced heparin analogs tested (**Figure 42**). The

difference between carboxyl-reduced heparin and heparin is statistically significant at a significance level of  $P = 0.05$  at molar ratios of approximately 70:1 and 35:1. The reversal levels for 6-*O*-desulfated heparin are significantly different from those of heparin at a significance level of  $P = 0.05$  for molar ratios between 140:1 and 35:1. These results indicate that each of the anionic groups on heparin tested is important for modulation of cecropin B anti-*P. aeruginosa* activity. As is seen with cecropin A, the 6-*O*-sulfate group on glucosamine may play a fundamental role in the interaction between cecropin B and heparin.

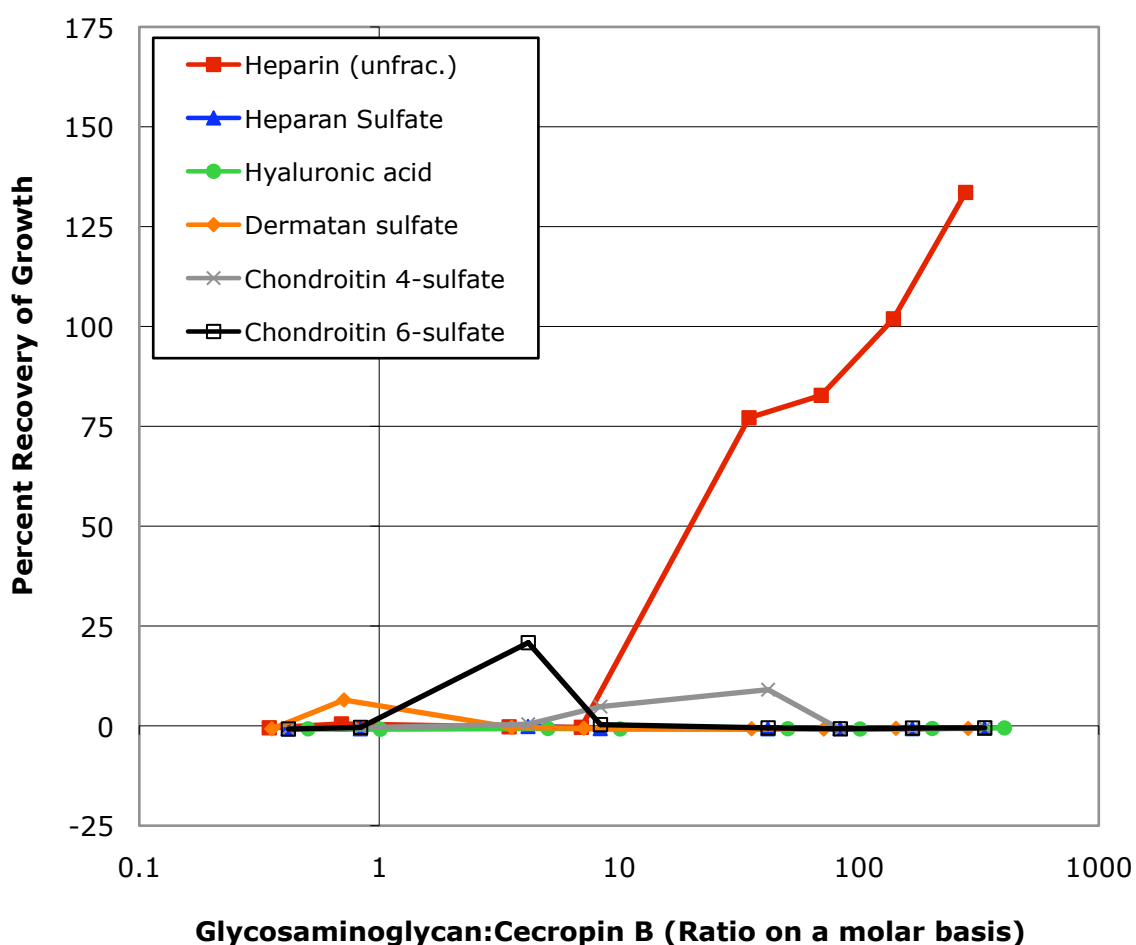


**Figure 41** Reversal of antimicrobial activity of cecropin B versus *P. aeruginosa* by GAGs. Data points represent the mean of duplicate measurements.

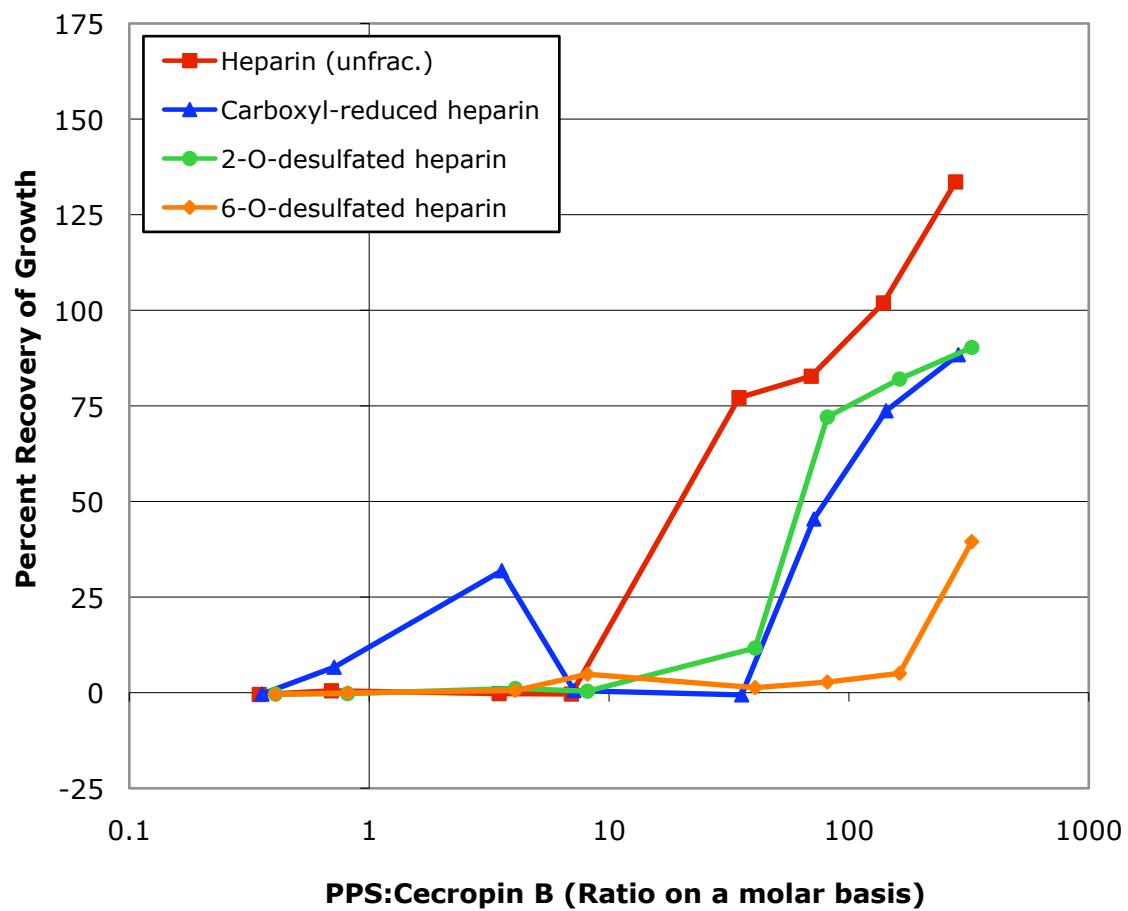


**Figure 42** Reversal of antimicrobial activity of cecropin B versus *P. aeruginosa* by heparin and charge-reduced heparin analogs. Mean of duplicate data points shown.

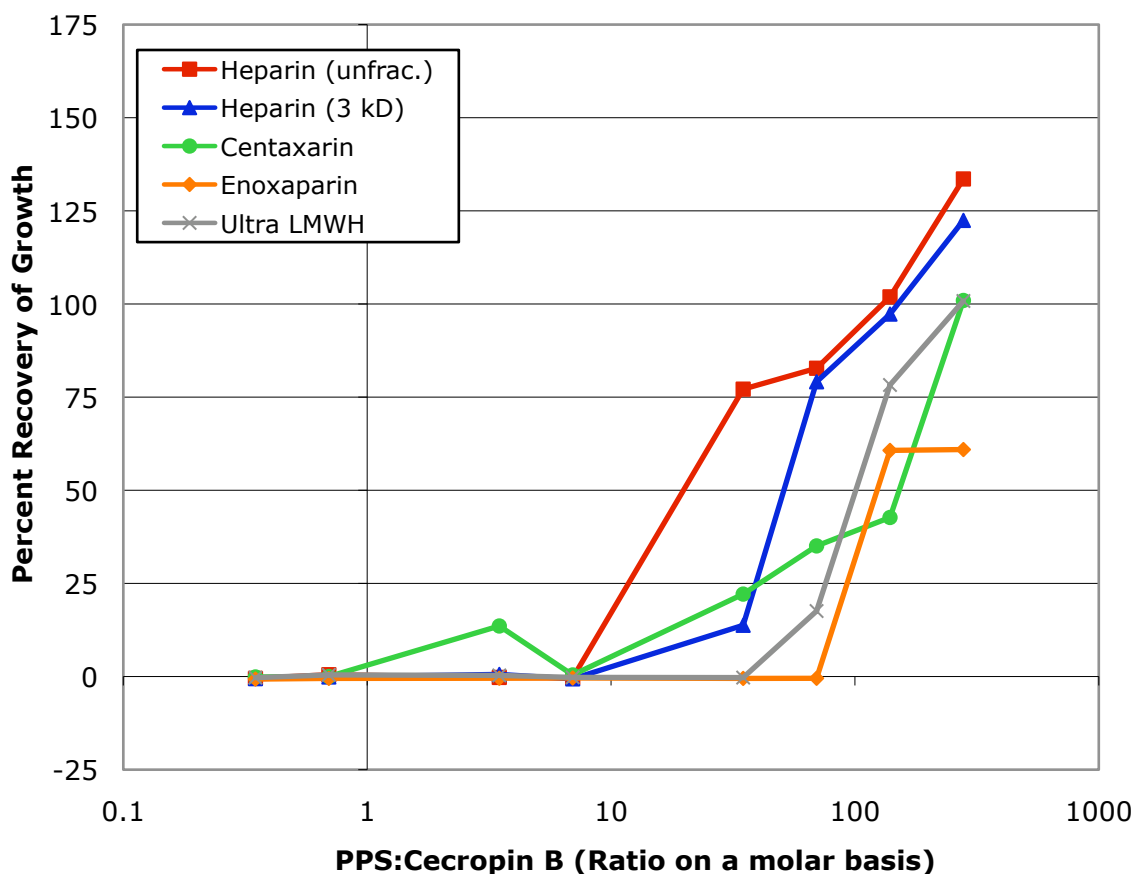


**Figure 43** Reversal of antimicrobial activity of cecropin B versus *P. aeruginosa* by heparin and LMWHs. Data points represent the mean of duplicate measurements.

A comparison of the reversal activity of heparin and the LMWHs shows that they all achieve full reversal of cecropin B anti-*P. aeruginosa* activity (**Figure 43**). Heparin differs significantly from enoxaparin and ultra LMWH at molar ratios between 140:1 and 35:1. Heparin and 3kD heparin show essentially the same reversal pattern.

Again, none of the PPSs tested were able to reverse the antimicrobial activity of cecropin B against *E. coli* (**Figure 44**). As discussed previously, this may be due to the unique two-helix structure that cecropins form when bound to the bacterial membrane or in hydrophobic environments (**Figure 3C**). Since the C-terminal helix is much more hydrophobic it likely serves as an anchor in the *E. coli* outer membrane. Thus, we



suggest that all of the PPSs tested are unable to disrupt the binding of the cecropin C-terminal helix to the outer membrane and, once this binding has occurred, are unable to bind the cationic N-terminal helix and modulate membrane permeability activity.

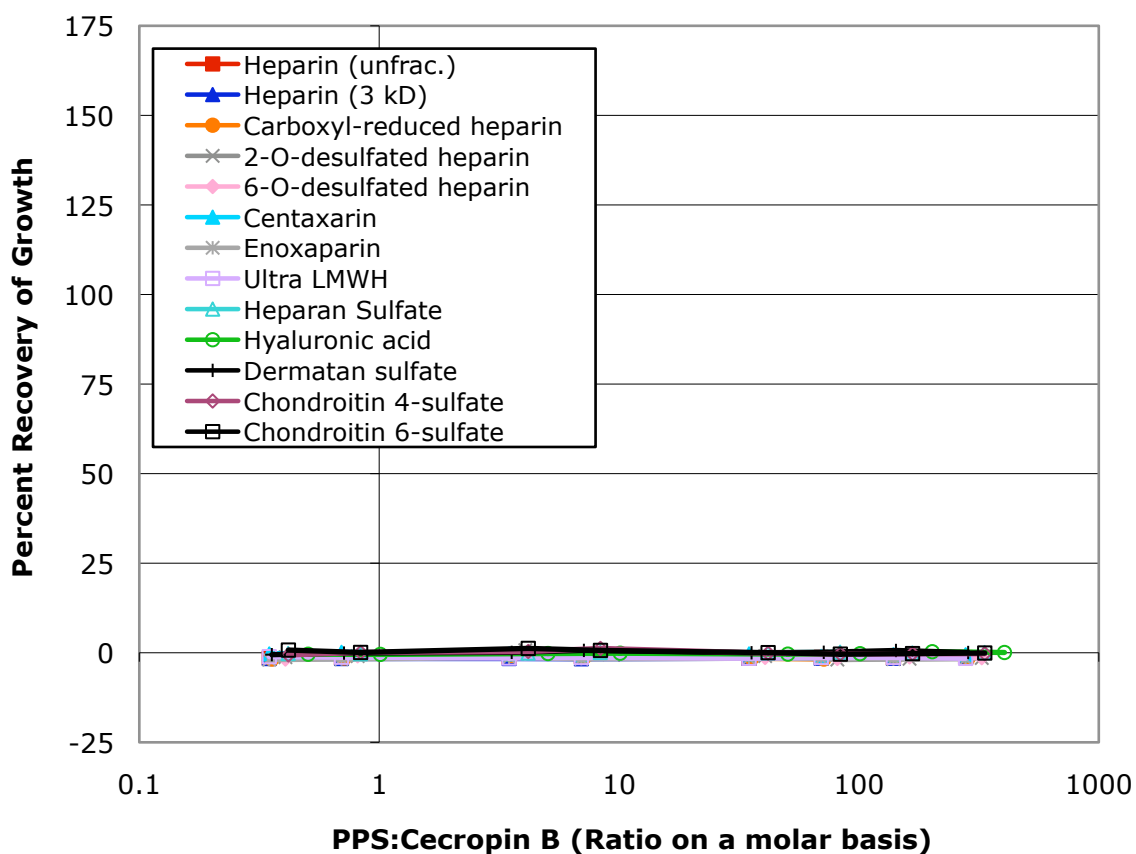
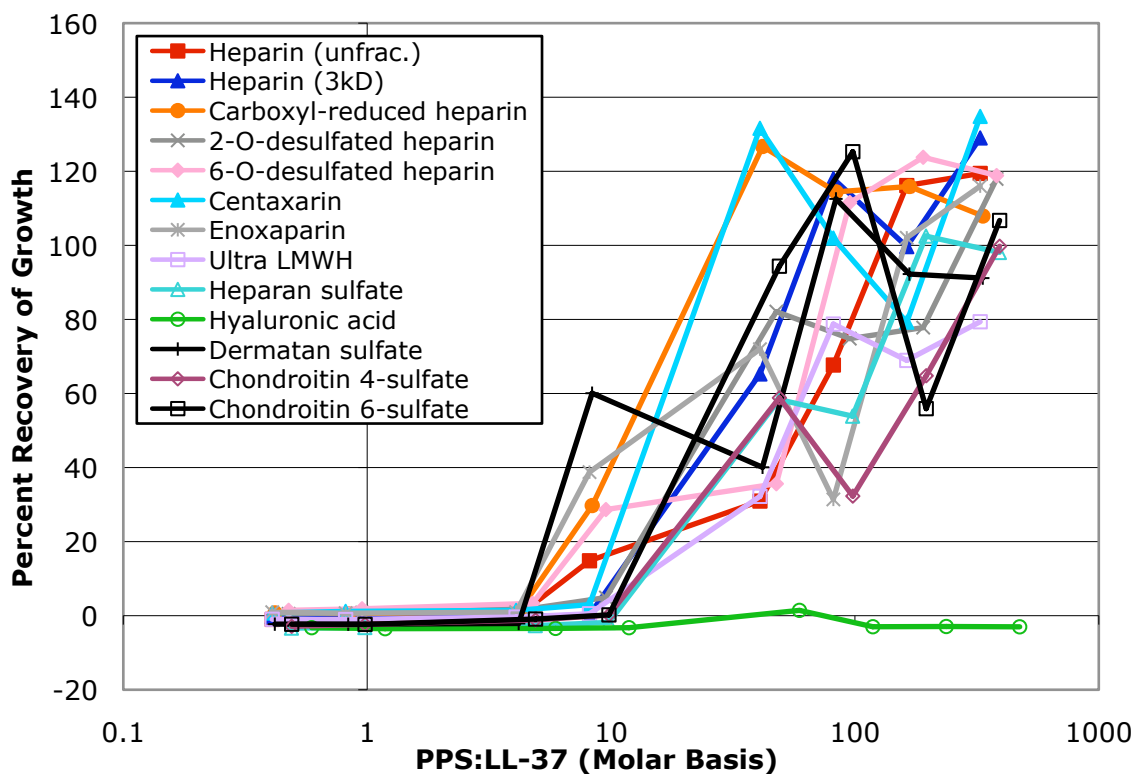


**Figure 44** Reversal of antimicrobial activity of cecropin B versus *E. coli* by GAGs, charge-reduced heparin analogs and LMWHs. Data points represent the mean of duplicate determinations.

#### 4.2.7 Modulation of LL-37 antimicrobial activity by GAGs, charge-reduced heparin analogs and LMWHs

All of the PPSs tested, with the exception of hyaluronic acid, were able to reverse the anti-*P. aeruginosa* activity of LL-37 (**Figure 45**). This is similar to the results of

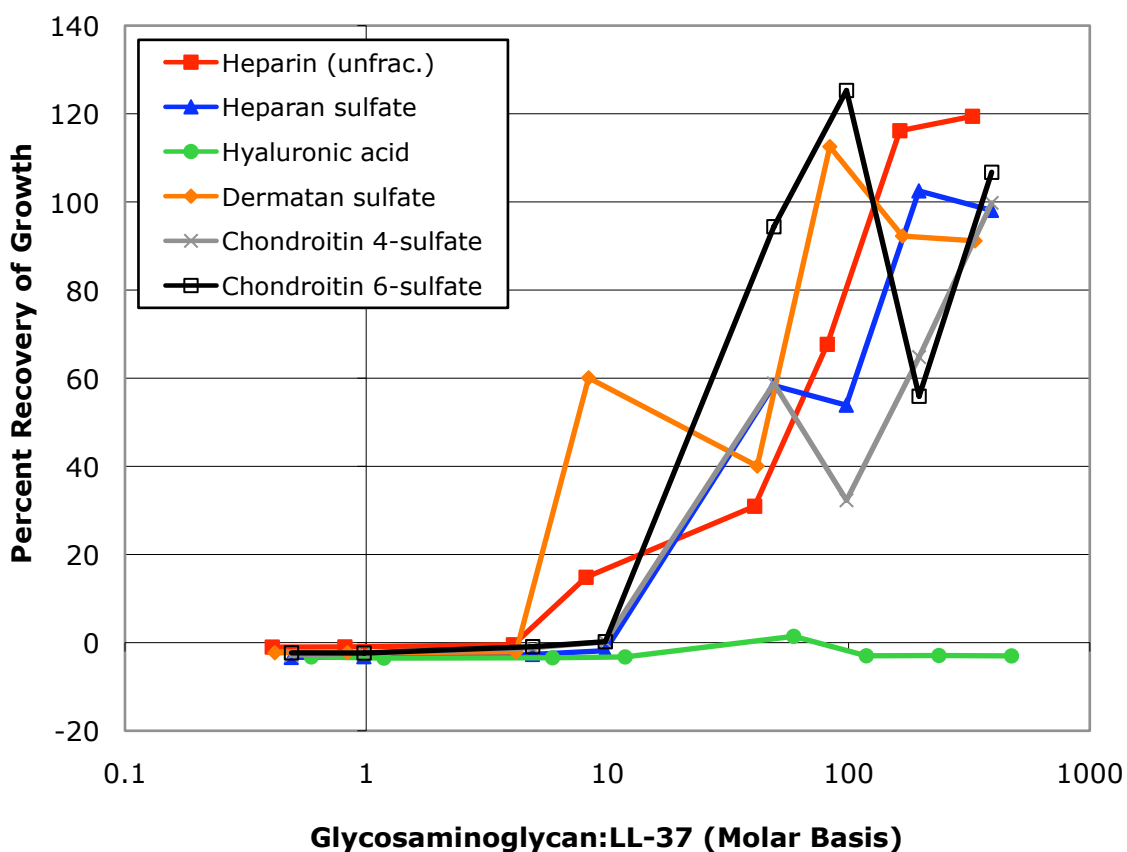
PPSs reversal of magainin II anti-*P. aeruginosa* activity, but in this case all of the PPSs were able to completely reverse LL-37 antimicrobial activity against *P. aeruginosa*. Additionally, all of the PPSs, except hyaluronic acid, reverse at roughly the same molar ratios of PPS:LL-37.



**Figure 45** Reversal of antimicrobial activity of LL-37 versus *P. aeruginosa* by GAGs. Average of duplicate data points shown.

Comparing the reversal patterns of LL-37 anti-*Pseudomonas* activity across GAGs, only HA shows significant differences in ability to reverse (**Figure 46**). These results are notably different from the GAG reversal patterns for magainin II, cecropin A and cecropin B against *P. aeruginosa*. With the cecropins, heparin is the only GAG that can reverse their anti-*Pseudomonas* activity. All of the GAGs except HA show some

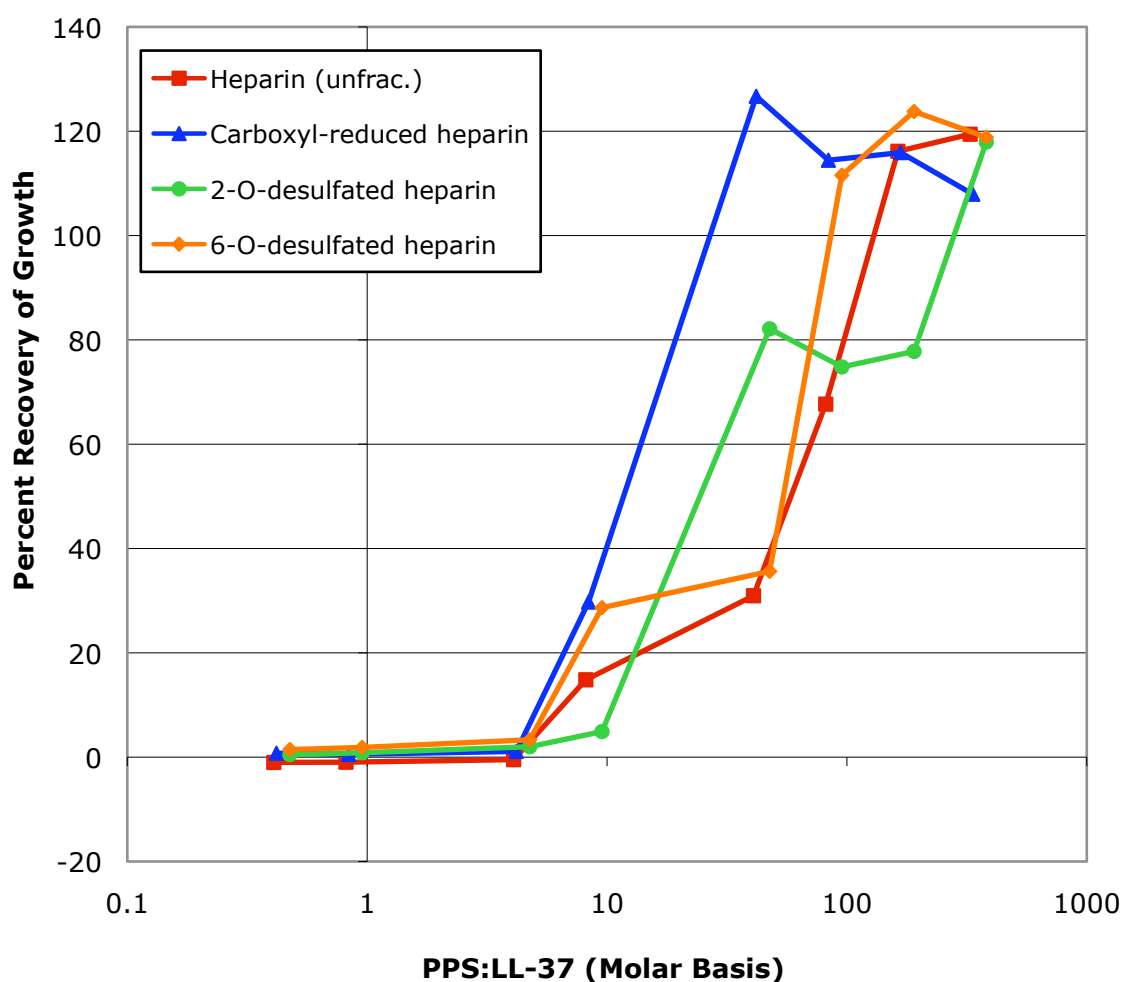
ability to reverse antimicrobial activity of magainin II against *P. aeruginosa*, but 10X more GAG was needed to reverse the activity as compared to heparin. These results indicate that heparin's increased anionic charge is not necessary for better reversal of LL-37 anti-*Pseudomonas* activity. This could also be interpreted as the ability to reverse the antimicrobial activity of LL-37 against *P. aeruginosa* is dependent upon overall charge rather than polysaccharide structure.



**Figure 46** Reversal of antimicrobial activity of LL-37 versus *P. aeruginosa* by GAGs. Average of duplicate data points shown.

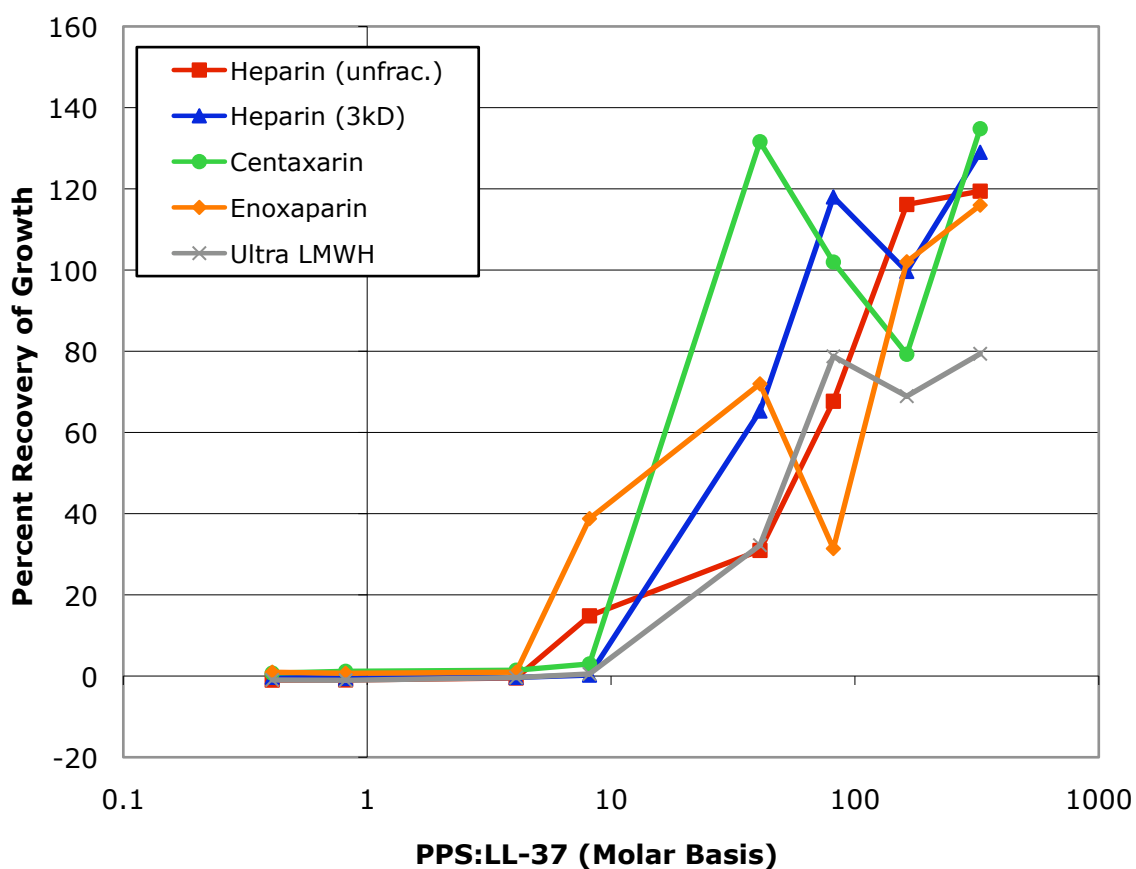
Another surprising result is seen looking at the ability of heparin versus the charge-reduced heparin analogs to negatively modulate the anti-*Pseudomonas* activity of

LL-37 (**Figure 47**). Carboxyl-reduced heparin is significantly better at reversing the antimicrobial activity of LL-37 against *P. aeruginosa* than heparin at a molar ratio of approximately 40:1. In addition, the removal of either the 2-sulfate on the uronic acid or the 6-sulfate on glucosamine does not significantly reduce the ability of the charge-reduced heparin analog to reverse the anti-*Pseudomonas* activity of LL-37. Again, this indicates that the higher anionic charge of heparin does not confer a better reversal activity for LL-37 anti-*Pseudomonas* activity.



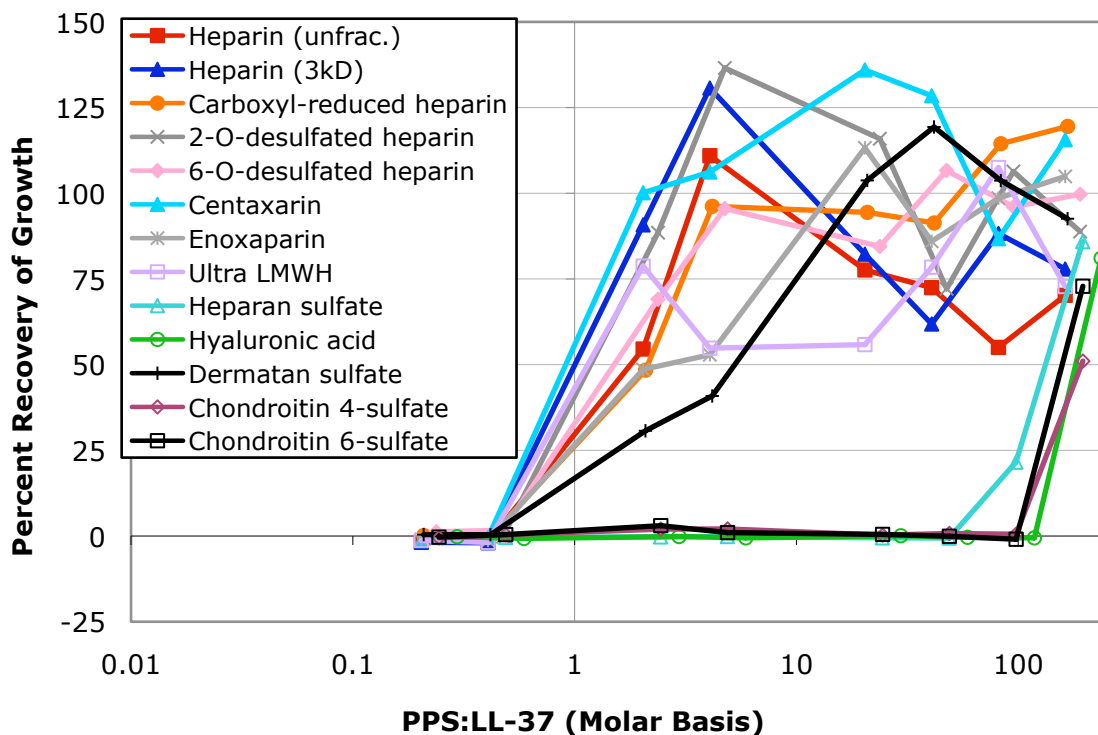
**Figure 47** Reversal of antimicrobial activity of LL-37 versus *P. aeruginosa* by heparin and charge-reduced heparin analogs. Average of duplicate data points shown.

Like the results for heparin and the charge-reduced heparin analogs, heparin and the LMWHs show similar abilities to reverse the anti-*Pseudomonas* activity of LL-37 (Figure 48). Centaxarin is the only LMWH that shows a significant difference from the reversal activity of heparin, and this is only at the molar ratio of 40:1. These results indicate that a higher molecular weight polysaccharide, or longer heparin molecule, does not confer an enhanced ability to negatively modulate LL-37 antimicrobial activity against *P. aeruginosa*. This is in contrast to the reversal of LP antimicrobial activity results where we saw that a longer molecular weight improved the antimicrobial modulatory activity of heparin.



**Figure 48** Reversal of antimicrobial activity of LL-37 versus *P. aeruginosa* by heparin and LMWHs. Average of duplicate data points shown.

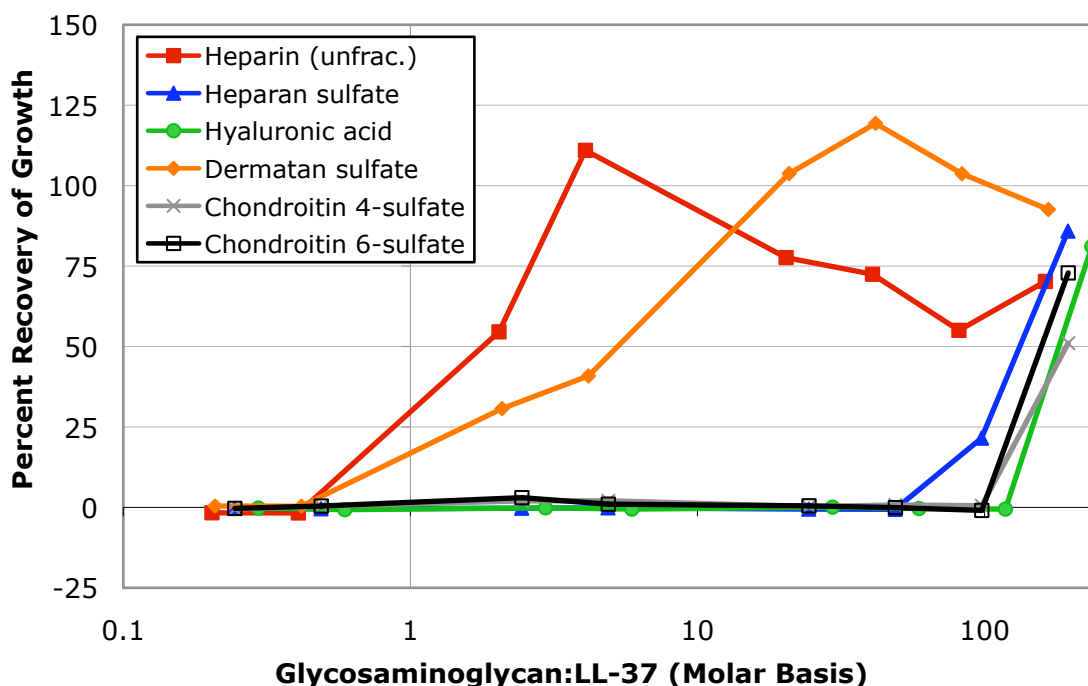
Many more of the PPSs tested show the ability to reverse the antimicrobial activity of LL-37 against *E. coli* as compared to the reversal patterns for magainin II, cecropin A and cecropin B (**Figure 49**). In addition, a molar ratio of less than 1:1 is required for many of the PPSs to reverse the anti-*E. coli* activity of LL-37 while molar ratios of greater than 10:1 are required to reverse the magainin II antimicrobial activity against *E. coli*. The most remarkable observation is that all of the PPSs, even hyaluronic acid, are able to reverse the antimicrobial activity of LL-37 against *E. coli*.



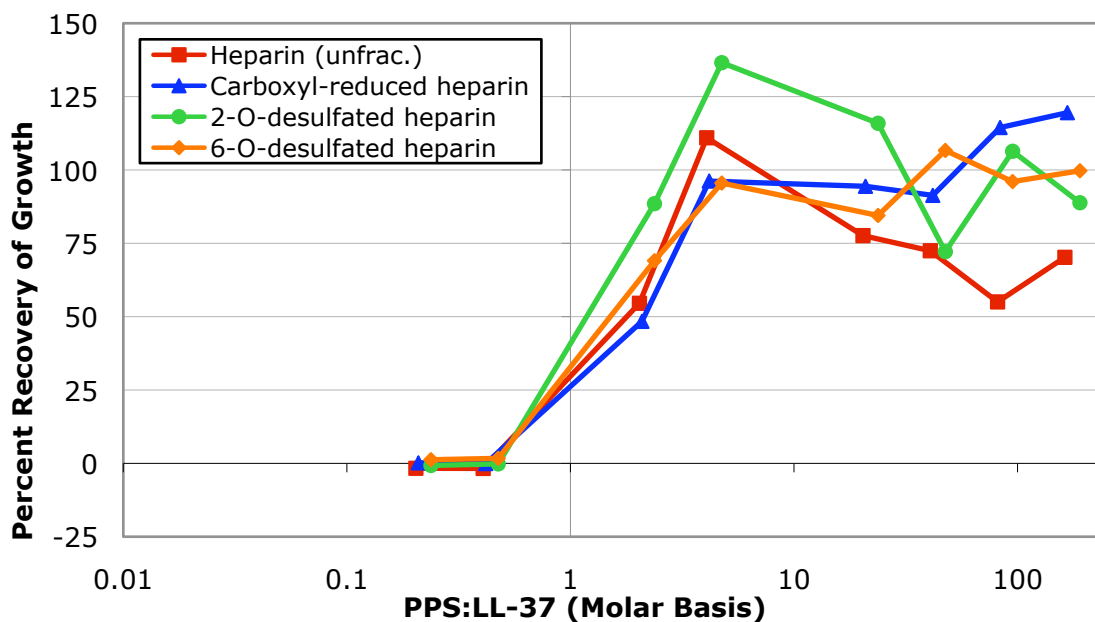
**Figure 49** Reversal of antimicrobial activity of LL-37 versus *E. coli* by GAGs, chemically-modified heparins and LMWHs. Average of duplicate data points shown.

Unlike with the other CAPs, all of the GAGs tested were able to reverse the antimicrobial activity of LL-37 against *E. coli* (**Figure 50**). In addition, all of the GAGs,

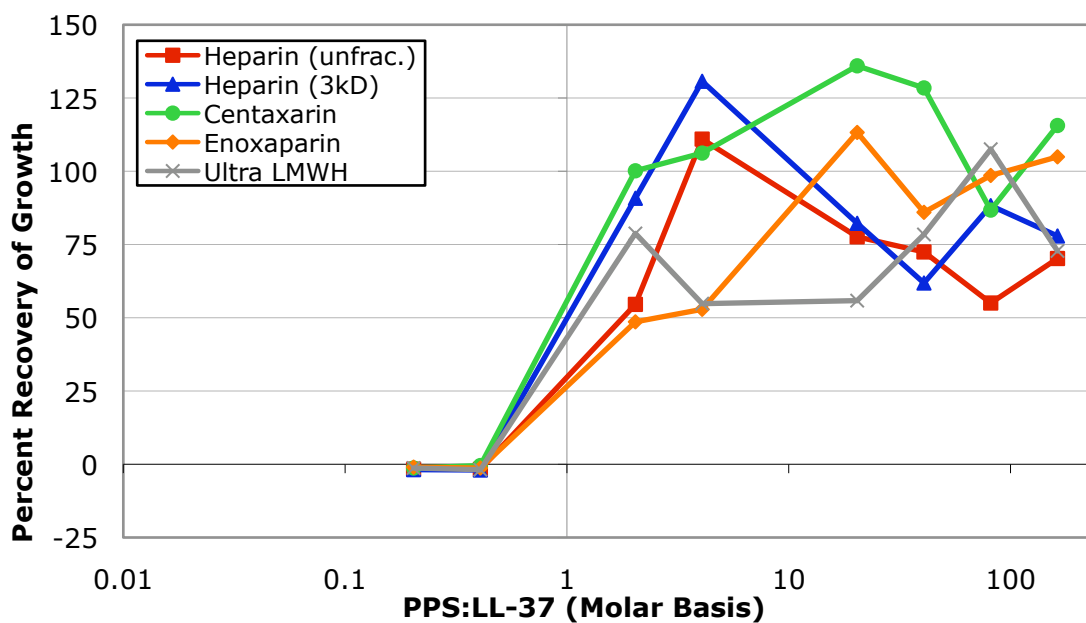
except C4S, were able to completely reverse the anti-*Escherichia* activity of LL-37. Another important result of these experiments is the strong reversal activity that DS exhibits against the anti-*Escherichia* activity of LL-37. DS is comparable to heparin as a negative modulator of the antimicrobial activity of LL-37 against *E. coli*. Alternatively, it takes approximately 400X more HS, C4S, C6S and HA as compared to heparin and DS to reverse the anti-*Escherichia* activity of LL-37. Additionally, the only reversal activity that was revealed in these experiments for HA is the reversal of the antimicrobial activity of LL-37 against *E. coli*. These data suggest that a higher anionic charge is required for reversal of the anti-*Escherichia* activity of LL-37 at low molar ratios. On the other hand, even polysaccharides that lack sulfate groups, such as HA, can reverse the antimicrobial activity at higher molar ratios, so the higher anionic charge is not an absolute requirement.



**Figure 50** Reversal of antimicrobial activity of LL-37 versus *E. coli* by GAGs. Average of duplicate data points shown.



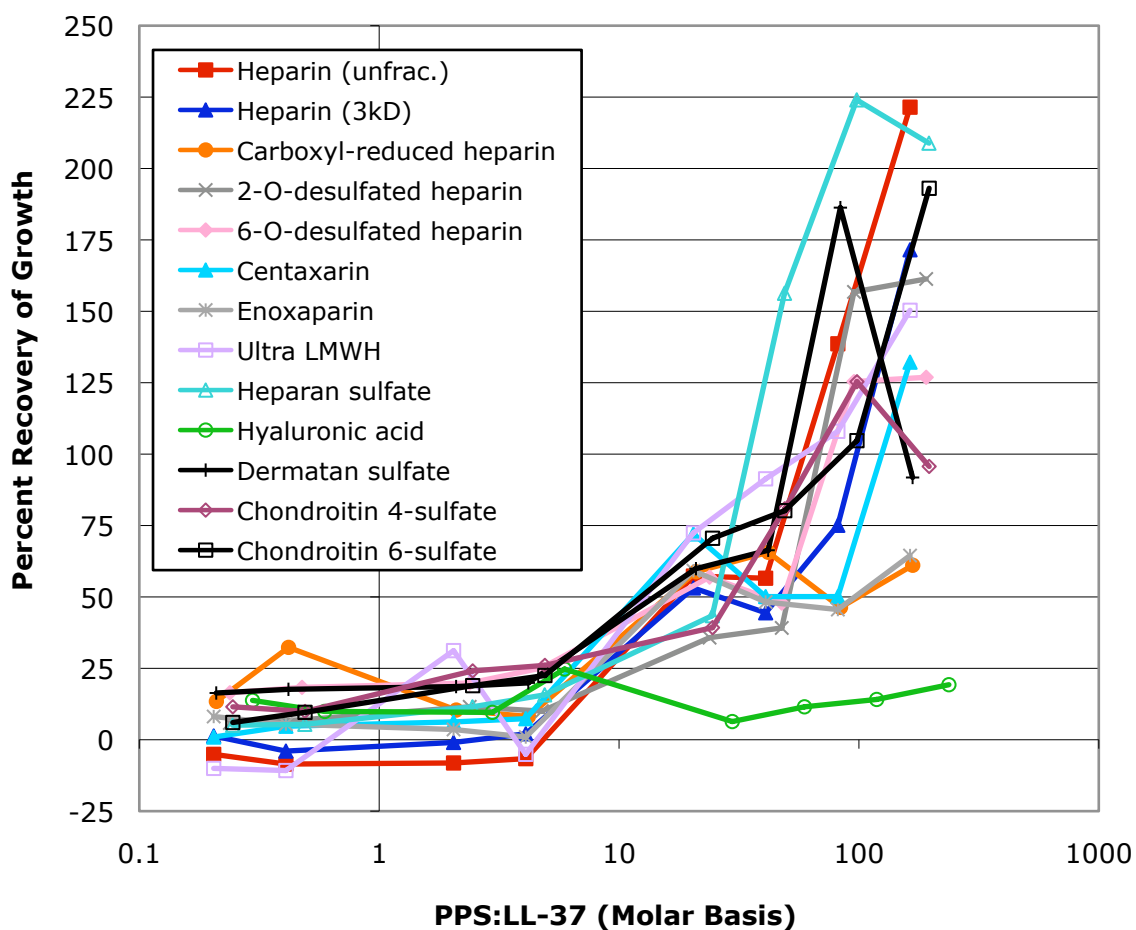
**Figure 51** Reversal of antimicrobial activity of LL-37 versus *E. coli* by heparin, chemically-modified heparin analogs. Average of duplicate data points shown.



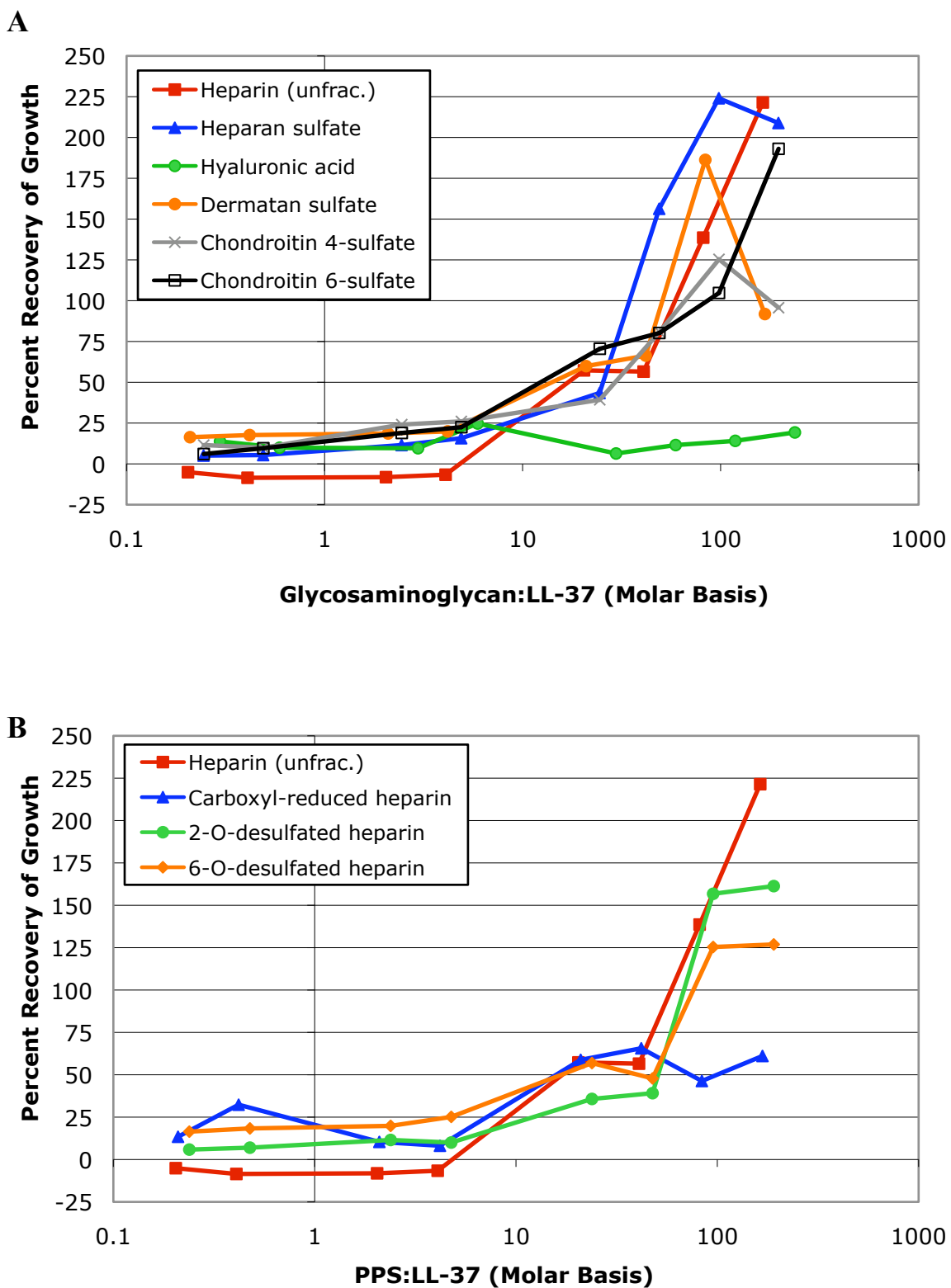
**Figure 52** Reversal of antimicrobial activity of LL-37 versus *E. coli* by heparin and LMWHs. Average of duplicate data points shown.



Removal of anionic charge did not affect heparin's ability to reverse the antimicrobial activity of LL-37 against *E. coli* (**Figure 51**). There was no significance difference between the reversal patterns of heparin, carboxyl-reduced heparin, 2-*O*-desulfated heparin and 6-*O*-desulfated heparin. These results indicate that the reversal of LL-37 antimicrobial activity against *E. coli* may be more dependant upon the structure of the PPS rather than the anionic charge. Similarly, a reduction in the molecular weight of heparin did not change its ability to reverse the antimicrobial activity of LL-37 against *E. coli* (**Figure 52**).



**Figure 53** Reversal of antimicrobial activity of LL-37 against *S. aureus* by GAGs, LMWHs and chemically-modified heparin analogs. Single data points shown.



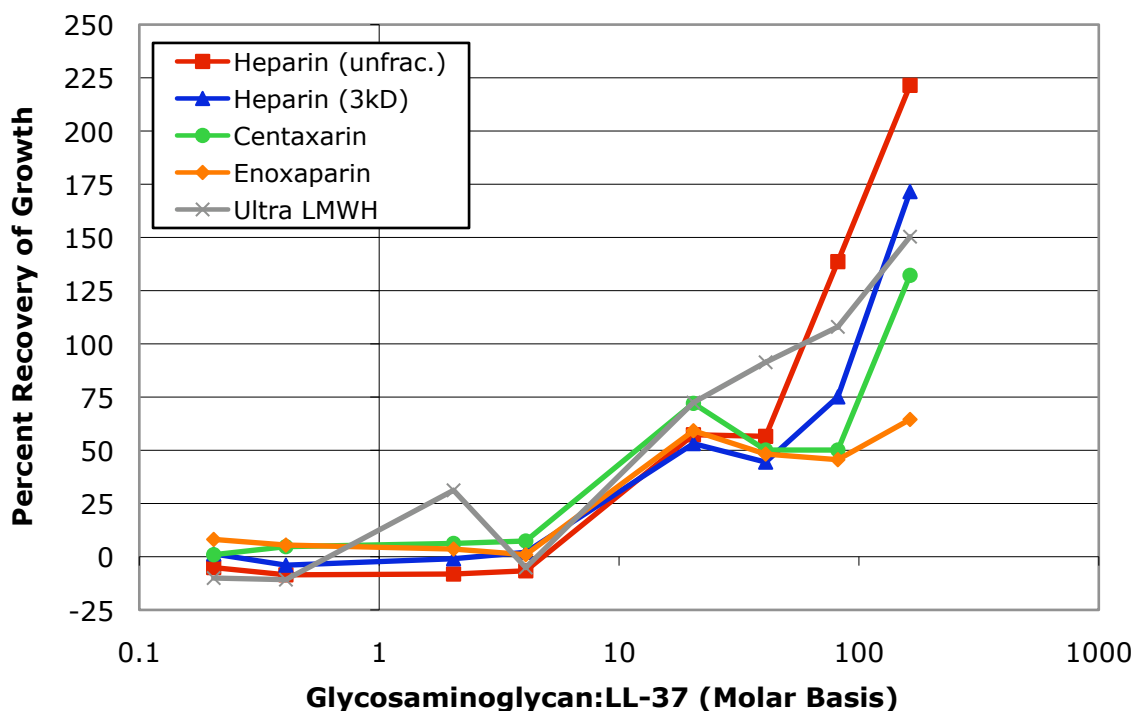


**Figure 55** Reversal of antimicrobial activity of LL-37 versus *S. aureus* by heparin and LMWHs. Single data points shown.

Due to the high MIC of LL-37 against *S. aureus* the experiment measuring the concentration dependent reversal of anti-*Staphylococcal* activity of LL-37 by GAGs, charge-reduced heparin analogs and LMWHs was only done once (**Figure 53**). Furthermore many of the PPSs tested appear to have supported the growth of *S. aureus*, leading to greater than 100% recovery of growth when compared to the growth controls in the experiment. These two issues make the data a little harder to interpret, but some generalizations can be made. First, all of the GAGs, charge-reduced heparin analogs and LMWHs tested, with the exception of HA, were able to reverse the antimicrobial activity of LL-37 against *S. aureus*. Secondly, HA was inactive as a negative modulator of LL-37 anti-*Staphylococcus* activity. Lastly, of the PPSs that reversed the antimicrobial activity of LL-37 against *S. aureus*, all were able to fully reverse antimicrobial activity except carboxyl-reduced heparin and enoxaparin.

### 4.3 Conclusions

The most significant result of these experiments was the realization that the CAP antimicrobial activity reversal patterns were not consistent across the bacterial species tested. Many respected researchers have suggested and discussed in the literature that such experiments reflect the affinities of the PPSs for each CAP. By testing the ability of the PPSs to negatively modulate the antimicrobial activity of the CAPs against two bacterial species (or three in the case of LL-37), we showed that each reversal activity is a unique interaction between the bacterial membrane, the CAP and the PPS. This is most likely due to differences in the bacterial membrane. No specific target, besides the overall anionic phospholipids in the bacterial membrane, has been found for the linear CAPs investigated here. In Chapter 5 the ability of GAGs to modulate cecropin A, cecropin B and LL-37 binding to components of Gram-negative and -positive membranes is investigated.

Overall, heparin was the best negative modulator of the antimicrobial activity of the CAPs tested. This is likely due to the high anionic charge of heparin. The higher molecular weight of unfractionated heparin as compared with the LMWHs may also contribute to the better reversal activity of heparin. HA, although much larger than the heparin used in our experiments, is not an effective modulator of antimicrobial activity, likely due to its low anionic charge.

HS, which is commonly thought of as interchangeable with heparin by many researchers, shows a much reduced reversal activity as compared to heparin. This implies that the higher anionic charge of heparin, or another property affected by its charge (such as its resulting structure) is responsible for its better reversal activity. The LMWHs were overall less active at reversing the antimicrobial activity of the CAPs as compared to heparin. Many medical professionals consider these therapeutic treatments essentially the same, thus these results may be important for elucidating why LMWHs are better overall therapies for anticoagulation.

Finally, although I have attempted to draw broad conclusions from these experiments, generalizations cannot be made regarding the affinities of the CAPs for the GAGs. We postulate that the bacterial membrane acts as a thermodynamic sink for the CAPs, and that the GAGs can only block the CAP from binding the bacterial membrane in solution. Thus, the results that we see in these experiments are a result of the GAGs reducing the effective concentration of CAPs to below the MIC at the bacterial membrane. As a result, we must assume that the interactions between the CAP, bacterial membrane and PPS are unique and dependent upon all three components of the interaction.

CHAPTER 5 MODULATION OF CATIONIC  
ANTIMICROBIAL PEPTIDE BINDING BACTERIAL  
MEMBRANE COMPONENTS BY  
GLYCOSAMINOGLYCANS

5.1 CAPs binding to lipopolysaccharides and lipoteichoic  
acid

5.1.1 Experimental techniques

The lipopolysaccharide- (LPS) and lipoteichoic acid- (LTA) binding properties of cecropin A, cecropin B and LL-37 were measured using an ELISA technique modified from a recent paper by Senyürek *et al.*<sup>357</sup> Aliquots of 125  $\mu\text{L}$  of 40 ng/mL *P. aeruginosa* 10 LPS (Sigma L8643) or *E. coli* 055:B5 LPS (Sigma L2637) in water were applied to the wells of a polystyrene microplates (Costar). The plates were incubated at room temperature in a bio-safety cabinet until dry and then heated at 60°C for 2 hours. The amount of CAP and primary and secondary antibody concentrations were optimized using cecropin B binding to *P. aeruginosa* LPS.

A variety of ELISA methods from the literature were analyzed for optimal blocking and CAP binding to immobilized LPS.<sup>357-361</sup> Plates were blocked with 300  $\mu\text{L}$  of a 1.0 mg/mL BSA solution in tris buffer (50 mM Tris-HCl, 50 mM NaCl, pH 8.0, ionic strength = 0.175) for 1 hour at room temperature. The plates were then washed three times using 300  $\mu\text{L}$ /well of tris buffer. Cecropin A, cecropin B or LL-37 was added at 50  $\mu\text{L}$ /well in a concentration range from 0-12.5  $\mu\text{M}$  and incubated at 37°C for one hour with shaking. The plates were subsequently rinsed three times with 300  $\mu\text{L}$ /well of tris buffer. Following this 100ng/mL primary antibody in 1.0 mg/mL BSA in tris buffer, rabbit polyclonal antibody to cecropin B (Abcam ab27571) for cecropin A and cecropin B or rabbit polyclonal antibody to LL37 (Innovagen PA-LL37100), was added at 100  $\mu\text{L}$ /well. After a one hour incubation at 37°C with shaking the plates were washed three

times with tris buffer. The secondary antibody, 100 ng/mL of goat polyclonal antibody to rabbit IgG labeled with horseradish peroxidase in 1.0 mg/mL BSA in tris buffer for all CAPs, was added at 100  $\mu$ L/well and incubated at 37°C for 30 minutes. The plates were washed four times with tris buffer. Hydrogen peroxide and tetramethylbenzidine, components of the DuoSet IC Substrate Buffer (R&D Systems), were mixed according to the manufactures directions, added to the plate at 50  $\mu$ L/well and incubated at room temperature for 30 minutes with shaking. 15  $\mu$ L H<sub>2</sub>SO<sub>4</sub> was added to each well to stop the action of horseradish peroxidase on the substrate, tetramethylbenzidine, and the plates were read at 450 nm to detect the amount of CAP bound to the immobilized LPS.

Data were analyzed using SigmaPlot (Systat Software Inc.). The affinity of CAPs for *P. aeruginosa* and *E. coli* LPS was calculated using **Equations 1-4**. **Equation 1** is used to calculate the binding constant (Kd) for one site saturation of a binding site. **Equation 2** is used to calculate the Kd for one site saturation of a binding site and takes into account nonspecific binding. Likewise, **Equation 3** is used to calculate the Kd for saturation of a two binding site model and **Equation 4** is used to calculate the Kd for saturation of a two binding site model plus nonspecific binding.

$$\text{Equation 1} \quad f(x) = \frac{B \max(abs(x))}{(Kd + abs(x))}$$

$$\text{Equation 2} \quad f(x) = \frac{B \max(abs(x))}{(Kd + abs(x))} + Ns(x)$$

$$\text{Equation 3} \quad f(x) = \frac{B \max_1(abs(x))}{(Kd_1 + abs(x))} + \frac{B \max_2(abs(x))}{(Kd_2 + abs(x))}$$

$$\text{Equation 4} \quad f(x) = \frac{B \max_1(abs(x))}{(Kd_1 + abs(x))} + \frac{B \max_2(abs(x))}{(Kd_2 + abs(x))} + Ns(x)$$

In **Equations 1-4**  $f(x)$  represents the absorbance at 450 nm,  $x$  represents the concentration of CAP in nM,  $B_{max}$  represents the binding maximum or total receptor number and  $K_d$  represents the binding constant.

### 5.1.2 Cecropin A binding to *P. aeruginosa* and *E. coli* LPS

The ELISA data from cecropin A binding to *P. aeruginosa* and *E. coli* LPS were analyzed using equations 1-4 (**Tables 5 and 6**). The one site saturation plus nonspecific binding model was selected as the best fit for cecropin A binding to both *P. aeruginosa* LPS and *E. coli* LPS. Cecropin A binds to *P. aeruginosa* LPS with a  $K_d$  of  $356 \pm 164$  nM and a  $B_{max}$  of  $0.46 \pm 0.07$ . Cecropin A binds to *E. coli* LPS with a  $K_d$  of  $133 \pm 56.5$  nM and a  $B_{max}$  of  $0.35 \pm 0.04$ . The binding data for cecropin A binding to *P. aeruginosa* LPS and *E. coli* LPS are shown in **Figures 56 and 57**.

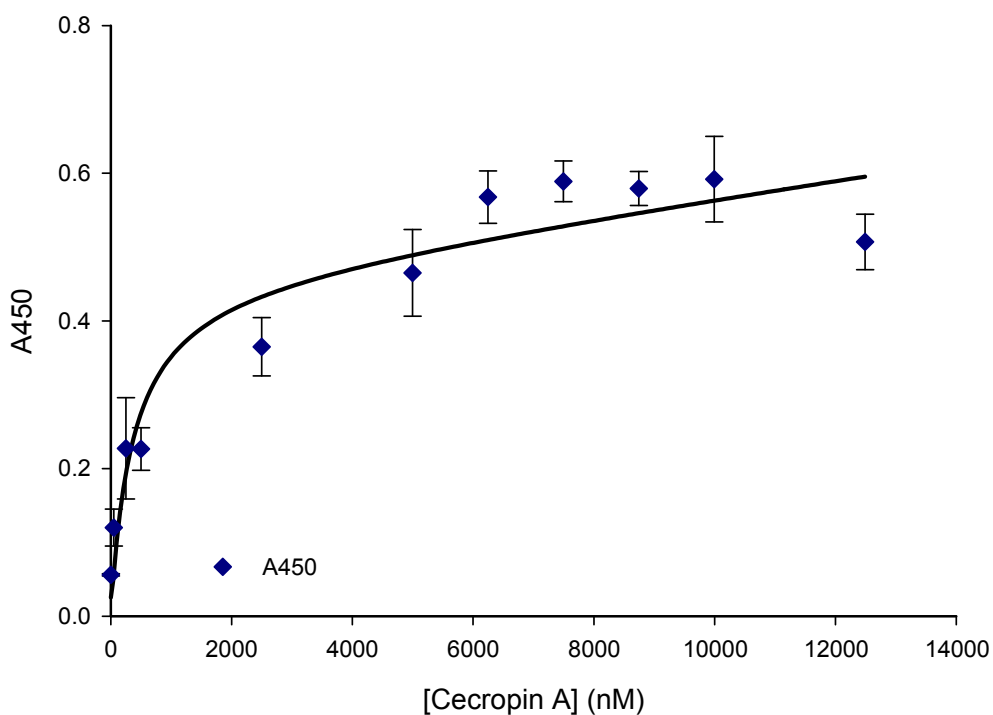


**Figure 56** Cecropin A binding to *P. aeruginosa* LPS. Mean of triplicate data points  $\pm$  standard error shown. Line shows the fit of **Equation 2**.



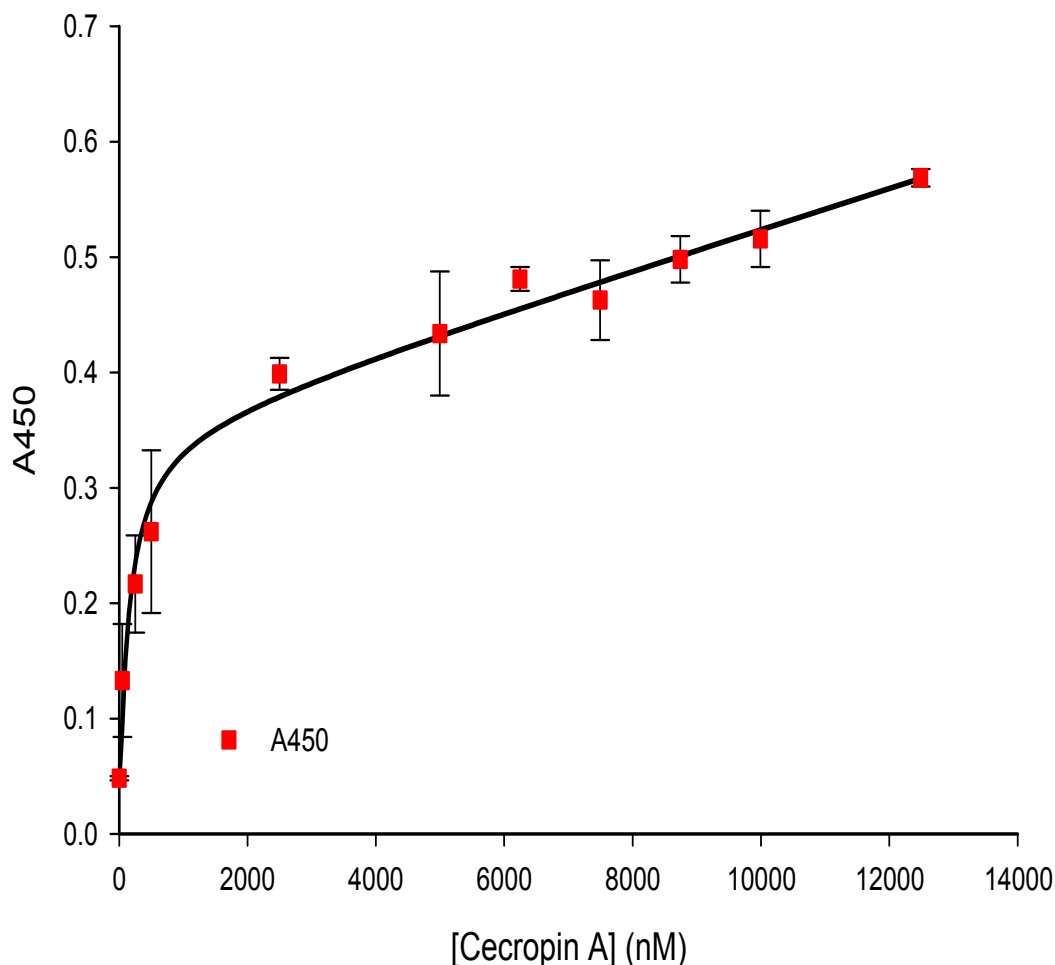


**Figure 57** Cecropin A binding to *E. coli* LPS. Data points represent the mean of triplicate measurements  $\pm$  standard error. Line shows the fit of **Equation 2**.

### 5.1.3 Cecropin B binding to *P. aeruginosa* and *E. coli* LPS

The ELISA data from cecropin B binding to *P. aeruginosa* and *E. coli* LPS were analyzed using equations 1-4 (**Tables 7 and 8**). The one site saturation binding model was selected as the best fit for cecropin B binding to both *P. aeruginosa* LPS and *E. coli* LPS. Cecropin B binds to *P. aeruginosa* LPS with a  $K_d$  of  $235 \pm 40.4$  nM and a  $B_{max}$  of  $1.66 \pm 0.04$ . Cecropin B binds to *E. coli* LPS with a  $K_d$  of  $270 \pm 50.0$  nM and a  $B_{max}$  of  $0.97 \pm 0.03$ . The binding data for cecropin B binding to *P. aeruginosa* LPS and *E. coli* LPS are shown in **Figure 58**.

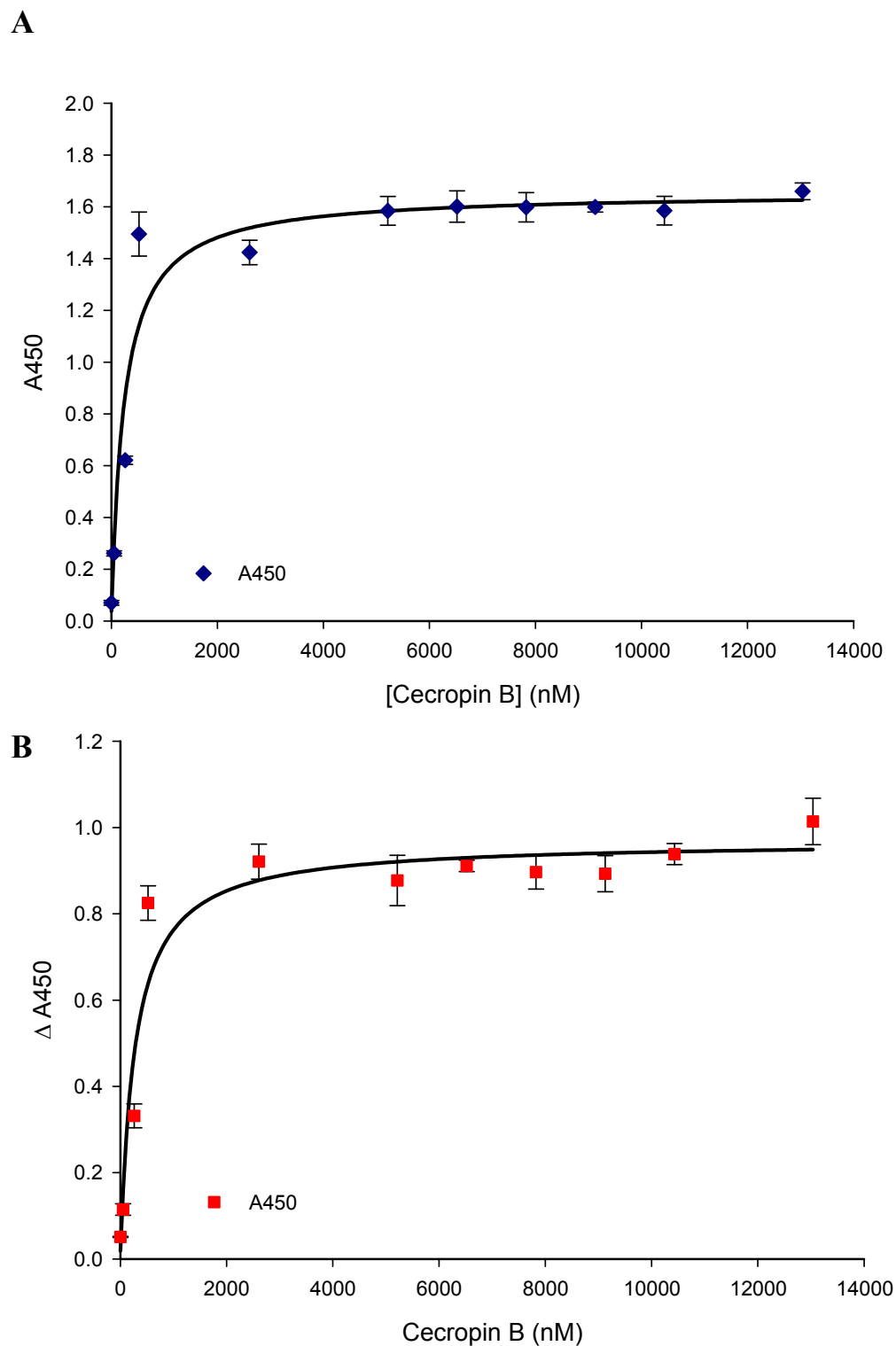


**Figure 58** Cecropin B binding to immobilized *P. aeruginosa* LPS (A) and *E. coli* LPS (B). Means of triplicate data points  $\pm$  standard error shown. Data in A and B is fit to **Equation 1**.

#### 5.1.4 LL-37 binding to *P. aeruginosa* and *E. coli* LPS

The results from LL-37 binding to *P. aeruginosa* and *E. coli* LPS were analyzed using equations 1-4 (**Tables 9** and **10**). The one site saturation binding model was selected as the best fit for LL-37 binding to both *P. aeruginosa* LPS and *E. coli* LPS. LL-37 binds to *P. aeruginosa* LPS with a  $K_d$  of  $69.2 \pm 7.72$  nM and a  $B_{max}$  of  $2.76 \pm 0.03$ . LL-37 binds to *E. coli* LPS with a  $K_d$  of  $224 \pm 22.1$  nM and a  $B_{max}$  of  $2.28 \pm 0.03$ . The binding data for LL-37 binding to *P. aeruginosa* LPS and *E. coli* LPS are shown in **Figures 59** and **60**.

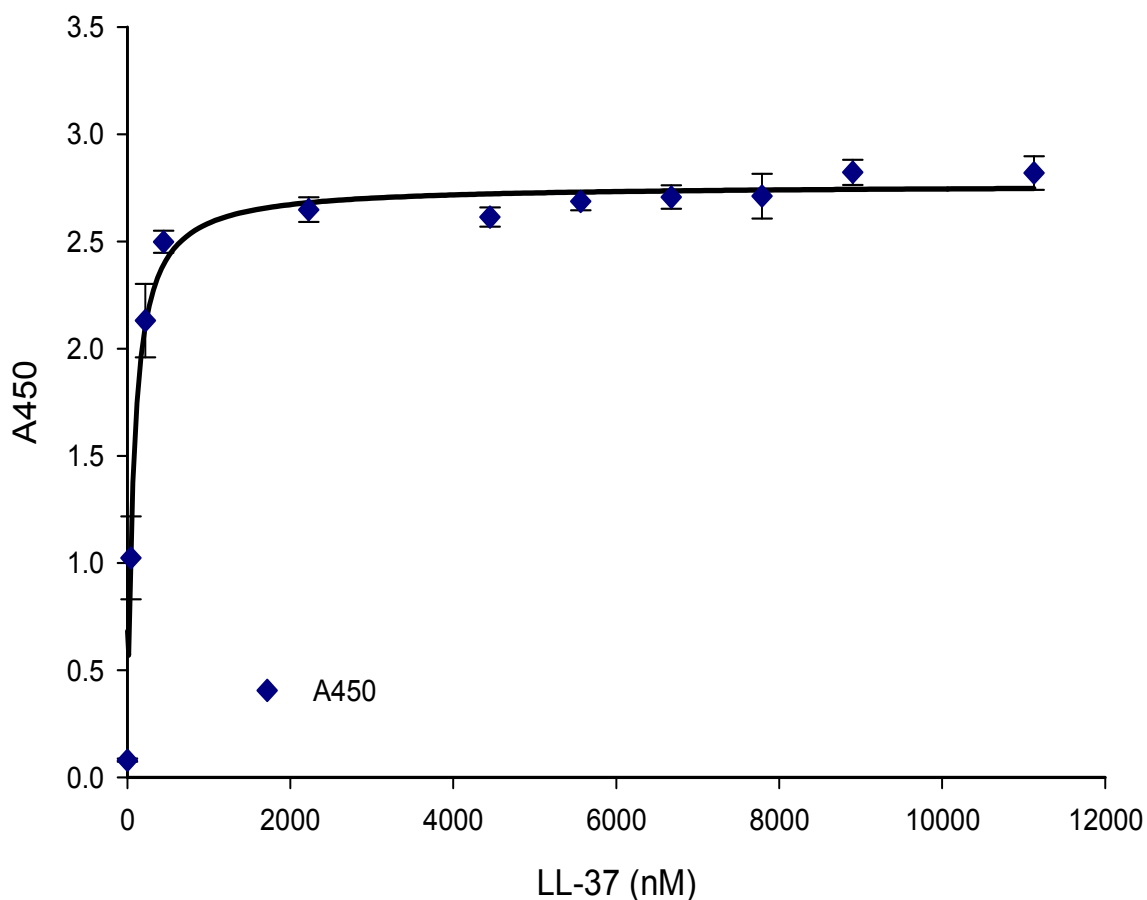


**Figure 59** LL-37 binding to immobilized *P. aeruginosa* LPS. Data points represent the mean of triplicate measurements  $\pm$  standard error. The fit of **Equation 1** is shown.

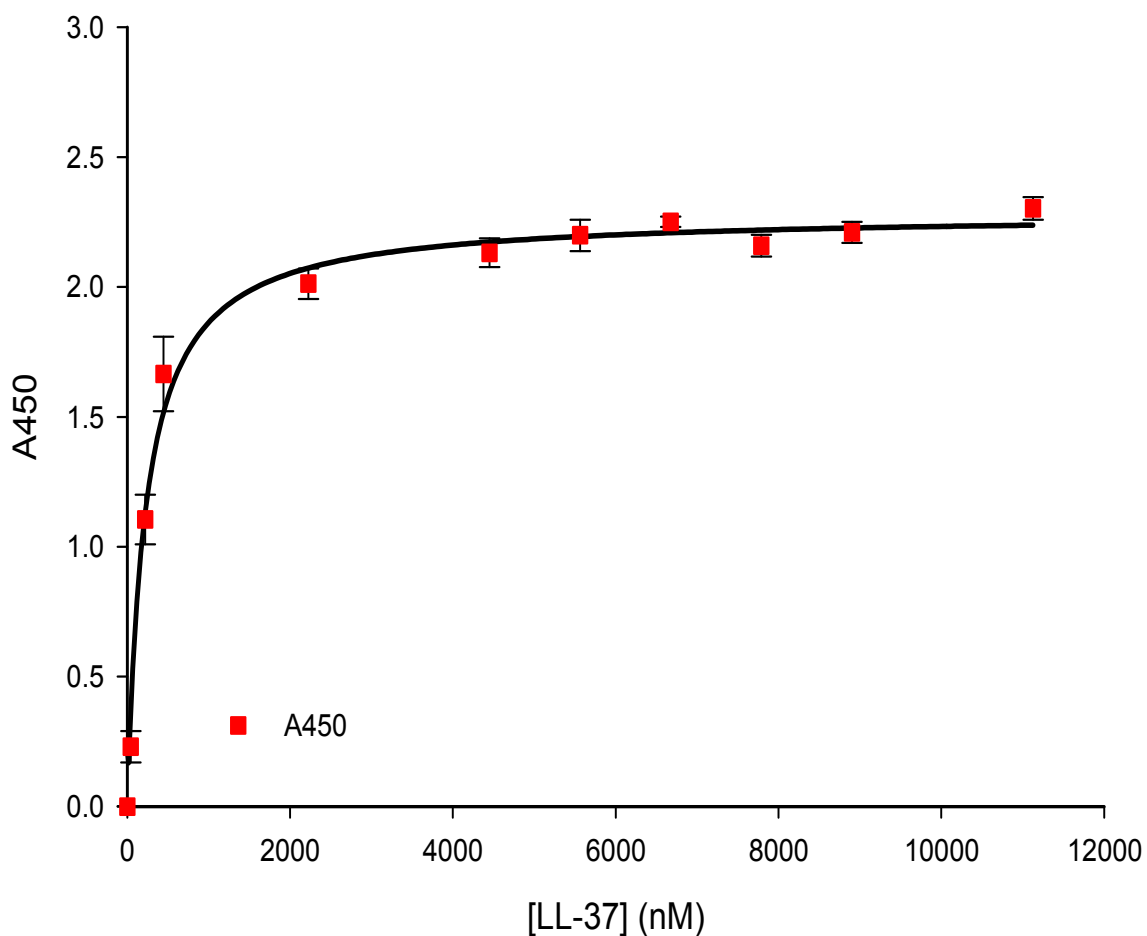


**Figure 60** LL-37 binding to immobilized *E. coli* LPS. The mean of triplicate data points  $\pm$  standard error is shown. Data are fit to **Equation 1**.

## 5.2 Evaluation of CAP affinity for LPS or LTA by competition binding assays

### 5.2.1 Experimental technique

Competitive binding assays were performed to determine the affinity of the CAPs for soluble *P. aeruginosa* LPS, *E. coli* LPS and *S. aureus* LTA. The reason for these experiments is twofold. First, we wanted to prove that free LPS could compete the CAP off of the immobilized *P. aeruginosa* or *E. coli* LPS. Secondly competition binding

provides a way to compare the affinities of the CAP for soluble *P. aeruginosa* LPS, *E. coli* LPS, *S. aureus* LTA and ultimately different GAGs. Plates were prepared and blocked as discussed in Section 5.1.1. Aliquots containing 0.1 µg Cecropin A, cecropin B or LL-37 in tris buffer containing 5 mM CaCl<sub>2</sub> and 1.0 mg/mL BSA were incubated with a series of concentrations of *P. aeruginosa* LPS, *E. coli* LPS or *S. aureus* LTA (Sigma L2515) overnight at 37°C with shaking. Three-50 µL aliquots of each sample were added to the plate and binding was allowed to occur for 1 hour at 37°C with shaking. Following binding the plates were washed 3X with tris buffer. A 100 ng/mL primary antibody solution was added at 100 µL/well and allowed to bind for 1 hour at 37°C with shaking. The plates were washed 3X with tris buffer at 300 µL/well, followed by the addition of 100 ng/mL secondary antibody at 100 UL/well. Next the plate was washed 4X with 300 µL tris buffer and 100 µL/well horseradish peroxidase substrate was added. After a 30 minute incubation at room temperature with shaking, 15 µL H<sub>2</sub>SO<sub>4</sub> was added to stop the reaction and the plate was read at 450 nm. Negative controls where the CAP was omitted were used in each case.

Data were analyzed using SigmaPlot. The affinity of CAPs for *P. aeruginosa* LPS, *E. coli* LPS or *S. aureus* LTA was calculated using **Equations 5 and 6**. **Equation 5** is used to calculate an EC<sub>50</sub>, or concentration required to displace 50% of the CAP from immobilized *P. aeruginosa* LPS or *E. coli* LPS, for one binding site competition. **Equation 6** is used to calculate an EC<sub>50</sub><sub>1</sub> and EC<sub>50</sub><sub>2</sub> for two binding sites. EC<sub>50</sub> values can be converted to inhibition constants (K<sub>i</sub>) using the equation of Cheng and Prusoff.<sup>362</sup>

$$\text{Equation 5} \quad f(x) = \min + \frac{(\max - \min)}{1 + 10^{x - \log(EC_{50})}}$$

$$\text{Equation 6} \quad f(x) = \min + (\max - \min) \left( \frac{F_1}{1 + 10^{x - \log(EC_{50_1})}} + \frac{F_2}{1 + 10^{x - \log(EC_{50_2})}} \right)$$

### 5.2.2 Measure of affinity of cecropin A for LPS and LTA

by competition binding assay

The results from the cecropin A LPS/LTA competition binding studies were analyzed using **Equations 5** and **6** and the  $K_d$  values previously calculated (**Tables 5** and **6**). Free *P. aeruginosa* LPS was able to compete cecropin A off the immobilized *P. aeruginosa* LPS (**Figure 61**). In addition, *E. coli* LPS and *S. aureus* LTA in solution were able to compete cecropin A off the immobilized *P. aeruginosa* LPS (**Figures 62** and **63**). *P. aeruginosa* LPS has an  $EC_{50}$  of  $30000 \pm 1.87$  nM. *E. coli* LPS has an  $EC_{50}$  of  $486 \pm 1.27$  nM and *S. aureus* LTA has an  $EC_{50}$  of  $2920 \pm 1.45$  nM (**Table 11**). It took much more *P. aeruginosa* LPS to compete off cecropin A compared to *E. coli* LPS and *S. aureus* LTA.

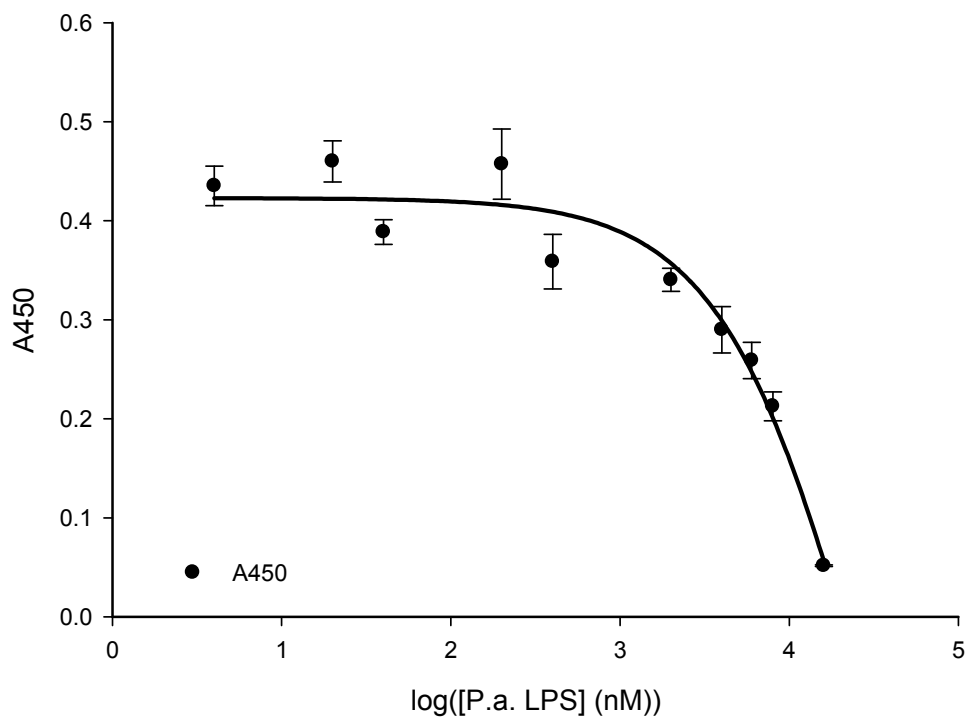


**Figure 61** Competition binding curve for free *P. aeruginosa* LPS binding cecropin A off *P. aeruginosa* LPS. Means of triplicate measurements  $\pm$  standard error. The fit of **Equation 5** is shown.

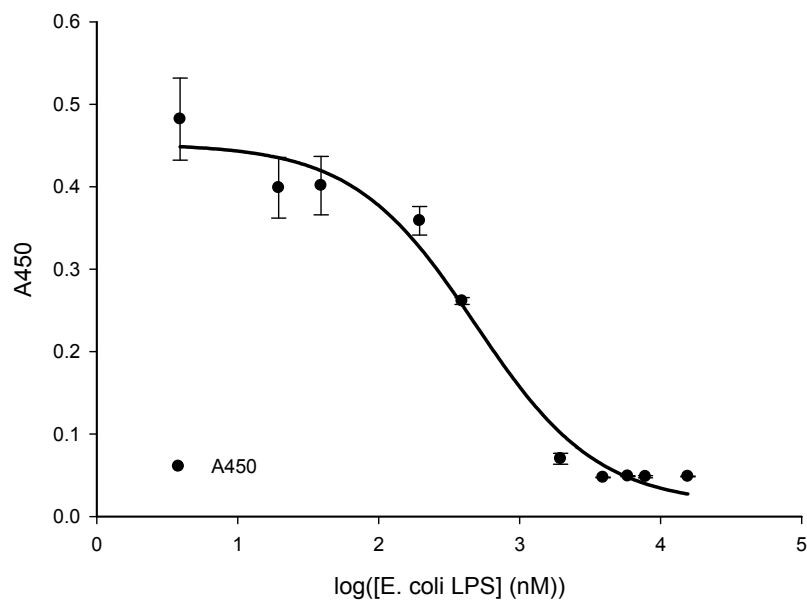


**Figure 62** Competition binding curve for *E. coli* LPS binding cecropin A on immobilized *P. aeruginosa* LPS. Data points represent the mean of triplicate determinations  $\pm$  standard error. The fit of **Equation 5** is shown.

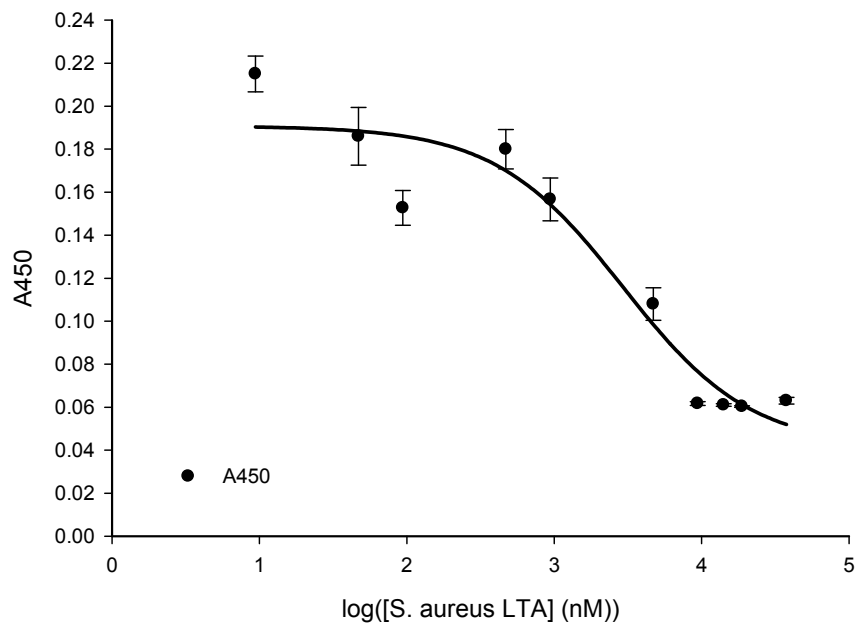


**Figure 63** Competition binding curve for *S. aureus* LTA binding cecropin A on *P. aeruginosa* LPS plates. Mean of triplicate data points  $\pm$  standard error shown. The fit of **Equation 5** is shown.

Free *E. coli* LPS was able to compete cecropin A off the immobilized *E. coli* LPS (Figure 64). Additionally, *P. aeruginosa* LPS and *S. aureus* LTA were able to compete cecropin A off the immobilized *E. coli* LPS plates (Figure 65). Free *E. coli* LPS has an EC50 of  $841 \pm 1.24$  nM while *P. aeruginosa* LPS gives an EC50 of  $17800 \pm 1.45$  nM and *S. aureus* LTA gives an EC50 of  $3890 \pm 1.51$  nM (Table 12).

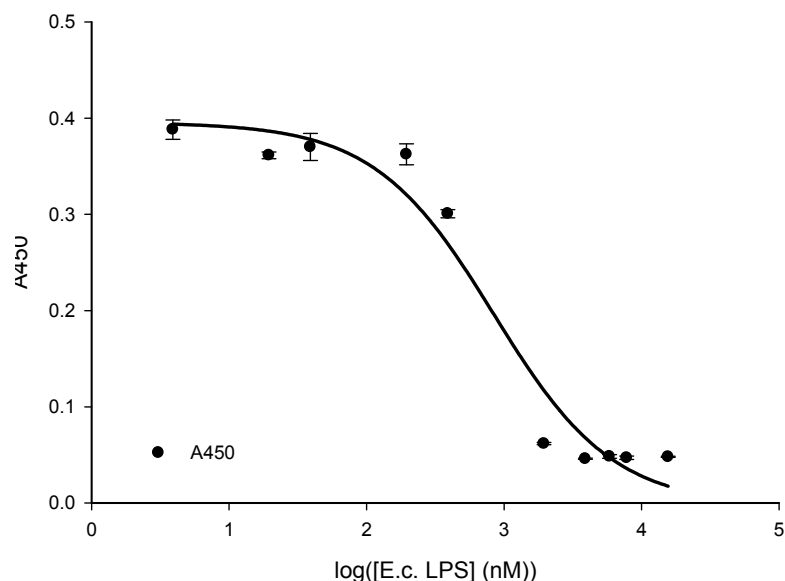


**Figure 64** Competition binding curve for free *E. coli* LPS binding cecropin A off *E. coli* LPS plates. Means of triplicate data points  $\pm$  standard error shown. The fit of Equation 5 is shown.

Taken together, the results of the cecropin A competitive binding assays show that cecropin A has a greater affinity for *E. coli* LPS as compared to *P. aeruginosa* LPS and *S. aureus* LTA. These results agree with the antimicrobial activity modulation experiments. I previously showed that none of the GAGs, charge-reduced heparin analogs and LMWHs tested can negatively modulate the anti-*Escherichia* activity of cecropin A. In contrast, all of the PPSs tested, with the exception of HA, were able to negatively modulate the antimicrobial activity of cecropin A against *P. aeruginosa*. Thus



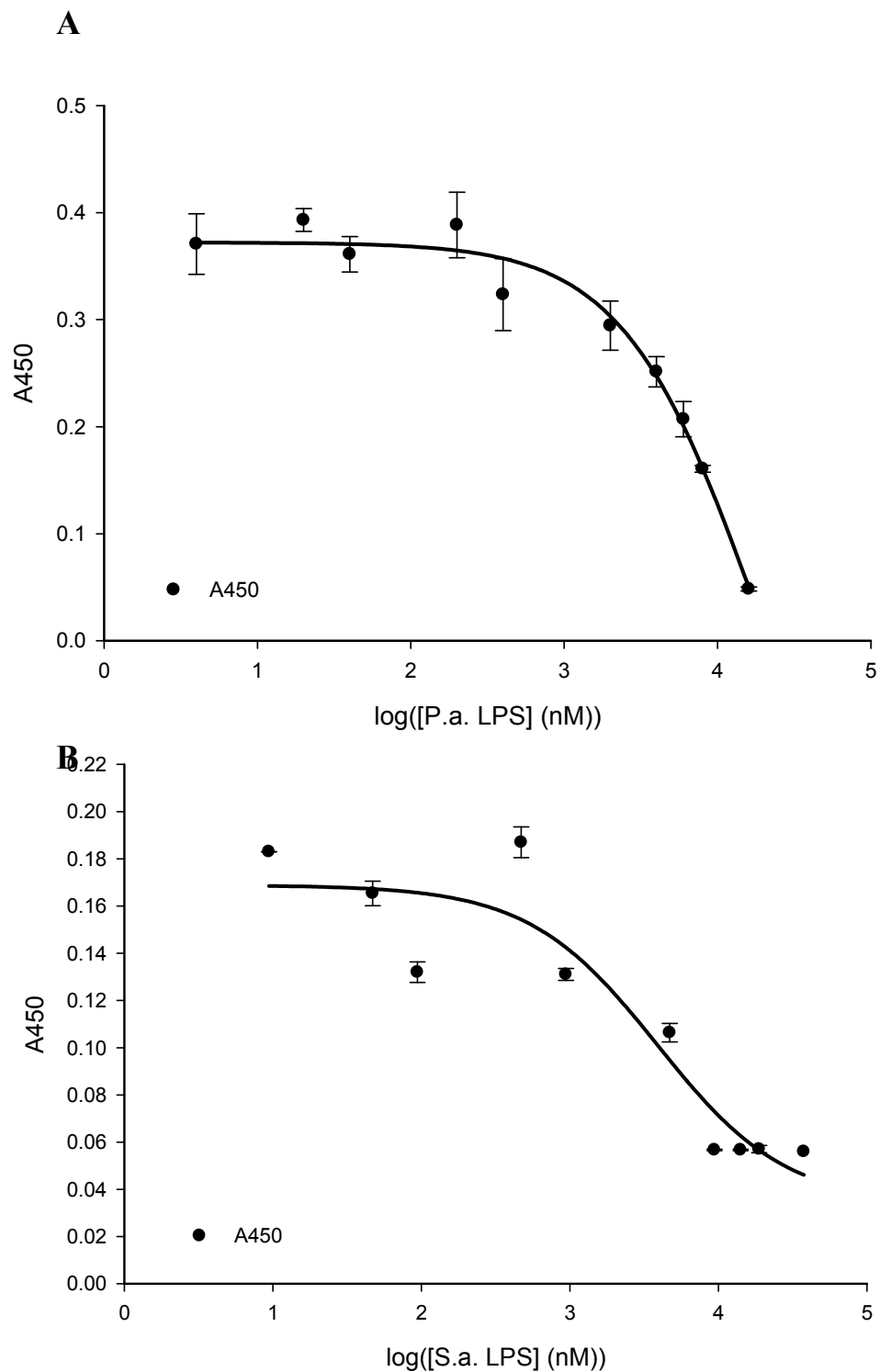


**Figure 65** Competition binding curves for *P. aeruginosa* LPS (A) and *S. aureus* LTA (B) competition binding cecropin A on *E. coli* LPS plates. Data points represent the mean of triplicate measurements  $\pm$  standard error. The fit of **Equation 5** is shown in A and B.

these results indicate that the greater affinity of cecropin A for *E. coli* LPS prevents the negative modulation of cecropin A anti-*Escherichia* activity. Since cecropin A has a lower affinity for *P. aeruginosa* LPS almost all of the PPSs tested were likely able to modulate cecropin A binding to the *P. aeruginosa* membrane, thus modulating the antimicrobial activity of cecropin A against *P. aeruginosa*. In addition, it is surprising that cecropin A has a higher affinity for *S. aureus* LTA as compared to its affinity for *P. aeruginosa* LPS since cecropin A is not active against *S. aureus* and other Gram-positive organisms.

### 5.2.3 Affinity of cecropin B for LPS and LTA measured by competition binding assay

The results from the cecropin B LPS/LTA competition binding assays and the K<sub>d</sub> values previously calculated (**Tables 7 and 8**). Soluble *P. aeruginosa* LPS was able to compete cecropin B off the immobilized *P. aeruginosa* LPS plate (**Figure 66**).

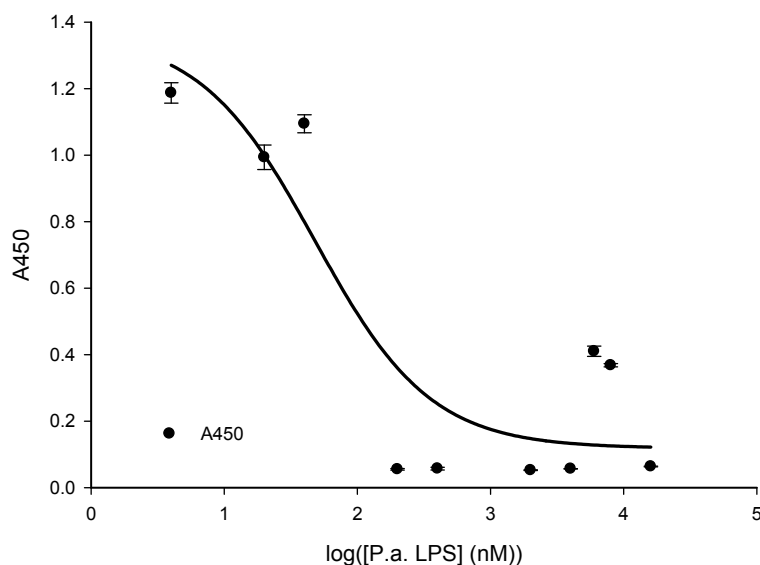


**Figure 66** *P. aeruginosa* LPS competition binding cecropin B on *P. aeruginosa* LPS. Data points represent the mean of triplicate determinations  $\pm$  standard error. The fit of **Equation 5** is shown.

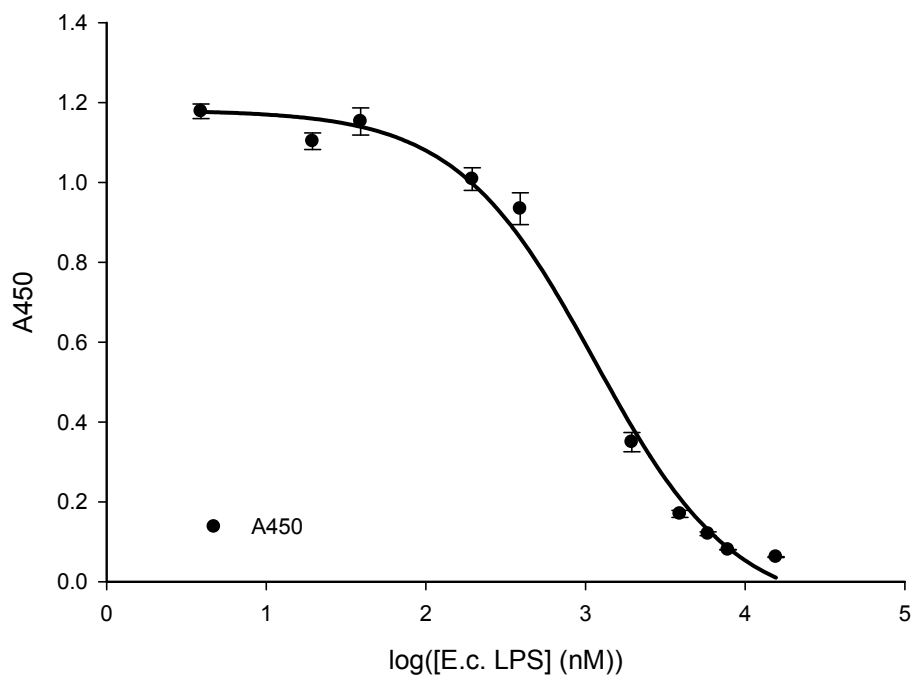


**Figure 67** Competition binding curve for *E. coli* LPS binding cecropin B on *P. aeruginosa* LPS. The means of triplicate data points  $\pm$  standard error are shown. Data are fit to **Equation 5**.

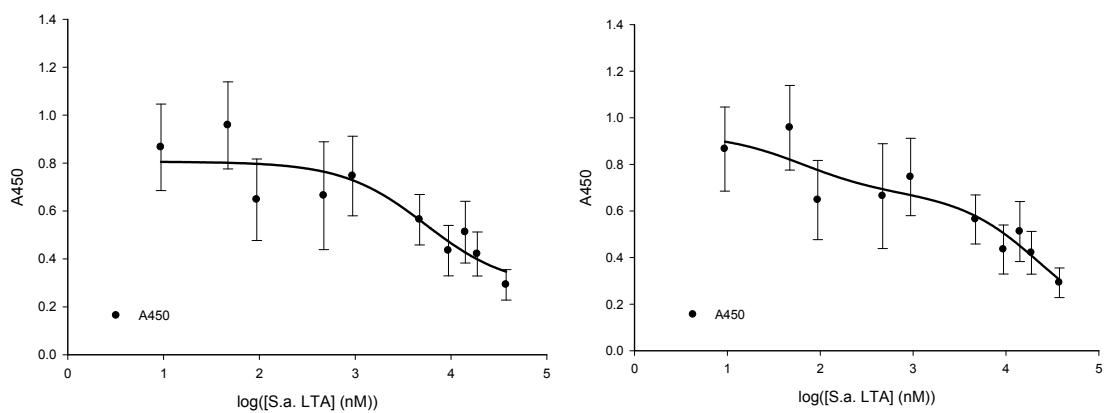


**Figure 68** Competition binding curves for *S. aureus* LTA binding cecropin B on immobilized *P. aeruginosa* LPS. The means of triplicate data points  $\pm$  standard error are shown. The fits of **Equation 5** (left) and **Equation 6** (right) are shown.

Additionally, *E. coli* LPS and *S. aureus* LTA were able to compete cecropin B off the immobilized *P. aeruginosa* LPS plate (**Figures 67 and 68**). Soluble *P. aeruginosa* LPS has an EC<sub>50</sub> value of  $48.1 \pm 1.57$  nM while *E. coli* LPS has an EC<sub>50</sub> value of  $1140 \pm 1.12$  nM and *S. aureus* LTA has an EC<sub>50</sub> value of  $5450 \pm 4.05$  nM (**Table 13**). The competition binding curve for *S. aureus* LTA fit a two binding site competition model as well (**Figure 68**).

Soluble *E. coli* LPS was able to compete cecropin B off of the immobilized *E. coli* LPS plate (**Figure 69**). *P. aeruginosa* LPS (**Figure 70**) and *S. aureus* LTA (**Figure 71**) were also able to compete cecropin B off of the immobilized *E. coli* LPS, although *S. aureus* LTA did not fully inhibit cecropin B binding to the plate in the concentrations tested. *E. coli* LPS has an EC<sub>50</sub> value of  $888 \pm 1.23$  nM, *P. aeruginosa* LPS has an EC<sub>50</sub> value of  $52.8 \pm 1.57$  nM and *S. aureus* LTA has an EC<sub>50</sub> value of  $13700 \pm 1.71$  nM (**Table 14**). The competition binding curve for *S. aureus* LTA binding cecropin B on immobilized *E. coli* LPS can be fit to a one- or two-site competition binding model.

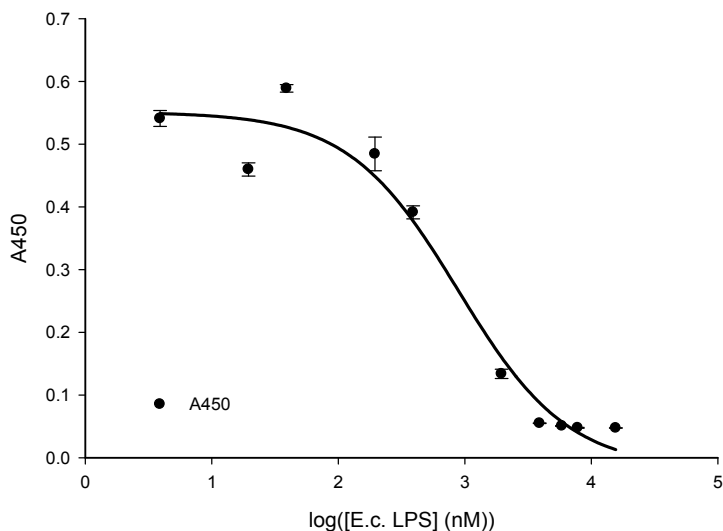


**Figure 69** *E. coli* LPS competition binding cecropin B on immobilized *E. coli* LPS. Means of triplicate data points  $\pm$  standard error shown. The line is fit to **Equation 5**.

Surprisingly these results do not agree with the results for the cecropin A LPS/LTA competition binding assays (Section 5.2.2). We expected cecropin A and cecropin B to behave similarly in these experiments due to the near identical antimicrobial activity modulation results found in Chapter 4. These results indicate that *P. aeruginosa* LPS has a greater affinity for cecropin B, followed by *E. coli* LPS and then *S. aureus* LTA. It is possible that other components of the bacterial membrane, such as other anionic components, play a larger role in the binding of cecropin B to the bacterial membrane. Additionally, these results suggest that cecropin B may bind to the *S. aureus* membrane in a different manner than for Gram-negative organisms. It is interesting to note that cecropin B has no activity against *S. aureus* yet is able to bind LTA from its membrane.

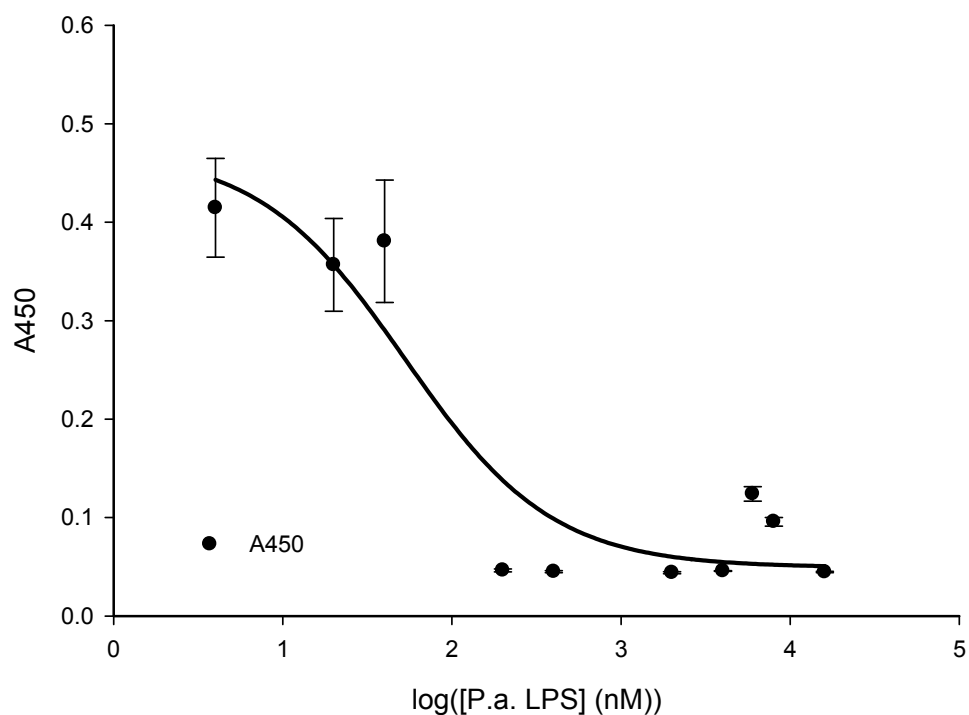


**Figure 70** Competition binding curve for *P. aeruginosa* LPS binding to cecropin B on *E. coli* LPS. Means of triplicate measurements are shown  $\pm$  standard error. The fit of **Equation 5** is shown.

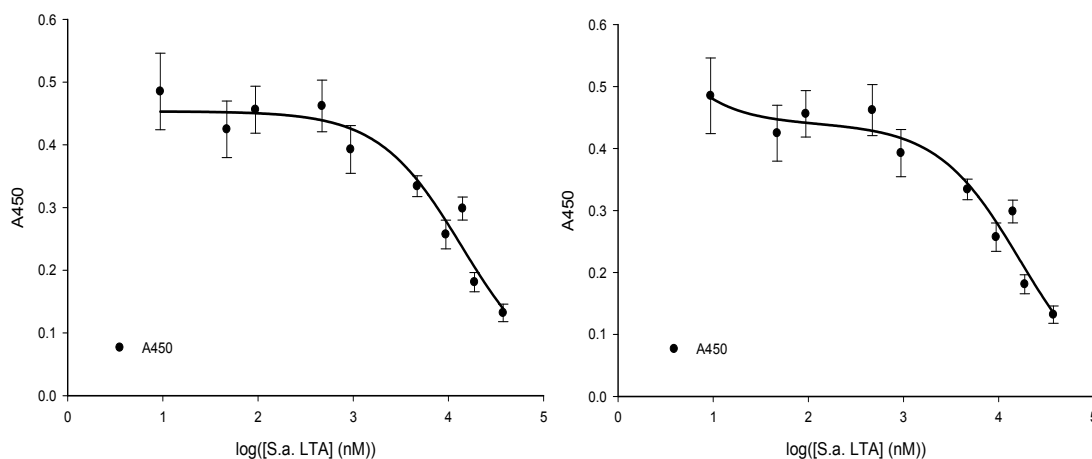


**Figure 71** Competition binding curves *S. aureus* LTA binding to cecropin B on immobilized *E. coli* LPS. Data points represent the mean of triplicate determinations  $\pm$  standard error. The fits of **Equation 5** (left) and **Equation 6** (right) are shown.

#### 5.2.4 Competition binding assays showing LL-37 affinity for LPS and LTA

Free *P. aeruginosa* LPS was able to completely block the binding of LL-37 to immobilized *P. aeruginosa* LPS. The data fit models for both one- and two-site

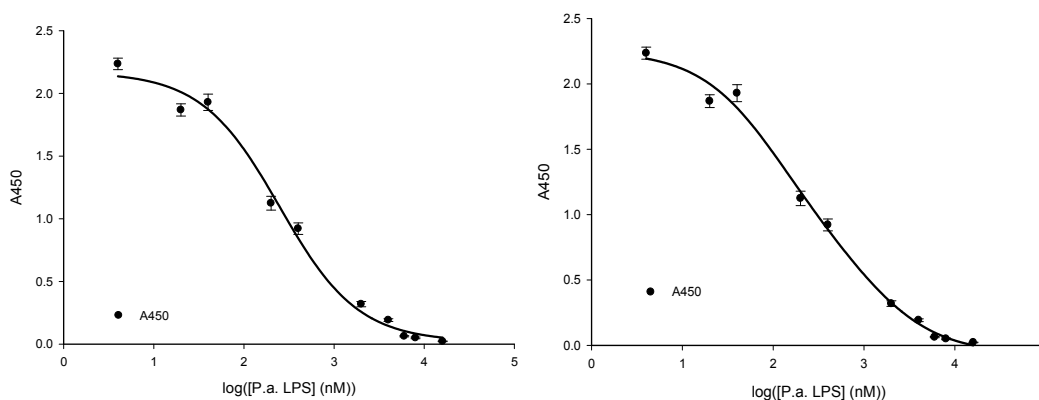


**Figure 72** Competition binding curves for free *P. aeruginosa* LPS binding to LL-37 on immobilized *P. aeruginosa* LPS. Data points represent the mean of triplicate measurements  $\pm$  standard error. Lines are the fit of **Equation 5** (left) and **Equation 6** (right).

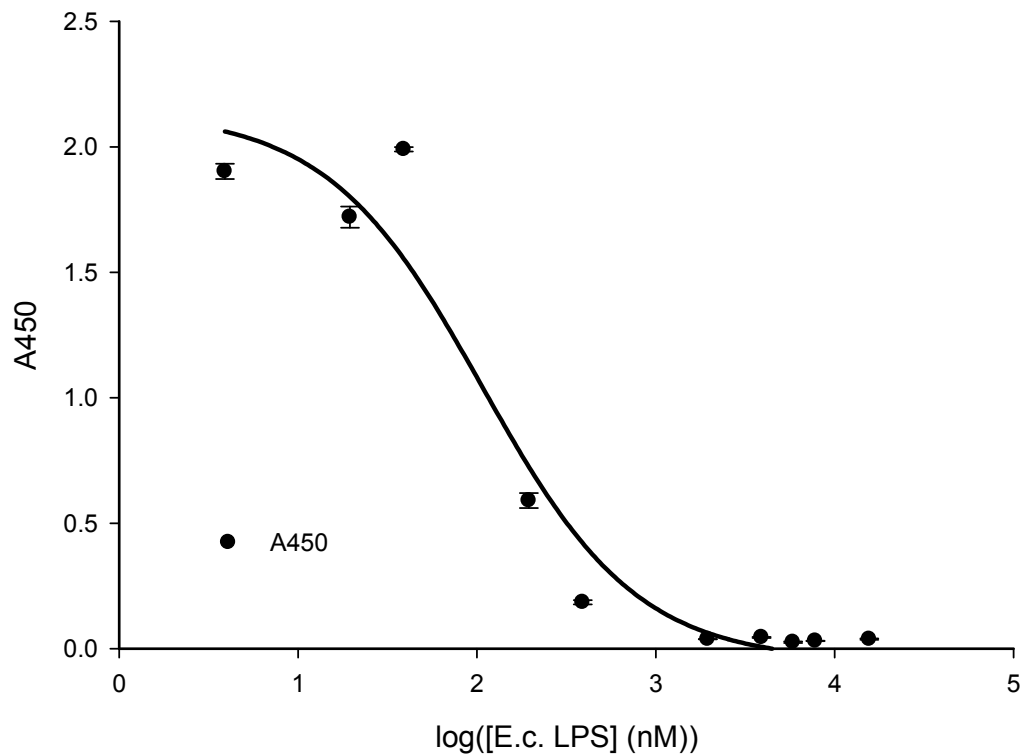


**Figure 73** Competition binding curves for *E. coli* LPS binding to cecropin B on *P. aeruginosa* LPS plates. The mean of triplicate data points  $\pm$  standard error is shown. Data are fit to **Equation 5**.

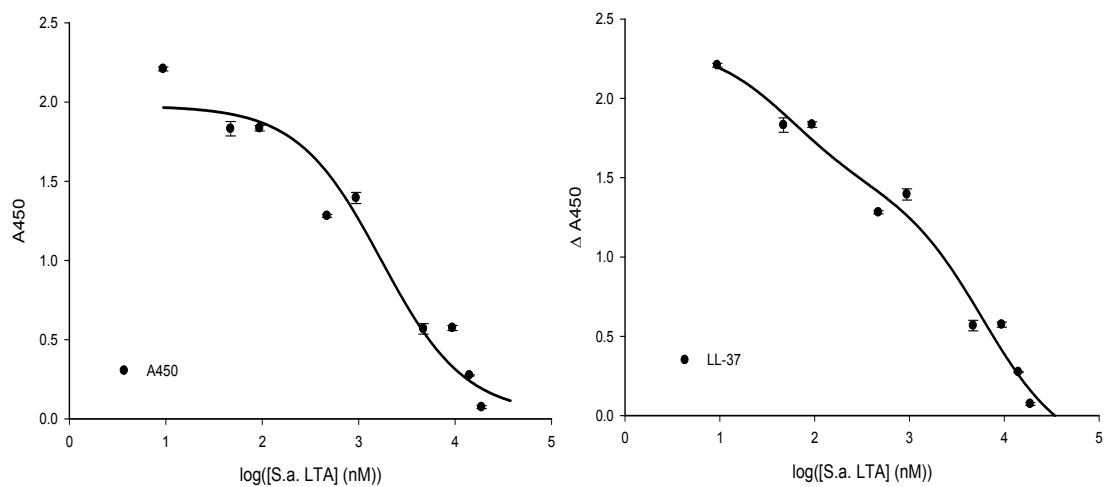


**Figure 74** Competition binding curves for *S. aureus* LTA competition binding to LL-37 on *P. aeruginosa* plates. The means of triplicate measurements  $\pm$  standard error are shown. Lines are fit to **Equation 5** (left) and **Equation 6** (right).

competition binding, but there was not a substantial improvement in the fit for the two-binding site competition model (**Figure 72**). *E. coli* LPS and *S. aureus* LTA were also able to completely block the binding of LL-37 to immobilized *P. aeruginosa* LPS (**Figures 73 and 74**). The competition binding data for *S. aureus* LTA fit both one- and two-site competition binding models. *P. aeruginosa* LPS binds LL-37 with an EC50 value of  $249 \pm 1.11$  nM, *E. coli* LPS binds with an EC50 value of  $107 \pm 1.24$  nM and *S. aureus* LTA binds with an EC50 value of  $1710 \pm 1.25$  nM (**Table 15**).

Free *E. coli* LPS was able to completely block LL-37 binding to immobilized *E. coli* LPS (**Figure 75**). Additionally, *P. aeruginosa* LPS and *S. aureus* LTA were also able to completely block LL-37 binding to immobilized *E. coli* LPS (**Figures 76 and 77**). The competition binding curves for *S. aureus* LTA fit both one- and two-binding competition models. Free *E. coli* LPS bound LL-37 with an EC50 value of  $81.9 \pm 1.91$  nM while *P. aeruginosa* LPS bound with an EC50 value of  $106 \pm 1.21$  nM and *S. aureus* LTA bound with an EC50 value of  $92.5 \pm 1.79$  nM (**Table 16**).

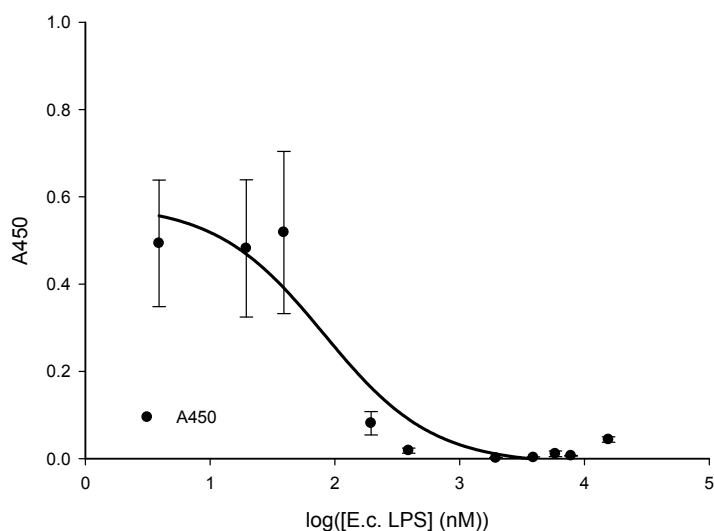


**Figure 75** Competition binding curve for free *E. coli* LPS binding to LL-37 on immobilized *E. coli* LPS. Data points represent the mean of triplicate measurements  $\pm$  standard error. Fit of **Equation 5** is shown.



From these data it appears that LL-37 binds to *P. aeruginosa* LPS, *E. coli* LPS and *S. aureus* LTA with similar affinities. This agrees with the results of the antimicrobial activity modulation data where almost all of the GAGs, charge-reduced heparin analogs and LMWHs were able to reverse the antimicrobial activity of LL-37 against the three different organisms.

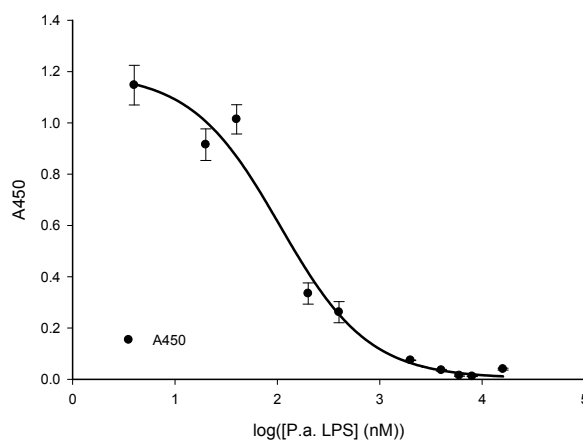


**Figure 76** Competition binding curve of *P. aeruginosa* LPS binding to LL-37 on immobilized *E. coli* LPS. Mean of triplicate data points  $\pm$  standard error shown. The line is fit to **Equation 5**.

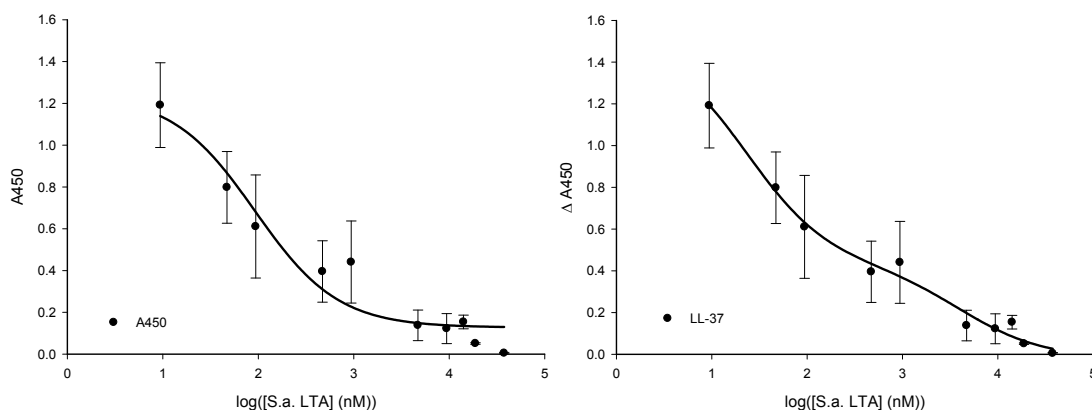


**Figure 77** Competition binding curves showing *S. aureus* LTA binding to LL-37 on *E. coli* LPS plates. The mean of triplicate measurements  $\pm$  standard error is shown. The fits of **Equation 5** (left) and **Equation 6** (right) are shown.

### 5.3 Competition binding assays measuring the affinity of CAPs for GAGs

#### 5.3.1 Experimental techniques

Competitive binding assays were employed to explore the affinity of GAGs for cecropin A, cecropin B and LL-37. Since these CAPs showed different affinity for *P. aeruginosa* LPS and *E. coli* LPS, these ELISA experiments were done using both immobilized *P. aeruginosa* LPS and *E. coli* LPS. We were especially interested in these experiments due to the different modulatory activities of the GAGs found when different target organisms were used in the antimicrobial activity reversal studies.

Plates were prepared and blocked as discussed in Section 5.1.1. Aliquots of 0.1  $\mu\text{g}$  cecropin A, cecropin B or LL-37 in tris buffer containing 5 mM  $\text{CaCl}_2$  and 1.0 mg/mL BSA was incubated with a series of concentrations of heparin, enoxaparin, HS, DS, HA or C4S overnight at 37°C with shaking. Three-50  $\mu\text{L}$  aliquots of each sample were added to the plate and binding was allowed to occur to 1 hour at 37°C with shaking. Following binding the plates were washed 3X with tris buffer. A 100 ng/mL primary antibody solution was added at 100  $\mu\text{L}$ /well and allowed to bind for 1 hour at 37°C with shaking. The plates were washed 3X with tris buffer at 300  $\mu\text{L}$ /well, followed by the addition of 100 ng/mL secondary antibody at 100  $\mu\text{L}$ /well. Next the plate was washed 4X with 300  $\mu\text{L}$  tris buffer and 100  $\mu\text{L}$ /well horseradish peroxidase substrate was added. After a 30 minute incubation at room temperature with shaking, 15  $\mu\text{L}$   $\text{H}_2\text{SO}_4$  was added to stop the reaction and the plate was read at 450 nm. Controls were included in these experiments where the CAP was omitted from the overnight incubation.

Due to the polydisperse nature of the GAGs used in these experiments, the average disaccharide molecular weights for each GAG were used in all calculations. Data were analyzed using SigmaPlot. The affinity of CAPs for the GAGs was calculated using **Equations 5 and 6**.

### 5.3.2 Competition binding studies for cecropin A and GAGs

Heparin, HS, DS, enoxaparin and C4S were able to block cecropin A binding to immobilized *P. aeruginosa* LPS (**Figures 78, 79 and 80**). HA was not able to block cecropin A binding to the immobilized *P. aeruginosa* LPS (**Figure 78**). The competition binding data for enoxaparin and C4S fit both the one- and two-site competition binding models. Cecropin A showed no affinity for the GAGs DS and HA.

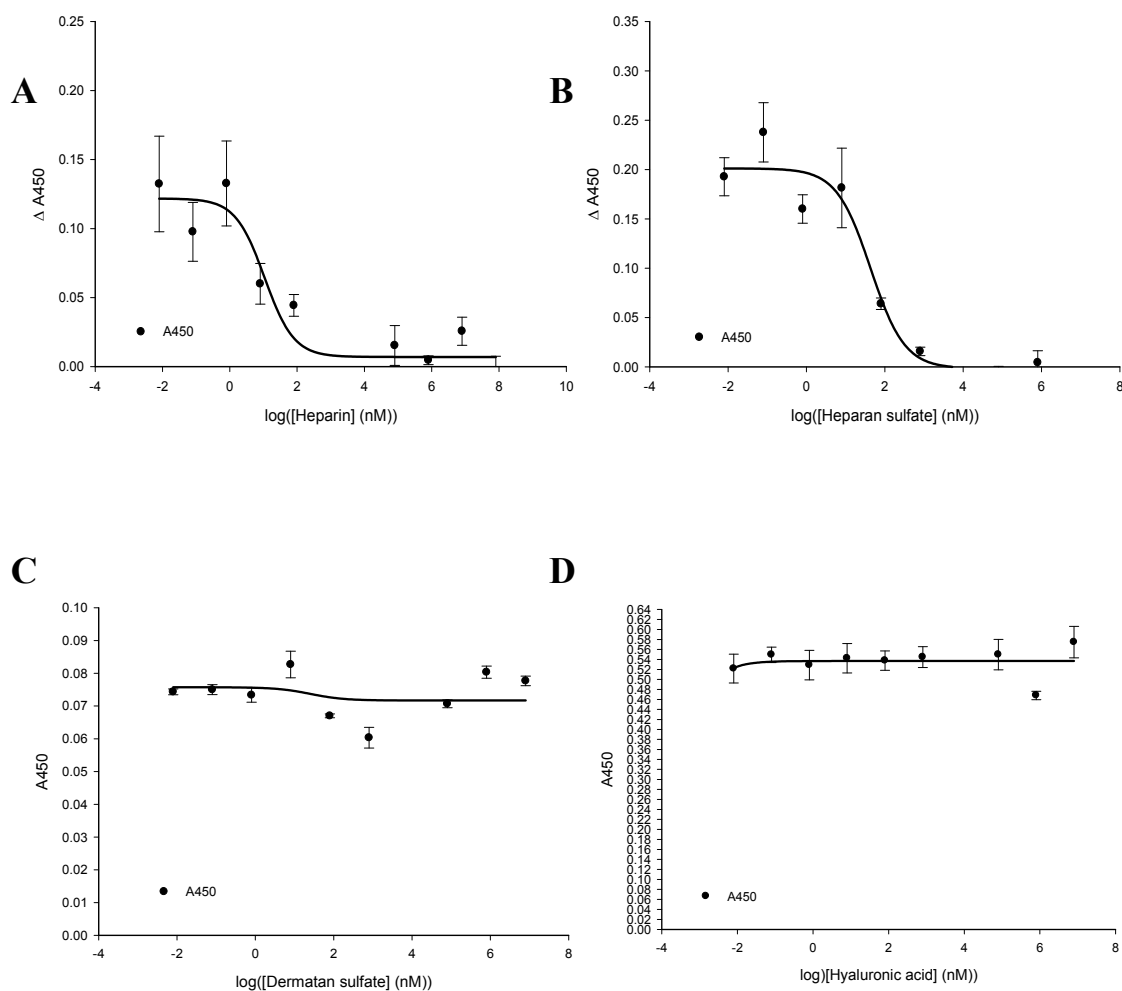


**Figure 78** Competition binding curves showing heparin (A), HS (B), DS (C) and HA (D) binding cecropin A on immobilized *P. aeruginosa* LPS. The fits of **Equation 5** are shown.

The calculated binding constants for the competition binding curves of the GAGs binding cecropin A on *P. aeruginosa* LPS is shown in **Table 17**. In order of highest affinity to lowest the GAGs rank heparin > HS > enoxaparin > C4S > HA and DS.

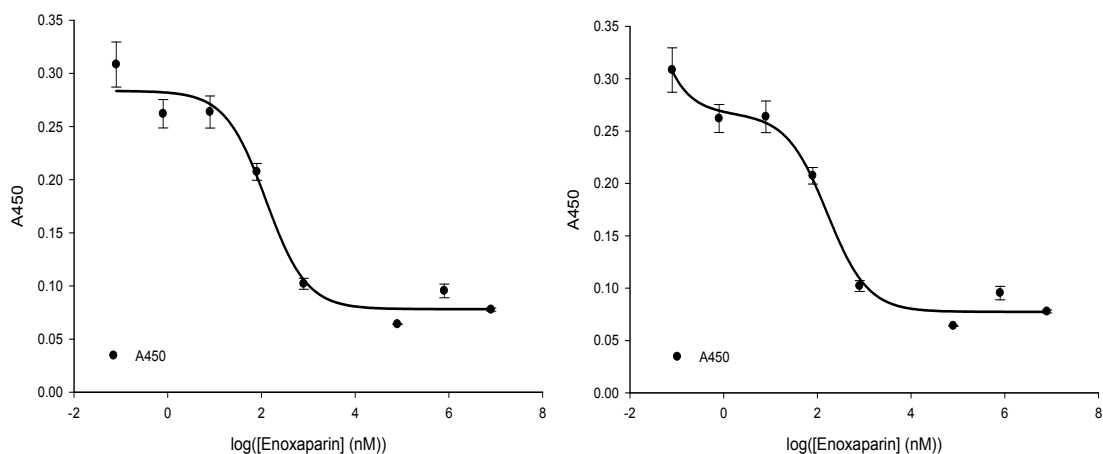


**Figure 79** Competition binding curves for enoxaparin binding cecropin A on *P. aeruginosa* LPS. The fits of **Equation 5** (left) and **Equation 6** (right) are shown.

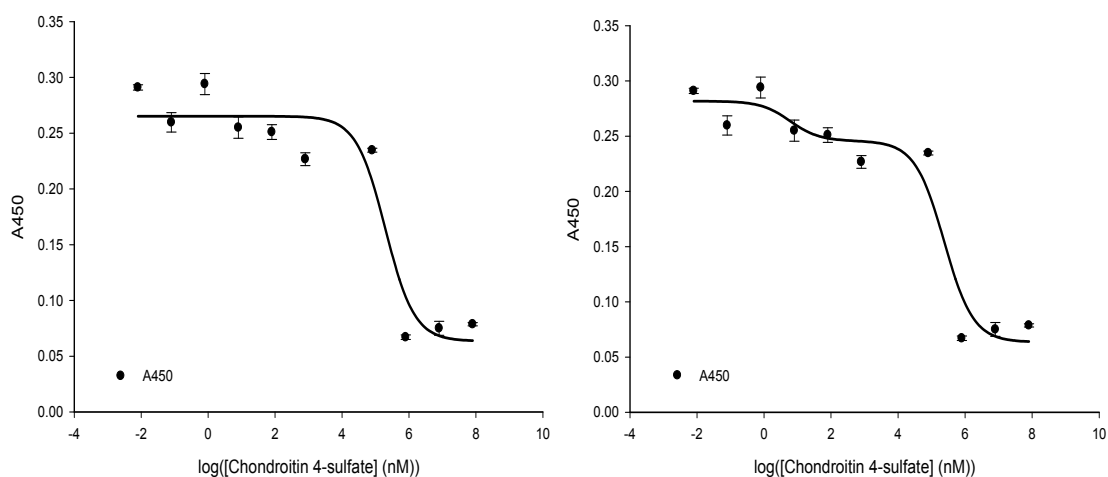


**Figure 80** Competition binding curves for C4S binding cecropin A on immobilized *P. aeruginosa* LPS. The fits of **Equation 5** (left) and **Equation 6** (right) are shown.

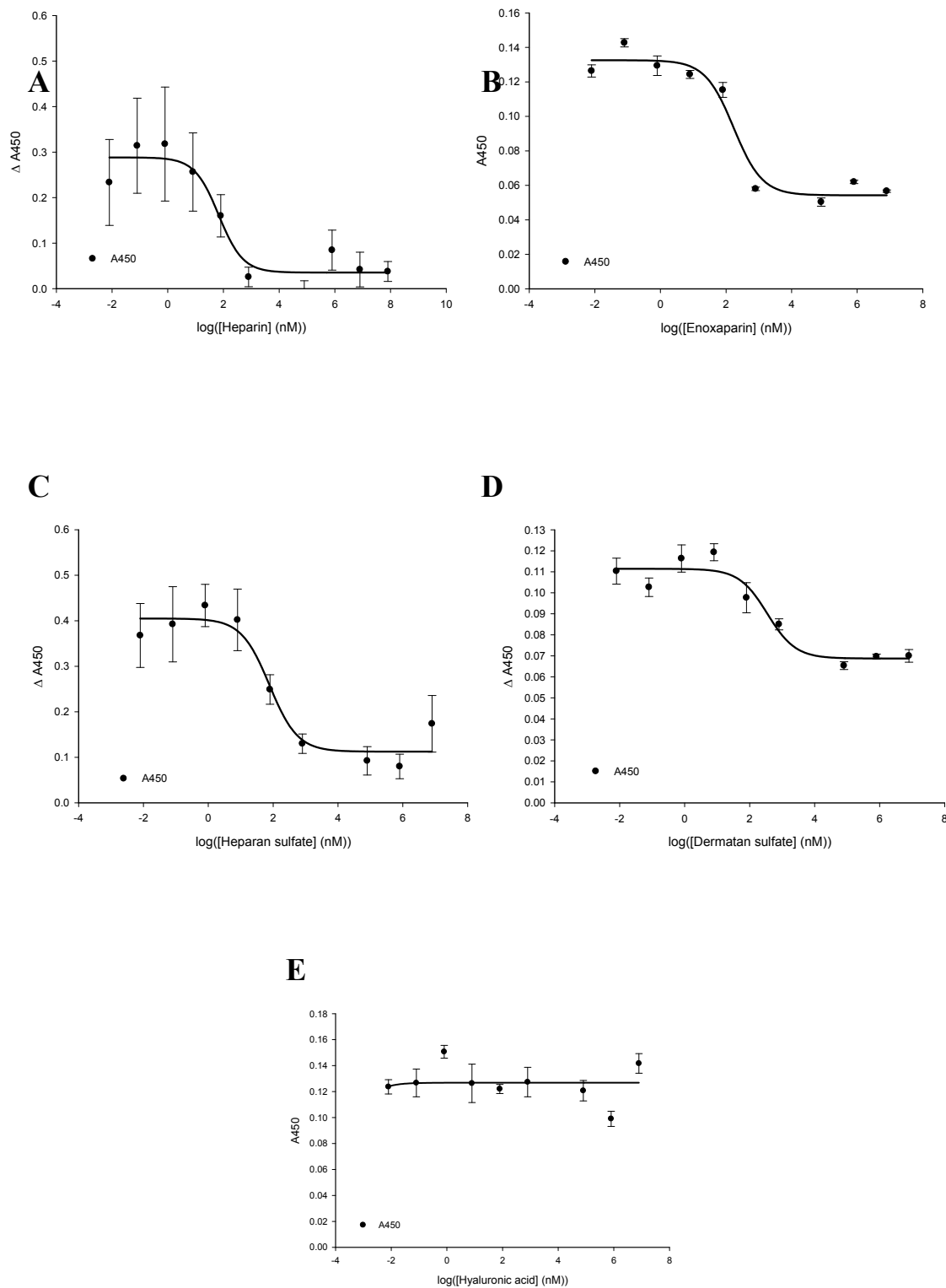


**Figure 81** Competition binding curves showing heparin (A), enoxaparin (B), HS (C), DS (D) and HA (E) binding cecropin A on immobilized *E. coli* LPS. The fit of Equation 5 is shown in A-E.

All of the GAGs tested, with the exception of HA were able to block cecropin A binding to immobilized *E. coli* LPS (**Figures 81 and 82**). The competition binding curves for C4S blocking LL-37 binding to immobilized *E. coli* LPS fit both the one- and two-binding site competition models (**Figure 82**). The calculated binding constants for the GAG-cecropin A-immobilized *E. coli* LPS competition binding studies are shown in **Table 18**. Heparin had the highest affinity, followed by HS, enoxaparin, DS, C4S and HA.

These results are surprising based on the results of the cecropin A antimicrobial reversal data. In those experiments heparin was the only GAG able to modulate the antimicrobial activity of cecropin A. Here all of the GAGs, with the exception of HA, show affinity for cecropin A. Additionally, DS shows a higher affinity for cecropin A when competing with *P. aeruginosa* LPS as compared to heparin.

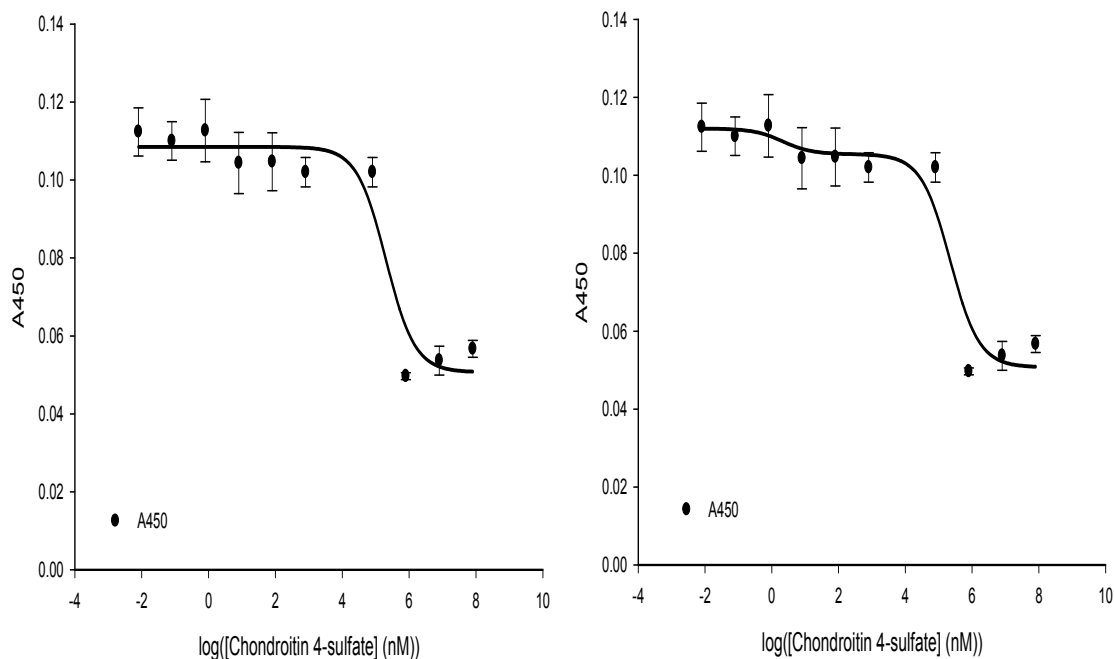


**Figure 82** Competition binding curves showing C4S binding cecropin A on immobilized *E. coli* LPS. The fits of **Equation 5** (left) and **Equation 6** (right) are shown.

### 5.3.3 Competition binding studies on cecropin B binding to GAGs

All of the GAGs tested, with the exception of HA, showed affinity for cecropin B when competing with immobilized *P. aeruginosa* LPS (**Figures 83, 84, 85 and 86**). The competition binding data for HS, HA and C4S and cecropin B on immobilized *P. aeruginosa* LPS fit the binding models for one- and two-sites (**Figures 84, 85 and 86**). Only the C4S competition binding data were a significantly better for the two-site competition binding model. The calculated binding constants for the GAGs binding

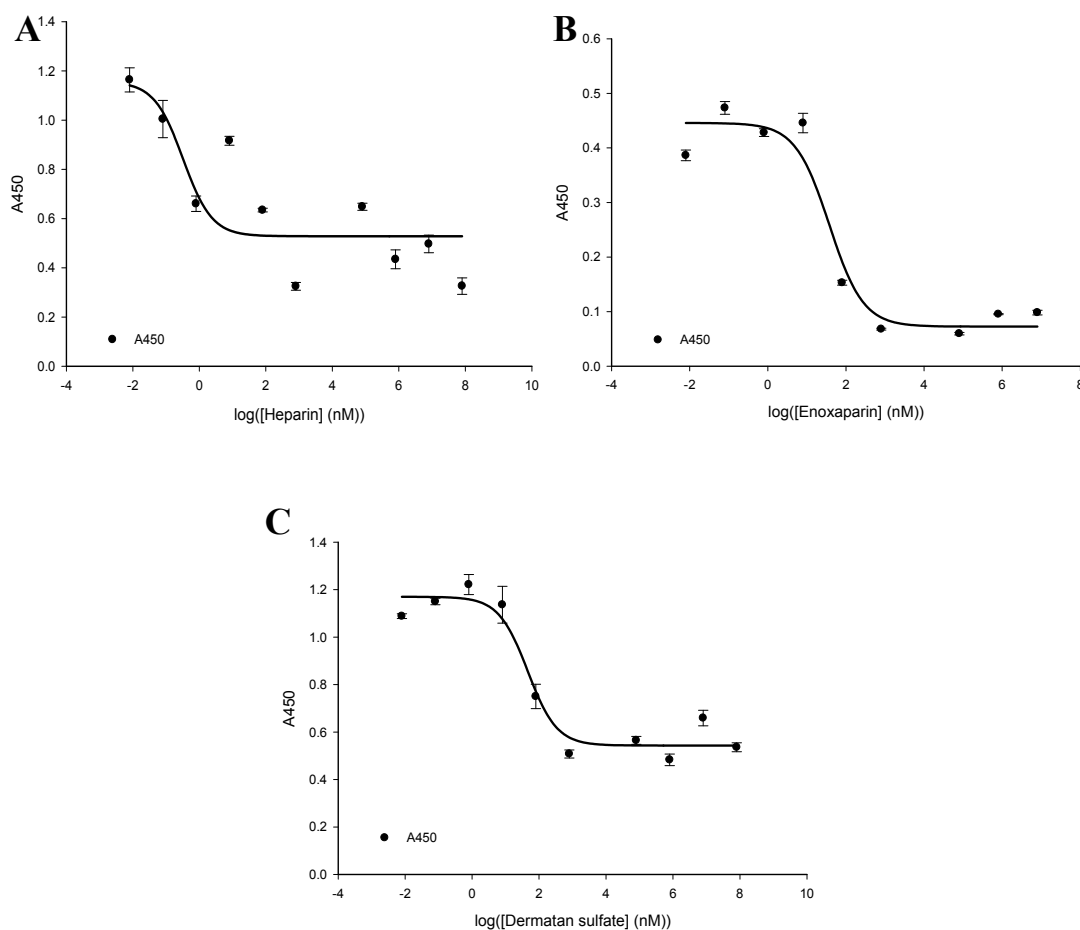


**Figure 83** Competition binding curves showing heparin (A), enoxaparin (B) and DS (C) binding to cecropin B on immobilized *P. aeruginosa* LPS. The fits of **Equation 5** are shown.

cecropin B on immobilized *P. aeruginosa* LPS is shown in **Table 19**. The GAGs in order from best affinity to worst are: heparin > HS > enoxaparin > DS > C4S > HA.

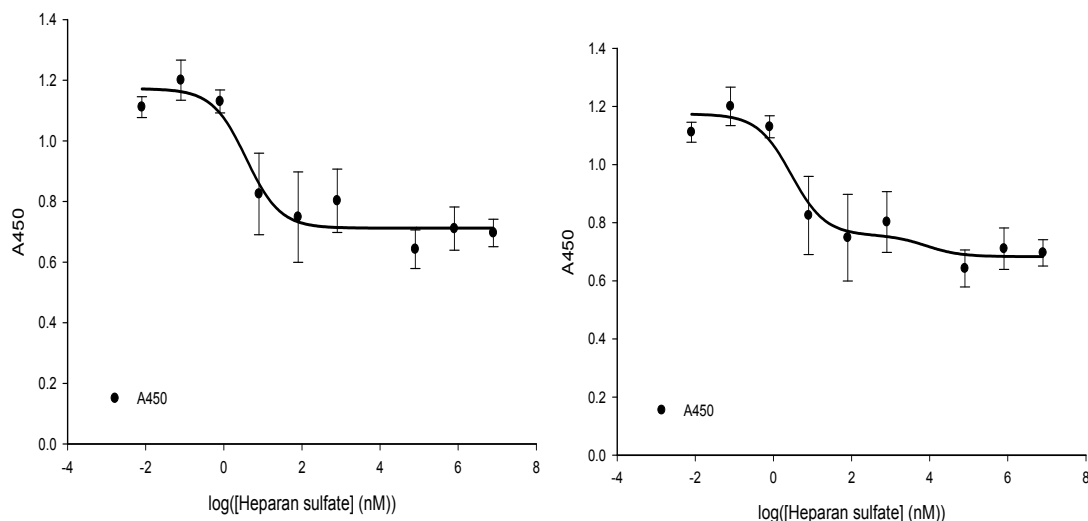


**Figure 84** Competition curves for HS binding cecropin B on immobilized *P. aeruginosa* LPS. Means of triplicate data points  $\pm$  standard error are shown. The fits of **Equation 5** (A) and **Equation 6** (B) are shown.

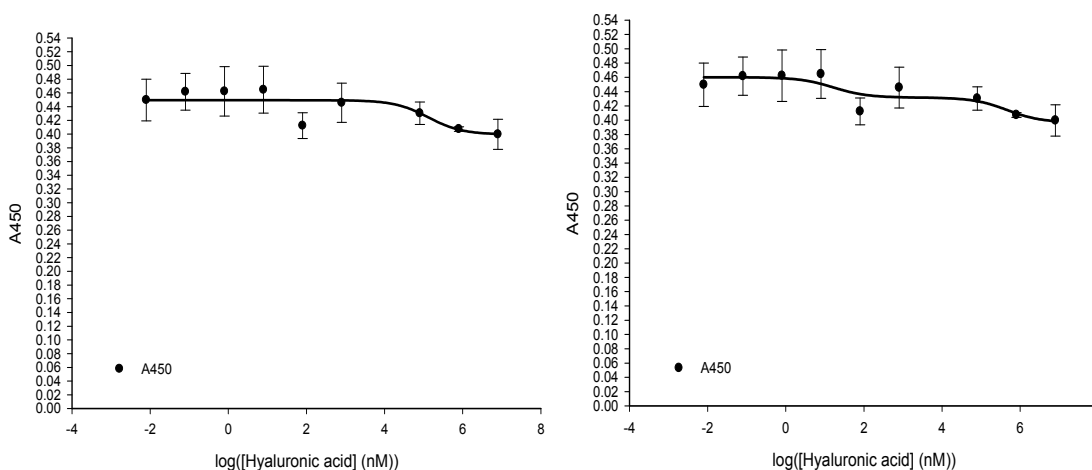


**Figure 85** Competition binding curves for HA binding to cecropin B on immobilized *P. aeruginosa* LPS. Data points represent the mean of triplicate measurements  $\pm$  standard error. The fits of **Equation 5** (left) and **Equation 6** (right) are shown.



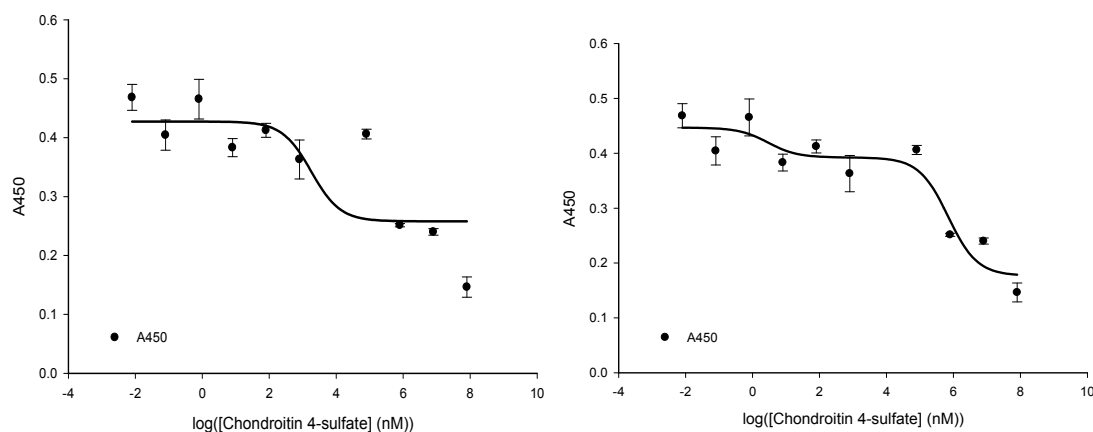


**Figure 86** Competition binding curves for C4S binding cecropin B on immobilized *P. aeruginosa* LPS. Means of triplicate determinations  $\pm$  standard error shown. The fits of **Equation 5** (left) and **Equation 6** (right) are shown.

All of the GAGs, with the exception of HA, are able to compete with *E. coli* LPS to bind cecropin B. The competition binding curves for enoxaparin, DS and C4S are better fit to a one-site competition binding model (**Figure 87**). Surprisingly, heparin and heparan sulfate both fit a two-site competition binding model better than a one-site competition binding model (**Figures 88 and 89**). Both heparin and HS appear to have a high affinity binding site and a much lower affinity binding site for cecropin B. The calculated binding constants for the GAG competition binding curves are presented in **Table 20**.

In the cecropin B competition binding studies heparin shows some of the highest affinity for the CAP, along with the LMWH and HS. It is intriguing to note that both heparin and HS fit the two-site competition binding model better with immobilized *E. coli* LPS. It is possible that the conformation of cecropin B bound to *E. coli* LPS allows it to be accessible to multiple binding sites on these two GAGs, while the conformation of cecropin B bound to *P. aeruginosa* LPS does not allow for this. Ultimately there are many binding sites along each GAG due to the high degree of heterogeneity, especially on HS.

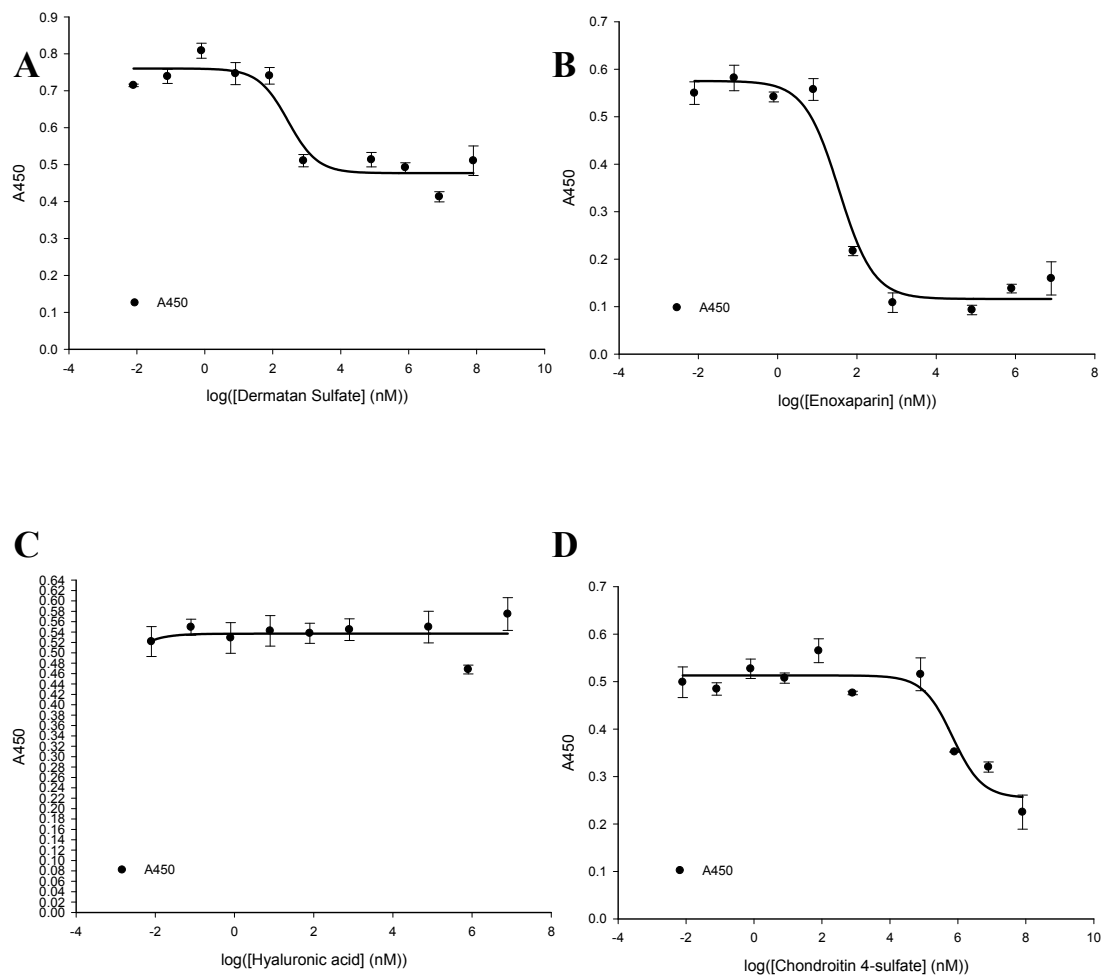


**Figure 87** Competition binding curves for DS (A), C4S (B), HA (C) and enoxaparin (D) binding to cecropin B on immobilized *E. coli* LPS. Means of triplicate data points  $\pm$  standard error shown. The fits of **Equation 5** are shown.

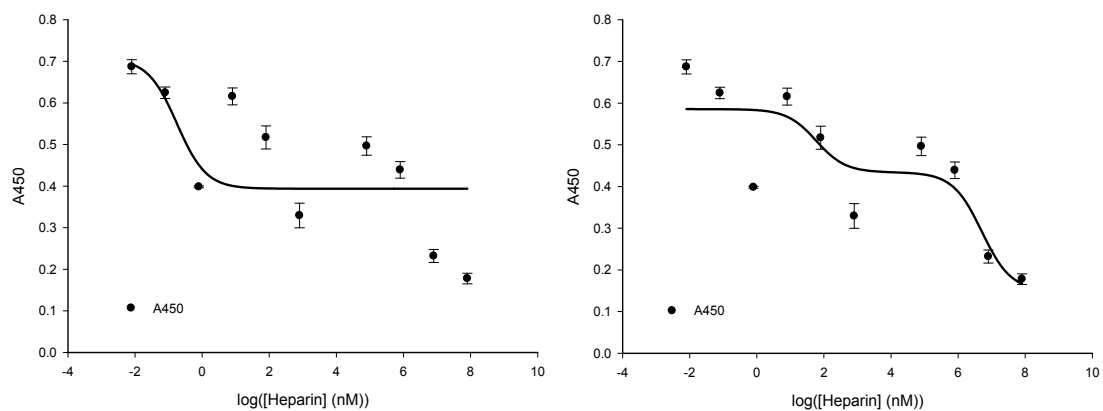


**Figure 88** Competition binding curves for heparin binding cecropin B on immobilized *E. coli* LPS. Data points represent the means of triplicate determinations  $\pm$  standard error. The fits of **Equation 5** (left) and **Equation 6** (right) are shown.

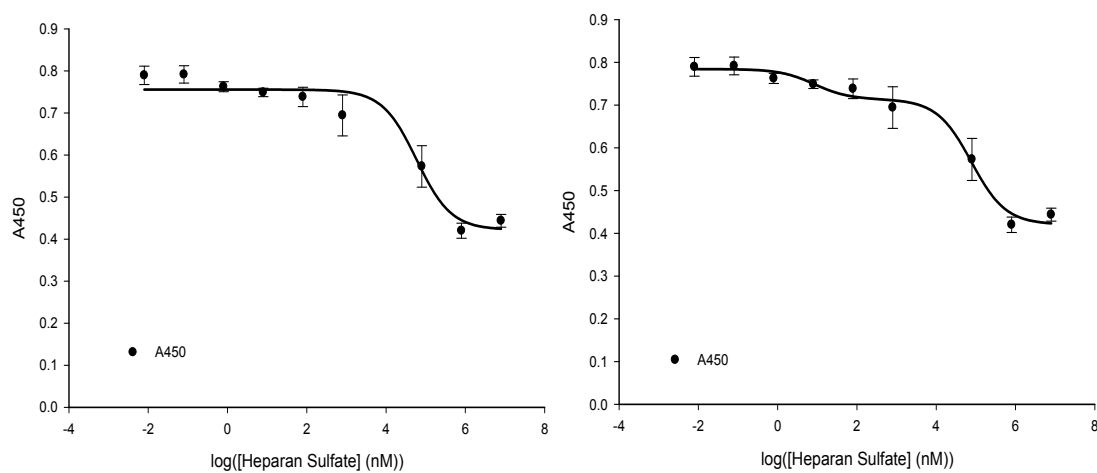


**Figure 89** Competition binding curves for HS binding to cecropin B on immobilized *E. coli* LPS. Data points represent the mean of triplicate measurements  $\pm$  standard error. Lines are fit to **Equation 5** (left) and **Equation 6** (right).

### 5.3.4 Competition binding studies for LL-37 and GAGs

In contrast to the competition binding studies for cecropin A and cecropin B, all of the GAGs tested were able to block the binding of LL-37 to *P. aeruginosa* LPS (**Figure 90**). Although heparin, enoxaparin and HA fit both the one- and two-site competition binding models, only heparin showed a significantly improved fit for the two-site competition binding model. The calculated binding constants for the GAGs competing LL-37 off of immobilized *P. aeruginosa* LPS is shown in **Table 21**. For the one-site competition binding model the GAGs rank in order of highest affinity to lowest DS > enoxaparin > HS > HA > heparin > C4S.

All of the GAGs, except C4S, were able to compete with immobilized *E. coli* LPS to bind LL-37 (**Figure 91**). The calculated binding constants for these competition binding curves are shown in **Table 22**. Only the enoxaparin competition binding curve fit the two-site competition binding model, but with little improvement over the one-site model. In order of highest affinity to lowest the GAGs rank: DS > heparin > HS > enoxaparin > HA > C4S.

DS shows the highest affinity for LL-37 on both immobilized *P. aeruginosa* LPS and *E. coli* LPS. This is surprising based on the results of the LL-37 antimicrobial activity modulatory activities of the GAGs. Based on the results of those experiments we would expect all of the GAGs, with the exception of HA, to show approximately equal affinities for LL-37 on either immobilized *P. aeruginosa* LPS or *E. coli* LPS. In these experiments we see that HA shows affinity for LL-37. These experiments also demonstrate that there is a clear difference between the GAG affinities for LL-37. In addition, it is interesting to note that enoxaparin binding to LL-37 on either immobilized *P. aeruginosa* LPS or *E. coli* LPS can fit a two-site competition binding model. It is possible that its lower molecular weight and therefore smaller size results in it binding closer to the immobilized LPS surface and allows it to come into contact with two LL-37 molecules.

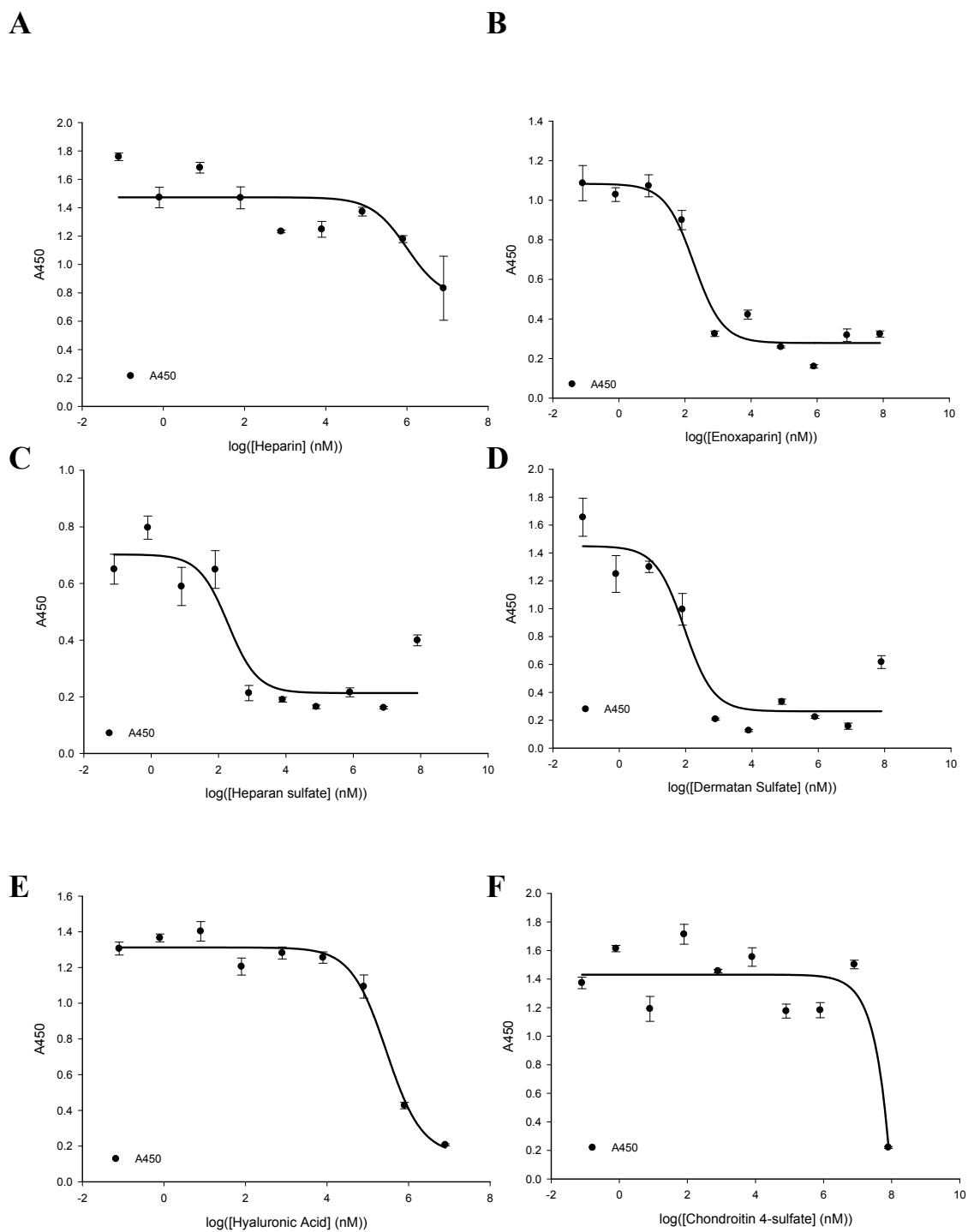


**Figure 90** Competition binding curves for heparin (A), enoxaparin (B), HS (C), DS (D), HA (E) and C4S (F) binding to LL-37 on immobilized *P. aeruginosa* LPS. The means of triplicate data points  $\pm$  standard error are shown. The fits of Equation 5 are shown.

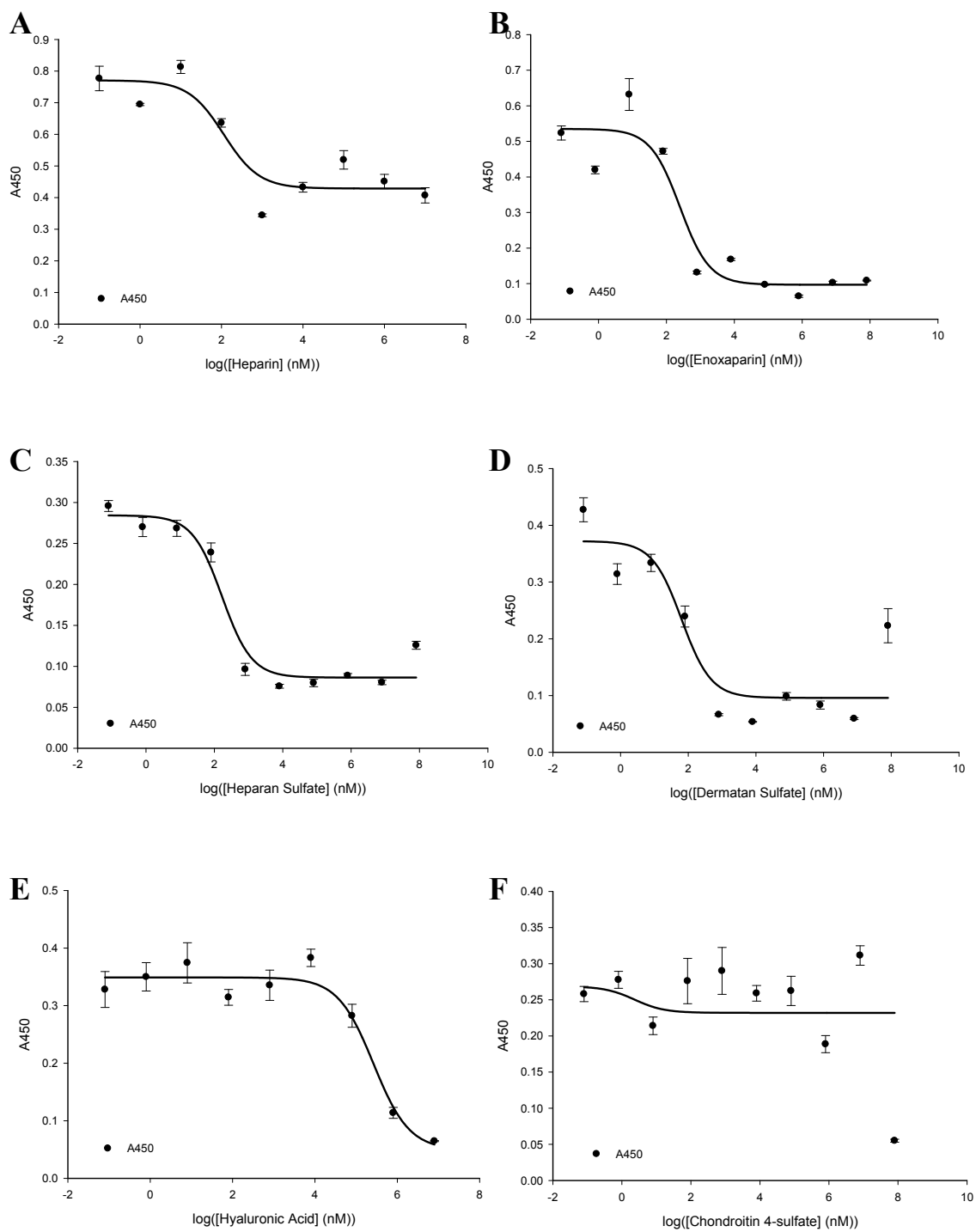


**Figure 91** Competition binding curves for heparin (A), enoxaparin (B), HS (C), DS (D), HA (E) and C4S (F) binding to LL-37 on immobilized *E. coli* LPS. Means of triplicate data points  $\pm$  standard error shown. The fits of Equation 5 are shown.

Binding Model	Kd (nM)	Bmax	Kd <sub>2</sub> (nM)	Bmax <sub>2</sub>	N.s.	R <sup>2</sup>
One site saturation	652 ± 186	0.584 ± 0.028				0.8344
One site saturation + nonspecific	356 ± 164	0.460 ± 0.0720			1.18 × 10 <sup>-5</sup> ± 7.41 × 10 <sup>-6</sup>	0.8427
Two site saturation	25.7 ± 48.5	0.179 ± 0.0820	3180 ± 2480	0.515 ± 0.0816		0.8737
Two site saturation ± nonspecific	25.7 ± 55.8	0.179 ± 0.110	3180 ± 6880	0.515 ± 0.539	7.07 × 10 <sup>-13</sup> ± 2.84 × 10 <sup>-5</sup>	0.8737

**Table 5** Binding constants calculated from cecropin A saturation of immobilized *P. aeruginosa* LPS.

Binding Model	Kd (nM)	Bmax	Kd <sub>2</sub> (nM)	Bmax <sub>2</sub>	N.s.	R <sup>2</sup>
One site saturation	396 ± 96.5	0.513 ± 0.0191				0.8528
One site saturation + nonspecific	133 ± 56.5	0.353 ± 0.0377			1.753×10 <sup>-5</sup> ± 4.334×10 <sup>-6</sup>	0.8924
Two site saturation	55.7 ± 45.6	0.261 ± 0.0634	7060 ± 6950	0.448 ± 0.138		0.8959
Two site saturation + nonspecific				DNC		

**Table 6** Binding constants calculated from cecropin A saturation of *E. coli* LPS.

Note: DNC indicates that the data did not converge to the binding model.



Binding Model	Kd (nM)	Bmax	Kd <sub>2</sub> (nM)	Bmax <sub>2</sub>	N.s.	R <sup>2</sup>
One site saturation	235± 40.4	1.655 ± 0.0395				0.930 5
One site saturation + nonspecific	235 ± 56.6	1.66 ± 0.119			3.92×10 <sup>-14</sup> ±1.24×10 <sup>-5</sup>	0.930 5
Two site saturation	235 ± 7240000	0.832 ± 3020000	235 ± 7320000	0.823 ± 3020000		0.930 5
Two site saturation ± nonspecific	235 ± 3020000	0.849 ± 3160000	235 ± 3220000	0.807 ± 3160000	1.55×10 <sup>-14</sup> ±1.62×10 <sup>-5</sup>	0.930 5

**Table 7** Binding constants calculated from cecropin B saturation of *P. aeruginosa* LPS.

Binding Model	Kd (nM)	Bmax	Kd <sub>2</sub> (nM)	Bmax <sub>2</sub>	N.s.	R <sup>2</sup>
One site saturation	270 ± 49.9	0.969 ± 0.0255				0.9220
One site saturation + nonspecific	270 ± 70.3	0.969 ± 0.0781			2.47×10 <sup>-14</sup> ± 8.04×10 <sup>-6</sup>	0.9220
Two site saturation	270 ± 8530000	0.492 ± 1220000	270 ± 8810000	0.476 ± 1220000		0.9220
Two site saturation ± nonspecific	270 ± 74800	0.501 ± 10.7	270 ± 80100	0.468 ± 10.7	6.92×10 <sup>-15</sup> ± 6.95×10 <sup>-11</sup>	0.9220

**Table 8** Calculated binding constants for cecropin B binding to immobilized *E. coli* LPS.

Binding Model	Kd (nM)	Bmax	Kd <sub>2</sub> (nM)	Bmax <sub>2</sub>	Ns	R <sup>2</sup>
One site saturation	69.2 ± 7.72	2.76 ± 0.0348				0.9691
One site saturation + nonspecific	66.4 ± 9.77	2.73 ± 0.0844			5.56×10 <sup>-6</sup>	0.9693
Two site saturation	69.2 ± 1580000	1.39 ± 1350000	69.2 ± 1590000	1.38 ± 1350000		0.9691
Two site saturation + nonspecific	66.4 ± 3470000	1.38 ± 9260000	66.4 ± 3520000	1.35 ± 9260000	5.56×10 <sup>-6</sup>	0.9693

**Table 9** Binding constants calculated for LL-37 binding to *P. aeruginosa* LPS.

Binding Model	Kd (nM)	Bmax	Kd <sub>2</sub> (nM)	Bmax <sub>2</sub>	Ns	R <sup>2</sup>
One site saturation	225 ±	2.28 ±				0.9780
	22.1	0.0317				
One site saturation + nonspecific	220 ±	2.26 ±			3.31×10 <sup>-6</sup>	0.9780
	30.5	0.0959				
Two site saturation	226 ±	1.14 ±	226 ±	1.14 ±		0.9780
	4630000	1240000	4650000	12400000		
Two site saturation + nonspecific	220 ±	1.16 ±	220 ±	1.10 ±	3.31×10 <sup>-6</sup>	0.9780
	23100000	1300000	24200000	1300000		

**Table 10** Calculated binding constants for LL-37 binding to *E. coli* LPS.

Free ligand	Kd	[Cecropin A] (nM)	One site competition			Two site competition				
			EC50 (nM)	Ki (nM)	R <sup>2</sup>	EC50 <sub>1</sub> (nM)	EC50 <sub>2</sub> (nM)	Ki <sub>1</sub> (nM)	Ki <sub>2</sub> (nM)	R <sup>2</sup>
<i>P. aeruginosa</i> LPS	356	500	29900 ± 1.87	13200	0.8962					DNC
<i>E. coli</i> LPS	356	500	486 ± 1.27	216	0.9461					DNC
<i>S. aureus</i> LTA	356	500	2920 ± 1.45	1300	0.8996					DNC

**Table 11** Binding constants calculated from LPS and LTA competition binding studies on cecropin A binding to immobilized *P. aeruginosa* LPS.

Note: DNC indicates that the data did not conform to the binding model.

Free ligand	Kd	[Cecropin A] (nM)	One site competition			Two site competition				
			EC50 (nM)	Ki (nM)	R <sup>2</sup>	EC50 <sub>1</sub> (nM)	EC50 <sub>2</sub> (nM)	Ki <sub>1</sub> (nM)	Ki <sub>2</sub> (nM)	R <sup>2</sup>
<i>P. aeruginosa</i> LPS	133	500	17800 ± 1.55	3740	0.9117	467 ± 32.9	41400 ± 9.32	98.3	8700	0.9153
<i>E. coli</i> LPS	133	500	841 ± 1.24	177	0.9626			DNC		
<i>S. aureus</i> LTA	133	500	3890 ± 1.51	818	0.8764			DNC		

**Table 12** Calculated binding values from LPS and LTA competition binding studies on cecropin A binding to immobilized *E. coli* LPS.

Note: DNC indicates that the data did not converge to the binding model.

Free ligand	Kd	[Cecropin B] (nM)	One site competition			Two site competition				
			EC50 (nM)	Ki (nM)	R <sup>2</sup>	EC50 <sub>1</sub> (nM)	EC50 <sub>2</sub> (nM)	Ki <sub>1</sub> (nM)	Ki <sub>2</sub> (nM)	R <sup>2</sup>
<i>P. aeruginosa</i> LPS	253	522	48.1 ± 1.57	15.7	0.8096			DNC		
<i>E. coli</i> LPS	253	522	1140 ± 1.12	374	0.9889			DNC		
<i>S. aureus</i> LTA	253	522	5450 ± 4.05	1780	0.3774	63.6 ± 36.9	23400 ± 15.3	20.8	7640	0.402

**Table 13** Calculated binding values from LPS and LTA competition binding studies on cecropin B binding to immobilized *P. aeruginosa* LPS.

Note: DNC indicates that the data did not converge to the binding model.

Free ligand	Kd	[Cecropin B] (nM)	One site competition			Two site competition				
			EC50 (nM)	Ki (nM)	R <sup>2</sup>	EC50 <sub>1</sub> (nM)	EC50 <sub>2</sub> (nM)	Ki <sub>1</sub> (nM)	Ki <sub>2</sub> (nM)	R <sup>2</sup>
<i>P. aeruginosa</i> LPS	270	522	52.8 ± 1.57	18.0	0.814			DNC		
<i>E. coli</i> LPS	270	522	888 ± 1.23	3300	0.965			DNC		
<i>S. aureus</i> LTA	270	522	13700 ± 1.71	4690	0.7984	0.156 ± 1×10 <sup>178</sup>	16900 ± 1.99	0.0532	5760	0.8057

**Table 14** Binding constants calculated from LPS and LTA competition binding assays on cecropin B binding to immobilized *E. coli* LPS.

Note: DNC indicates that the data did not converge to the binding model.



Free ligand	Kd	[LL-37] (nM)	One site competition			Two site competition				
			EC50 (nM)	Ki (nM)	R <sup>2</sup>	EC50 <sub>1</sub> (nM)	EC50 <sub>2</sub> (nM)	Ki <sub>1</sub> (nM)	Ki <sub>2</sub> (nM)	R <sup>2</sup>
<i>P. aeruginosa</i> LPS	69.2	445	249 ± 1.11	33.6	0.9875	98.4 ± 1.74	1100 ± 2.25	13.2	148	0.9902
<i>E. coli</i> LPS	69.2	445	107 ± 1.24	14.4	0.9524			DNC		
<i>S. aureus</i> LTA	69.2	445	1710 ± 1.25	230	0.956	54.0 ± 1.77	6080 ± 1.35	7.27	818	0.9808

**Table 15** Calculated binding constants for LL-37 binding to *P. aeruginosa* LPS.

Note: DNC indicates that the data did not converge to the binding model.

Free ligand	Kd	[LL-37] (nM)	One site competition			Two site competition				
			EC50 (nM)	Ki (nM)	R <sup>2</sup>	EC50 <sub>1</sub> (nM)	EC50 <sub>2</sub> (nM)	Ki <sub>1</sub> (nM)	Ki <sub>2</sub> (nM)	R <sup>2</sup>
<i>P. aeruginosa</i> LPS	226	445	106 ± 1.21	35.7	0.9635			DNC		
<i>E. coli</i> LPS	226	445	81.9 ± 1.91	27.6	0.6910			DNC		
<i>S. aureus</i> LTA	226	445	92.5 ± 1.79	31.1	0.7127	23.2 ± 4.09	4200 ± 8.61	7.81	1410	0.7547

**Table 16** Calculated binding constants for LL-37 binding to *E. coli* LPS.

Free ligand	Kd (nM)	[Ligand] (nM)	One Site Competition			Two Site Competition				
			EC50 (nM)	Ki (nM)	R <sup>2</sup>	EC50 <sub>1</sub> (nM)	EC50 <sub>2</sub> (nM)	Ki <sub>1</sub> (nM)	Ki <sub>2</sub> (nM)	R <sup>2</sup>
Heparin	356	499	10.8 ± 2.07	4.51	0.7080			DNC		
Enoxaparin	356	499	125 ± 1.33	55.3	0.9483	1.31×10 <sup>-3</sup> ± 6.37×10 <sup>136</sup>	162 ± 1.43	5.83×10 <sup>-4</sup>	71.8	0.9620
Heparan sulfate	356	499	43.4 ± 1.56	18.1	0.8825			DNC		
Dermatan sulfate	356	499		DNC				DNC		
Hyaluronic acid	356	499		DNC				DNC		
Chondroitin 4-sulfate	356	499	197000 ± 1.42	87400	0.9171	6.00 ± 6.48	237000 ± 1.48	2.67	106000	0.9360

**Table 17** Binding constants calculated for GAG competition binding assays on cecropin A binding to immobilized *P. aeruginosa* LPS.

Note: DNC indicates that the data did not converge to binding model.

Free ligand	Kd (nM)	[Ligand] (nM)	One Site Competition			Two Site Competition				
			EC50 (nM)	Ki (nM)	R <sup>2</sup>	EC50 <sub>1</sub> (nM)	EC50 <sub>2</sub> (nM)	Ki <sub>1</sub> (nM)	Ki <sub>2</sub> (nM)	R <sup>2</sup>
Heparin	133	499	67.4 ± 2.86	14.2	0.5450			DNC		
Enoxaparin	133	499	171 ± 1.32	39.4	0.9507			DNC		
Heparan sulfate	133	499	77.0 ± 2.06	16.2	0.7235			DNC		
Dermatan sulfate	133	499	349 ± 1.69	73.5	0.8429			DNC		
Hyaluronic acid	133	499		DNC				DNC		
Chondroitin 4-sulfate	133	499	202000 ± 1.62	46500	0.8544	2.12 ± 119	222000 ± 1.74	0.489	51100	0.8616

**Table 18** Binding constants calculated for GAG competition binding assays on cecropin A binding to immobilized *E.coli* LPS.

Note: DNC indicates that the data did not converge to binding model.

Free ligand	Kd (nM)	[Ligand] (nM)	One Site Competition			Two Site Competition				
			EC50 (nM)	Ki (nM)	R <sup>2</sup>	EC50 <sub>1</sub> (nM)	EC50 <sub>2</sub> (nM)	Ki <sub>1</sub> (nM)	Ki <sub>2</sub> (nM)	R <sup>2</sup>
Heparin	253	522	0.324 ± 2.27	0.106	0.6343				DNC	
Enoxaparin	253	522	37.5 ± 1.33	12.3	0.9498				DNC	
Heparan sulfate	253	522	3.74 ± 2.26	1.22	0.6821	2.87 ± 3.05	8300 ± 1330000	0.938	2710	0.6929
Dermatan sulfate	253	522	45.9 ± 1.40	15.0	0.9253				DNC	
Hyaluronic acid	253	522	132000 ± 9.97	43000	0.188	16.6 ± 76.3	463000 ± 64.2	5.41	151000	0.2362
Chondroitin 4-sulfate	253	522	1790 ± 3.50	584	0.566	2.90 ± 12.1	694000 ± 1.82	0.948	227000	0.8344

**Table 19** Calculated binding constants for GAG competition binding studies for cecropin B binding to *P. aeruginosa* LPS.

Note: DNC indicates that the data did not converge to the binding model.

Free ligand	Kd (nM)	[Ligand] (nM)	One Site Competition			Two Site Competition				
			EC50 (nM)	Ki (nM)	R <sup>2</sup>	EC50 <sub>1</sub> (nM)	EC50 <sub>2</sub> (nM)	Ki <sub>1</sub> (nM)	Ki <sub>2</sub> (nM)	R <sup>2</sup>
Heparin	133	522	67.4 ± 2.86	14.2	0.5450	58.8 ± 5.32	5100000 ± 3.14	20.1	17400	0.7122
Enoxaparin	133	522	35.3 ± 1.31	12.1	0.9535			DNC		
Heparan sulfate	133	522	59100 ± 1.54	20200	0.8859	8.49 ± 6.38	77300 ± 1.58	2.90	26400	0.9129
Dermatan sulfate	133	522	279 ± 1.60	95.4	0.8721			DNC		
Hyaluronic acid	133	522		DNC				DNC		
Chondroitin 4-sulfate	133	522	694000 ± 1.60	237000	0.8333			DNC		

**Table 20** Binding constants calculated from GAG competition binding curves on cecropin B binding to immobilized *E. coli* LPS.

Note: DNC indicates that the data did not converge to the binding model.

Free ligand	Kd (nM)	[Ligand] (nM)	One Site Competition			Two Site Competition				
			EC50 (nM)	Ki (nM)	R <sup>2</sup>	EC50 <sub>1</sub> (nM)	EC50 <sub>2</sub> (nM)	Ki <sub>1</sub> (nM)	Ki <sub>2</sub> (nM)	R <sup>2</sup>
Heparin	69.2	445	999000 ± 2.67	134000	0.5141	78.3 ± 3.25	7220000 ± 24.3	10.5	972000	0.7352
Enoxaparin	69.2	445	185 ± 1.37	24.9	0.9367	170 ± 1.56	47100 ± 6740	22.9	6330	0.9375
Heparan sulfate	69.2	445	192 ± 1.79	25.8	0.810			DNC		
Dermatan sulfate	69.2	445	92.7 ± 1.55	12.5	0.8681			DNC		
Hyaluronic acid	69.2	445	286000 ± 1.24	38500	0.9650	22.3 ± 17.6	323000 ± 1.27	3.00	43500	0.9698
Chondroitin 4-sulfate	69.2	445	220000000000 ± 10 <sup>1112.373</sup>	29560000000	0.7606			DNC		

**Table 21** Binding constants for GAG competition binding assays for LL-37 binding immobilized *P. aeruginosa* LPS.

Note: DNC indicates that the data did not converge to the binding model.

Free ligand	Kd (nM)	[Ligand] (nM)	One Site Competition			Two Site Competition				
			EC50 (nM)	Ki (nM)	R <sup>2</sup>	EC50 <sub>1</sub> (nM)	EC50 <sub>2</sub> (nM)	Ki <sub>1</sub> (nM)	Ki <sub>2</sub> (nM)	R <sup>2</sup>
Heparin	226	445	114 ± 1.71	38.4	0.8232			DNC		
Enoxaparin	226	445	249 ± 1.50	83.9	0.9002	240 ± 1.78	86100 ± 2270000000	80.6	29000	0.9004
Heparan sulfate	226	445	167 ± 1.32	56.3	0.9472			DNC		
Dermatan sulfate	226	445	63.9 ± 1.73	21.5	0.8049			DNC		
Hyaluronic acid	226	445	265000 ± 1.51	89100	0.8839			DNC		
Chondroitin 4-sulfate	226	445	2.31 ± 624	0.777	0.0279			DNC		

**Table 22** Binding constants calculated from GAG competition binding curves on LL-37 binding to immobilized *E. coli* LPS.

Note: DNC indicates that the data did not converge to the binding model.



5.4 Correlation between LL-37 affinity for  
glycosaminoglycans and the ability of glycosaminoglycans  
to reversal of antimicrobial activity of LL-37

Scatter plots were used to correlate the concentration of GAGs required to reverse the antimicrobial activity of LL-37 against both *P. aeruginosa* and *E. coli* with the  $K_i$  values calculated for the GAGs binding LL-37 competitively on either *P. aeruginosa* or *E. coli* LPS (**Figures 92** and **93**). Fitting these data to a linear regression can identify correlation. The fits of the linear regression to both sets of data can be seen in **Figures 92** and **93**.

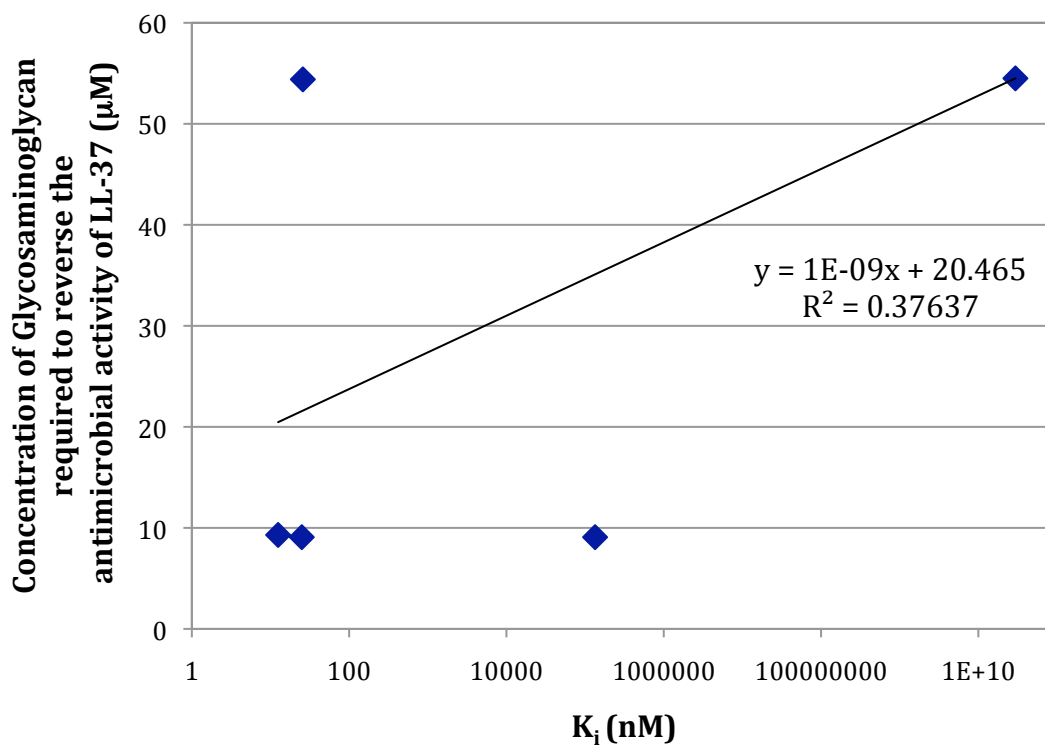


**Figure 92** Correlation plot comparing the concentration of GAG required to reverse the antimicrobial activity of LL-37 against *P. aeruginosa* vs. the  $K_i$  value for each GAG binding LL-37 on *P. aeruginosa* LPS. A linear fit is shown for the data.

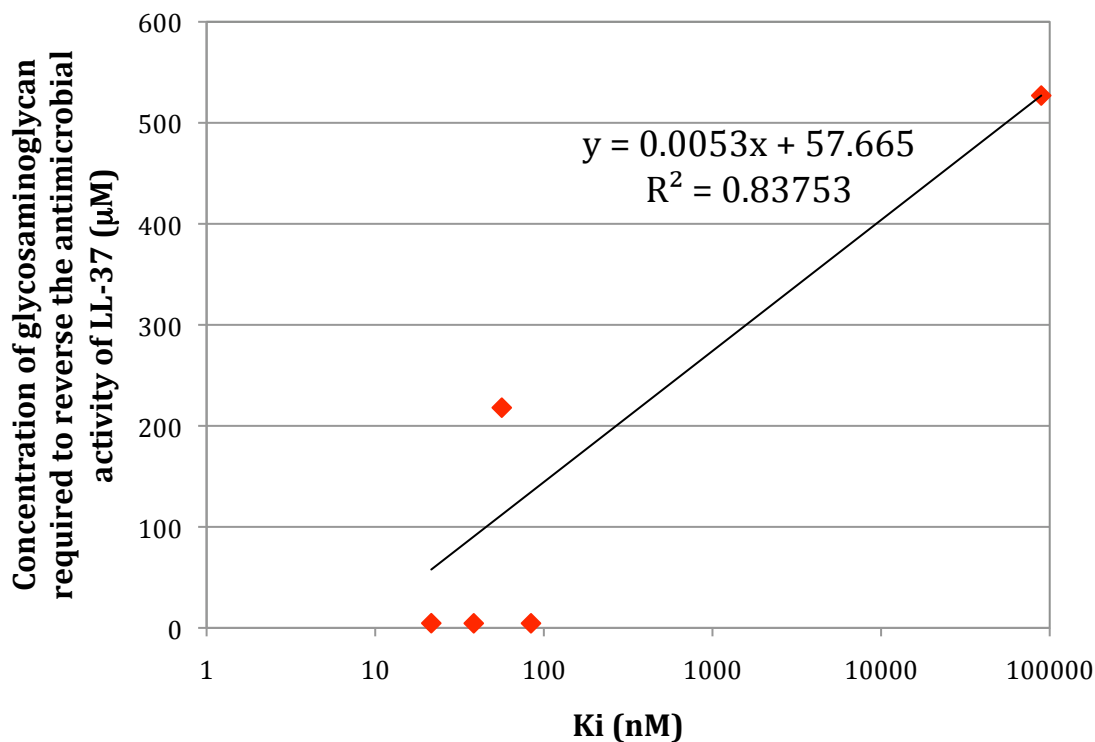


**Figure 93** Correlation plot comparing the concentration of GAG required to reverse the antimicrobial activity of LL-37 against *E. coli* vs. the  $K_i$  value for each GAG binding LL-37 on *E. coli* LPS. A linear fit is shown for the data.

Looking at the correlation plots in **Figures 92** and **93**, we can see that the affinity of LL-37 for the GAGs correlates more strongly to the ability of the GAGs to reverse the antimicrobial activity of LL-37 against *E. coli*. However, not all of the data points show strong correlation, such as in the case of Enoxaparin. In **Figure 93** Enoxaparin has a low  $K_i$  value, indicating a high affinity for LL-37, yet it requires a larger concentration to reverse the antimicrobial activity of LL-37 against *E. coli* as compared to heparin and DS, two GAGs that have similar  $K_i$  values. Correlations for the concentration of GAGs required to reverse the antimicrobial activity of cecropins A and B with the  $K_i$  values calculated for the GAGs binding either cecropin competitively on *P. aeruginosa* or *E.*

*coli* LPS could not be examined due to the low number of GAGs that reversed the antimicrobial activities of the cecropins against *P. aeruginosa* and *E. coli*.

### 5.5 Conclusions

In these experiments I measured the affinity of cecropin A, cecropin B and LL-37 for components of Gram-negative and -positive membranes. This provided insight into the affinity of the CAPs for the bacterial membranes of *P. aeruginosa*, *E. coli* and *S. aureus*. I found that there were significant differences between the affinities of cecropin A and cecropin B for the Gram-negative and -positive components, a result that wasn't expected based on the similarity of the peptide sequences. Cecropin A has a higher affinity for *E. coli* LPS while cecropin B has a higher affinity for *P. aeruginosa* LPS. Based on the results of the antimicrobial activity reversal data we expected to see that both cecropins show higher affinities for *E. coli* LPS. In addition, both cecropins showed affinity for *S. aureus* LTA, despite having no antimicrobial activity against this organism. Another surprising result was that LL-37 has similar affinities for *P. aeruginosa* LPS, *E. coli* LPS and *S. aureus* LTA. We expected the affinities to show significant differences based on the MIC values determined for LL-37. This likely indicates that there are additional binding components on the bacterial membrane involved in the antimicrobial activity of LL-37.

All of the GAGs tested showed affinities for cecropin A, cecropin B and LL-37. Overall, heparin showed the highest affinity for cecropin A, cecropin B and LL-37 on immobilized *P. aeruginosa* and *E. coli* LPS. Although CAP affinities were calculated for the GAGs, these results do not completely agree with the results from the reversal of antimicrobial activity experiments. Since we are working with a very simple representation of the bacterial membrane, this indicates that other factors may play a role in the CAPs binding to the bacterial membrane. Since specific bacterial membrane targets for cecropin A, cecropin B and LL-37 have not been elucidated it is difficult to

postulate what other components of the bacterial membrane GAGs are blocking the CAPs from binding. Yet again, these results indicate that GAG interactions with CAPs are complex and are dependent upon all factors of the system.

I also looked for a correlation between the concentration of GAG required to reverse the antimicrobial activity of LL-37 and the calculated affinities of LL-37 for each GAG. No clear correlations were evident between the affinity of LL-37 for the GAGs and the ability of the GAGs to negatively modulate the antimicrobial activity of LL-37. Since the ionic strength of the buffer used in the ELISA affinity assays is higher than the ionic strength used in earlier studies, it is possible that the affinity of LL-37 for each GAG in the two studies differs. Overall, these results indicate that the simplified models that we are using are not sufficient to be able to predict the ability of GAGs to modulate the antimicrobial activity of LL-37 based upon the affinity of LL-37 for each GAG.

Due to the highly basic properties of these peptides, it is likely that they bind to many targets non-specifically. While the affinity experiments presented in this chapter indicate that some or all of the GAGs have high affinities for the linear CAPs studied in this work, this affinity clearly does not solely account for the ability of select GAGs to modulate the antimicrobial activity of these CAPs. As has been suggested in this chapter, it is likely that a combination of factors, one being the affinity of the CAP for a GAG, results in the antimicrobial activity modulatory effects of the GAGs on each CAP.

CHAPTER 6 PROTECTION OF CATIONIC  
ANTIMICROBIAL PEPTIDES FROM PROTEOLYTIC  
DEGRADATION BY GLYCOSAMINOGLYCANS

6.1 Inhibition of trypsin and *Pseudomonas aeruginosa*  
elastase by glycosaminoglycans

Before we could test the ability of GAGs to protect cecropin A, cecropin B and LL-37 from proteolytic degradation we had to test the ability of GAGs to inhibit trypsin and *P. aeruginosa* elastase. Heparin is a potent regulator of serine proteases in the coagulation cascade.<sup>155</sup> In addition, heparin and other GAGs are known to inhibit human neutrophil elastase and interact with cathepsin G and protect against inhibition.<sup>363,364</sup> Furthermore, Redini *et al.* showed the *P. aeruginosa* elastase (PAELA) is not inhibited by heparin. However, the authors noted that PAELA showed inhibition by heparin when elastin, rather than a labeled peptide was used at the substrate for PAELA.<sup>210</sup>

6.1.1 Experimental techniques

The Pierce Quanticleave protease assay kit (#23236) was used to detect the activity of trypsin. This kit uses succinylated casein as the substrate for proteases and trinitrobenzenesulfonic acid (TNBSA) to detect primary amines exposed by protease cleavage. Dixon plots were used to determine the trypsin inhibitory activities of each GAG. For this assay, two different concentrations of substrate are used with a fixed amount of trypsin and range of concentrations of GAGs. Succinylated casein in the amount of 100 or 50  $\mu$ g was added to a 100 mM-0.01 mM GAG concentration range, TNBSA and 38.8 U trypsin in 50 mM sodium borate buffer, pH 8.0, in a 96-well microplate. The absorbance at 450 nm was read every 30 seconds in a BioTek ELx808 microplate reader for a total of 30 minutes. Each reaction condition was done in triplicate. Since this experiment is sensitive to free amines and many of the GAGs contain some primary amines, controls wells of GAG, TNBSA and trypsin were run.

Following the experiment, the initial velocity ( $V_0$ ) of each reaction condition was calculated by determining the slope of the A450 vs. time plots. To correct for the signal caused by GAG alone the initial velocity of the GAG controls was subtracted from the initial velocity of the samples, giving a corrected  $V_0$  for each reaction condition. The Grubbs test (**Equation 7**) was used to detect outliers in the data and a critical value of 2.21 or 2.29, depending on the number of samples in the data set, was used to exclude values. Less than half of the data sets had a data point excluded.

$$\text{Equation 7} \quad Z = \frac{|mean - x|}{SD}$$

Following the calculation of  $V_0$  for the two concentrations of succinylated casein with each GAG, the Dixon plots were created. To do this,  $1/V_0$  for each GAG data set was plotted against the GAG concentration and fit to a linear regression equation. The inhibition constant ( $K_i$ ) for the GAG is calculated from the X-coordinate at the intersection of the two linear fit lines (**Figure 94**).

A modified TNBSA-based assay was used to detect the effect of GAGs on PAELA activity. Rao *et al.* reported that succinylated elastin can be used as a substrate in the assay described above to measure the activity of elastase.<sup>365</sup> Since different inhibition potentials for heparin were seen depending on the substrate used by Redini *et al.*, we chose to use succinylated elastin to measure the inhibition of PAELA by GAGs<sup>210</sup>. Succinylated elastin was prepared according to the method of Rao *et al.* Briefly, soluble elastin (Sigma #E6527) was dissolved in 50 mM sodium borate buffer, pH 8.0, and 0.04 (w/w) succinic anhydride was added. The mixture was stirred at room temperature for 1 hour while maintaining the pH of the solution at 8.0 with the addition of 1M NaOH. Following the reaction the product was dialyzed extensively in 50 mM sodium borate buffer, pH 8.0. The concentration of succinylated elastin was determined using the Pierce Micro BCA protein assay kit (product #23235) and soluble elastin

standards. The degree of succinylation was tested using TNBSA and no primary amines were detected after 30 minutes at 37°C.

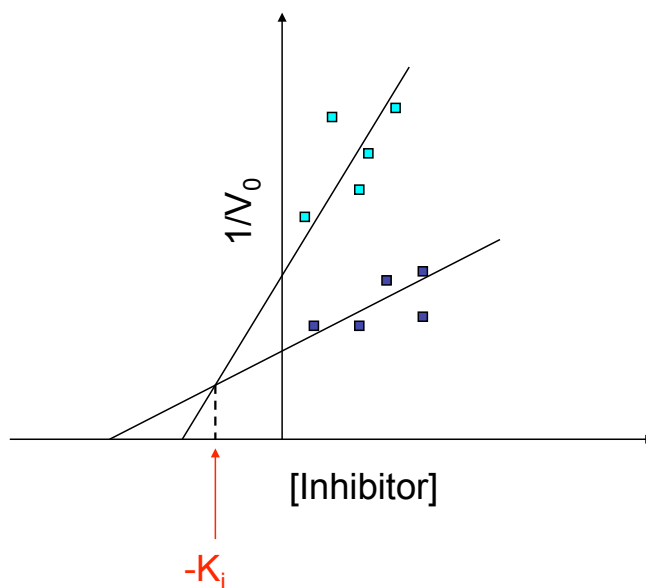


**Figure 94** Example of a Dixon plot and determination of the inhibition constant.

The effect of GAGs on the activity of PAELA was measured much in the same way as for trypsin activity. Succinylated elastin in the amount of 100 or 50  $\mu\text{g}$ , 0.2 U PAELA, a 100 mM-0.01 mM GAG concentration range and TNBSA were added to the wells of a 96-well microplate. The absorbance at 450 nm was read every 30 seconds in a Biotek ELx808 microplate reader for a total of 30 minutes and each reaction condition was done in triplicate. Controls for GAGs with TNBSA were also ran.  $V_0$  and  $K_i$  values were calculated for PAELA activity as described for trypsin activity. GM6001, a matrix metalloproteinase inhibitor that has activity against PAELA, was also used in these experiments as a positive control.<sup>366</sup> Due to the polydisperse nature of the GAGs used in these experiments, the average disaccharide molecular weight was used in all calculations for these experiments.

### 6.1.2 Results

The  $K_i$  values for heparin, enoxaparin, ardeparin, DS and HA against trypsin are shown in **Table 23**. Heparin, enoxaparin and HA showed some inhibition of trypsin while ardeparin and DS did not. HA was the most potent inhibitor of trypsin tested, but it is still not a very active trypsin inhibitor.

Glycosaminoglycan	Calculated $K_i$
Heparin	7.02 M
Enoxaparin	207 mM
Ardeparin	No inhibition
Dermatan sulfate	No inhibition
Hyaluronic acid	1.78 mM

**Table 23** Calculated inhibition constants for GAGs inhibiting trypsin.

The calculated  $K_i$  values for heparin, HS, DS, C4S, C6S, HA and GM6001 against PAELA are shown in **Table 24**. Heparin, DS, HA and GM6001 inhibited PAELA while HS, C4S and C6S showed no inhibition. GM6001 was the most potent inhibitor tested followed by HA.

Although we saw some inhibition of trypsin and PAELA by GAGs, the lowest  $K_i$  for a GAG was in the mM or greater range. However, much more protease was used in the protease inhibition experiments than in the CAP protection assays and it is possible that the GAG levels approached the inhibition constant. With this knowledge we continued the experiments and measured the ability of GAGs to protect cecropin A, cecropin B and LL-37 from proteolytic degradation. Knowing that it took large amounts of GAG to inhibit trypsin and PAELA gave us confidence that we would see protection of the CAP instead of inhibition of the protease in the next experiments.



Glycosaminoglycan	Calculated Ki
Heparin	5.10 mM
Heparan sulfate	No inhibition
Dermatan sulfate	19.2 mM
Chondroitin 4-sulfate	No inhibition
Chondroitin 6-sulfate	No inhibition
Hyaluronic acid	3.39 mM
GM6001	70.1 nM

**Table 24** Calculated inhibition constants for GAGs inhibiting *P. aeruginosa* elastase.

## 6.2 Protection of CAPs from trypsin degradation by GAGs

### 6.2.1 Experimental technique

To monitor the protection of cecropin A, cecropin B and LL-37 from proteolytic degradation by a range of concentrations of GAGs we chose to use polyacrylamide gel electrophoresis (PAGE). This method has been utilized in the past by Schmidtchen *et al.* to measure the degradation of LL-37 by bacterial proteinases.<sup>42</sup> This method had the advantage of being able to run multiple samples at once for a relatively low cost. However, because we chose to use this method, multiple experiments were not run and only single data points were collected from the experiments. Tris-tricine PAGE was used because we were interested in separating the CAPs from the smaller peptides produced by trypsin or PAELA cleavage<sup>367</sup>.

The optimal concentration of trypsin or PAELA was first determined. Eight micrograms of Cecropin A, cecropin B or LL-37 were incubated with a range of concentrations of trypsin or PAELA in for 30 minutes at 37°C. Loading buffer was added and the samples were boiled for 5 minutes to inactivate the protease and denature the CAP and protease. The samples were loaded onto Bio-Rad 16.5% tris-tricine Ready Gels (catalog #161-1125) along with two low molecular weight markers (MWMs). The

gels were ran in a Bio-Rad mini-PROTEAN gel electrophoresis cell using an initial voltage of 30 V and a running voltage of 100 V. Following electrophoresis, the gels were fixed using a methanol/acetic acid solution and visualized using Pierce GelCode Blue stain reagent. After destaining the gels were dried using gel drying frames and scanned. Two amounts of protease were chosen to follow the protection of the CAPs by GAGs.

To measure the protection of cecropin A, cecropin B or LL-37 from proteolytic degradation 8  $\mu$ g CAP was incubated with a range of concentrations of GAG and trypsin or PAELA for 30 minutes at 37°C. The samples were prepared by adding loading buffer and boiling to denature and inactivate the enzyme, run on tris-tricine gels, visualized and scanned as described above. The image processing program Image J was used to measure the pixel values for each band on the gels. The percentage of intact LL-37 was calculated for each GAG-CAP sample and graphed using excel.

#### 6.2.2 Protection of LL-37 from trypsin degradation by GAGs

The optimal incubation time and concentrations of trypsin were chosen to study the degradation of LL-37 by trypsin (**Figure 95**). A 30 minute incubation time showed the digestion of LL-37 more clearly than a 15 minute incubation time. A 30 minute incubation time was subsequently used for all other experiments. In these experiments we were interested in following the overall protection of LL-37 as well as determining if select peptides were protected by specific GAGs. Thus two concentrations of trypsin were used in the protection studies. 1 BAEE unit trypsin (Lane 7, **Figure 95**) was chosen to follow the overall protection of LL-37 because this amount of trypsin was sufficient to completely degrade LL-37. 100 mU BAEE trypsin (Lane 8, **Figure 95**) was used to determine if select peptides were protected by specific GAGs because this amount of trypsin yielded smaller peptides after a 30 minute digestion period and these were visible on the tris-tricine gel.

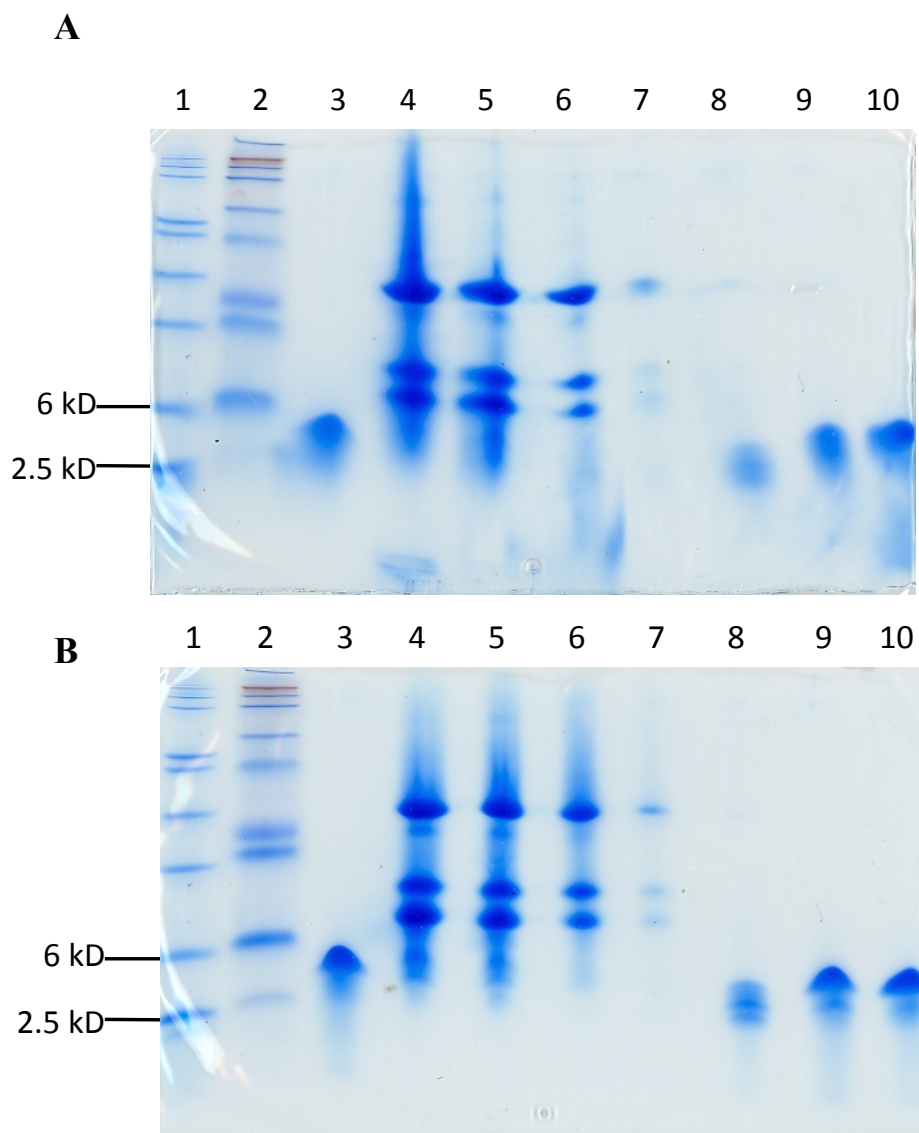


**Figure 95** Concentration-dependent trypsin digestion of LL-37. 15 minute (A) and 30 minute (B) digestions shown. Lanes 1-2: MWMs, Lane 3: LL-37, Lanes 4-10: LL-37 + trypsin. Lane 4 contains 1000 U. 1:10 trypsin dilutions were used in subsequent lanes, giving 1 mU trypsin in lane 10.

The tris-tricine gels for GAGs protecting LL-37 from 1 U trypsin are shown in **Figures 96** and **97**. Although the protection of LL-37 from 100 mU trypsin was also followed using tris-tricine gels, the sensitivity of the gels and Image J were not sufficient to determine if specific peptides were protected.

The percentage of LL-37 protected from trypsin degradation by the GAGs can be seen in **Figure 98**. Surprisingly, heparin was one of the least effective GAGs at protecting LL-37. DS, C4S and C6S were all able to protect LL-37 from trypsin degradation at less than 1:1 molar ratios. In fact, C4S and C6S protected LL-37 from trypsin degradation down to 0.01:1 molar ratios. HA was slightly better at protecting LL-37 than heparin while HS was slightly worse than heparin at protecting LL-37 from trypsin degradation. It is also surprising to note that C6S, enoxaparin and ardeparin have optimal protection concentrations. This is very evident with enoxaparin and ardeparin in **Figure 97 D&E**.

Based on the results of the antimicrobial activity modulation we would expect to see little difference between the abilities of the GAGs to protect LL-37. However, based on the results of LPS binding modulation we would expect C4S to be the worst GAG tested for protecting LL-37 against trypsin degradation.

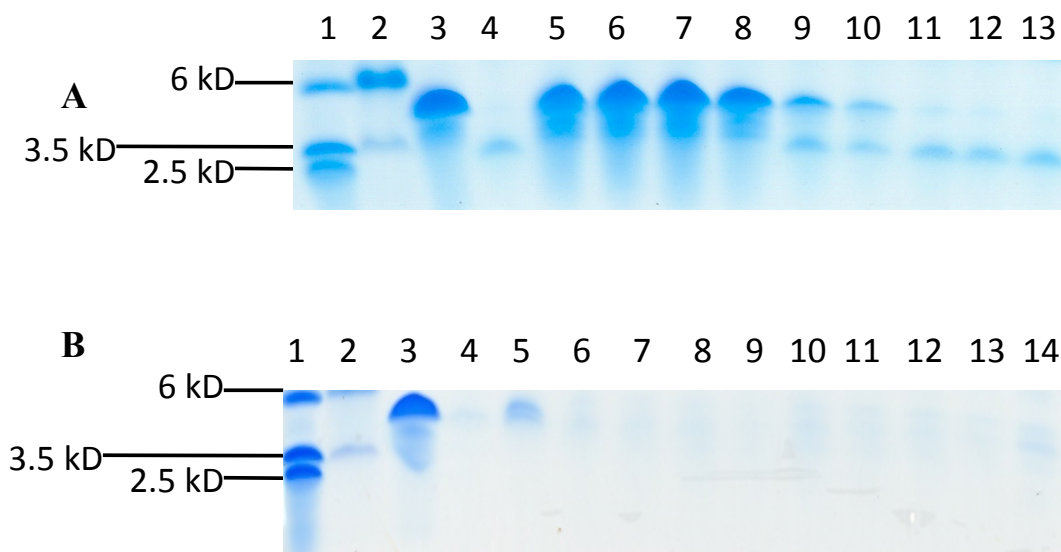


**Figure 96** Tris-tricine PAGE showing concentration-dependent protection of LL-37 from trypsin degradation by heparin (A) and HS (B). Lanes 1-2: MWMs, Lane 3: LL-37, Lane 4: LL-37 + 1 U trypsin, Lanes 5-14: LL-37, 1 U trypsin + GAGs.

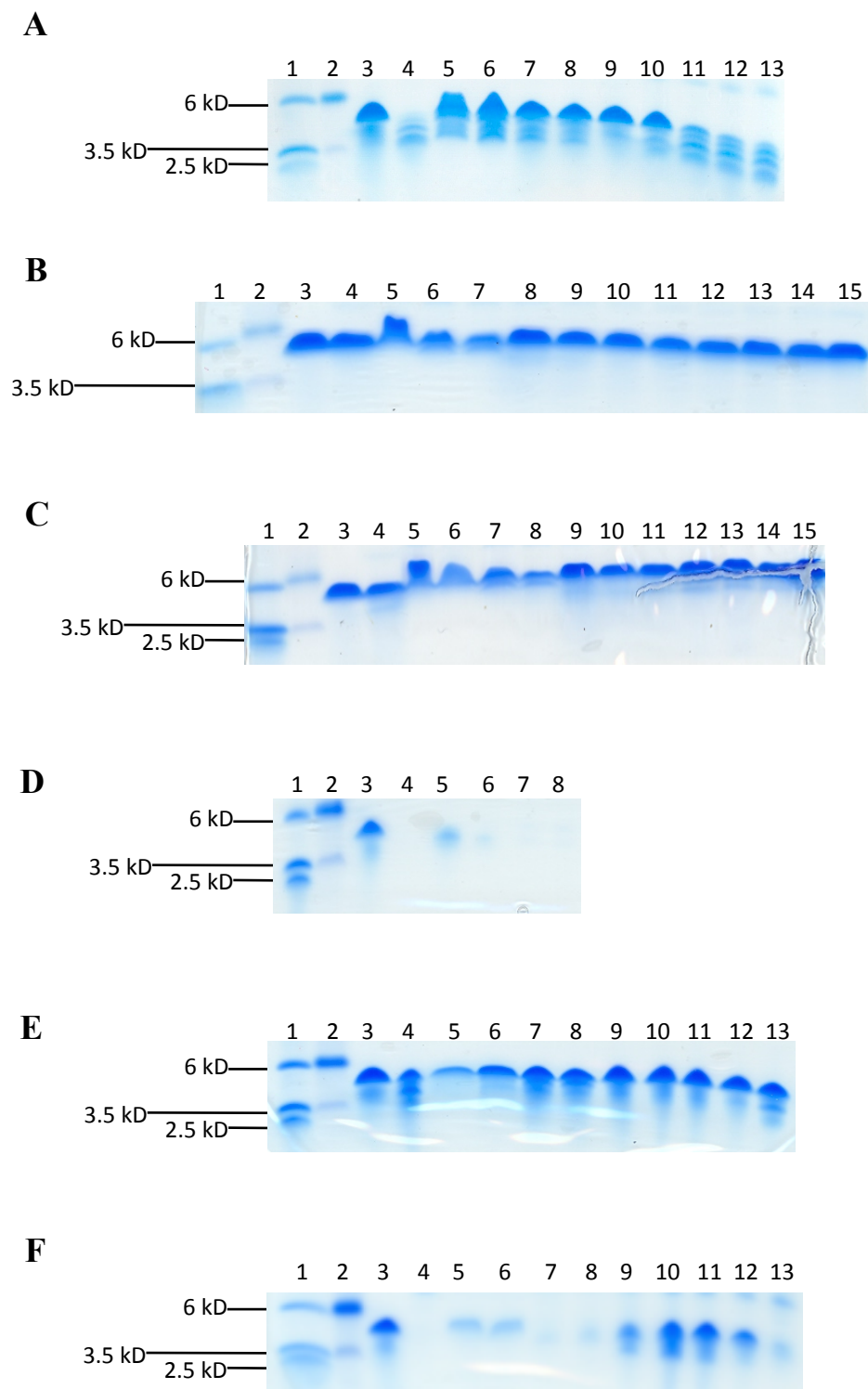


**Figure 97** Tris-tricine PAGE showing concentration-dependent protection of LL-37 from trypsin degradation by DS (A), C4S (B), C6S (C), HA (D), enoxaparin (E), and ardeparin (F). Lanes 1-2: MWMs, Lane 3: LL-37, Lane 4: LL-37 + 1 U trypsin, Lanes 5-15: LL-37, 1 U trypsin + GAGs.

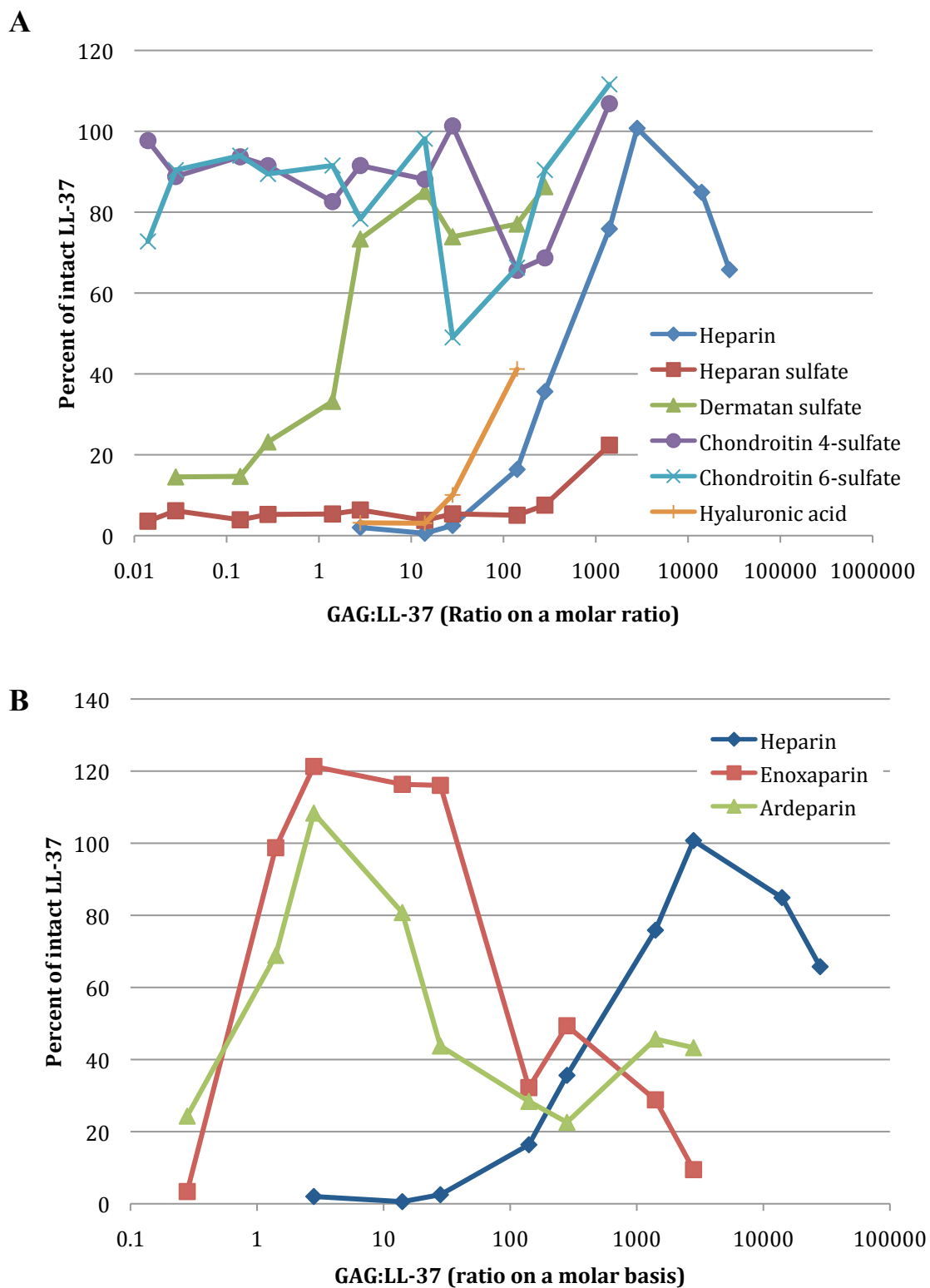


**Figure 98** Concentration-dependent protection of LL-37 from trypsin degradation by GAGs (A) and heparin and LMWHs (B).

### 6.2.3 Protection of cecropin A from trypsin degradation by GAGs

Based on the results of the cecropin A digestion with trypsin (**Figure 99**) we chose to use 5.5 U trypsin to measure the total protection of LL-37 and 550 mU to monitor the protection of specific peptide fragments by specific GAGs. Cecropin A is more resistant to trypsin degradation than LL-37, as evidenced by the larger amount of trypsin needed to completely degrade cecropin A.

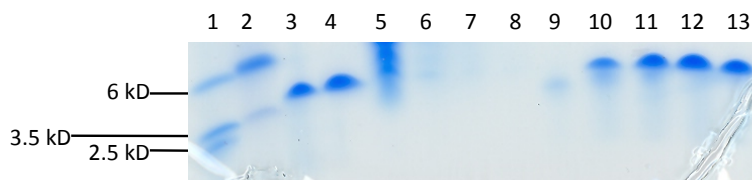


**Figure 99** Concentration-dependent digestion of cecropin A by trypsin. Lanes 1-2: MWMs, Lanes 3-4: cecropin A, Lanes 5-13: cecropin A + trypsin. Lane 5 contains 5,500 U of trypsin. 1:10 dilutions of trypsin were used in subsequent lanes, where lane 13 has 55 nU of trypsin.

For cecropin A, heparin is the best GAG tested at protecting from trypsin degradation (**Figures 100** and **101**). DS does not protect cecropin A from trypsin degradation and while HA provides approximately the same level of protection for cecropin A and LL-37. Interestingly, there is a significant difference between the ability of the LMWHs to protect cecropin A from degradation, as opposed to what was seen for LL-37. These results are in line with the result of the antimicrobial activity modulation where heparin was the best negative modulator of antimicrobial activity. These results are also in line with calculated affinities of cecropin A for the GAGs. Heparin had the lowest calculated  $EC_{50}$ , followed by enoxaparin, DS and HA. Only ardeparin showed a slight optimal protection window of concentrations in these experiments.

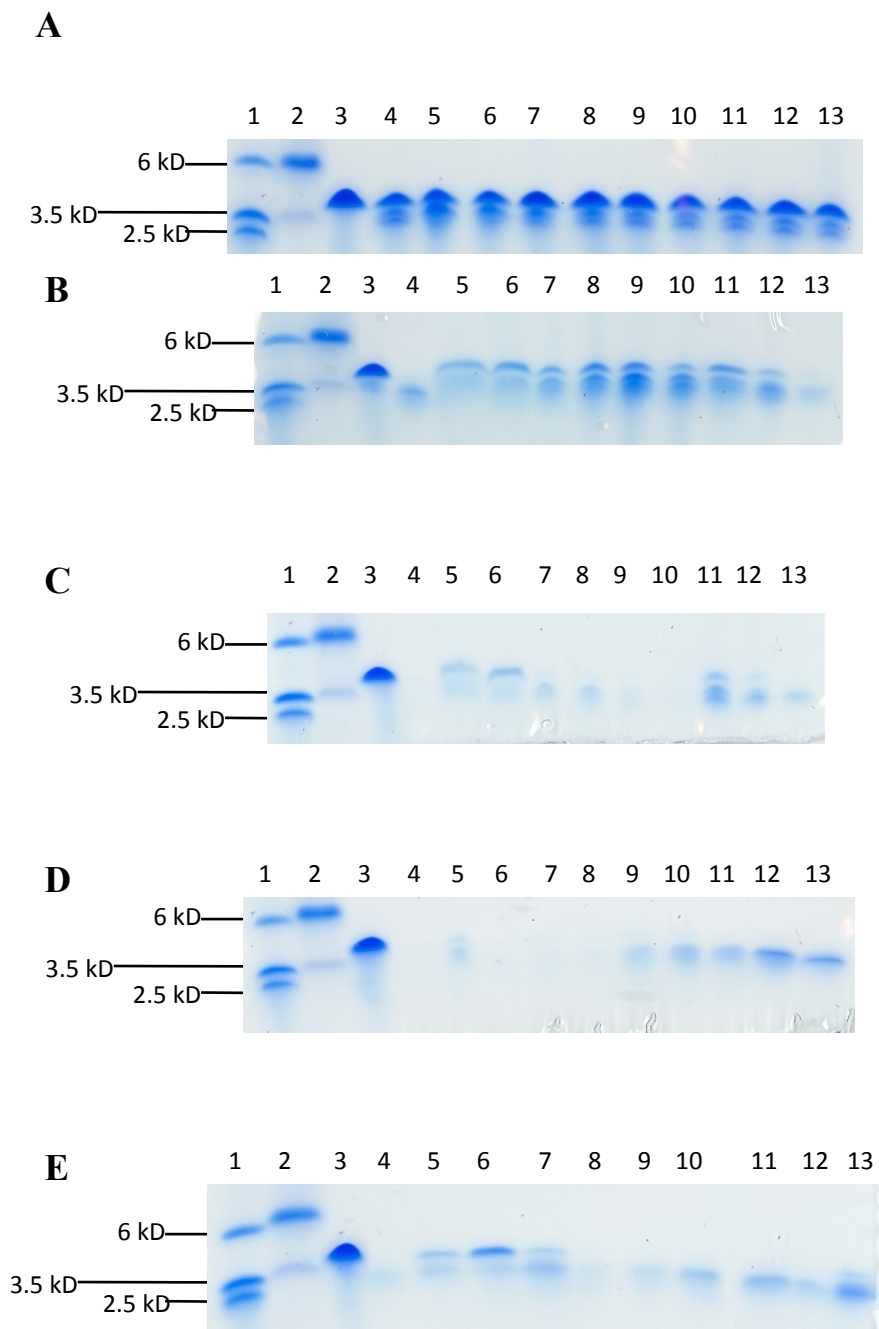


**Figure 100** Tris-tricine PAGE showing concentration-dependent protection of cecropin A from trypsin degradation by heparin (A), enoxaparin (B), ardeparin (C), dermatan sulfate (D) and hyaluronic acid (E). Lanes 1-2: MWMs, Lane 3: cecropin A, Lane 4: cecropin A + 5.5 U trypsin, Lanes 5-13: cecropin A, 5.5 U trypsin and GAGs.



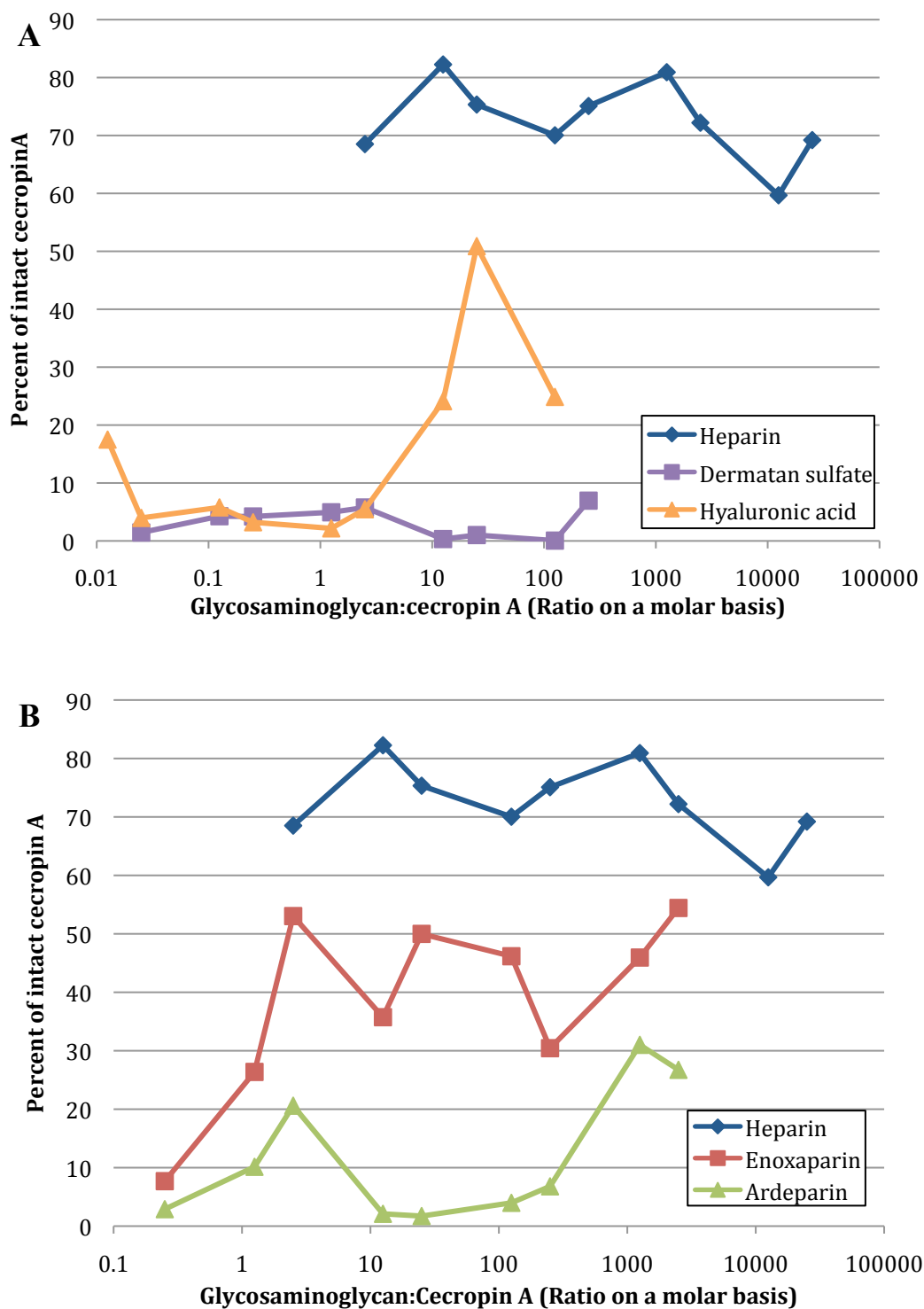


**Figure 101** Concentration-dependent protection of cecropin A by heparin, dermatan sulfate and hyaluronic acid (A) and heparin and LMWHs (B).

#### 6.2.4 Protection of cecropin B from trypsin degradation by GAGs

As for the other CAPs tested, a range of concentrations of trypsin was tested to determine the best amount to be used for experiments studying the ability of GAGs to protect cecropin B from trypsin degradation (**Figure 102**). Five hundred and fifty mU of trypsin was the amount selected to measure the protection of cecropin B from trypsin degradation. Fifty-five mU was the amount selected to observe the protection of select peptide fragments by specific GAGs.

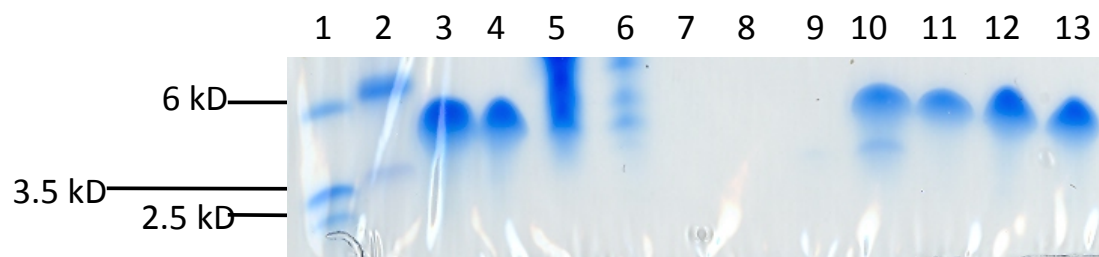


**Figure 102** Concentration-dependent digestion of cecropin B by trypsin. Lanes 1-2: MWMs, Lane 3: cecropin B, Lanes 4-13: cecropin B + trypsin. Lane 4 contains 55,000 U of trypsin. 1:10 dilutions of trypsin were used in subsequent lanes, where lane 13 has 55 nU of trypsin.

For cecropin B, heparin is the best GAG tested for protection from trypsin degradation. Even though heparin achieves the highest level of protection, heparin, ardeparin and HA all show protection of cecropin B starting at a molar ratio of 1:1. Again, a large difference between cecropin A and cecropin B was seen. Unlike what was seen for cecropin A, 3 of the 4 GAGs tested appear to have a concentration range of optimal protection (**Figures 104 and 105**). This is also surprising given the fact that some of the GAGs with the optimal protection windows, such as DS and HA, did not display this type of protection for the other CAPs tested with trypsin degradation.

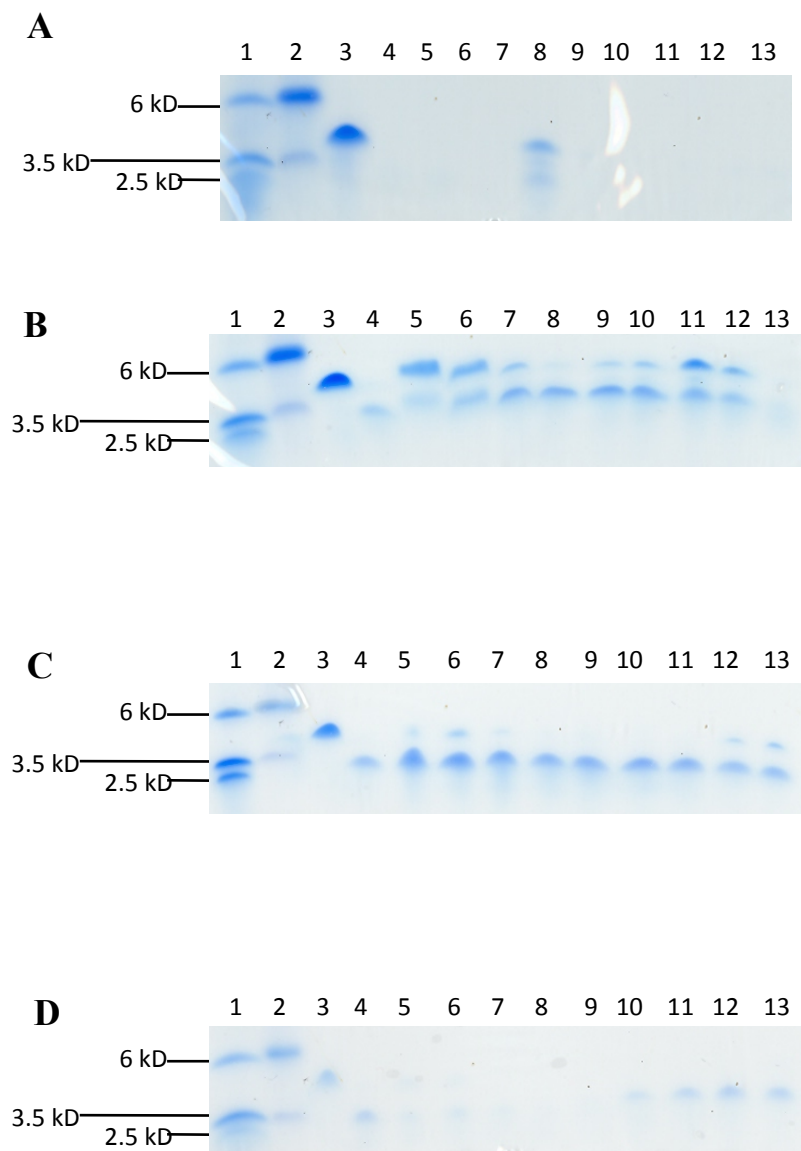


**Figure 103** Tris-tricine PAGE showing concentration-dependent protection of cecropin B by heparin (A), ardeparin (B), dermatan sulfate (C) and hyaluronic acid (D). Lanes 1-2: MWMs, Lane 3: cecropin B, Lane 4: cecropin B + 550 mU trypsin, Lanes 5-13: cecropin B, 550 U trypsin + GAGs.

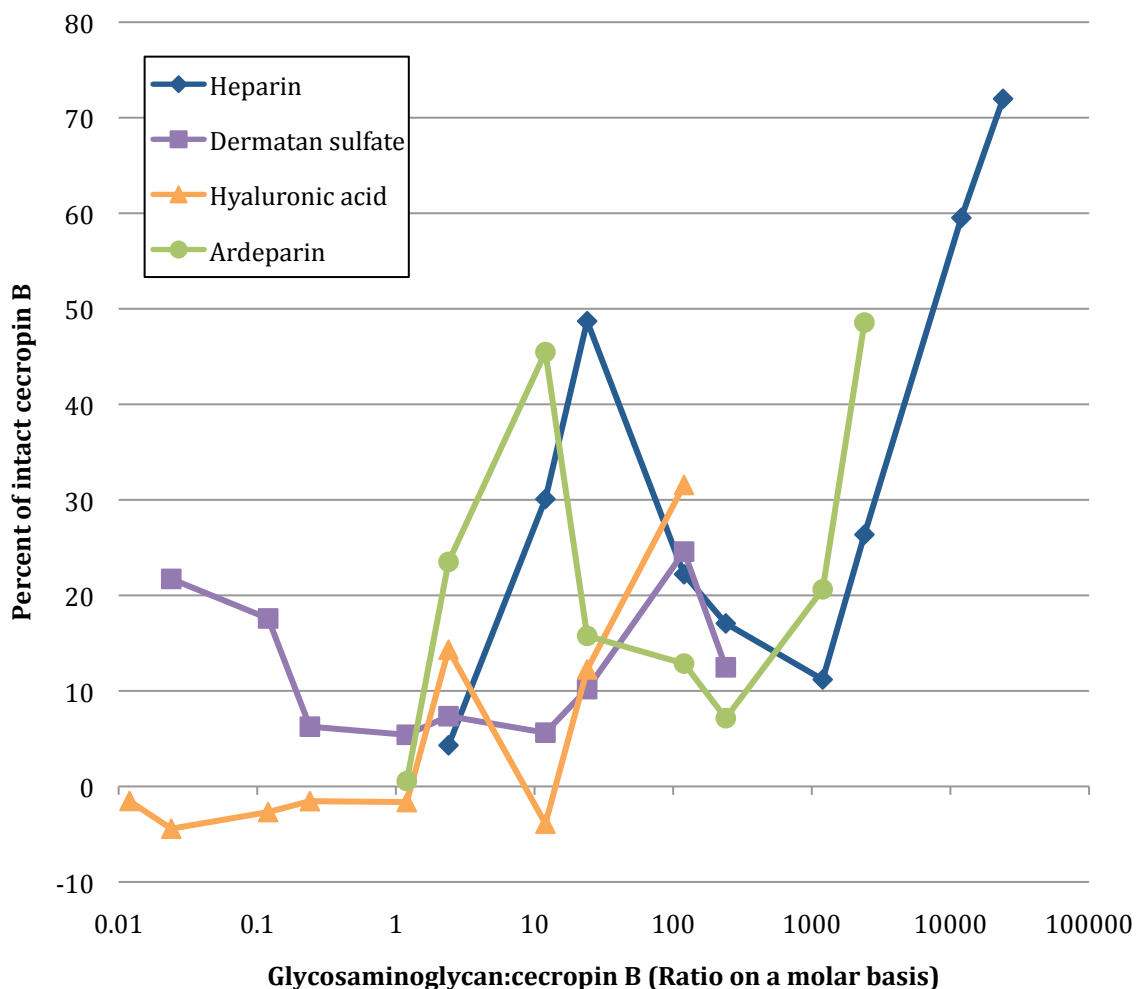


**Figure 104** Concentration-dependent protection of cecropin B from trypsin degradation by GAGs.

### 6.3 Protection of LL-37 from *Pseudomonas aeruginosa* elastase degradation by glycosaminoglycans

As was done for LL-37, cecropin A and cecropin B with trypsin, LL-37 was incubated with a range of concentrations of PAELA. This allowed for the determination of the best amounts of PAELA to use to study the protection of LL-37 from PAELA degradation by GAGs (**Figure 105**). Ten mU PAELA was selected to measure the

complete protection of LL-37 by GAGs and 1 mU PAELA was selected to study the protection of select peptide fragments by GAGs.

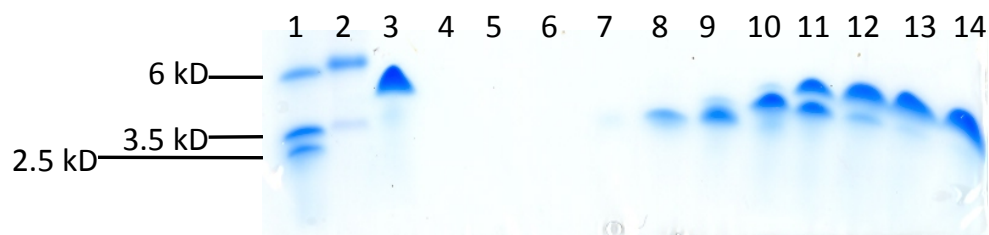


**Figure 105** Concentration-dependent PAELA digestion of LL-37. Lanes 1-2: MWMs, Lane 3: LL-37, Lanes 4-14: LL-37 + PAELA. Lane 4 contains 10.0 U of PAELA. 1:10 dilutions of PAELA were used in subsequent lanes, where lane 14 contains 1.0 nU PAELA.

The results of LL-37 protection from PAELA degradation (**Figures 106, 107 and 108**) are very similar to the results for the protection of LL-37 from trypsin degradation. Here again we see that all concentrations of C4S and C6S are able to completely protect LL-37 from PAELA degradation. All of the C4S and C6S concentrations tested were able to protect LL-37 from trypsin degradation. Both DS and HA are able to protect LL-37 from PAELA degradation at lower molar ratios than heparin. Moreover, heparin is the worst GAG tested for protection of LL-37 against PAELA degradation. Another interesting result of these experiments is that DS, enoxaparin and ardeparin show an optimal range of concentrations for LL-37 protection. This is unique considering the fact that DS did not show an optimal range of concentrations for protection of LL-37, cecropin A or cecropin B against trypsin degradation. While all of the other GAGs achieve complete LL-37 protection against PAELA at a molar ratio of approximately 10:1, it requires approximately 100X more heparin to achieve full protection of LL-37. These results are not consistent with either the LL-37 antimicrobial activity modulation activities of GAGs or the calculated affinities of the GAGs for LL-37.

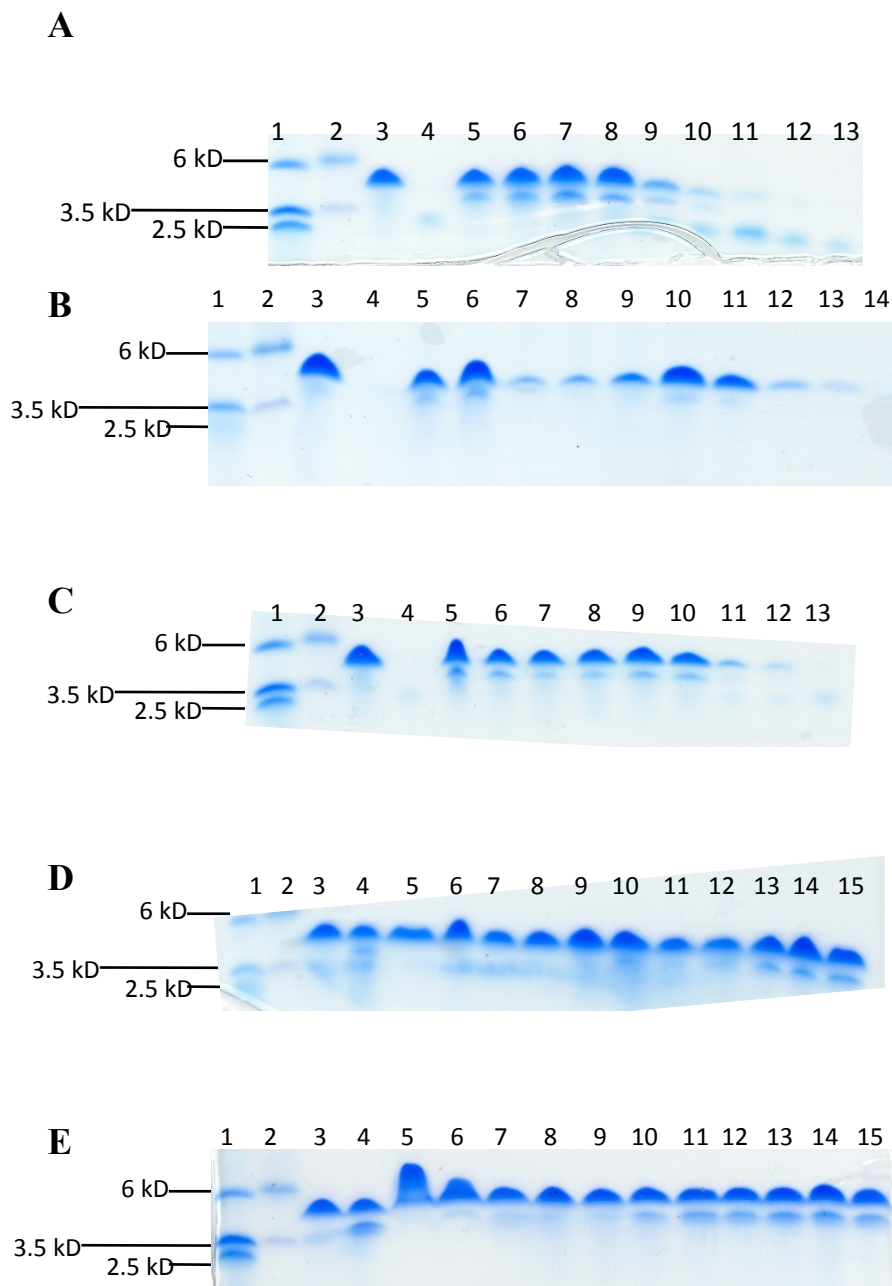


**Figure 106** Tris-tricine PAGE showing concentration-dependent protection of LL-37 from PAELA degradation by heparin (A), HS (B), DS (C), C4S (D) and C6S (E). Lanes 1-2: MWMs, Lane 3: LL-37, Lane 4: LL-37 + 10 mU PAELA, Lanes 5-15: LL-37, 10 mU PAELA + GAGs.

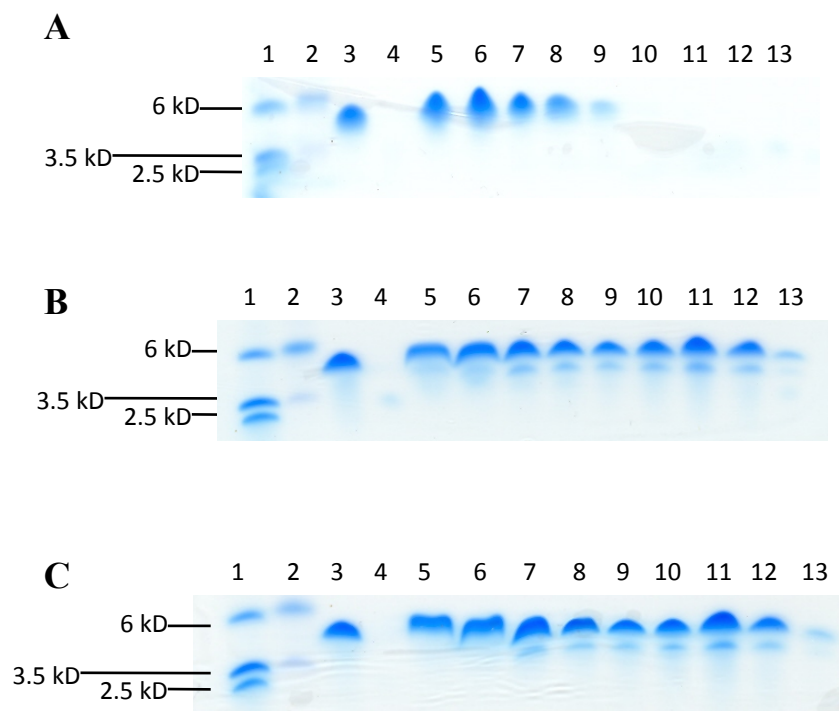


**Figure 107** Tris-tricine PAGE showing concentration-dependent protection of LL-37 from PAELA degradation by HA (A), enoxaparin (B) and ardeparin (C).

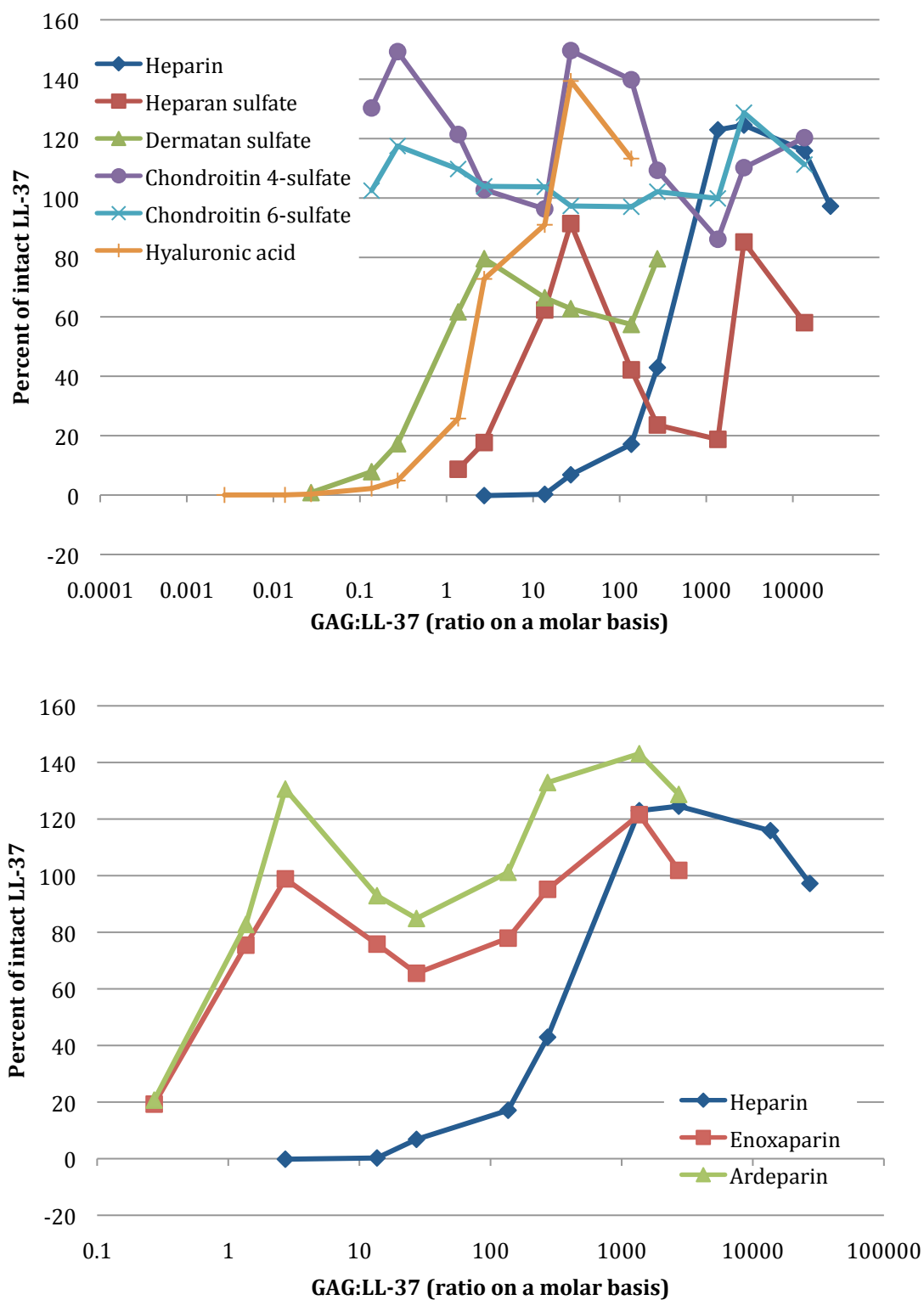


**Figure 108** Concentration-dependent protection of LL-37 from PAELA degradation by GAGs (A) and heparin and LMWHs (B).



#### 6.4 Conclusions

I found that a portion of the GAGs tested inhibit trypsin and PAELA. Hyaluronic acid was the most potent inhibitor with nM inhibition constants for trypsin and PAELA. Heparin showed inhibitory activity against both trypsin and PAELA, while enoxaparin inhibited trypsin and DS inhibited PAELA. Thus it is possible that these GAGs are inhibiting the proteolytic activity of trypsin and PAELA instead of protecting the CAPs. However, these experiments were an initial investigation into the inhibitory activity of GAGs against trypsin and PAELA. To achieve more reliable results I would suggest calculating an inhibitory constant from a more complex model of enzyme inhibition than a Dixon plot.

These data shows that GAGs have the ability to protect cecropin A, cecropin B and LL-37 from proteolytic degradation. Schmidtchen *et al.* previously reported the LL-37-protective activities of DS, C4S and C6S against PAELA<sup>42</sup>. However, the protective abilities of heparin, HA and LMWHs were not measured and the researchers did not examine the protective abilities in a concentration-dependent manner.

C4S and C6S exhibited the best proteolytic degradation protective activities. This was a surprising conclusion given that C4S has the lowest calculated affinity for the CAPs and they are some of the least active GAGs tested for negative modulation of CAP antimicrobial activity. It is very possible that LL-37 forms a complex with C4S or C6S. The tris-tricine gels show this possibility where a higher molecular weight band is detected in lanes with higher C4S or C6S concentrations.

Another surprising result was the low protective activity of heparin. Based on the calculated affinities for the CAPs and heparin's ability to negatively modulate the CAP antimicrobial activities at low heparin:CAP molar ratios we would have expected heparin to be one of the best GAGs tested for protection from proteolytic degradation. That being said, heparin was the best GAG tested at protecting cecropin A from trypsin degradation.

Finally, many of the GAGs tested showed optimal concentration ranges for protection of CAP degradation by proteases. There are several possibilities to explain this phenomenon, but the simplest may be that this is an effect of the experimental techniques used. We chose to use tris-tricine PAGE to measure the ability of the GAGs to protect CAPs from proteolytic degradation with the knowledge that there were some disadvantages to the method. Since we only have single data points for these experiments it is possible that repeating the experiments and reporting the data using error bars would eliminate this effect. Our results could also be improved by using a more quantitative method, such as HPLC, to follow the amount of LL-37 protected from trypsin in PAELA degradation. Interactions between the CAP and GAG could also explain the optimal protective concentration ranges observed. It is possible that the GAGs and CAP formed aggregates at specific concentrations, thus shielding and protecting the CAPs from the protease. It is also possible that binding between the CAP and GAG caused changes in the secondary structure of the CAP, thus masking the protease cleavage sites of the CAPs.

These data indicates that GAGs can protect CAPs from proteolytic degradation, but this is just an initial study. As stated above, these experiments need to be repeated to ensure that this is not a singular phenomenon observed. Additionally, further work is needed to investigate the reason for the optimal GAG protective concentration ranges observed. This work indicates that GAGs may play a physiological role in protecting CAPs from proteolytic degradation at cell surfaces and following CAP release from storage vesicles. It also suggests that heparinoids and other polymers based on GAGs could serve as protective molecules for CAP therapeutics.

## CHAPTER 7 CONCLUSIONS AND FUTURE DIRECTIONS

In this work I showed that GAGs and other PPSs modulate the antimicrobial activities, proteolytic degradation and bacterial membrane component binding of CAPs. When we first started this work we expected to find that specific GAGs were the best universal modulators due to their charge and structure. Instead we found that the modulatory activity of the GAG is dependent upon the three components in the system: the bacteria, the CAP and the GAG, for example. In this case the modulatory activity of the GAG on the antimicrobial activity of the CAP is dependent upon the affinity of the CAP for the GAG, the affinity of the CAP for the bacteria and the affinity of the bacteria for the GAG. In some cases, such as what is seen with the lack of antimicrobial activity modulation against *E. coli*, the affinity of the CAP for the target is too great to be disrupted by the PPSs.

Especially for cecropin A and cecropin B, where they have the amphipathic helix and hydrophobic helix in their structure (**Figure 3**), we hypothesize that the bacterial membrane acts as a thermodynamic sink for the peptide. No matter the concentration used, none of the GAGs were able to modulate the antimicrobial activity of the cecropins against *E. coli*. These results indicate that the cecropins bind tightly to the bacterial membrane through their hydrophobic helix and GAGs cannot disrupt the antibacterial activity because the peptide is already anchored in the membrane. The GAGs were able to disrupt the cecropins binding to immobilized *E. coli* LPS, indicating that other bacterial membrane components likely play key roles in anchoring cecropin A and cecropin B to the membrane.

The  $\alpha$ -helical rod-shaped peptides investigated in this work, magainin II and LL-37, were more susceptible to the modulatory activities of the GAGs and PPSs. However, these peptides are still selectively modulated by the more anionic GAGs. Although

several groups are now looking at interactions between CAPs and GAGs, much of what they report may be oversimplified compared to the interactions between endogenous CAPs and GAGs *in vivo*.

While this work indicates that GAGs can protect CAPs from proteolytic degradation, a more detailed study is needed to draw specific conclusions. Additionally, in the past 5 years interest has shifted from the antimicrobial activity of CAPs to their immunostimulatory activities. Since GAGs are found in abundance at cell surfaces and in secretory granules it is very likely that GAGs will modulate the immunostimulatory activities of CAPs as well.

## REFERENCES

1. Bals, R. Epithelial antimicrobial peptides in host defense against infection. *Respir Res* **2000**, *1* (3), 141-50.
2. Tollin, M.; Bergman, P.; Svenberg, T.; Jornvall, H.; Gudmundsson, G.H.; Agerberth, B. Antimicrobial peptides in the first line defence of human colon mucosa. *Peptides* **2003**, *24* (4), 523-30.
3. Ganz, T.; Selsted, M.E.; Szklarek, D.; Harwig, S.S.; Daher, K.; Bainton, D.F.; Lehrer, R.I. Defensins. Natural peptide antibiotics of human neutrophils. *J Clin Invest* **1985**, *76* (4), 1427-35.
4. Zeya, H.I.; Spitznagel, J.K. Antimicrobial specificity of leukocyte lysosomal cationic proteins. *Science* **1966**, *154* (752), 1049-51.
5. Ganz, T.; Lehrer, R.I. Defensins. *Pharmacol Ther* **1995**, *66* (2), 191-205.
6. Powers, J.P.; Hancock, R.E. The relationship between peptide structure and antibacterial activity. *Peptides* **2003**, *24* (11), 1681-91.
7. Lehrer, R.I. Primate defensins. *Nat Rev Microbiol* **2004**, *2* (9), 727-38.
8. Vizioli, J.; Salzet, M. Antimicrobial peptides from animals: focus on invertebrates. *Trends Pharmacol Sci* **2002**, *23* (11), 494-6.
9. Zasloff, M. Antimicrobial peptides of multicellular organisms. *Nature* **2002**, *415* (6870), 389-95.
10. Palffy, R.; Gardlik, R.; Behuliak, M.; Kadasi, L.; Turna, J.; Celec, P. On the physiology and pathophysiology of antimicrobial peptides. *Mol Med* **2009**, *15* (1-2), 51-9.
11. Marshall, S.H.; Arenas, G. Antimicrobial peptides: A natural alternative to chemical antibiotics and a potential for applied biotechnology. *Electronic Journal of Biotechnology* **2003**, *6*, 271-284.
12. Gallo, R.L.; Murakami, M.; Ohtake, T.; Zaiou, M. Biology and clinical relevance of naturally occurring antimicrobial peptides. *J Allergy Clin Immunol* **2002**, *110* (6), 823-31.
13. Huang, H.J.; Ross, C.R.; Blecha, F. Chemoattractant properties of PR-39, a neutrophil antibacterial peptide. *J Leukoc Biol* **1997**, *61* (5), 624-9.
14. Garcia, J.R.; Jaumann, F.; Schulz, S.; Krause, A.; Rodriguez-Jimenez, J.; Forssmann, U.; Adermann, K.; Kluver, E.; Vogelmeier, C.; Becker, D.; Hedrich, R.; Forssmann, W.G.; Bals, R. Identification of a novel, multifunctional beta-defensin (human beta-defensin 3) with specific antimicrobial activity. Its interaction with plasma membranes of *Xenopus* oocytes and the induction of macrophage chemoattraction. *Cell Tissue Res* **2001**, *306* (2), 257-64.

15. De, Y.; Chen, Q.; Schmidt, A.P.; Anderson, G.M.; Wang, J.M.; Wooters, J.; Oppenheim, J.J.; Chertov, O. LL-37, the neutrophil granule- and epithelial cell-derived cathelicidin, utilizes formyl peptide receptor-like 1 (FPRL1) as a receptor to chemoattract human peripheral blood neutrophils, monocytes, and T cells. *J Exp Med* **2000**, *192* (7), 1069-74.
16. Gallo, R.L.; Ono, M.; Povsic, T.; Page, C.; Eriksson, E.; Klagsbrun, M.; Bernfield, M. Syndecans, cell surface heparan sulfate proteoglycans, are induced by a proline-rich antimicrobial peptide from wounds. *Proc Natl Acad Sci U S A* **1994**, *91* (23), 11035-9.
17. Dorschner, R.A.; Pestonjamas, V.K.; Tamakuwala, S.; Ohtake, T.; Rudisill, J.; Nizet, V.; Agerberth, B.; Gudmundsson, G.H.; Gallo, R.L. Cutaneous injury induces the release of cathelicidin anti-microbial peptides active against group A Streptococcus. *J Invest Dermatol* **2001**, *117* (1), 91-7.
18. Heilborn, J.D.; Nilsson, M.F.; Kratz, G.; Weber, G.; Sorensen, O.; Borregaard, N.; Stahle-Backdahl, M. The cathelicidin anti-microbial peptide LL-37 is involved in re-epithelialization of human skin wounds and is lacking in chronic ulcer epithelium. *J Invest Dermatol* **2003**, *120* (3), 379-89.
19. Burton, M.F.; Steel, P.G. The chemistry and biology of LL-37. *Nat Prod Rep* **2009**, *26* (12), 1572-84.
20. Utsugi, T.; Schroit, A.J.; Connor, J.; Bucana, C.D.; Fidler, I.J. Elevated expression of phosphatidylserine in the outer membrane leaflet of human tumor cells and recognition by activated human blood monocytes. *Cancer Res* **1991**, *51* (11), 3062-6.
21. Dobrzynska, I.; Szachowicz-Petelska, B.; Sulkowski, S.; Figaszewski, Z. Changes in electric charge and phospholipids composition in human colorectal cancer cells. *Mol Cell Biochem* **2005**, *276* (1-2), 113-9.
22. Yoon, W.H.; Park, H.D.; Lim, K.; Hwang, B.D. Effect of O-glycosylated mucin on invasion and metastasis of HM7 human colon cancer cells. *Biochem Biophys Res Commun* **1996**, *222* (3), 694-9.
23. Burdick, M.D.; Harris, A.; Reid, C.J.; Iwamura, T.; Hollingsworth, M.A. Oligosaccharides expressed on MUC1 produced by pancreatic and colon tumor cell lines. *J Biol Chem* **1997**, *272* (39), 24198-202.
24. Ehrenstein, G.; Lecar, H. Electrically gated ionic channels in lipid bilayers. *Q Rev Biophys* **1977**, *10* (1), 1-34.
25. Dempsey, C.E. The actions of melittin on membranes. *Biochim Biophys Acta* **1990**, *1031* (2), 143-61.
26. Pokorny, A.; Birkbeck, T.H.; Almeida, P.F. Mechanism and kinetics of delta-lysin interaction with phospholipid vesicles. *Biochemistry* **2002**, *41* (36), 11044-56.
27. Pokorny, A.; Almeida, P.F. Kinetics of dye efflux and lipid flip-flop induced by delta-lysin in phosphatidylcholine vesicles and the mechanism of graded release by amphipathic, alpha-helical peptides. *Biochemistry* **2004**, *43* (27), 8846-57.

28. Chan, D.I.; Prenner, E.J.; Vogel, H.J. Tryptophan- and arginine-rich antimicrobial peptides: structures and mechanisms of action. *Biochim Biophys Acta* **2006**, *1758* (9), 1184-202.
29. Papo, N.; Shai, Y. Can we predict biological activity of antimicrobial peptides from their interactions with model phospholipid membranes? *Peptides* **2003**, *24* (11), 1693-703.
30. Matsuzaki, K.; Murase, O.; Fujii, N.; Miyajima, K. An antimicrobial peptide, magainin 2, induced rapid flip-flop of phospholipids coupled with pore formation and peptide translocation. *Biochemistry* **1996**, *35* (35), 11361-8.
31. Ludtke, S.J.; He, K.; Heller, W.T.; Harroun, T.A.; Yang, L.; Huang, H.W. Membrane pores induced by magainin. *Biochemistry* **1996**, *35* (43), 13723-8.
32. Huang, H.W. Action of antimicrobial peptides: two-state model. *Biochemistry* **2000**, *39* (29), 8347-52.
33. Shai, Y. Mode of action of membrane active antimicrobial peptides. *Biopolymers* **2002**, *66* (4), 236-48.
34. Pouny, Y.; Rapaport, D.; Mor, A.; Nicolas, P.; Shai, Y. Interaction of antimicrobial dermaseptin and its fluorescently labeled analogues with phospholipid membranes. *Biochemistry* **1992**, *31* (49), 12416-23.
35. Hancock, R.E.; Chapple, D.S. Peptide antibiotics. *Antimicrob Agents Chemother* **1999**, *43* (6), 1317-23.
36. Hong, R.W.; Shchepetov, M.; Weiser, J.N.; Axelsen, P.H. Transcriptional profile of the Escherichia coli response to the antimicrobial insect peptide cecropin A. *Antimicrob Agents Chemother* **2003**, *47* (1), 1-6.
37. Nizet, V.; Ohtake, T.; Lauth, X.; Trowbridge, J.; Rudisill, J.; Dorschner, R.A.; Pestonjamas, V.; Piraino, J.; Huttner, K.; Gallo, R.L. Innate antimicrobial peptide protects the skin from invasive bacterial infection. *Nature* **2001**, *414* (6862), 454-7.
38. Gregory, S.M.; Cavanaugh, A.; Journigan, V.; Pokorny, A.; Almeida, P.F. A quantitative model for the all-or-none permeabilization of phospholipid vesicles by the antimicrobial peptide cecropin A. *Biophys J* **2008**, *94* (5), 1667-80.
39. Brogden, K.A. Antimicrobial peptides: pore formers or metabolic inhibitors in bacteria? *Nat Rev Microbiol* **2005**, *3* (3), 238-50.
40. Taggart, C.C.; Greene, C.M.; Smith, S.G.; Levine, R.L.; McCray, P.B., Jr.; O'Neill, S.; McElvaney, N.G. Inactivation of human beta-defensins 2 and 3 by elastolytic cathepsins. *J Immunol* **2003**, *171* (2), 931-7.
41. Sieprawska-Lupa, M.; Mydel, P.; Krawczyk, K.; Wojcik, K.; Puklo, M.; Lupa, B.; Suder, P.; Silberring, J.; Reed, M.; Pohl, J.; Shafer, W.; McAleese, F.; Foster, T.; Travis, J.; Potempa, J. Degradation of human antimicrobial peptide LL-37 by Staphylococcus aureus-derived proteinases. *Antimicrob Agents Chemother* **2004**, *48* (12), 4673-9.

42. Schmidtchen, A.; Frick, I.M.; Andersson, E.; Tapper, H.; Bjorck, L. Proteinases of common pathogenic bacteria degrade and inactivate the antibacterial peptide LL-37. *Mol Microbiol* **2002**, *46* (1), 157-68.
43. Bergsson, G.; Reeves, E.P.; McNally, P.; Chotirmall, S.H.; Greene, C.M.; Greally, P.; Murphy, P.; O'Neill, S.J.; McElvaney, N.G. LL-37 complexation with glycosaminoglycans in cystic fibrosis lungs inhibits antimicrobial activity, which can be restored by hypertonic saline. *J Immunol* **2009**, *183* (1), 543-51.
44. Dong, Z.; Katar, M.; Linebaugh, B.E.; Sloane, B.F.; Berk, R.S. Expression of cathepsins B, D and L in mouse corneas infected with *Pseudomonas aeruginosa*. *Eur J Biochem* **2001**, *268* (24), 6408-16.
45. Minarowska, A.; Minarowski, L.; Karwowska, A.; Sands, D.; Dabrowska, E. The activity of cathepsin D in saliva of cystic fibrosis patients. *Folia Histochem Cytobiol* **2007**, *45* (3), 165-8.
46. Chen, Y.; Vasil, A.I.; Rehaume, L.; Mant, C.T.; Burns, J.L.; Vasil, M.L.; Hancock, R.E.; Hodges, R.S. Comparison of biophysical and biologic properties of alpha-helical enantiomeric antimicrobial peptides. *Chem Biol Drug Des* **2006**, *67* (2), 162-73.
47. Rozek, A.; Powers, J.P.; Friedrich, C.L.; Hancock, R.E. Structure-based design of an indolicidin peptide analogue with increased protease stability. *Biochemistry* **2003**, *42* (48), 14130-8.
48. Svenson, J.; Stensen, W.; Brandsdal, B.O.; Haug, B.E.; Monrad, J.; Svendsen, J.S. Antimicrobial peptides with stability toward tryptic degradation. *Biochemistry* **2008**, *47* (12), 3777-88.
49. Schiemann, F.; Brandt, E.; Gross, R.; Lindner, B.; Mittelstadt, J.; Sommerhoff, C.P.; Schulmistrat, J.; Petersen, F. The cathelicidin LL-37 activates human mast cells and is degraded by mast cell tryptase: counter-regulation by CXCL4. *J Immunol* **2009**, *183* (4), 2223-31.
50. Metz-Boutigue, M.H.; Jolles, J.; Mazurier, J.; Schoentgen, F.; Legrand, D.; Spik, G.; Montreuil, J.; Jolles, P. Human lactotransferrin: amino acid sequence and structural comparisons with other transferrins. *Eur J Biochem* **1984**, *145* (3), 659-76.
51. Masson, P.L.; Heremans, J.F.; Dive, C.H. An iron-binding protein common to many external secretions. *Clinica Chimica Acta* **1966**, *14* (6), 735-739.
52. Bullen, J.J.; Armstrong, J.A. The role of lactoferrin in the bactericidal function of polymorphonuclear leucocytes. *Immunology* **1979**, *36* (4), 781-91.
53. Tomita, M.; Bellamy, W.; Takase, M.; Yamauchi, K.; Wakabayashi, H.; Kawase, K. Potent antibacterial peptides generated by pepsin digestion of bovine lactoferrin. *J Dairy Sci* **1991**, *74* (12), 4137-42.
54. Vorland, L.H. Lactoferrin: a multifunctional glycoprotein. *APMIS* **1999**, *107* (11), 971-81.



55. Weinberg, E.D. Human lactoferrin: a novel therapeutic with broad spectrum potential. *J Pharm Pharmacol* **2001**, *53* (10), 1303-10.
56. Levay, P.F.; Viljoen, M. Lactoferrin: a general review. *Haematologica* **1995**, *80* (3), 252-67.
57. Mann, D.M.; Romm, E.; Migliorini, M. Delineation of the glycosaminoglycan-binding site in the human inflammatory response protein lactoferrin. *J Biol Chem* **1994**, *269* (38), 23661-7.
58. Wu, H.F.; Monroe, D.M.; Church, F.C. Characterization of the glycosaminoglycan-binding region of lactoferrin. *Arch Biochem Biophys* **1995**, *317* (1), 85-92.
59. Vorland, L.H.; Ulvatne, H.; Andersen, J.; Haukland, H.; Rekdal, O.; Svendsen, J.S.; Gutteberg, T.J. Lactoferricin of bovine origin is more active than lactoferricins of human, murine and caprine origin. *Scand J Infect Dis* **1998**, *30* (5), 513-7.
60. Hwang, P.M.; Zhou, N.; Shan, X.; Arrowsmith, C.H.; Vogel, H.J. Three-dimensional solution structure of lactoferricin B, an antimicrobial peptide derived from bovine lactoferrin. *Biochemistry* **1998**, *37* (12), 4288-98.
61. Bellamy, W.; Takase, M.; Yamauchi, K.; Wakabayashi, H.; Kawase, K.; Tomita, M. Identification of the bactericidal domain of lactoferrin. *Biochim Biophys Acta* **1992**, *1121* (1-2), 130-6.
62. Schibli, D.J.; Hwang, P.M.; Vogel, H.J. The structure of the antimicrobial active center of lactoferricin B bound to sodium dodecyl sulfate micelles. *FEBS Lett* **1999**, *446* (2-3), 213-7.
63. Kang, J.H.; Lee, M.K.; Kim, K.L.; Hahn, K.S. Structure-biological activity relationships of 11-residue highly basic peptide segment of bovine lactoferrin. *Int J Pept Protein Res* **1996**, *48* (4), 357-63.
64. Zasloff, M. Magainins, a class of antimicrobial peptides from *Xenopus* skin: isolation, characterization of two active forms, and partial cDNA sequence of a precursor. *Proc Natl Acad Sci U S A* **1987**, *84* (15), 5449-53.
65. Bulet, P.; Stocklin, R.; Menin, L. Anti-microbial peptides: from invertebrates to vertebrates. *Immunol Rev* **2004**, *198*, 169-84.
66. Zasloff, M.; Martin, B.; Chen, H.C. Antimicrobial activity of synthetic magainin peptides and several analogues. *Proc Natl Acad Sci U S A* **1988**, *85* (3), 910-3.
67. Cruciani, R.A.; Barker, J.L.; Zasloff, M.; Chen, H.C.; Colamonici, O. Antibiotic magainins exert cytolytic activity against transformed cell lines through channel formation. *Proc Natl Acad Sci U S A* **1991**, *88* (9), 3792-6.
68. Ohsaki, Y.; Gazdar, A.F.; Chen, H.C.; Johnson, B.E. Antitumor activity of magainin analogues against human lung cancer cell lines. *Cancer Res* **1992**, *52* (13), 3534-8.

69. Soballe, P.W.; Maloy, W.L.; Myrnga, M.L.; Jacob, L.S.; Herlyn, M. Experimental local therapy of human melanoma with lytic magainin peptides. *Int J Cancer* **1995**, *60* (2), 280-4.
70. Bessalle, R.; Kapitkovsky, A.; Gorea, A.; Shalit, I.; Fridkin, M. All-D-magainin: chirality, antimicrobial activity and proteolytic resistance. *FEBS Lett* **1990**, *274* (1-2), 151-5.
71. Wade, D.; Boman, A.; Wahlin, B.; Drain, C.M.; Andreu, D.; Boman, H.G.; Merrifield, R.B. All-D amino acid-containing channel-forming antibiotic peptides. *Proc Natl Acad Sci U S A* **1990**, *87* (12), 4761-5.
72. Pathak, N.; Salas-Auvert, R.; Ruche, G.; Janna, M.H.; McCarthy, D.; Harrison, R.G. Comparison of the effects of hydrophobicity, amphiphilicity, and alpha-helicity on the activities of antimicrobial peptides. *Proteins* **1995**, *22* (2), 182-6.
73. Matsuzaki, K.; Nakamura, A.; Murase, O.; Sugishita, K.; Fujii, N.; Miyajima, K. Modulation of magainin 2-lipid bilayer interactions by peptide charge. *Biochemistry* **1997**, *36* (8), 2104-11.
74. Ludtke, S.J.; He, K.; Wu, Y.; Huang, H.W. Cooperative membrane insertion of magainin correlated with its cytolytic activity. *Biochim Biophys Acta* **1994**, *1190* (1), 181-4.
75. Marion, D.; Zasloff, M.; Bax, A. A two-dimensional NMR study of the antimicrobial peptide magainin 2. *FEBS Lett* **1988**, *227* (1), 21-6.
76. Matsuzaki, K.; Harada, M.; Funakoshi, S.; Fujii, N.; Miyajima, K. Physicochemical determinants for the interactions of magainins 1 and 2 with acidic lipid bilayers. *Biochim Biophys Acta* **1991**, *1063* (1), 162-70.
77. Williams, R.W.; Starman, R.; Taylor, K.M.; Gable, K.; Beeler, T.; Zasloff, M.; Covell, D. Raman spectroscopy of synthetic antimicrobial frog peptides magainin 2a and PGLa. *Biochemistry* **1990**, *29* (18), 4490-6.
78. Jackson, M.; Mantsch, H.H.; Spencer, J.H. Conformation of magainin-2 and related peptides in aqueous solution and membrane environments probed by Fourier transform infrared spectroscopy. *Biochemistry* **1992**, *31* (32), 7289-93.
79. Bechinger, B. Structure and functions of channel-forming peptides: magainins, cecropins, melittin and alamethicin. *J Membr Biol* **1997**, *156* (3), 197-211.
80. Matsuzaki, K.; Sugishita, K.; Fujii, N.; Miyajima, K. Molecular basis for membrane selectivity of an antimicrobial peptide, magainin 2. *Biochemistry* **1995**, *34* (10), 3423-9.
81. Bechinger, B.; Zasloff, M.; Opella, S.J. Structure and orientation of the antibiotic peptide magainin in membranes by solid-state nuclear magnetic resonance spectroscopy. *Protein Sci* **1993**, *2* (12), 2077-84.
82. Matsuzaki, K.; Mitani, Y.; Akada, K.Y.; Murase, O.; Yoneyama, S.; Zasloff, M.; Miyajima, K. Mechanism of synergism between antimicrobial peptides magainin 2 and PGLa. *Biochemistry* **1998**, *37* (43), 15144-53.

83. Tachi, T.; Epand, R.F.; Epand, R.M.; Matsuzaki, K. Position-dependent hydrophobicity of the antimicrobial magainin peptide affects the mode of peptide-lipid interactions and selective toxicity. *Biochemistry* **2002**, *41* (34), 10723-31.
84. Matsuzaki, K.; Murase, O.; Tokuda, H.; Funakoshi, S.; Fujii, N.; Miyajima, K. Orientational and aggregational states of magainin 2 in phospholipid bilayers. *Biochemistry* **1994**, *33* (11), 3342-9.
85. Matsuzaki, K. Magainins as paradigm for the mode of action of pore forming polypeptides. *Biochim Biophys Acta* **1998**, *1376* (3), 391-400.
86. Huang, H.W. Molecular mechanism of antimicrobial peptides: the origin of cooperativity. *Biochim Biophys Acta* **2006**, *1758* (9), 1292-302.
87. Haukland, H.H.; Ulvatne, H.; Sandvik, K.; Vorland, L.H. The antimicrobial peptides lactoferricin B and magainin 2 cross over the bacterial cytoplasmic membrane and reside in the cytoplasm. *FEBS Lett* **2001**, *508* (3), 389-93.
88. Imura, Y.; Choda, N.; Matsuzaki, K. Magainin 2 in action: distinct modes of membrane permeabilization in living bacterial and mammalian cells. *Biophys J* **2008**, *95* (12), 5757-65.
89. Boman, H.G.; Hultmark, D. Cell-free immunity in insects. *Annu Rev Microbiol* **1987**, *41*, 103-26.
90. Dickinson, L.; Russell, V.; Dunn, P.E. A family of bacteria-regulated, cecropin D-like peptides from *Manduca sexta*. *J Biol Chem* **1988**, *263* (36), 19424-9.
91. Kaaya, G.P.; Flyg, C.; Boman, H.G. Insect immunity: Induction of cecropin and attacin-like antibacterial factors in the haemolymph of *Glossina morsitans morsitans*. *Insect Biochemistry* **1987**, *17* (2), 309-315.
92. Kanai, A.; Natori, S. Cloning of gene cluster for sarcotoxin I, antibacterial proteins of *Sarcophaga peregrina*. *FEBS Lett* **1989**, *258* (2), 199-202.
93. Kylsten, P.; Samakovlis, C.; Hultmark, D. The cecropin locus in *Drosophila*; a compact gene cluster involved in the response to infection. *EMBO J* **1990**, *9* (1), 217-24.
94. Samakovlis, C.; Kimbrell, D.A.; Kylsten, P.; Engstrom, A.; Hultmark, D. The immune response in *Drosophila*: pattern of cecropin expression and biological activity. *EMBO J* **1990**, *9* (9), 2969-76.
95. Samakovlis, C.; Kylsten, P.; Kimbrell, D.A.; Engstrom, A.; Hultmark, D. The andropin gene and its product, a male-specific antibacterial peptide in *Drosophila melanogaster*. *EMBO J* **1991**, *10* (1), 163-9.
96. Kimbrell, D.A. Insect antibacterial proteins: not just for insects and against bacteria. *Bioessays* **1991**, *13* (12), 657-63.
97. Gudmundsson, G.H.; Lidholm, D.A.; Asling, B.; Gan, R.; Boman, H.G. The cecropin locus. Cloning and expression of a gene cluster encoding three antibacterial peptides in *Hyalophora cecropia*. *J Biol Chem* **1991**, *266* (18), 11510-7.

98. Hultmark, D. Immune reactions in *Drosophila* and other insects: a model for innate immunity. *Trends Genet* **1993**, *9* (5), 178-83.
99. Lee, J.Y.; Boman, A.; Sun, C.X.; Andersson, M.; Jornvall, H.; Mutt, V.; Boman, H.G. Antibacterial peptides from pig intestine: isolation of a mammalian cecropin. *Proc Natl Acad Sci U S A* **1989**, *86* (23), 9159-62.
100. Boman, H.G.; Faye, I.; Gudmundsson, G.H.; Lee, J.Y.; Lidholm, D.A. Cell-free immunity in *Cecropia*. A model system for antibacterial proteins. *Eur J Biochem* **1991**, *201* (1), 23-31.
101. Andreu, D.; Merrifield, R.B.; Steiner, H.; Boman, H.G. N-terminal analogues of cecropin A: synthesis, antibacterial activity, and conformational properties. *Biochemistry* **1985**, *24* (7), 1683-8.
102. Boman, H.G. Antibacterial peptides: basic facts and emerging concepts. *J Intern Med* **2003**, *254* (3), 197-215.
103. Diaz-Achirica, P.; Prieto, S.; Ubach, J.; Andreu, D.; Rial, E.; Rivas, L. Permeabilization of the mitochondrial inner membrane by short cecropin-A-melittin hybrid peptides. *Eur J Biochem* **1994**, *224* (1), 257-63.
104. Gazit, E.; Boman, A.; Boman, H.G.; Shai, Y. Interaction of the mammalian antibacterial peptide cecropin P1 with phospholipid vesicles. *Biochemistry* **1995**, *34* (36), 11479-88.
105. Steiner, H.; Andreu, D.; Merrifield, R.B. Binding and action of cecropin and cecropin analogues: antibacterial peptides from insects. *Biochim Biophys Acta* **1988**, *939* (2), 260-6.
106. Steiner, H.; Hultmark, D.; Engstrom, A.; Bennich, H.; Boman, H.G. Sequence and specificity of two antibacterial proteins involved in insect immunity. *Nature* **1981**, *292* (5820), 246-8.
107. Hultmark, D. *Drosophila* as a model system for antibacterial peptides. *Ciba Found Symp* **1994**, *186*, 107-19; discussion 120-2.
108. Merrifield, R.B.; Vizioli, L.D.; Boman, H.G. Synthesis of the antibacterial peptide cecropin A (1-33). *Biochemistry* **1982**, *21* (20), 5020-31.
109. Fernandez, I.; Ubach, J.; Reig, F.; Andreu, D.; Pons, M. Effect of succinylation on the membrane activity and conformation of a short cecropin A-melittin hybrid peptide. *Biopolymers* **1994**, *34* (9), 1251-8.
110. Hugosson, M.; Andreu, D.; Boman, H.G.; Glaser, E. Antibacterial peptides and mitochondrial presequences affect mitochondrial coupling, respiration and protein import. *Eur J Biochem* **1994**, *223* (3), 1027-33.
111. Moore, A.J.; Devine, D.A.; Bibby, M.C. Preliminary experimental anticancer activity of cecropins. *Pept Res* **1994**, *7* (5), 265-9.
112. Chen, H.M.; Wang, W.; Smith, D.; Chan, S.C. Effects of the anti-bacterial peptide cecropin B and its analogs, cecropins B-1 and B-2, on liposomes, bacteria, and cancer cells. *Biochim Biophys Acta* **1997**, *1336* (2), 171-9.

113. Hui, L.; Leung, K.; Chen, H.M. The combined effects of antibacterial peptide cecropin A and anti-cancer agents on leukemia cells. *Anticancer Res* **2002**, *22* (5), 2811-6.
114. Holak, T.A.; Engstrom, A.; Kraulis, P.J.; Lindeberg, G.; Bennich, H.; Jones, T.A.; Gronenborn, A.M.; Clore, G.M. The solution conformation of the antibacterial peptide cecropin A: a nuclear magnetic resonance and dynamical simulated annealing study. *Biochemistry* **1988**, *27* (20), 7620-9.
115. Fink, J.; Boman, A.; Boman, H.G.; Merrifield, R.B. Design, synthesis and antibacterial activity of cecropin-like model peptides. *Int J Pept Protein Res* **1989**, *33* (6), 412-21.
116. Bulet, P.; Stocklin, R. Insect antimicrobial peptides: structures, properties and gene regulation. *Protein Pept Lett* **2005**, *12* (1), 3-11.
117. Agerberth, B.; Charo, J.; Werr, J.; Olsson, B.; Idali, F.; Lindbom, L.; Kiessling, R.; Jornvall, H.; Wigzell, H.; Gudmundsson, G.H. The human antimicrobial and chemotactic peptides LL-37 and alpha-defensins are expressed by specific lymphocyte and monocyte populations. *Blood* **2000**, *96* (9), 3086-93.
118. Bals, R.; Wang, X.; Zasloff, M.; Wilson, J.M. The peptide antibiotic LL-37/hCAP-18 is expressed in epithelia of the human lung where it has broad antimicrobial activity at the airway surface. *Proc Natl Acad Sci U S A* **1998**, *95* (16), 9541-6.
119. Sorensen, O.E.; Follin, P.; Johnsen, A.H.; Calafat, J.; Tjabringa, G.S.; Hiemstra, P.S.; Borregaard, N. Human cathelicidin, hCAP-18, is processed to the antimicrobial peptide LL-37 by extracellular cleavage with proteinase 3. *Blood* **2001**, *97* (12), 3951-9.
120. Zanetti, M.; Gennaro, R.; Romeo, D. Cathelicidins: a novel protein family with a common proregion and a variable C-terminal antimicrobial domain. *FEBS Lett* **1995**, *374* (1), 1-5.
121. Sorensen, O.E.; Gram, L.; Johnsen, A.H.; Andersson, E.; Bangsboll, S.; Tjabringa, G.S.; Hiemstra, P.S.; Malm, J.; Egesten, A.; Borregaard, N. Processing of seminal plasma hCAP-18 to ALL-38 by gastricsin: a novel mechanism of generating antimicrobial peptides in vagina. *J Biol Chem* **2003**, *278* (31), 28540-6.
122. Zanetti, M. Cathelicidins, multifunctional peptides of the innate immunity. *J Leukoc Biol* **2004**, *75* (1), 39-48.
123. Malm, J.; Sorensen, O.; Persson, T.; Frohm-Nilsson, M.; Johansson, B.; Bjartell, A.; Lilja, H.; Stahle-Backdahl, M.; Borregaard, N.; Egesten, A. The human cationic antimicrobial protein (hCAP-18) is expressed in the epithelium of human epididymis, is present in seminal plasma at high concentrations, and is attached to spermatozoa. *Infect Immun* **2000**, *68* (7), 4297-302.
124. Frohm, M.; Agerberth, B.; Ahangari, G.; Stahle-Backdahl, M.; Liden, S.; Wigzell, H.; Gudmundsson, G.H. The expression of the gene coding for the antibacterial peptide LL-37 is induced in human keratinocytes during inflammatory disorders. *J Biol Chem* **1997**, *272* (24), 15258-63.

125. Stie, J.; Jesaitis, A.V.; Lord, C.I.; Gripenrog, J.M.; Taylor, R.M.; Burritt, J.B.; Jesaitis, A.J. Localization of hCAP-18 on the surface of chemoattractant-stimulated human granulocytes: analysis using two novel hCAP-18-specific monoclonal antibodies. *J Leukoc Biol* **2007**, *82* (1), 161-72.
126. Durr, U.H.; Sudheendra, U.S.; Ramamoorthy, A. LL-37, the only human member of the cathelicidin family of antimicrobial peptides. *Biochim Biophys Acta* **2006**, *1758* (9), 1408-25.
127. Johansson, J.; Gudmundsson, G.H.; Rottenberg, M.E.; Berndt, K.D.; Agerberth, B. Conformation-dependent antibacterial activity of the naturally occurring human peptide LL-37. *J Biol Chem* **1998**, *273* (6), 3718-24.
128. Gordon, Y.J.; Huang, L.C.; Romanowski, E.G.; Yates, K.A.; Proske, R.J.; McDermott, A.M. Human cathelicidin (LL-37), a multifunctional peptide, is expressed by ocular surface epithelia and has potent antibacterial and antiviral activity. *Curr Eye Res* **2005**, *30* (5), 385-94.
129. Turner, J.; Cho, Y.; Dinh, N.N.; Waring, A.J.; Lehrer, R.I. Activities of LL-37, a cathelin-associated antimicrobial peptide of human neutrophils. *Antimicrob Agents Chemother* **1998**, *42* (9), 2206-14.
130. Lopez-Garcia, B.; Lee, P.H.; Yamasaki, K.; Gallo, R.L. Anti-fungal activity of cathelicidins and their potential role in *Candida albicans* skin infection. *J Invest Dermatol* **2005**, *125* (1), 108-15.
131. De Smet, K.; Contreras, R. Human antimicrobial peptides: defensins, cathelicidins and histatins. *Biotechnol Lett* **2005**, *27* (18), 1337-47.
132. Niyonsaba, F.; Iwabuchi, K.; Someya, A.; Hirata, M.; Matsuda, H.; Ogawa, H.; Nagaoka, I. A cathelicidin family of human antibacterial peptide LL-37 induces mast cell chemotaxis. *Immunology* **2002**, *106* (1), 20-6.
133. Soehnlein, O.; Zernecke, A.; Eriksson, E.E.; Rothfuchs, A.G.; Pham, C.T.; Herwald, H.; Bidzhekov, K.; Rottenberg, M.E.; Weber, C.; Lindbom, L. Neutrophil secretion products pave the way for inflammatory monocytes. *Blood* **2008**, *112* (4), 1461-71.
134. Zheng, Y.; Niyonsaba, F.; Ushio, H.; Nagaoka, I.; Ikeda, S.; Okumura, K.; Ogawa, H. Cathelicidin LL-37 induces the generation of reactive oxygen species and release of human alpha-defensins from neutrophils. *Br J Dermatol* **2007**, *157* (6), 1124-31.
135. Wan, M.; Sabirsh, A.; Wetterholm, A.; Agerberth, B.; Haeggstrom, J.Z. Leukotriene B4 triggers release of the cathelicidin LL-37 from human neutrophils: novel lipid-peptide interactions in innate immune responses. *FASEB J* **2007**, *21* (11), 2897-905.
136. Niyonsaba, F.; Someya, A.; Hirata, M.; Ogawa, H.; Nagaoka, I. Evaluation of the effects of peptide antibiotics human beta-defensins-1/-2 and LL-37 on histamine release and prostaglandin D(2) production from mast cells. *Eur J Immunol* **2001**, *31* (4), 1066-75.

137. Bowdish, D.M.; Davidson, D.J.; Speert, D.P.; Hancock, R.E. The human cationic peptide LL-37 induces activation of the extracellular signal-regulated kinase and p38 kinase pathways in primary human monocytes. *J Immunol* **2004**, *172* (6), 3758-65.
138. Scott, M.G.; Davidson, D.J.; Gold, M.R.; Bowdish, D.; Hancock, R.E. The human antimicrobial peptide LL-37 is a multifunctional modulator of innate immune responses. *J Immunol* **2002**, *169* (7), 3883-91.
139. Tjabringa, G.S.; Aarbiou, J.; Ninaber, D.K.; Drijfhout, J.W.; Sorensen, O.E.; Borregaard, N.; Rabe, K.F.; Hiemstra, P.S. The antimicrobial peptide LL-37 activates innate immunity at the airway epithelial surface by transactivation of the epidermal growth factor receptor. *J Immunol* **2003**, *171* (12), 6690-6.
140. Murakami, M.; Lopez-Garcia, B.; Braff, M.; Dorschner, R.A.; Gallo, R.L. Postsecretory processing generates multiple cathelicidins for enhanced topical antimicrobial defense. *J Immunol* **2004**, *172* (5), 3070-7.
141. Gough, M.; Hancock, R.E.; Kelly, N.M. Antiendotoxin activity of cationic peptide antimicrobial agents. *Infect Immun* **1996**, *64* (12), 4922-7.
142. Gandhi, N.S.; Mancera, R.L. The structure of glycosaminoglycans and their interactions with proteins. *Chem Biol Drug Des* **2008**, *72* (6), 455-82.
143. Capila, I.; Linhardt, R.J. Heparin-protein interactions. *Angew Chem Int Ed Engl* **2002**, *41* (3), 391-412.
144. Braswell, E. Heparin: molecular weight and degradation studies. *Biochim Biophys Acta* **1968**, *158* (1), 103-16.
145. Dol, F.; Petitou, M.; Lormeau, C.J.; Choay, J.; Caranobe, C.; Sie, P.; Saivin, S.; Houin, G.; Boneu, B. Pharmacologic Properties of a Low Molecular Weight Dermatan Sulfate: Comparison with Unfractionated Dermatan Sulfate. *The Journal of Laboratory and Clinical Medicine* **1990**, *115* (1), 43 - 51.
146. Mourao, P.A.S.; Salac, M.L.B. The Effect of Chondroitin Sulfate Molecular Weight and Degree of Sulfation on the Activity of a Sulfotransferase from Chicken Embryo Epiphyseal Cartilages. *Molecular and Cellular Biochemistry* **1983**, *57*, 47 - 60.
147. Griffin, C.C.; Linhardt, R.J.; Van Gorp, C.L.; Toida, T.; Hileman, R.E.; Schubert, R.L., 2nd; Brown, S.E. Isolation and characterization of heparan sulfate from crude porcine intestinal mucosal peptidoglycan heparin. *Carbohydr Res* **1995**, *276* (1), 183-97.
148. Hopwood, J.J.; Robinson, H.C. The Molecular-Weight Distribution of Glycosaminoglycans. *Biochemical Journal* **1973**, *135*, 631 - 637.
149. Taylor, K.R.; Gallo, R.L. Glycosaminoglycans and Their Proteoglycans: Host-Associated Molecular Patterns for Initiation and Modulation of Inflammation. *Federation of the American Societies for Experimental Biology Journal* **2006**, *20*, 9 - 22.

150. *Essentials of Glycobiology*. Second ed.; The Consortium of Glycobiology: La Jolla, 2009.
151. Metcalfe, D.D.; Lewis, R.A.; Silbert, J.E.; Rosenberg, R.D.; Wasserman, S.I.; Austen, K.F. Isolation and characterization of heparin from human lung. *J Clin Invest* **1979**, *64* (6), 1537-43.
152. Stevens, R.L.; Fox, C.C.; Lichtenstein, L.M.; Austen, K.F. Identification of chondroitin sulfate E proteoglycans and heparin proteoglycans in the secretory granules of human lung mast cells. *Proc Natl Acad Sci U S A* **1988**, *85* (7), 2284-7.
153. Thompson, H.L.; Schulman, E.S.; Metcalfe, D.D. Identification of chondroitin sulfate E in human lung mast cells. *J Immunol* **1988**, *140* (8), 2708-13.
154. Almond, A. Hyaluronan. *Cell Mol Life Sci* **2007**, *64* (13), 1591-6.
155. Rabenstein, D.L. Heparin and heparan sulfate: structure and function. *Nat Prod Rep* **2002**, *19* (3), 312-31.
156. Lindahl, U.; Kjellen, L. Heparin or heparan sulfate--what is the difference? *Thromb Haemost* **1991**, *66* (1), 44-8.
157. Esko, J.D.; Lindahl, U. Molecular diversity of heparan sulfate. *J Clin Invest* **2001**, *108* (2), 169-73.
158. Mulloy, B.; Forster, M.J.; Jones, C.; Davies, D.B. N.m.r. and molecular-modelling studies of the solution conformation of heparin. *Biochem J* **1993**, *293* (Pt 3), 849-58.
159. Mulloy, B.; Forster, M.J.; Jones, C.; Drake, A.F.; Johnson, E.A.; Davies, D.B. The effect of variation of substitution on the solution conformation of heparin: a spectroscopic and molecular modelling study. *Carbohydr Res* **1994**, *255*, 1-26.
160. Wu, C.W.; Jayaraman, G.; Chien, K.Y.; Liu, Y.J.; Lyu, P.C. Influence of peptide conformation on oligosaccharide binding characteristics--a study using apamin-based chimeric peptide. *Peptides* **2003**, *24* (12), 1853-61.
161. Record, M.T., Jr.; Lohman, M.L.; De Haseth, P. Ion effects on ligand-nucleic acid interactions. *J Mol Biol* **1976**, *107* (2), 145-58.
162. Hirsh, J.; Warkentin, T.E.; Raschke, R.; Granger, C.; Ohman, E.M.; Dalen, J.E. Heparin and low-molecular-weight heparin: mechanisms of action, pharmacokinetics, dosing considerations, monitoring, efficacy, and safety. *Chest* **1998**, *114* (5 Suppl), 489S-510S.
163. Rota, C.; Liverani, L.; Spelta, F.; Mascellani, G.; Tomasi, A.; Iannone, A.; Vismara, E. Free radical generation during chemical depolymerization of heparin. *Anal Biochem* **2005**, *344* (2), 193-203.
164. Guerrini, M.; Guglieri, S.; Naggi, A.; Sasisekharan, R.; Torri, G. Low molecular weight heparins: structural differentiation by bidimensional nuclear magnetic resonance spectroscopy. *Semin Thromb Hemost* **2007**, *33* (5), 478-87.



165. Casu, B.; Guerrini, M.; Torri, G. Structural and conformational aspects of the anticoagulant and anti-thrombotic activity of heparin and dermatan sulfate. *Curr Pharm Des* **2004**, *10* (9), 939-49.
166. Sugahara, K.; Mikami, T.; Uyama, T.; Mizuguchi, S.; Nomura, K.; Kitagawa, H. Recent advances in the structural biology of chondroitin sulfate and dermatan sulfate. *Curr Opin Struct Biol* **2003**, *13* (5), 612-20.
167. Itano, N. Simple primary structure, complex turnover regulation and multiple roles of hyaluronan. *J Biochem* **2008**, *144* (2), 131-7.
168. Turley, E.A.; Noble, P.W.; Bourguignon, L.Y. Signaling properties of hyaluronan receptors. *J Biol Chem* **2002**, *277* (7), 4589-92.
169. Jiang, D.; Liang, J.; Noble, P.W. Hyaluronan in tissue injury and repair. *Annu Rev Cell Dev Biol* **2007**, *23*, 435-61.
170. Ponting, J.; Howell, A.; Pye, D.; Kumar, S. Prognostic relevance of serum hyaluronan levels in patients with breast cancer. *Int J Cancer* **1992**, *52* (6), 873-6.
171. Ropponen, K.; Tammi, M.; Parkkinen, J.; Eskelinen, M.; Tammi, R.; Lipponen, P.; Agren, U.; Alhava, E.; Kosma, V.M. Tumor cell-associated hyaluronan as an unfavorable prognostic factor in colorectal cancer. *Cancer Res* **1998**, *58* (2), 342-7.
172. Toole, B.P. Hyaluronan: from extracellular glue to pericellular cue. *Nat Rev Cancer* **2004**, *4* (7), 528-39.
173. Toole, B.P.; Wight, T.N.; Tammi, M.I. Hyaluronan-cell interactions in cancer and vascular disease. *J Biol Chem* **2002**, *277* (7), 4593-6.
174. Wight, T.N.; Merrilees, M.J. Proteoglycans in atherosclerosis and restenosis: key roles for versican. *Circ Res* **2004**, *94* (9), 1158-67.
175. Laurent, T.C.; Laurent, U.B.; Fraser, J.R. The structure and function of hyaluronan: An overview. *Immunol Cell Biol* **1996**, *74* (2), A1-7.
176. Funderburgh, J.L.; Caterson, B.; Conrad, G.W. Distribution of proteoglycans antigenically related to corneal keratan sulfate proteoglycan. *J Biol Chem* **1987**, *262* (24), 11634-40.
177. Konkle, B.A.; Bauer, T.L.; Arepally, G.; Cines, D.B.; Poncz, M.; McNulty, S.; Edie, R.N.; Mannion, J.D. Heparin-induced thrombocytopenia: bovine versus porcine heparin in cardiopulmonary bypass surgery. *Ann Thorac Surg* **2001**, *71* (6), 1920-4.
178. Sim, J.-S.; Im, A.-R.; Cho, S.M.; Jang, H.J.; Jo, J.H.; Kim, Y.S. Evaluation of chondroitin sulfate in shark cartilage powder as a dietary supplement: Raw materials and finished products. *Food Chemistry* **2007**, *101* (2), 532-539.

179. Manna, F.; Dentini, M.; Desideri, P.; De Pita, O.; Mortilla, E.; Maras, B. Comparative chemical evaluation of two commercially available derivatives of hyaluronic acid (hylaform from rooster combs and restylane from streptococcus) used for soft tissue augmentation. *J Eur Acad Dermatol Venereol* **1999**, *13* (3), 183-92.
180. Taylor, R.L.; Shively, J.E.; Conrad, H.E., Stoichiometric reduction of uronic acid carboxyl groups in polysaccharides. In *Methods in Carbohydrate Chemistry*, Whistler, RL; *al., e*, Eds. Academic Press: New York, 1976; Vol. VII, pp 149-151.
181. Brown, K.J.; Hendry, I.A.; Parish, C.R. Evidence that carboxyl-reduced heparin fails to potentiate acidic fibroblast growth factor activity due to an inability to interact with cell surface heparin receptors. *Exp Cell Res* **1995**, *217* (1), 132-9.
182. Ishihara, M.; Kariya, Y.; Kikuchi, H.; Minamisawa, T.; Yoshida, K. Importance of 2-O-sulfate groups of uronate residues in heparin for activation of FGF-1 and FGF-1. *Journal of Biochemistry (Tokyo)* **1997**, *121*, 345-349.
183. Ayotte, L.; Perlin, A.S. N.M.R. spectroscopic observations related to the function of sulfate groups in heparin. Calcium binding vs. biological activity. *Carbohydrate Research* **1986**, *145*, 267-277.
184. Jaseja, M.; Rej, R.N.; Sauriol, F.; Perlin, A.S. Novel regio- and stereoselective modifications of heparin in alkaline solution. Nuclear magnetic resonance spectroscopic evidence. *Canadian Journal of Chemistry* **1989**, *67*, 1449-1456.
185. Matsuo, M.; Takano, R.; Kamei-Hayashi, K.; Hara, S. A novel regioselective desulfation of polysaccharide sulfates: Specific 6Odesulfation with N,O-bis(trimethylsilyl)acetamide. *Carbohydrate Research* **1993**, *241*, 209-215.
186. Takano, R.; Ye, Z.; Ta, T.-V.; Hayashi, K.; Kariya, Y.; Hara, S. Specific 6-O-desulfation of heparin. *Carbohydrate Letters* **1998**, *3*, 71-77.
187. Danishefsky, I.; Siskovic, E. Conversion of Carboxyl Groups of Mucopolysaccharides in Amides of Amino Acid Esters. *Carbohydr Res* **1971**, *16*, 199-205.
188. Davis, M.E.; Brewster, M.E. Cyclodextrin-based pharmaceuticals: past, present and future. *Nat Rev Drug Discov* **2004**, *3* (12), 1023-35.
189. Pagington, J.S. beta-Cyclodextrin: the success of molecular inclusion. *Chemistry in Britain* **1987**, *23* (5), 455-458.
190. Uekama, K.; Hirayama, F.; Irie, T. Cyclodextrin Drug Carrier Systems. *Chem Rev* **1998**, *98* (5), 2045-2076.
191. Loftsson, T.; Brewster, M.E. Pharmaceutical applications of cyclodextrins. 1. Drug solubilization and stabilization. *J Pharm Sci* **1996**, *85* (10), 1017-25.
192. Javan, C.M.; Gooderham, N.J.; Edwards, R.J.; Davies, D.S.; Shaunak, S. Anti-HIV type 1 activity of sulfated derivatives of dextrin against primary viral isolates of HIV type 1 in lymphocytes and monocyte-derived macrophages. *AIDS Res Hum Retroviruses* **1997**, *13* (10), 875-80.

193. Shaunak, S.; Gooderham, N.J.; Edwards, R.J.; Payvandi, N.; Javan, C.M.; Baggett, N.; MacDermot, J.; Weber, J.N.; Davies, D.S. Infection by HIV-1 blocked by binding of dextrin 2-sulphate to the cell surface of activated human peripheral blood mononuclear cells and cultured T-cells. *Br J Pharmacol* **1994**, *113* (1), 151-8.
194. McClure, M.O.; Moore, J.P.; Blanc, D.F.; Scotting, P.; Cook, G.M.; Keynes, R.J.; Weber, J.N.; Davies, D.; Weiss, R.A. Investigations into the mechanism by which sulfated polysaccharides inhibit HIV infection in vitro. *AIDS Res Hum Retroviruses* **1992**, *8* (1), 19-26.
195. D'Cruz, O.J.; Uckun, F.M. Clinical development of microbicides for the prevention of HIV infection. *Curr Pharm Des* **2004**, *10* (3), 315-36.
196. D'Cruz, O.J.; Uckun, F.M. Preclinical and Clinical Profile of Emmelle (Dextrin-2-Sulfate) - a Potential Anti-HIV Microbicide. *Journal of Applied Research* **2005**, *5* (1), 26-34.
197. Harenberg, J. Review of pharmacodynamics, pharmacokinetics, and therapeutic properties of sulodexide. *Med Res Rev* **1998**, *18* (1), 1-20.
198. Weiss, R.; Niecestro, R.; Raz, I. The role of sulodexide in the treatment of diabetic nephropathy. *Drugs* **2007**, *67* (18), 2681-96.
199. Buchanan, M.R.; Liao, P.; Smith, L.J.; Ofosu, F.A. Prevention of thrombus formation and growth by antithrombin III and heparin cofactor II-dependent thrombin inhibitors: importance of heparin cofactor II. *Thromb Res* **1994**, *74* (5), 463-75.
200. Witvrouw, M.; De Clercq, E. Sulfated polysaccharides extracted from sea algae as potential antiviral drugs. *Gen Pharmacol* **1997**, *29* (4), 497-511.
201. Mahner, C.; Lechner, M.D.; Nordmeier, E. Synthesis and characterisation of dextran and pullulan sulphate. *Carbohydr Res* **2001**, *331* (2), 203-8.
202. Schaeffer, D.J.; Krylov, V.S. Anti-HIV activity of extracts and compounds from algae and cyanobacteria. *Ecotoxicol Environ Saf* **2000**, *45* (3), 208-27.
203. Morelli, F.; Carlier, P.; Giannini, G.; De Luigi, M.C.; Dejana, A.M.; Ruzzenenti, M.R. Hypercholesterolemia and LDL apheresis. *Int J Artif Organs* **2005**, *28* (10), 1025-31.
204. Cardin, A.D.; Weintraub, H.J. Molecular modeling of protein-glycosaminoglycan interactions. *Arteriosclerosis* **1989**, *9* (1), 21-32.
205. Sobel, M.; Soler, D.F.; Kermode, J.C.; Harris, R.B. Localization and characterization of a heparin binding domain peptide of human von Willebrand factor. *J Biol Chem* **1992**, *267* (13), 8857-62.
206. Hileman, R.E.; Fromm, J.R.; Weiler, J.M.; Linhardt, R.J. Glycosaminoglycan-protein interactions: definition of consensus sites in glycosaminoglycan binding proteins. *Bioessays* **1998**, *20* (2), 156-67.

207. Margalit, H.; Fischer, N.; Ben-Sasson, S.A. Comparative analysis of structurally defined heparin binding sequences reveals a distinct spatial distribution of basic residues. *J Biol Chem* **1993**, *268* (26), 19228-31.
208. Stevens, R.L.; Adachi, R. Protease-proteoglycan complexes of mouse and human mast cells and importance of their beta-tryptase-heparin complexes in inflammation and innate immunity. *Immunol Rev* **2007**, *217*, 155-67.
209. Evangelista, V.; Piccardoni, P.; Maugeri, N.; De Gaetano, G.; Cerletti, C. Inhibition by heparin of platelet activation induced by neutrophil-derived cathepsin G. *Eur J Pharmacol* **1992**, *216* (3), 401-5.
210. Redini, F.; Tixier, J.M.; Petitou, M.; Choay, J.; Robert, L.; Hornebeck, W. Inhibition of leucocyte elastase by heparin and its derivatives. *Biochem J* **1988**, *252* (2), 515-9.
211. Finotti, P.; Pagetta, A.; Corvaja, C. Role of reducing terminals in unfractionated and low-molecular-mass heparins in causing free radical generation and loss of structure and activity of trypsin. *Int J Biol Macromol* **1999**, *26* (2-3), 135-44.
212. Finotti, P. Biphasic pattern of heparin-induced oxidative degradation of trypsin in the presence of glucose. *Biochimie* **1997**, *79* (6), 351-8.
213. Zhang, Y.; Scandura, J.M.; Van Nostrand, W.E.; Walsh, P.N. The mechanism by which heparin promotes the inhibition of coagulation factor XIa by protease nexin-2. *J Biol Chem* **1997**, *272* (42), 26139-44.
214. Thorne, K.J.I.; Norman, J.M.; Haydock, S.F.; Lammas, D.A.; Duffus, P.H. ANTIBODY-DEPENDENT CELL-MEDIATED CYTO-TOXICITY AGAINST IBR-INFECTED BOVINE KIDNEY-CELLS BY RUMINANT NEUTROPHILS - THE ROLE OF LYSOSOMAL CATIONIC PROTEIN. *Immunology* **1984**, *53* (2), 275-282.
215. Gennaro, R.; Skerlavaj, B.; Romeo, D. PURIFICATION, COMPOSITION, AND ACTIVITY OF 2 BACTENECINS, ANTIBACTERIAL PEPTIDES OF BOVINE NEUTROPHILS. *Infect. Immun.* **1989**, *57* (10), 3142-3146.
216. Park, P.W.; Pier, G.B.; Hinkes, M.T.; Bernfield, M. Exploitation of syndecan-1 shedding by *Pseudomonas aeruginosa* enhances virulence. *Nature* **2001**, *411* (6833), 98-102.
217. Weiss; Elsbach; Olsson; Odeberg, H. Purification and characterization of a potent bactericidal and membrane active protein from the granules of human polymorphonuclear leukocytes. *J Biol Chem* **1978**, *253*, 2664-2672.
218. Little, R.G.; Kelner, D.N.; Lim, E.; Burke, D.J.; Conlon, P.J. Functional domains of recombinant bactericidal/permeability increasing protein (rBPI23). *J Biol Chem* **1994**, *269*, 1865-1872.
219. Klocek, G.; Seelig, J. Melittin interaction with sulfated cell surface sugars. *Biochemistry* **2008**, *47* (9), 2841-9.

220. James, S.; Gibbs, B.F.; Toney, K.; Bennett, H.P. Purification of antimicrobial peptides from an extract of the skin of *Xenopus laevis* using heparin-affinity HPLC: characterization by ion-spray mass spectrometry. *Anal Biochem* **1994**, *217* (1), 84-90.
221. Bosch, T.C.; Augustin, R.; Anton-Erxleben, F.; Fraune, S.; Hemmrich, G.; Zill, H.; Rosenstiel, P.; Jacobs, G.; Schreiber, S.; Leippe, M.; Stanisak, M.; Grotzinger, J.; Jung, S.; Podschun, R.; Bartels, J.; Harder, J.; Schroder, J.M. Uncovering the evolutionary history of innate immunity: the simple metazoan *Hydra* uses epithelial cells for host defence. *Dev Comp Immunol* **2009**, *33* (4), 559-69.
222. Cho, J.H.; Park, C.B.; Yoon, Y.G.; Kim, S.C. Lumbricin I, a novel proline-rich antimicrobial peptide from the earthworm: purification, cDNA cloning and molecular characterization. *Biochim Biophys Acta* **1998**, *1408* (1), 67-76.
223. Pan, W.; Liu, X.; Ge, F.; Han, J.; Zheng, T. Perinerin, a Novel Antimicrobial Peptide Purified from the Clamworm *Perinereis aibuhitensis* Grube and Its Partial Characterization. *J Biochem* **2004**, *135* (3), 297-304.
224. Park, C.J.; Park, C.B.; Hong, S.S.; Lee, H.S.; Lee, S.Y.; Kim, S.C. Characterization and cDNA cloning of two glycine- and histidine-rich antimicrobial peptides from the roots of shepherd's purse, *Capsella bursa-pastoris*. *Plant Mol Biol* **2000**, *44* (2), 187-97.
225. Egorov, T.A.; Odintsova, T.I.; Pukhalsky, V.A.; Grishin, E.V. Diversity of wheat anti-microbial peptides. *Peptides* **2005**, *26* (11), 2064-73.
226. Park, C.B.; Lee, J.H.; Park, I.Y.; Kim, M.S.; Kim, S.C. A novel antimicrobial peptide from the loach, *Misgurnus anguillicaudatus*. *FEBS Lett* **1997**, *411* (2-3), 173-8.
227. Minn, I.; Kim, H.S.; Kim, S.C. Antimicrobial peptides derived from pepsinogens in the stomach of the bullfrog, *Rana catesbeiana*. *Biochim Biophys Acta* **1998**, *1407* (1), 31-9.
228. Hirata, M.; Shimomura, Y.; Yoshida, M.; Morgan, J.G.; Palings, I.; Wilson, D.; Yen, M.H.; Wright, S.C.; Larrick, J.W. Characterization of a rabbit cationic protein (CAP18) with lipopolysaccharide-inhibitory activity. *Infect Immun* **1994**, *62* (4), 1421-6.
229. Larrick, J.W.; Hirata, M.; Zheng, H.; Zhong, J.; Bolin, D.; Cavaillon, J.M.; Warren, H.S.; Wright, S.C. A novel granulocyte-derived peptide with lipopolysaccharide-neutralizing activity. *J Immunol* **1994**, *152* (1), 231-40.
230. Shimazaki, K.; Tazume, T.; Uji, K.; Tanaka, M.; Kumura, H.; Mikawa, K.; Shimo-Oka, T. Properties of a heparin-binding peptide derived from bovine lactoferrin. *J Dairy Sci* **1998**, *81* (11), 2841-9.
231. Harder, J.; Schroder, J.M. RNase 7, a novel innate immune defense antimicrobial protein of healthy human skin. *J Biol Chem* **2002**, *277* (48), 46779-84.
232. Kim, H.S.; Cho, J.H.; Park, H.W.; Yoon, H.; Kim, M.S.; Kim, S.C. Endotoxin-neutralizing antimicrobial proteins of the human placenta. *J Immunol* **2002**, *168* (5), 2356-64.

233. Yang, D.; Rosenberg, H.F.; Chen, Q.; Dyer, K.D.; Kurosaka, K.; Oppenheim, J.J. Eosinophil-derived neurotoxin (EDN), an antimicrobial protein with chemotactic activities for dendritic cells. *Blood* **2003**, *102* (9), 3396-403.
234. Wehkamp, J.; Harder, J.; Wehkamp, K.; Wehkamp-von Meissner, B.; Schlee, M.; Enders, C.; Sonnenborn, U.; Nuding, S.; Bengmark, S.; Fellermann, K.; Schroder, J.M.; Stange, E.F. NF-kappaB- and AP-1-mediated induction of human beta defensin-2 in intestinal epithelial cells by Escherichia coli Nissle 1917: a novel effect of a probiotic bacterium. *Infect Immun* **2004**, *72* (10), 5750-8.
235. Blackberg, L.; Hernell, O. Isolation of lactoferrin from human whey by a single chromatographic step. *FEBS Lett* **1980**, *109* (2), 180-3.
236. Zou, S.; Magura, C.E.; Hurley, W.L. Heparin-binding properties of lactoferrin and lysozyme. *Comp Biochem Physiol B* **1992**, *103* (4), 889-95.
237. Imber, M.J.; Pizzo, S.V. Clearance and binding of native and defucosylated lactoferrin. *Biochem J* **1983**, *212* (2), 249-57.
238. McAbee, D.D.; Esbensen, K. Binding and endocytosis of apo- and holo-lactoferrin by isolated rat hepatocytes. *J Biol Chem* **1991**, *266* (35), 23624-23631.
239. Ziere, G.J.; van Dijk, M.C.M.; Bijsterbosch, M.K.; van Berkel, T.J.C. Lactoferrin uptake by the rat liver. Characterization of the recognition site and effect of selective modification of arginine residues. *J Biol Chem* **1992**, *267* (16).
240. Andersen, J.H.; Jenssen, H.; Sandvik, K.; Gutteberg, T.J. Anti-HSV activity of lactoferrin and lactoferricin is dependent on the presence of heparan sulphate at the cell surface. *J Med Virol* **2004**, *74* (2), 262-71.
241. Risso, A.; Zanetti, M.; Gennaro, R. Cytotoxicity and apoptosis mediated by two peptides of innate immunity. *Cell Immunol* **1998**, *189* (2), 107-15.
242. Schroder-Borm, H.; Bakalova, R.; Andra, J. The NK-lysin derived peptide NK-2 preferentially kills cancer cells with increased surface levels of negatively charged phosphatidylserine. *FEBS Lett* **2005**, *579* (27), 6128-34.
243. Klaassen, C.D.; Boles, J.W. Sulfation and sulfotransferases 5: the importance of 3'-phosphoadenosine 5'-phosphosulfate (PAPS) in the regulation of sulfation. *FASEB J* **1997**, *11* (6), 404-18.
244. Fadnes, B.; Rekdal, O.; Uhlin-Hansen, L. The anticancer activity of lytic peptides is inhibited by heparan sulfate on the surface of the tumor cells. *BMC Cancer* **2009**, *9*, 183.
245. Guibinga, G.H.; Miyanojara, A.; Esko, J.D.; Friedmann, T. Cell surface heparan sulfate is a receptor for attachment of envelope protein-free retrovirus-like particles and VSV-G pseudotyped MLV-derived retrovirus vectors to target cells. *Mol Ther* **2002**, *5* (5 Pt 1), 538-46.
246. Ueda, M.; Matsumoto, S.; Hayashi, S.; Kobayashi, N.; Noguchi, H. Cell surface heparan sulfate proteoglycans mediate the internalization of PDX-1 protein. *Cell Transplant* **2008**, *17* (1-2), 91-7.

247. Wang, Y.; Agerberth, B.; Lothgren, A.; Almstedt, A.; Johansson, J. Apolipoprotein A-I binds and inhibits the human antibacterial/cytotoxic peptide LL-37. *J Biol Chem* **1998**, *273* (50), 33115-8.
248. Andersson, E.; Rydengard, V.; Sonesson, A.; Morgelin, M.; Bjorck, L.; Schmidtchen, A. Antimicrobial activities of heparin-binding peptides. *Eur J Biochem* **2004**, *271* (6), 1219-26.
249. Penc, S.F.; Pomahac, B.; Winkler, T.; Dorschner, R.A.; Eriksson, E.; Herndon, M.; Gallo, R.L. Dermatan sulfate released after injury is a potent promoter of fibroblast growth factor-2 function. *J Biol Chem* **1998**, *273* (43), 28116-21.
250. Baranska-Rybak, W.; Sonesson, A.; Nowicki, R.; Schmidtchen, A. Glycosaminoglycans inhibit the antibacterial activity of LL-37 in biological fluids. *J Antimicrob Chemother* **2006**, *57* (2), 260-5.
251. Scherpereel, A.; Depontieu, F.; Grigoriu, B.; Cavestri, B.; Tsiopoulos, A.; Gentina, T.; Jourdain, M.; Pugin, J.; Tonnel, A.B.; Lassalle, P. Endocan, a new endothelial marker in human sepsis. *Crit Care Med* **2006**, *34* (2), 532-7.
252. Gotte, M. Syndecans in inflammation. *FASEB J* **2003**, *17* (6), 575-91.
253. Nordahl, E.A.; Rydengard, V.; Nyberg, P.; Nitsche, D.P.; Morgelin, M.; Malmsten, M.; Bjorck, L.; Schmidtchen, A. Activation of the complement system generates antibacterial peptides. *Proc Natl Acad Sci U S A* **2004**, *101* (48), 16879-84.
254. Nelson, A.; Berkestedt, I.; Schmidtchen, A.; Ljunggren, L.; Bodelsson, M. Increased levels of glycosaminoglycans during septic shock: relation to mortality and the antibacterial actions of plasma. *Shock* **2008**, *30* (6), 623-7.
255. Gudmundsson, G.H.; Agerberth, B. Neutrophil antibacterial peptides, multifunctional effector molecules in the mammalian immune system. *J Immunol Methods* **1999**, *232* (1-2), 45-54.
256. Stern, R.; Asari, A.A.; Sugahara, K.N. Hyaluronan fragments: an information-rich system. *Eur J Cell Biol* **2006**, *85* (8), 699-715.
257. Jiang, D.; Liang, J.; Fan, J.; Yu, S.; Chen, S.; Luo, Y.; Prestwich, G.D.; Mascarenhas, M.M.; Garg, H.G.; Quinn, D.A.; Homer, R.J.; Goldstein, D.R.; Bucala, R.; Lee, P.J.; Medzhitov, R.; Noble, P.W. Regulation of lung injury and repair by Toll-like receptors and hyaluronan. *Nat Med* **2005**, *11* (11), 1173-9.
258. Taylor, K.R.; Yamasaki, K.; Radek, K.A.; Di Nardo, A.; Goodarzi, H.; Golenbock, D.; Beutler, B.; Gallo, R.L. Recognition of hyaluronan released in sterile injury involves a unique receptor complex dependent on Toll-like receptor 4, CD44, and MD-2. *J Biol Chem* **2007**, *282* (25), 18265-75.
259. Morioka, Y.; Yamasaki, K.; Leung, D.; Gallo, R.L. Cathelicidin antimicrobial peptides inhibit hyaluronan-induced cytokine release and modulate chronic allergic dermatitis. *J Immunol* **2008**, *181* (6), 3915-22.

260. Djanani, A.; Mosheimer, B.; Kaneider, N.C.; Ross, C.R.; Ricevuti, G.; Patsch, J.R.; Wiedermann, C.J. Heparan sulfate proteoglycan-dependent neutrophil chemotaxis toward PR-39 cathelicidin. *J Inflamm (Lond)* **2006**, *3*, 14.
261. Ohtake, T.; Fujimoto, Y.; Ikuta, K.; Saito, H.; Ohhira, M.; Ono, M.; Kohgo, Y. Proline-rich antimicrobial peptide, PR-39 gene transduction altered invasive activity and actin structure in human hepatocellular carcinoma cells. *Br J Cancer* **1999**, *81* (3), 393-403.
262. Kaneider, N.C.; Djanani, A.; Wiedermann, C.J. Heparan sulfate proteoglycan-involving immunomodulation by cathelicidin antimicrobial peptides LL-37 and PR-39. *ScientificWorldJournal* **2007**, *7*, 1832-8.
263. Tokumaru, S.; Sayama, K.; Shirakata, Y.; Komatsuzawa, H.; Ouhara, K.; Hanakawa, Y.; Yahata, Y.; Dai, X.; Tohyama, M.; Nagai, H.; Yang, L.; Higashiyama, S.; Yoshimura, A.; Sugai, M.; Hashimoto, K. Induction of keratinocyte migration via transactivation of the epidermal growth factor receptor by the antimicrobial peptide LL-37. *J Immunol* **2005**, *175* (7), 4662-8.
264. Schmidtchen, A.; Frick, I.M.; Bjorck, L. Dermatan sulphate is released by proteinases of common pathogenic bacteria and inactivates antibacterial alpha-defensin. *Mol Microbiol* **2001**, *39* (3), 708-13.
265. Kuschert, G.S.; Coulin, F.; Power, C.A.; Proudfoot, A.E.; Hubbard, R.E.; Hoogewerf, A.J.; Wells, T.N. Glycosaminoglycans interact selectively with chemokines and modulate receptor binding and cellular responses. *Biochemistry* **1999**, *38* (39), 12959-68.
266. Xiao, W.; Hsu, Y.P.; Ishizaka, A.; Kirikae, T.; Moss, R.B. Sputum cathelicidin, urokinase plasminogen activation system components, and cytokines discriminate cystic fibrosis, COPD, and asthma inflammation. *Chest* **2005**, *128* (4), 2316-26.
267. Weiner, D.J.; Bucki, R.; Janmey, P.A. The antimicrobial activity of the cathelicidin LL37 is inhibited by F-actin bundles and restored by gelsolin. *Am J Respir Cell Mol Biol* **2003**, *28* (6), 738-45.
268. Bucki, R.; Byfield, F.J.; Janmey, P.A. Release of the antimicrobial peptide LL-37 from DNA/F-actin bundles in cystic fibrosis sputum. *Eur Respir J* **2007**, *29* (4), 624-32.
269. Felgentreff, K.; Beisswenger, C.; Griese, M.; Gulder, T.; Bringmann, G.; Bals, R. The antimicrobial peptide cathelicidin interacts with airway mucus. *Peptides* **2006**, *27* (12), 3100-6.
270. Mummert, D.I.; Takashima, A.; Ellinger, L.; Mummert, M.E. Involvement of hyaluronan in epidermal Langerhans cell maturation and migration in vivo. *J Dermatol Sci* **2003**, *33* (2), 91-7.
271. Mummert, M.E.; Mohamadzadeh, M.; Mummert, D.I.; Mizumoto, N.; Takashima, A. Development of a peptide inhibitor of hyaluronan-mediated leukocyte trafficking. *J Exp Med* **2000**, *192* (6), 769-79.



272. Yang, B.; Zhang, L.; Turley, E.A. Identification of two hyaluronan-binding domains in the hyaluronan receptor RHAMM. *J Biol Chem* **1993**, *268* (12), 8617-23.
273. Zaleski, K.J.; Kolodka, T.; Cywes-Bentley, C.; McLoughlin, R.M.; Delaney, M.L.; Charlton, B.T.; Johnson, W.; Tzianabos, A.O. Hyaluronic acid binding peptides prevent experimental staphylococcal wound infection. *Antimicrob Agents Chemother* **2006**, *50* (11), 3856-60.
274. Rydengard, V.; Olsson, A.K.; Morgelin, M.; Schmidtchen, A. Histidine-rich glycoprotein exerts antibacterial activity. *FEBS J* **2007**, *274* (2), 377-89.
275. Malmsten, M.; Davoudi, M.; Schmidtchen, A. Bacterial killing by heparin-binding peptides from PRELP and thrombospondin. *Matrix Biol* **2006**, *25* (5), 294-300.
276. Ringstad, L.; Schmidtchen, A.; Malmsten, M. Effect of peptide length on the interaction between consensus peptides and DOPC/DOPA bilayers. *Langmuir* **2006**, *22* (11), 5042-50.
277. Mader, J.S.; Smyth, D.; Marshall, J.; Hoskin, D.W. Bovine lactoferricin inhibits basic fibroblast growth factor- and vascular endothelial growth factor165-induced angiogenesis by competing for heparin-like binding sites on endothelial cells. *Am J Pathol* **2006**, *169* (5), 1753-66.
278. Elliott, S.D. A Proteolytic Enzyme Produced by Group a Streptococci with Special Reference to Its Effect on the Type-Specific M Antigen. *J Exp Med* **1945**, *81* (6), 573-592.
279. Berge, A.; Bjorck, L. Streptococcal cysteine proteinase releases biologically active fragments of streptococcal surface proteins. *J Biol Chem* **1995**, *270* (17), 9862-7.
280. Herwald, H.; Collin, M.; Muller-Esterl, W.; Bjorck, L. Streptococcal cysteine proteinase releases kinins: a virulence mechanism. *J Exp Med* **1996**, *184* (2), 665-73.
281. Kapur, V.; Majesky, M.W.; Li, L.L.; Black, R.A.; Musser, J.M. Cleavage of interleukin 1 beta (IL-1 beta) precursor to produce active IL-1 beta by a conserved extracellular cysteine protease from *Streptococcus pyogenes*. *Proc Natl Acad Sci U S A* **1993**, *90* (16), 7676-80.
282. Kapur, V.; Topouzis, S.; Majesky, M.W.; Li, L.L.; Hamrick, M.R.; Hamill, R.J.; Patti, J.M.; Musser, J.M. A conserved *Streptococcus pyogenes* extracellular cysteine protease cleaves human fibronectin and degrades vitronectin. *Microb Pathog* **1993**, *15* (5), 327-46.
283. Lukomski, S.; Montgomery, C.A.; Rurangirwa, J.; Geske, R.S.; Barrish, J.P.; Adams, G.J.; Musser, J.M. Extracellular cysteine protease produced by *Streptococcus pyogenes* participates in the pathogenesis of invasive skin infection and dissemination in mice. *Infect Immun* **1999**, *67* (4), 1779-88.

284. Fukushima, J.; Yamamoto, S.; Morihara, K.; Atsumi, Y.; Takeuchi, H.; Kawamoto, S.; Okuda, K. Structural gene and complete amino acid sequence of *Pseudomonas aeruginosa* IFO 3455 elastase. *J Bacteriol* **1989**, *171* (3), 1698-704.
285. Makinen, M.W.; Troyer, J.M.; van der Werff, H.; Berendsen, H.J.; van Gunsteren, W.F. Dynamical structure of carboxypeptidase A. *J Mol Biol* **1989**, *207* (1), 201-16.
286. Morihara, K.; Tsuzuki, H.; Oka, T.; Inoue, H.; Ebata, M. *Pseudomonas Aeruginosa* Elastase. Isolation, Crystallization, and Preliminary Characterization. *J Biol Chem* **1965**, *240*, 3295-304.
287. Okuda, K.; Morihara, K.; Atsumi, Y.; Takeuchi, H.; Kawamoto, S.; Kawasaki, H.; Suzuki, K.; Fukushima, J. Complete nucleotide sequence of the structural gene for alkaline proteinase from *Pseudomonas aeruginosa* IFO 3455. *Infect Immun* **1990**, *58* (12), 4083-8.
288. Su, Y.A.; Sulavik, M.C.; He, P.; Makinen, K.K.; Makinen, P.L.; Fiedler, S.; Wirth, R.; Clewell, D.B. Nucleotide sequence of the gelatinase gene (*gelE*) from *Enterococcus faecalis* subsp. *liquefaciens*. *Infect Immun* **1991**, *59* (1), 415-20.
289. Schmidtchen, A. Degradation of antiproteases, complement and fibronectin in chronic leg ulcers. *Acta Derm Venereol* **2000**, *80* (3), 179-84.
290. Schmidtchen, A.; Holst, E.; Tapper, H.; Bjorck, L. Elastase-producing *Pseudomonas aeruginosa* degrade plasma proteins and extracellular products of human skin and fibroblasts, and inhibit fibroblast growth. *Microb Pathog* **2003**, *34* (1), 47-55.
291. Park, P.W.; Pier, G.B.; Preston, M.J.; Goldberger, O.; Fitzgerald, M.L.; Bernfield, M. Syndecan-1 shedding is enhanced by LasA, a secreted virulence factor of *Pseudomonas aeruginosa*. *J Biol Chem* **2000**, *275* (5), 3057-64.
292. Nikaido, H. Molecular basis of bacterial outer membrane permeability revisited. *Microbiol Mol Biol Rev* **2003**, *67* (4), 593-656.
293. Bos, M.P.; Robert, V.; Tommassen, J. Biogenesis of the gram-negative bacterial outer membrane. *Annu Rev Microbiol* **2007**, *61*, 191-214.
294. Luirink, J.; von Heijne, G.; Houben, E.; de Gier, J.W. Biogenesis of inner membrane proteins in *Escherichia coli*. *Annu Rev Microbiol* **2005**, *59*, 329-55.
295. Raetz, C.R.; Reynolds, C.M.; Trent, M.S.; Bishop, R.E. Lipid A modification systems in gram-negative bacteria. *Annu Rev Biochem* **2007**, *76*, 295-329.
296. Raetz, C.R.; Whitfield, C. Lipopolysaccharide endotoxins. *Annu Rev Biochem* **2002**, *71*, 635-700.
297. Miyake, K. Innate recognition of lipopolysaccharide by Toll-like receptor 4-MD-2. *Trends Microbiol* **2004**, *12* (4), 186-92.
298. Raetz, C.R. Biochemistry of endotoxins. *Annu Rev Biochem* **1990**, *59*, 129-70.

299. Rietschel, E.T.; Kirikae, T.; Schade, F.U.; Mamat, U.; Schmidt, G.; Loppnow, H.; Ulmer, A.J.; Zahringer, U.; Seydel, U.; Di Padova, F.; et al. Bacterial endotoxin: molecular relationships of structure to activity and function. *FASEB J* **1994**, *8* (2), 217-25.
300. Galloway, S.M.; Raetz, C.R. A mutant of *Escherichia coli* defective in the first step of endotoxin biosynthesis. *J Biol Chem* **1990**, *265* (11), 6394-402.
301. Muller-Loennies, S.; Holst, O.; Lindner, B.; Brade, H. Isolation and structural analysis of phosphorylated oligosaccharides obtained from *Escherichia coli* J-5 lipopolysaccharide. *Eur J Biochem* **1999**, *260* (1), 235-49.
302. Muller-Loennies, S.; Lindner, B.; Brade, H. Structural analysis of oligosaccharides from lipopolysaccharide (LPS) of *Escherichia coli* K12 strain W3100 reveals a link between inner and outer core LPS biosynthesis. *J Biol Chem* **2003**, *278* (36), 34090-101.
303. Vinogradov, E.V.; Van Der Drift, K.; Thomas-Oates, J.E.; Meshkov, S.; Brade, H.; Holst, O. The structures of the carbohydrate backbones of the lipopolysaccharides from *Escherichia coli* rough mutants F470 (R1 core type) and F576 (R2 core type). *Eur J Biochem* **1999**, *261* (3), 629-39.
304. Nikaido, H.; Vaara, M. Molecular basis of bacterial outer membrane permeability. *Microbiol Rev* **1985**, *49* (1), 1-32.
305. de Cock, H.; Brandenburg, K.; Wiese, A.; Holst, O.; Seydel, U. Non-lamellar structure and negative charges of lipopolysaccharides required for efficient folding of outer membrane protein PhoE of *Escherichia coli*. *J Biol Chem* **1999**, *274* (8), 5114-9.
306. Hagge, S.O.; de Cock, H.; Gutschmann, T.; Beckers, F.; Seydel, U.; Wiese, A. Pore formation and function of phosphoprotein PhoE of *Escherichia coli* are determined by the core sugar moiety of lipopolysaccharide. *J Biol Chem* **2002**, *277* (37), 34247-53.
307. Frirdich, E.; Whitfield, C. Lipopolysaccharide inner core oligosaccharide structure and outer membrane stability in human pathogens belonging to the Enterobacteriaceae. *J Endotoxin Res* **2005**, *11* (3), 133-44.
308. Appelmelk, B.J.; An, Y.Q.; Hekker, T.A.; Thijs, L.G.; MacLaren, D.M.; de Graaf, J. Frequencies of lipopolysaccharide core types in *Escherichia coli* strains from bacteraemic patients. *Microbiology* **1994**, *140* (Pt 5), 1119-24.
309. Gibb, A.P.; Barclay, G.R.; Poxton, I.R.; di Padova, F. Frequencies of lipopolysaccharide core types among clinical isolates of *Escherichia coli* defined with monoclonal antibodies. *J Infect Dis* **1992**, *166* (5), 1051-7.
310. Amor, K.; Heinrichs, D.E.; Frirdich, E.; Ziebell, K.; Johnson, R.P.; Whitfield, C. Distribution of core oligosaccharide types in lipopolysaccharides from *Escherichia coli*. *Infect Immun* **2000**, *68* (3), 1116-24.
311. Currie, C.G.; Poxton, I.R. The lipopolysaccharide core type of *Escherichia coli* O157:H7 and other non-O157 verotoxin-producing *E. coli*. *FEMS Immunol Med Microbiol* **1999**, *24* (1), 57-62.

312. Stenutz, R.; Weintraub, A.; Widmalm, G. The structures of Escherichia coli O-polysaccharide antigens. *FEMS Microbiol Rev* **2006**, *30* (3), 382-403.
313. Pier, G.B. Pseudomonas aeruginosa lipopolysaccharide: a major virulence factor, initiator of inflammation and target for effective immunity. *Int J Med Microbiol* **2007**, *297* (5), 277-95.
314. Beckmann, F.; Moll, H.; Jager, K.E.; Zahringer, U. Preliminary communication 7-O-carbamoyl-L-glycero-D-manno-heptose: a new core constituent in the lipopolysaccharide of Pseudomonas aeruginosa. *Carbohydr Res* **1995**, *267* (2), C3-7.
315. Bystrova, O.V.; Knirel, Y.A.; Lindner, B.; Kocharova, N.A.; Kondakova, A.N.; Zahringer, U.; Pier, G.B. Structures of the core oligosaccharide and O-units in the R- and SR-type lipopolysaccharides of reference strains of Pseudomonas aeruginosa O-serogroups. *FEMS Immunol Med Microbiol* **2006**, *46* (1), 85-99.
316. Bystrova, O.V.; Shashkov, A.S.; Kocharova, N.A.; Knirel, Y.A.; Zahringer, U.; Pier, G.B. Elucidation of the structure of the lipopolysaccharide core and the linkage between the core and the O-antigen in Pseudomonas aeruginosa immunotype 5 using strong alkaline degradation of the lipopolysaccharide. *Biochemistry (Mosc)* **2003**, *68* (8), 918-25.
317. Wilkinson, S.G. Composition and structure of lipopolysaccharides from Pseudomonas aeruginosa. *Rev Infect Dis* **1983**, *5 Suppl 5*, S941-9.
318. Bystrova, O.V.; Shashkov, A.S.; Kocharova, N.A.; Knirel, Y.A.; Lindner, B.; Zahringer, U.; Pier, G.B. Structural studies on the core and the O-polysaccharide repeating unit of Pseudomonas aeruginosa immunotype 1 lipopolysaccharide. *Eur J Biochem* **2002**, *269* (8), 2194-203.
319. Knirel, Y.A.; Bystrova, O.V.; Shashkov, A.S.; Lindner, B.; Kocharova, N.A.; Senchenkova, S.N.; Moll, H.; Zahringer, U.; Hatano, K.; Pier, G.B. Structural analysis of the lipopolysaccharide core of a rough, cystic fibrosis isolate of Pseudomonas aeruginosa. *Eur J Biochem* **2001**, *268* (17), 4708-19.
320. Sadovskaya, I.; Brisson, J.R.; Thibault, P.; Richards, J.C.; Lam, J.S.; Altman, E. Structural characterization of the outer core and the O-chain linkage region of lipopolysaccharide from Pseudomonas aeruginosa serotype O5. *Eur J Biochem* **2000**, *267* (6), 1640-50.
321. Raymond, C.K.; Sims, E.H.; Kas, A.; Spencer, D.H.; Kutuyavin, T.V.; Ivey, R.G.; Zhou, Y.; Kaul, R.; Clendenning, J.B.; Olson, M.V. Genetic variation at the O-antigen biosynthetic locus in Pseudomonas aeruginosa. *J Bacteriol* **2002**, *184* (13), 3614-22.
322. Morath, S.; von Aulock, S.; Hartung, T. Structure/function relationships of lipoteichoic acids. *J Endotoxin Res* **2005**, *11* (6), 348-56.
323. Fournier, B.; Philpott, D.J. Recognition of Staphylococcus aureus by the innate immune system. *Clin Microbiol Rev* **2005**, *18* (3), 521-40.
324. Bhakdi, S.; Klonisch, T.; Nuber, P.; Fischer, W. Stimulation of monokine production by lipoteichoic acids. *Infect Immun* **1991**, *59* (12), 4614-20.

325. Cleveland, M.G.; Gorham, J.D.; Murphy, T.L.; Tuomanen, E.; Murphy, K.M. Lipoteichoic acid preparations of gram-positive bacteria induce interleukin-12 through a CD14-dependent pathway. *Infect Immun* **1996**, *64* (6), 1906-12.
326. Danforth, J.M.; Strieter, R.M.; Kunkel, S.L.; Arenberg, D.A.; VanOtteren, G.M.; Standiford, T.J. Macrophage inflammatory protein-1 alpha expression in vivo and in vitro: the role of lipoteichoic acid. *Clin Immunol Immunopathol* **1995**, *74* (1), 77-83.
327. Keller, R.; Fischer, W.; Keist, R.; Bassetti, S. Macrophage response to bacteria: induction of marked secretory and cellular activities by lipoteichoic acids. *Infect Immun* **1992**, *60* (9), 3664-72.
328. Standiford, T.J.; Arenberg, D.A.; Danforth, J.M.; Kunkel, S.L.; VanOtteren, G.M.; Strieter, R.M. Lipoteichoic acid induces secretion of interleukin-8 from human blood monocytes: a cellular and molecular analysis. *Infect Immun* **1994**, *62* (1), 119-25.
329. von Aulock, S.; Morath, S.; Hareng, L.; Knapp, S.; van Kessel, K.P.; van Strijp, J.A.; Hartung, T. Lipoteichoic acid from *Staphylococcus aureus* is a potent stimulus for neutrophil recruitment. *Immunobiology* **2003**, *208* (4), 413-22.
330. von Aulock, S.; Schroder, N.W.; Traub, S.; Gueinzius, K.; Lorenz, E.; Hartung, T.; Schumann, R.R.; Hermann, C. Heterozygous toll-like receptor 2 polymorphism does not affect lipoteichoic acid-induced chemokine and inflammatory responses. *Infect Immun* **2004**, *72* (3), 1828-31.
331. Peschel, A.; Sahl, H.G. The co-evolution of host cationic antimicrobial peptides and microbial resistance. *Nat Rev Microbiol* **2006**, *4* (7), 529-36.
332. Neuhaus, F.C.; Baddiley, J. A continuum of anionic charge: structures and functions of D-alanyl-teichoic acids in gram-positive bacteria. *Microbiol Mol Biol Rev* **2003**, *67* (4), 686-723.
333. Abachin, E.; Poyart, C.; Pellegrini, E.; Milohanic, E.; Fiedler, F.; Berche, P.; Trieu-Cuot, P. Formation of D-alanyl-lipoteichoic acid is required for adhesion and virulence of *Listeria monocytogenes*. *Mol Microbiol* **2002**, *43* (1), 1-14.
334. Kristian, S.A.; Datta, V.; Weidenmaier, C.; Kansal, R.; Fedtke, I.; Peschel, A.; Gallo, R.L.; Nizet, V. D-alanylation of teichoic acids promotes group A streptococcus antimicrobial peptide resistance, neutrophil survival, and epithelial cell invasion. *J Bacteriol* **2005**, *187* (19), 6719-25.
335. Peschel, A.; Otto, M.; Jack, R.W.; Kalbacher, H.; Jung, G.; Gotz, F. Inactivation of the *dlt* operon in *Staphylococcus aureus* confers sensitivity to defensins, protegrins, and other antimicrobial peptides. *J Biol Chem* **1999**, *274* (13), 8405-10.
336. Poyart, C.; Pellegrini, E.; Marceau, M.; Baptista, M.; Jaubert, F.; Lamy, M.C.; Trieu-Cuot, P. Attenuated virulence of *Streptococcus agalactiae* deficient in D-alanyl-lipoteichoic acid is due to an increased susceptibility to defensins and phagocytic cells. *Mol Microbiol* **2003**, *49* (6), 1615-25.

337. Peschel, A.; Jack, R.W.; Otto, M.; Collins, L.V.; Staubitz, P.; Nicholson, G.; Kalbacher, H.; Nieuwenhuizen, W.F.; Jung, G.; Tarkowski, A.; van Kessel, K.P.; van Strijp, J.A. Staphylococcus aureus resistance to human defensins and evasion of neutrophil killing via the novel virulence factor MprF is based on modification of membrane lipids with l-lysine. *J Exp Med* **2001**, *193* (9), 1067-76.
338. Oku, Y.; Kurokawa, K.; Ichihashi, N.; Sekimizu, K. Characterization of the Staphylococcus aureus mprF gene, involved in lysinylation of phosphatidylglycerol. *Microbiology* **2004**, *150* (Pt 1), 45-51.
339. Staubitz, P.; Neumann, H.; Schneider, T.; Wiedemann, I.; Peschel, A. MprF-mediated biosynthesis of lysylphosphatidylglycerol, an important determinant in staphylococcal defensin resistance. *FEMS Microbiol Lett* **2004**, *231* (1), 67-71.
340. Ernst, R.K.; Guina, T.; Miller, S.I. Salmonella typhimurium outer membrane remodeling: role in resistance to host innate immunity. *Microbes Infect* **2001**, *3* (14-15), 1327-34.
341. Miller, S.I.; Ernst, R.K.; Bader, M.W. LPS, TLR4 and infectious disease diversity. *Nat Rev Microbiol* **2005**, *3* (1), 36-46.
342. Shafer, W.M.; Casey, S.G.; Spitznagel, J.K. Lipid A and resistance of Salmonella typhimurium to antimicrobial granule proteins of human neutrophil granulocytes. *Infect Immun* **1984**, *43* (3), 834-8.
343. Guo, L.; Lim, K.B.; Poduje, C.M.; Daniel, M.; Gunn, J.S.; Hackett, M.; Miller, S.I. Lipid A acylation and bacterial resistance against vertebrate antimicrobial peptides. *Cell* **1998**, *95* (2), 189-98.
344. Otto, M. Bacterial evasion of antimicrobial peptides by biofilm formation. *Curr Top Microbiol Immunol* **2006**, *306*, 251-8.
345. Vuong, C.; Voyich, J.M.; Fischer, E.R.; Braughton, K.R.; Whitney, A.R.; DeLeo, F.R.; Otto, M. Polysaccharide intercellular adhesin (PIA) protects Staphylococcus epidermidis against major components of the human innate immune system. *Cell Microbiol* **2004**, *6* (3), 269-75.
346. Blann, A.D.; Khoo, C.W. The prevention and treatment of venous thromboembolism with LMWHs and new anticoagulants. *Vasc Health Risk Manag* **2009**, *5*, 693-704.
347. Ghosh, T.; Chattopadhyay, K.; Marschall, M.; Karmakar, P.; Mandal, P.; Ray, B. Focus on antivirally active sulfated polysaccharides: from structure-activity analysis to clinical evaluation. *Glycobiology* **2009**, *19* (1), 2-15.
348. Yamada, S.; Sugahara, K. Potential therapeutic application of chondroitin sulfate/dermatan sulfate. *Curr Drug Discov Technol* **2008**, *5* (4), 289-301.
349. Dodgson, K.S. Determination of inorganic sulphate in studies on the enzymic and non-enzymic hydrolysis of carbohydrate and other sulphate esters. *Biochem J* **1961**, *78*, 312-9.
350. Dodgson, K.S.; Price, R.G. A note on the determination of the ester sulphate content of sulphated polysaccharides. *Biochem J* **1962**, *84*, 106-10.

351. Christman, J.F.; Doherty, D.G. The antimicrobial action of heparin. *J Bacteriol* **1956**, *72* (4), 433-5.
352. de Leeuw, E.; Burks, S.R.; Li, X.; Kao, J.P.; Lu, W. Structure-dependent functional properties of human defensin 5. *FEBS Lett* **2007**, *581* (3), 515-20.
353. Shain, H.; Homer, K.A.; Beighton, D. Degradation and utilisation of chondroitin sulphate by *Streptococcus intermedius*. *J Med Microbiol* **1996**, *44* (5), 372-80.
354. Christman, J.F.; Doherty, D.G. Microbial utilization of heparin. *J Bacteriol* **1956**, *72* (4), 429-32.
355. Sallman, B.; Birkeland, J.M.; Gray, C.T. Hyaluronic acid utilization by hemolytic streptococci in relation to possible hyaluronidase function in pathogenesis. *Proc Soc Exp Biol Med* **1951**, *76* (3), 467-71.
356. Salyers, A.A.; O'Brien, M.; Kotarski, S.F. Utilization of chondroitin sulfate by *Bacteroides thetaiotaomicron* growing in carbohydrate-limited continuous culture. *J Bacteriol* **1982**, *150* (3), 1008-15.
357. Senyurek, I.; Paulmann, M.; Sinnberg, T.; Kalbacher, H.; Deeg, M.; Gutschmann, T.; Hermes, M.; Kohler, T.; Gotz, F.; Wolz, C.; Peschel, A.; Schitteck, B. Dermcidin-derived peptides show a different mode of action than the cathelicidin LL-37 against *Staphylococcus aureus*. *Antimicrob Agents Chemother* **2009**, *53* (6), 2499-509.
358. Yu, X.Q.; Kanost, M.R. Immulectin-2, a lipopolysaccharide-specific lectin from an insect, *Manduca sexta*, is induced in response to gram-negative bacteria. *J Biol Chem* **2000**, *275* (48), 37373-81.
359. Li, C.; Ng, M.L.; Zhu, Y.; Ho, B.; Ding, J.L. Tandem repeats of Sushi3 peptide with enhanced LPS-binding and -neutralizing activities. *Protein Eng* **2003**, *16* (8), 629-35.
360. Koizumi, N.; Morozumi, A.; Imamura, M.; Tanaka, E.; Iwahana, H.; Sato, R. Lipopolysaccharide-binding proteins and their involvement in the bacterial clearance from the hemolymph of the silkworm *Bombyx mori*. *Eur J Biochem* **1997**, *248* (1), 217-24.
361. Gonzalez, M.; Romestand, B.; Fievet, J.; Huvet, A.; Lebart, M.C.; Gueguen, Y.; Bachere, E. Evidence in oyster of a plasma extracellular superoxide dismutase which binds LPS. *Biochem Biophys Res Commun* **2005**, *338* (2), 1089-97.
362. Cheng, Y.; Prusoff, W.H. Relationship between the inhibition constant (K<sub>1</sub>) and the concentration of inhibitor which causes 50 per cent inhibition (I<sub>50</sub>) of an enzymatic reaction. *Biochem Pharmacol* **1973**, *22* (23), 3099-108.
363. Walsh, R.L.; Dillon, T.J.; Scicchitano, R.; McLennan, G. Heparin and heparan sulphate are inhibitors of human leucocyte elastase. *Clin Sci (Lond)* **1991**, *81* (3), 341-6.
364. Ermolieff, J.; Boudier, C.; Laine, A.; Meyer, B.; Bieth, J.G. Heparin protects cathepsin G against inhibition by protein proteinase inhibitors. *J Biol Chem* **1994**, *269* (47), 29502-8.

365. Rao, S.K.; Mathrubutham, M.; Karteron, A.; Sorensen, K.; Cohen, J.R. A versatile microassay for elastase using succinylated elastin. *Anal Biochem* **1997**, *250* (2), 222-7.
366. Grobelny, D.; Poncz, L.; Galaray, R.E. Inhibition of human skin fibroblast collagenase, thermolysin, and *Pseudomonas aeruginosa* elastase by peptide hydroxamic acids. *Biochemistry* **1992**, *31* (31), 7152-7154.
367. Schagger, H. Tricine-SDS-PAGE. *Nat Protoc* **2006**, *1* (1), 16-22.